DISSERTATION

MOLECULAR GENETICS OF HERBICIDE RESISTANCE IN PALMER AMARANTH (*AMARANTHUS PALMERI*): METABOLIC TEMBOTRIONE RESISTANCE AND GEOGRAPHIC ORIGIN OF GLYPHOSATE RESISTANCE

Submitted by

Anita Küpper

Department of Bioagricultural Sciences and Pest Management

In partial fulfillment of the requirements

For the Degree of Doctor of Philosophy

Colorado State University

Fort Collins, Colorado

Spring 2018

Doctoral Committee:

Advisor: Todd A. Gaines

Franck E. Dayan
Scott J. Nissen
Anireddy S. N. Reddy

ABSTRACT

MOLECULAR GENETICS OF HERBICIDE RESISTANCE IN PALMER AMARANTH (*AMARANTHUS PALMERI*): METABOLIC TEMBOTRIONE RESISTANCE AND GEOGRAPHIC ORIGIN OF GLYPHOSATE RESISTANCE

Palmer amaranth (*Amaranthus palmeri*) is a major weed in U.S. cotton and soybean production systems, partly because it evolved resistance to five different herbicide modes of action. Resistance to the 4-hydroxyphenylpyruvate dioxygenase (HPPD)-inhibitor tembotrione in a population from Nebraska (NER) is due to enhanced metabolism. This type of non-target-site resistance is especially troublesome because of its potential for cross-resistance. Tembotrione-susceptible (NES) and NER formed the same tembotrione metabolites but NER exhibited faster 4-hydroxylation followed by glycosylation. The T_{50} value (time for 50% production of the maximum 4-hydroxylation product) was 4.9 and 11.9 h for NER and NES, respectively. Hydroxylation is typically catalyzed by cytochrome P450 monooxygenases (CYPs). Metabolism differences between NER and NES were most prominent under 28°C conditions and herbicide application at the four-leaf stage. An RNA-Seq transcriptome analysis was conducted with Pseudo-F_2 tembotrione-resistant and -susceptible individuals originating from three separate NER x NES crosses that were sampled before, six, and twelve h after treatment (HAT). Differential gene expression analysis identified CYP72A219 and CYP81E8 as strong candidates for metabolic resistance. The contigs were constitutively expressed in resistant plants, as were the contigs for several glycosyltransferases (GTs), oxidase, and glutathione-S-transferase (GST). Exposure to tembotrione further increased their expression in both resistant and susceptible plants.

Originally native to the Southwest, *A. palmeri* has spread throughout the country. In 2004 a population was identified with resistance to glyphosate, a herbicide heavily relied on in modern no-tillage and transgenic glyphosate-resistant crop systems. Glyphosate resistance in the species is now highly

prevalent in USA and was also discovered in Brazil in 2015. This was confirmed by species identification with a genetic marker, dose-response studies, shikimate accumulation assay, and *EPSPS* copy number assay. The Brazilian population was also resistant to sulfonylurea and imidazolinone ALS inhibitor herbicides conferred by two different alleles for target-site mutations in the *ALS* gene ($W_{574}L$ and $S_{653}N$). The degree of genetic relatedness among eight different populations of glyphosate-resistant (GR) and –susceptible (GS) *A. palmeri* from various geographic regions in USA was investigated by analyzing patterns of phylogeography and diversity to ascertain whether resistance evolved independently or spread from outside to an Arizona locality (AZ-R). Shikimate accumulation and *EPSPS* genomic copy assays confirmed resistance or susceptibility. With a set of 1,351 single nucleotide polymorphisms (SNPs), discovered by genotyping-by-sequencing (GBS), UPGMA phylogenetic analysis, principal component analysis, Bayesian model-based clustering, and pairwise comparisons of genetic distances were conducted. A GR population from Tennessee and two GS populations from Georgia and Arizona were identified as genetically distinct while the remaining GS populations from Kansas, Arizona, and Nebraska clustered together with two GR populations from Arizona and Georgia. Within the latter group, AZ-R was most closely related to the GS populations from Kansas and Arizona followed by the GR population from Georgia. GR populations from Georgia and Tennessee were genetically distinct from each other. The data suggest the following two possible scenarios: either glyphosate resistance was introduced to the Arizona locality from the east, or resistance evolved independently in Arizona. Glyphosate resistance in the Georgia and Tennessee localities most likely evolved separately. Thus, modern farmers need to continue to diversify weed management practices and prevent seed dispersal to mitigate herbicide resistance evolution in *A. palmeri*.

ACKNOWLEDGEMENTS

I want to thank Stephen Duke who encouraged me to apply for a PhD in the weed research laboratory of Colorado State University. I would also like to thank my committee, Franck Dayan, Scott Nissen, and Anireddy Reddy. I am deeply indebted to Todd Gaines who has been a phenomenal advisor. He provided an educational, safe, and supportive environment with continuous guidance and allowed me to explore any scientific area I wanted to pursue. I also learned a tremendous amount about herbicide resistance from Roland Beffa who has taken on a role equivalent to a co-advisor. He has been a dedicated and excellent brainstorming partner and mentor over the years. I would also like to thank Patrick Tranel, Christopher Preston, Philip Westra, Harish Manmathan, Paul Neve and his lab, Dale Shaner, and William McCloskey for their advice.

I am grateful to have studied alongside many great graduate students in the weed lab of which many have helped me along the way: Darci Giacomini, Eric Westra, Dean Pettinga, Olivia Todd, John Coyle, Tom Getts, Kallie Kessler, Christopher van Horn, Mirella Ortiz, Neeta Soni, Derek Sebastian, Raven Bough, Rachel Seedorf, Kristen Tanz, Shannon Clark, Adrien Quicke, Abigail Barker, and Hudson Takano. I especially want to thank Karl Ravet and Eric Patterson for teaching me lab techniques and bioinformatic tools, as well as Marcelo Figueiredo for many discussions on resistance, help in the radioactivity lab and shouting out “Courage!” whenever I needed to hear it. Also, I would like to thank the people from other labs, John Long, Graham Tuttle, Jessica Warren, Stacy Endriss, Taylor Person, Craig Beil, Paul Tanger, Federico Martin, Michael Friedman, Stephen Cohen, Becky Gullberg, Margret Fleming, Justin Lee, and Tammy Brenner for their support. Many hourly workers have helped me with labor-intensive planting, harvest and seed cleaning of Palmer amaranth over the years, I want to especially acknowledge Tyler Hicks, Tyler Todd, Dillon Thompson, Jessica Scarpin, Colton Hankins, Hailey Meiners, Nicholas McKenna, Mitch Hoffman, Henrique Scatena, Bryna Burns, Beatrice Bachur, Rachel Chayer, and Crystal Sparks. I would also like to thank Susana Gonzales, Veronika Brabetz, Julia

Unger, Thomas Schubel, Rebecka Dücker, Johannes Hermann, Ragnhild Paul, Bodo Peters, Harry Strek and especially Falco Peter from Bayer's Herbicide Resistance Competence Center for all their advice and help during my visit. Furthermore, I want to thank Janet Dill for always having a smile on her face and guiding me through the bureaucracy of a PhD program as well as Elden Pemberton for his friendly reminders. Funding was generously provided by Bayer CropScience, Dow AgroSciences and the USDA National Institute of Food and Agriculture Hatch fund.

I am grateful to my "American parents" Billie and David Novy for their visits and support from Minnesota as well as my actual parents Luzie and Anton Küpper for supporting my decision to go to graduate school on the other side of the globe, visiting me in the U.S. three times, regularly sending big packages with German candy and skyping with me almost every Saturday morning for the past four years. I want to especially thank my father for showing an interest in my research and for having read about the devices I use and science I do to be able to have challenging discussions with me. Finally, I want to thank Curtis Hildebrandt who, no matter the circumstances, has been my rock throughout the entire PhD program.

TABLE OF CONTENTS

ABSTRACT ii

ACKNOWLEDGEMENTS iv

1. INTRODUCTION 1

FIGURES 16

REFERENCES 19

2. TEMBOTRIONE DETOXIFICATION IN HPPD-INHIBITOR RESISTANT PALMER AMARANTH (*AMARANTHUS PALMERI* S. WATS) 24

INTRODUCTION 24
MATERIALS AND METHODS 26
RESULTS 30
DISCUSSION 33
CONCLUSION 38
TABLES 40
FIGURES 41

REFERENCES 45

3. IDENTIFICATION OF GENES INVOLVED IN METABOLISM-BASED TEMBOTRIONE RESISTANCE IN PALMER AMARANTH (*AMARANTHUS PALMERI*) BY RNA-SEQ TRANSCRIPTOME ANALYSIS 49

INTRODUCTION 49
MATERIALS AND METHODS 51
RESULTS 55
DISCUSSION 58
TABLES 63
FIGURES 65

REFERENCES 70

4. MULTIPLE RESISTANCE TO GLYPHSATE AND ALS INHIBITORS IN PALMER AMARANTH (*AMARANTHUS PALMERI*) IDENTIFIED IN BRAZIL 75

INTRODUCTION 75
MATERIALS AND METHODS 76
RESULTS AND DISCUSSION 82
TABLES 87
FIGURES 90

REFERENCES 93

5. POPULATION GENETIC STRUCTURE IN GLYPHOSATE-RESISTANT AND -SUSCEPTIBLE PALMER AMARANTH (*AMARANTHUS PALMERI*) POPULATIONS USING GENOTYPING-BY-SEQUENCING (GBS) 96
INTRODUCTION 96
MATERIALS AND METHODS 98
RESULTS 102
DISCUSSION 107
CONCLUSION 111
TABLES 113
FIGURES 116

REFERENCES 121

6. OUTLOOK 127

7. APPENDIX A 128
METHODS 128
RESULTS 130
FIGURES 132

8. APPENDIX B 135
TABLES 135

9. APPENDIX C 139
TABLES 139
FIGURES 141

1. INTRODUCTION

The increasing global demand for agricultural production

From 1961 to 2014 the amount of arable land within the global land area has increased from 9.7% to 10.9%. The lowest arable land areas are found in Oceania and the highest in Asia. In Europe, India, and Bangladesh over 29% of the land mass is defined as arable land (FAO, 2014). However, also from 1961 to 2014, the world population has increased from 3.1 to 7.3 billion people, an increase of over 135% (Worldometers, 2017). The world population is expected to reach 9 billion by mid of the century (Pretty et al., 2010) and even 12.3 billion by 2100 (Gerland et al., 2014). Additionally, the lifespan of people is expected to extend as well (Murphy et al., 2013).

Aside from the continuously growing global population, production demands are expected to increase further due to the continuing industrialization of developing countries and the growth of financial income and wealth. The following affluence shifts the dietary structure of people (Kearney, 2010), creating a demand for a variety of energy-dense foods like livestock, animal products, and sugar which are expected to replace carbohydrate-rich foods (Tomlinson, 2013; Henchion et al., 2014). These energy-dense foods require an increase of crop production for animal feed since it takes more calories to produce an animal product than the product contributes to the overall food system. As examples, it requires about 2.6 kilos of corn to produce one kilo of chicken and seven kilos of corn to produce one kilo of beef (Leibtag, 2008). Consequently, 36% of the calories derived from crops are produced for animal feed (Cassidy et al., 2013) and 75% of all agricultural land is used for animal production (Foley et al., 2011). Even though food production has significantly intensified over the past decades, it is estimated that it needs to increase by over 70% to meet global demand in the future (Alexandratos et al., 2006; Pretty et al., 2010).

In addition to the challenge of providing food security, human-edible calories are now also diverted for biofuel production (Cassidy et al., 2013). The demand for the production of bioethanol and

biodiesel raises the demands on agricultural yield especially in USA and Brazil since most of these fuels come from corn and sugarcane (Ajanovic, 2011). In 2012, ethanol fuel production was at 83.1 billion liters with 51% of total sugarcane production being used to produce bioethanol on 4.9 Mha, constituting roughly 6% of the global crop production (Cassidy et al., 2013). From 2000 to 2010, biofuel production has increased by 450% (Cassidy et al., 2013). Another 43 billion liters in ethanol are expected to be necessary to produce until 2025 (Lima et al., 2014).

Furthermore, climate change is becoming a contributor in the challenge for sufficient agricultural production since agriculture is highly dependent on temperature and rainfall. Erosion and desertification lead to a decrease in the amount of arable land available while floods, droughts, heatwaves, and natural catastrophes like storms increase the likelihood of crop losses (Smith and Gregory, 2013). The failure to provide a stable source of food production can lead to socio-economic implications like hunger, political destabilization, and migration.

Even though food production already underwent a "green revolution" that doubled the production per unit surface area in some crops with the help of fertilizers and improved crop varieties (Carvalho, 2006; 2017), this trend is reaching a plateau and will not be sufficient to feed the growing world population. To avoid this crisis, it is crucial to narrow the yield gap by increasing per-area productivity, limit the range of food commodities and promote equal access and utilization of the current food sources. Since more food must be produced on the same surface area of land, it is important to seek technological solutions which help further intensify agricultural production.

Agricultural weeds

The greatest causes for crop loss are abiotic and biotic stressors such as lack of water, temperature, and nutrients as well as the presence of animal pests (insects, nematodes, rodents, and birds), pathogens (fungi and bacteria), and plants (weeds). All these stressors reduce crop yield, which is calculated by the difference in attainable yield and actual yield. Within biotic stressors, uncontrolled weeds have the highest potential yield loss with an estimated attainable yield loss from 23 – 44% (Fried et

al., 2017) to up to 80% (Oerke, 2002). In most crops weeds are the most important pest group, which is facilitated by crop monocultures, frequent disturbances, and high resource availability. Estimated yield loss due to weeds in corn and soybean in the U.S. and Canada range from $26.7 and $16.2 billion annual loss, respectively (Soltani et al., 2016; 2017).

A weed is defined as "a plant that is not valued where it is growing and is usually of vigorous growth; especially: one that tends to overgrow or choke out more desirable plants" (Merriam-Webster, 2004). Many weeds are opportunistic pioneer plants and thus well adapted to thrive in disturbed soils and survive in a wide range of ecological conditions. Some readily adapt to agriculture by becoming dominant species within a certain type of crop or cropping system. These undesired plants compete with crops for inorganic and organic nutrients, light, space, and water and thus decrease the amount and often quality of food produced. Some weeds are allelopathic and affect crop production via the release of harmful compounds. They can also interfere with the harvest and contaminate it with their seeds. Various weeds cause health issues such as allergic reactions due to pollen or they harm humans or poison cattle through toxic compounds that protect them from herbivory. In arid environments, some weeds can pose a fire hazard that can start or maintain wild fires. Again, others act as hosts for harmful crop pests and diseases (Zimdahl, 2013). In the U.S., 73% of weeds are non-native (Pimentel et al., 2005) compared to only 18% of all plants (Fried et al., 2017). Many of these weeds are R-strategists, species that rapidly produce high amounts of offspring and live in unstable environments, with an annual life span that produce large amounts of seeds at a fast growth rate (Fried et al., 2017). What makes weeds especially challenging compared to other pests is the fact that it is difficult to kill an undesirable plant within a field of other plants since they are all in the same kingdom.

Over the last century, farmers have practiced weed control via biological, mechanical, and chemical means, often in combination. Biological methods range from crop rotation to the planting of cover crops, the use of biological predators, and the breeding of resilient crop varieties. Mechanical/cultivation techniques encompass plowing to bury seeds, tilling, hoeing/harrowing and hand-weeding to control weeds after germination, weed seed destruction during harvest, and burn-downs.

Delayed drilling and the planting of higher seed rates are also being utilized as mechanical measures. Chemical tactics include the usage of synthetic and biological herbicides (Oerke, 2006). The last two methods are the most successful in controlling weeds.

Herbicides

Once people abandoned nomadic lifestyles, settled and started to practice agriculture, which required physical cultural weed control (ploughing/hand weeding). Then the usage of inorganic copper salts and sulphuric acid ushered the era of chemical weed control over a century ago (Hamill et al., 2004). In the 1940s, 2,4-dichlorophenoxyacetic acid (2,4-D) and 2-methyl-4-chlorophenoxyacetic acid (MCPA) were introduced and due to their selective nature found wide application in monocot crops like cereals. Since then over 300 different herbicidal active ingredients were brought to market (Heap, 2014; 2018). Herbicides have played an important role in agriculture due to their relative low cost, high efficacy, and success killing up to 99% of weeds targeted (Delye et al., 2013). If herbicides were not available, U.S. crop productivity would be less than 80% of what it is now (Owen, 2011). However, they also increased the dependence of farmers on chemicals, especially since the introduction of crops containing herbicide resistance traits. This has raised questions about the environmental fate and safety of herbicides and introduced additional problems such as the evolution of resistance that now threatens the successful application of this technology.

Some herbicide chemistries act non-selectively (broad-spectrum) and are used as “burndown herbicides” because they eradicate most plants. Other herbicides work selectively, killing only certain plants while leaving others unharmed. This is typically based on physiological differences such as differences in metabolism rates. Selectivity can be increased by the usage of safeners that enhance detoxification processes that allow desired crops to metabolize the herbicide quicker and therefore save them from harm. Some herbicides work only in the areas of direct contact (e.g. paraquat) and do not translocate within the plant. Others work systemically and are transported, either actively or passively, to the target site. Herbicides can be applied either pre- or post-emergence. Pre-emergence applications kill

weeds before they are able to emerge from the soil, post-emergence applications target actively growing weeds by penetrating through roots or shoots, translocating to the site of action where they accumulate and then bind to the target protein to block its function (Delye et al., 2013). Protein inhibition ceases the production of downstream products such as amino acids which are essential for the plant, ultimately causing its death (e.g. glyphosate stops the production of tyrosine, tryptophan, and phenylalanine). Inhibition can also lead to the accumulation of upstream intermediates to a degree that is toxic to the plant (e.g. ammonia accumulation in response to glufosinate) or cause biochemical changes that lead to the production of reactive oxygen species (ROS) which destroy plant cells (e.g. free radicals formed from PPO inhibitors).

To date there are 27 registered modes of actions of herbicides that target light processes, cell metabolism, or growth/cell division with the last mode of action having been registered in 1984. Herbicides are classified according to their target site, site of action, and their chemical class by two different widely used systems: One by the Herbicide Resistance Action Committee (HRAC) and one by the Weed Science Society of America (WSSA), both created in the 1990s. The first system is based on letters and used world-wide while the latter system is based on numbers and only used in North America. Australia also uses a separate classification system.

In 2016 the global herbicide market was valued at $23.97 billion and is estimated to increase to $34.10 billion in 2022 with Latin America and Asia/Pacific being the areas with fastest growth. The market is expected to develop towards bio-based and save products to address ecological and health concerns from regulatory authorities and consumers (GlobeNewswire, 2017). Over the past years the global agro-industry has undergone large-scale high-profile mergers and acquisitions. Currently, about 80% of the herbicide market share is divided between a total of four companies only: Bayer/Monsanto, ChemChina/Syngenta/ADAMA, Dow Dupont, and BASF (AgroNews, (2017)). Despite the high demand, no new modes of action have been commercialized in over three decades. This is partly owed to the high market share of glyphosate which diminished efforts for new herbicide discovery (Duke, 2012). With the evolution of herbicide-resistant weeds, especially to glyphosate, the pressure on the current remaining

modes of action will increase dramatically. Additionally, the rise of herbicide-resistant weeds threatens the practice of chemical weed control as a whole (Yuan et al., 2007).

Herbicide resistance

Theory of evolution has been described by Jean-Baptiste Lamarck in the early 19th century followed by Charles Darwin, Alfred Russel Wallace, and Gregor Mendel, all of which elaborated on the idea of natural selection. They realized that Nature occasionally produced variants of the common phenotype of a species. If this variation within an individual impart it a competitive advantage over other individuals, it was likely to be passed on to the offspring thereby driving population shifts and finally evolutionary change of the species. To put it in Siddhartha Mukherjee's words: "Freaks became norms, and norms became extinct. Monster by monster, evolution advanced." (Mukherjee, 2017). Selection acts on biological features and therefore the selection for the genes causing them is a passive process with the phenotype dragging the genotype behind it (Mukherjee, 2017). The more severe the selection pressure, the more obvious the shifts.

Variants emerge through genetic variation stemming from mutations that result in new alleles. These mutations can occur naturally and randomLy and have played a crucial role in the successful adaptation of existing species to environmental changes and ultimately in the evolution of new species. Thus, the evolution of adaptation mechanisms – such as resistance to pesticides or antibiotica - is a common occurrence in insects, fungi, bacteria, and mammals, as long as individuals are forced by continuous selection pressure to evolve to ensure the species' survival.

In plants, resistance to herbicides evolves when a mutation changes the genotype in a way that it allows for better survival following a herbicide application. If the resistant genotype is not eradicated and selection with the same herbicide persists, it will reproduce and its offspring will become the primary variant in the population. Resistance genes can spread rapidly via pollen and seed movement and sometimes even through gene flow or hybridization with other species (Franssen et al., 2001; Perez-Jones et al., 2010). Over time, plants will adapt to any repeated single method of removal, no matter if hand

weeding (Barrett, 1983) or chemicals. The speed at which resistance will evolve and successfully persist in the population depends on the molecular structure of the target enzyme (Preston et al., 1996), the structure of the herbicide molecule, as well as the weed's mutation rate, initial frequency of resistance alleles, inheritance, fitness, mating system, and gene flow (Jasieniuk et al., 1996b). If the mutation is advantageous will it continue to persist in the population.

The Weed Science Society of America (WSSA) defines herbicide resistance as "the inherited ability of a plant to survive and reproduce following exposure to a dose of herbicide normally lethal to the wild type". A similar definition by the Herbicide Resistance Action Committee (HRAC) says that herbicide resistance is the "naturally occurring inheritable ability of some weed biotypes within a given weed population to survive a herbicide treatment that should, under normal use conditions, effectively control that weed population." Alternatively, a plant species can also be naturally tolerant to a herbicide without any previous selection pressure. In that case a herbicide is selective for that species.
Herbicide resistance can be conferred by either target-site or non-target site mechanisms. Target-site resistance is the easier to investigate because it is mostly monogenic and involves an altered target enzyme (Yuan et al., 2007). The mechanism is caused by a mutation leading to a single amino acid substitution or deletion that leads to a structural change in the herbicide-binding site of the target enzyme allowing the protein to continue to function in the presence of the herbicide (Figure 1-1b). Other target-site resistance mechanisms encompass enzyme overexpression and target gene amplification where the target enzyme has been produced so numerously that the normally effective herbicide rate fails to kill the plant (Figure 1-1d).

Non-target site resistance includes all types of resistance that do not modify the herbicide-targeted enzyme such as reduced herbicide uptake or translocation, sequestration (Powles and Shaner, 2001), rapid necrosis/defoliation, delayed germination, or enhanced metabolism which detoxifies the active ingredient into inactive compounds before it can reach its target site (Figure 1-1c). Aside from a few exceptions (e.g. paraquat and glyphosate (Calderbank and Slade, 1976; Bradshaw et al., 1997)), most plants can detoxify herbicides to a certain degree which explains the selectivity of some herbicides. For example, in the case

of chlorsulfuron, wheat can metabolize the active ingredient more rapidly than weeds. Some weeds metabolize chlorsulfuron as well but at a rate too slow to allow them to survive. However, weeds can evolve to enhance their herbicide metabolism by e.g. increased expression of genes involved in metabolism of xenobiotics that increase their rates of detoxification to the point where they manage to survive an application. Previous research suggests that target-site resistance mechanisms are most likely to occur after frequent application with high doses of herbicide while non-target site resistance mechanisms evolve incrementally in quantitative changes (mostly polygenic) and are more likely to evolve with low dose applications (Gardner et al., 1998; Neve and Powles, 2005; Renton et al., 2011; Busi et al., 2013). Reduction of herbicide rates allows for selection of a broad range of alleles ("gene stacking") that would not have enabled survival to field rates on their own (Delye, 2013). Non-target-site resistance can confer cross-resistance which is defined by a single resistance mechanism conferring resistance to several herbicides. On the other hand, the presence of two or more resistance mechanisms is called multiple resistance, even if they confer resistance to the same herbicide (Powles and Shaner, 2001; Vencill et al., 2012).

Herbicide resistance was not of practical concern until the 1970s when groundsel (*Senecio vulgaris*) evolved resistance to triazines (Ryan, 1970; Scott and Putwain, 1981). Today, resistance to almost all available modes of action and cropping systems can be found in 487 different species of weeds (Heap, 2018). The modes of action with the fastest evolution of resistance and the highest number of resistant species are triazines, ALS-, and ACCase inhibitors while resistance evolution to synthetic auxins is slowest to emerge. Some herbicides are more prone to resistance evolution than others, which depends on their mode of action. As an example, if the herbicide acts as a non-competitive inhibitor, a small change in the herbicide's binding site may be enough to confer resistance but not interfere with the plant's essential biochemical pathways while competitive inhibitors do not allow for enzyme changes without affecting the plant's own protein synthesis. Even though resistance to different modes of action evolves at a different rate, it is inevitable that it will occur to any chemistry, new or old, if the selection pressure is high enough.

Certain weeds have shown propensity to evolve resistance and cases of multiple resistance are rising. Among the most troublesome of them are annual ryegrass (*Lolium rigidum*), barnyardgrass (*Echinochloa crus-gallis*), annual bluegrass (*Poa annua*), Indian goosegrass (*Eleusine indica*), and English ryegrass (*Lolium perenne*) which have evolved resistance to up to 13 different sites of action. Even though monocots are at the top of the list, four different *Amaranthus* species (Palmer amaranth (*A. palmeri*), green amaranth (*A. hybridus*), common waterhemp (*A. tuberculatus*), and redroot pigweed (*A. retroflexus*)) make the top list of resistant dicots with resistance having evolved to up to six different sites of action (Heap, 2018). All these plants have features in common which increase the chance of a mutation to occur and for it to spread: They produce high amounts of seed, have high genetic diversity, an annual life cycle and spread via pollen.

Resistance to HPPD inhibitors and glyphosate

This dissertation contains projects on herbicides tembotrione and glyphosate. Tembotrione is part of a class of herbicides that target the enzyme 4-hydroxyphenylpyruvate dioxygenase (HPPD). HPPD catalyzes the conversion of 4-hydroxyphenylpyruvate (HPP), derived from tyrosine, to homogentisate which is the precursor for α-tocopherols and plastoquinone (Lee et al., 1998) (Figure 1-2). If HPPD is inhibited, photosynthesis, carotenoid biosynthesis (Norris et al., 1995), and the protection of biological membranes against oxidative stress are impaired (Foyer et al., 1994; Ruiz-Sola and Rodríguez-Concepción, 2012). This leads to the characteristic bleaching and necrosis symptoms in treated plants before they die. Tembotrione finds wide application in corn because the crop is able to metabolize most of the herbicide within 24 hours whereas targeted weeds do not (Schulte and Köcher, 2009). Currently, 13 HPPD inhibitors are commercially available which can be divided into the three categories pyrazolones, isoxazoles (diketonitriles), and triketones (Wang et al., 2015). Triketone herbicides are structural analogues to the natural phytotoxin leptospermone. Their group is the last mode of action to be introduced, with sulcotrione having been brought to market in the early 1990s and tembotrione as late as 2007.

Over the following years, resistance to HPPD inhibitors was reported in *A. palmeri* from Kansas, Nebraska, and Wisconsin (Jhala et al., 2014; Nakka et al., 2017; Heap, 2018) as well as *A. tuberculatus* from Illinois, Iowa, Nebraska, and Missouri (Hausman et al., 2011; McMullan and Green, 2011; Schultz et al., 2015; Nakka et al., 2017). Enhanced metabolism is the main mechanism of resistance in both species (Kaundun et al., 2017; Küpper et al., 2017a; Nakka et al., 2017; Oliveira et al., 2017). So far, no other species have been reported to have evolved resistance to this mode of action.

Glyphosate, or *N*-phosphonomethyl glycine, is the most widely used herbicide in the world (Baylis, 2000), partly owed to the wide adoption of transgenic glyphosate-resistant crops (Roundup Ready). The onset of genetically modified crops led to the often exclusive use of glyphosate over large areas since the herbicide kills every plant and only leaves the transgenic crop alive. This allowed farmers greater flexibility with their applications, a reduction in the total amount of herbicides sprayed, the cost for labor and machinery, and the adoption of the practice of conservation tillage reducing soil erosion. By 2014, 89, 91, and 94% of U.S. corn, cotton and soybean acres planted, respectively, were herbicide-resistant varieties (USDA, 2017). However, this development also made farmers more reliable on glyphosate as weed control, abandoning deep cultivation. This favors the germination of seeds in shallow soil depths (Ward et al., 2013).

Glyphosate is a systemic, broad-spectrum herbicide with good translocation properties. Its low volatility, fast sorption to soil minerals, short half-life due to the fast degradation by microorganisms, and targeting of a pathway that animals do not have make it environmentally and toxicologically favorable when compared to other groups of herbicides and earned it the title “once in a century herbicide” (Duke and Powles, 2008a). Glyphosate inhibits the enzyme 5-enolpyruvylshikimate-3-phosphate synthase (EPSPS) in the shikimate pathway which plays a role in the production of the aromatic amino acids tyrosine, tryptophan, and phenylalanine. These proteins are important for downstream pathways such as auxins, pathogen defense, flavonoids, and plastoquinones. Glyphosate competes with the enzyme substrate phosphoenolpyruvate (PEP) with a tighter binding to the EPSPS-(shikimate-3-phosphate) S3P complex than PEP itself (Alibhai and Stallings, 2001) (Figure 1-3). If the complex works, it forms EPSP

and inorganic phosphate (Pi) (Pollegioni et al., 2011). If it is inhibited, S3P accumulates and degrades to shikimate which leads to plant injury (Shaner et al., 2005). Symptoms of chlorosis start at the growing points, followed by necrosis 4-20 d after application (Shaner, 2014). Glyphosate is absorbed via the foliage and therefore does not interfere with new germination after application.

The non-selective post-emergence herbicide was introduced commercially by Monsanto in 1974 as an acid molecule formulated as a salt. For a long time it was assumed that target-site-based resistance would never evolve since it proved to be difficult to obtain a resistant form of EPSPS that was still catalytically active (Bradshaw et al., 1997). For the following two decades glyphosate-resistant weeds did not seem to exist. However, in 1996 a population of *L. rigidum* from a field in Australia was reported to be resistant after glyphosate had been applied for 15 years (Powles et al., 1998; Pratley et al., 1999). Then, reduced sensitivity of EPSPS to glyphosate was found in *E. indica* from Malaysia. To date a total of 48 different species have evolved resistance to glyphosate (Heap, 2018). So far, several glyphosate resistance mechanisms have been identified ranging from point mutations (several substitutions with Pro106 (e.g. TIPS) being the most prominent (Baerson et al., 2002; Sammons and Gaines, 2014; Yu et al., 2015)) to vacuole sequestration (Ge et al., 2010; Ge et al., 2012), reduced cellular uptake (Shaner, 2009) and rapid necrosis (Norsworthy et al., 2010). However, the most problematic resistance mechanism is EPSPS gene amplification which enables the overexpression of the target enzyme. Thus, the plant has enough uninhibited EPSPS available to survive glyphosate application (Gaines et al., 2010). The EPSPS gene copies are associated with various other genetic elements and are dispersed across all chromosomes of the genome (Gaines et al., 2010; Gaines et al., 2013; Molin et al., 2017a), making the genome of glyphosate-resistant individuals 7-13% larger than the genome of glyphosate-susceptible ones (Molin et al., 2017a). These observations make the number of resistance mechanisms for glyphosate more numerous than to any other herbicide (Sammons and Gaines, 2014).

Palmer amaranth

The weed investigated in this dissertation is Palmer amaranth (*Amaranthus palmeri* s. Wats.) which currently poses a major threat to many U.S. food production systems (Beckie, 2011). The species has undergone an unprecedented expansion in the U.S. and managed to evolve resistance to multiple different herbicide modes of action.

Originally, *A. palmeri* was native to Northwestern Mexico and the U.S. Southwest where several Native American tribes consumed its leaves and seeds. Over the past decades, the species has established itself in the eastern and northern U.S. states as a weedy invader of artificial habitats (Sauer, 1957; Ward et al., 2013) and can even be found in Canada today (Kartescz, 2014) (Figure 1-4A). *A. palmeri* first became a problem in the mid-1990s in cotton fields in the Southern U.S. (Webster and Nichols, 2012). Its economic impact became worse once the species evolved wide-spread resistance to glyphosate. In 2015, a survey conducted by the Weed Science Society of America (WSSA) ranked *A. palmeri* as the most troublesome weed in the U.S due its devastating impact on crop yields (WSSA, 2016). The plant also compromises harvest efficiency through plant stems getting stuck in harvest equipment (Smith et al., 2000). Yield losses due to crop competition from *A. palmeri* can reach up to 65% in cotton (Rowland et al., 1999), 79% in soybean (Bensch et al., 2003), 91% in corn (Massinga et al., 2001), and 94% in sweet potato (Meyers et al., 2010; Ward et al., 2013).

A. palmeri can be distinguished from the other 75 species in the *Amaranthaceae* family by its dioecious nature, smooth stem and diamond-shaped leaves with petioles as long as the leaf (Figure 1-4B). Some leaves have a light V-shaped chevron on their surface. In contrast to male plants, females feel prickly and can produce up to a million seeds per individual that are very small (1 to 2 mm) and can easily be dispersed via water, wind, animals, manure, plowing, and harvest. *A. palmeri* emerge from within the top 3 cm of soil and can complete its lifecycle quickly. Even though no data is available for *A. palmeri*, previous studies have shown that the seeds of *A. tuberculatus* and *A. retroflexus* were still viable 17 years after burial (Burnside et al., 1996). The male plants of *A. palmeri* also produce a prodigious amount of pollen which can spread alleles up to 300 m (Sosnoskie et al., 2012). The weed has a long

germination period starting in spring continuing throughout the growing season. This allows it to avoid pre-emergence as well as post-emergence non-residual herbicide applications. Furthermore, *A. palmeri* can live under dry conditions since it is a C4 plant (Wang et al., 1992). It has 2n = 34 chromosomes (Gaines et al., 2012) and a genome size of 0.95 pg (929 Mbp) (Rayburn et al., 2005).

The weed's proliferation is largely owed to its high genetic variability, annual life cycle, high seed production, obligate outcrossing nature, and gene flow via wind-borne pollen movement (Franssen et al., 2001; Sellers et al., 2003; Ward et al., 2013), all of which are characteristics that allow a plant to adapt quickly to a changing environment and facilitate the spread of advantageous alleles.

The first report of herbicide resistance in *A. palmeri* was against the microtubule inhibitor trifluralin in 1989. Resistance to photosystem (PS) II and acetolactate synthase (ALS) was discovered in the 1990s. In 2004, the first case of glyphosate resistance was identified in Georgia (Culpepper et al., 2006) followed by Arkansas, North and South Carolina, and Tennessee (Scott et al., 2007; Norsworthy et al., 2008; Steckel et al., 2008). Glyphosate-resistant *A. palmeri* are now found in 26 U.S. States (Figure 1-5) which makes it especially troublesome for farmers. In recent years the weed also evolved resistance to HPPD inhibitors and protoporphyrinogen oxidase (PPO) inhibitors. So far resistant *A. palmeri* plants can be found in four different countries with multiple resistance to up to three modes of action (Heap, 2018).

Findings of this dissertation

Regardless of if one supports the usage of herbicides or not, it cannot be overlooked that herbicides play a crucial part in modern high-yielding agricultural production systems and will most likely continue to play an even greater role in the future unless or until alternative more successful technologies are discovered and commercialized. However, the continued success of herbicides is threatened by the lack of new mode of action discovery and commercialization due to the cost of registration and the inability of many chemistries to meet environmental safety standards. In order to preserve the usefulness of chemical weed control tools, it is important to gain an understanding of how

weeds adapt and evolve resistance to them and how these traits spread to other fields. Such knowledge will inform and improve application recommendations for customers and enable research and development departments in companies to find novel solutions to overcome resistance. Furthermore, a good understanding of resistance genes facilitates cheap and high-throughput diagnostics to give farmers a fast estimate of which herbicides still work in their field before the spraying season starts, avoiding costly and unnecessary applications. Also, such knowledge can be usable to create tolerant crops, help with the discovery of safeners and/or allow to develop useful targets for synergists and future technologies like RNA interference (RNAi). Just as weeds adapt to selection pressure from herbicides, farmers need to adapt their herbicide formulations and techniques to control weeds in the future. It has become apparent that the ability of *A. palmeri* to quickly evolve resistance to several modes of action over large acreages of agricultural land is a particular threat for the current herbicide-based system, especially cotton, soybean, and corn.

The aim of this dissertation was to expand the knowledge of enhanced metabolism as a mechanism of resistance to HPPD inhibitors and to gain an understanding of the distribution, dispersal patterns and evolution of glyphosate resistance in the weed species *A. palmeri.*

To address these topics, the second chapter of this dissertation investigates enhanced metabolism of the HPPD-inhibitor tembotrione in a resistant *A. palmeri* population from Nebraska. Tembotrione metabolites were identified and quantified to understand the differences in the detoxification process of resistant and susceptible plants. The experiments showed that increased hydroxylation of the parent compound steered by one or more gene(s) from the family of CYPs is likely to be the main mechanism of resistance. Several other possible mechanisms of resistance were excluded. Building on this knowledge, in chapter three the two candidate genes for resistance, CYPA219 and CYP81E8, were identified via an RNA-Sequencing experiment on three Pseudo-F_2-crosses made from tembotrione-resistant and -susceptible parent individuals. Chapter four characterizes the first glyphosate- and ALS-inhibitor-resistant *A. palmeri* population identified in Brazil by determining dose-response curves, shikimate accumulation, *EPSPS* gene copy number and *ALS* gene mutations. Finally, in chapter five several geographically distant

glyphosate-resistant and -susceptible *A. palmeri* populations from the United States were investigated for independent evolution events or resistance spread based on single nucleotide polymorphisms generated by genotyping-by-sequencing (GBS). The study found that glyphosate resistance reported from Georgia and Tennessee were most likely distinct evolution events while resistance in the south-west could have either evolved independently or been introduced from the east.

FIGURES

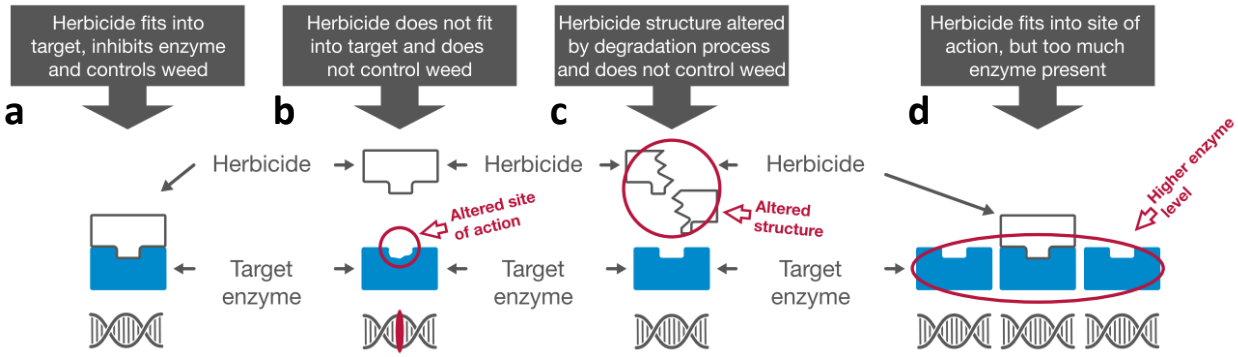

Figure 1-1: The most common herbicide resistance mechanisms. A: functional herbicide, b: target-site mutation, c: enhanced metabolism, d: target gene amplification (modified from (BayerCropScience, 2015).

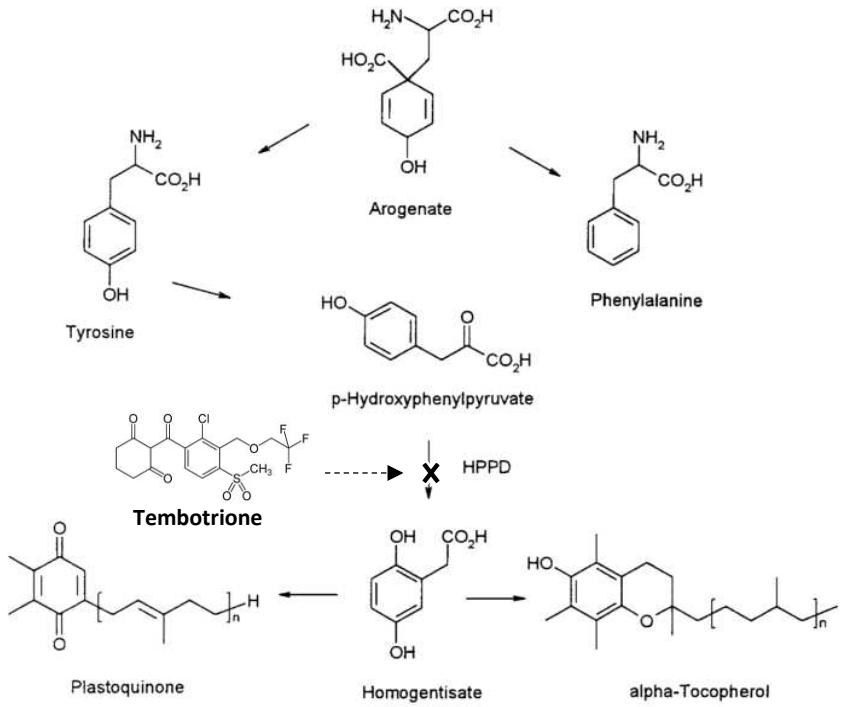

Figure 1-2: The 4-hydroxyphenylpyruvate pathway modified from (Lee et al., 1998) showing the site of action of tembotrione.

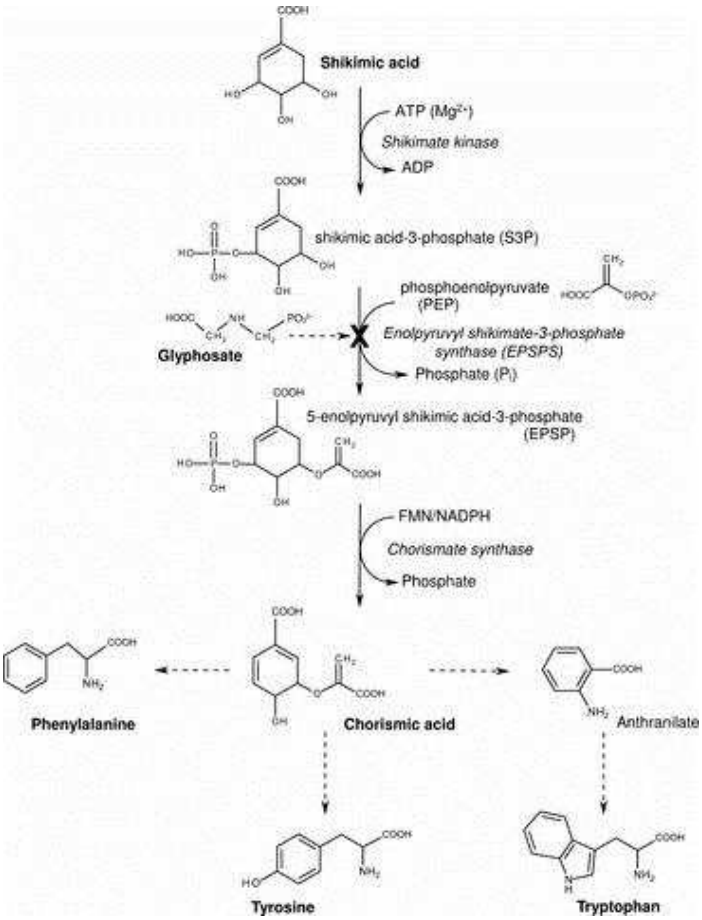

Figure 1-3: Glyphosate inhibition site in the shikimate pathway (Pollegioni et al., 2011).

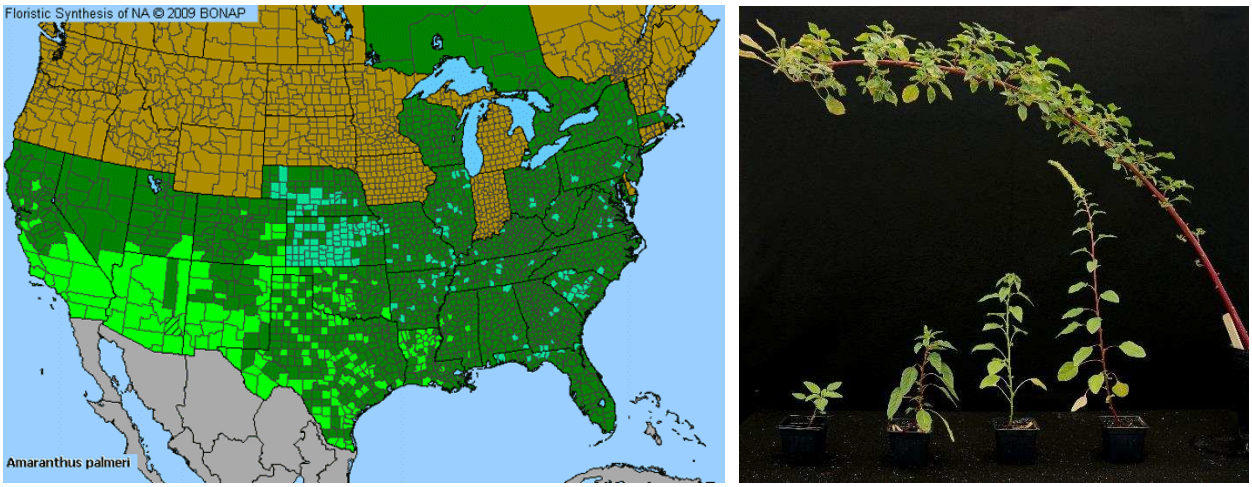

Figure 1-4: A. Distribution of *A. palmeri* in the United States (2009), brown: species not present in the state, green: species present in the state, light green: species is prominent (Kartescz, 2014). B. Different growing states of *A. palmeri*.

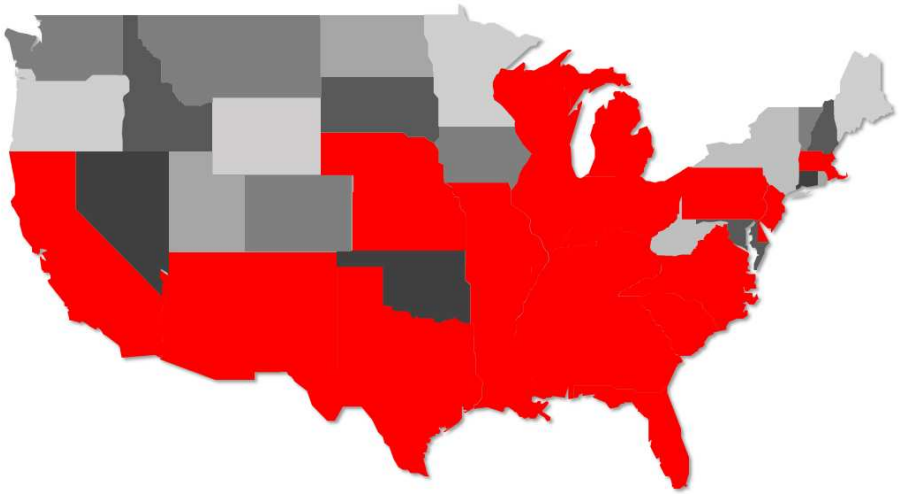

Figure 1-5: U.S. states with glyphosate-resistant *A. palmeri* as of 2018 (map made according to the database of (Heap, 2018))

REFERENCES

AgroNews. (2017). 2016 Analysis of new patterns and future trends in global agriculture, http://news.agropages.com/News/NewsDetail---21111.htm.

Ajanovic, A. (2011). Biofuels versus food production: does biofuels production increase food prices? *Energy* 36(4), 2070-2076.

Alexandratos, N., Bruinsma, J., Bödeker, G., Schmidhuber, J., Broca, S., Shetty, P., et al. (2006). World agriculture: Towards 2030/2050. Interim report. Prospects for food, nutrition, agriculture and major commodity groups.

Alibhai, M.F., and Stallings, W.C. (2001). Closing down on glyphosate inhibition—with a new structure for drug discovery. *Proc. Natl. Acad. Sci. USA* 98(6), 2944-2946.

Baerson, S.R., Rodriguez, D.J., Tran, M., Feng, Y., Biest, N.A., and Dill, G.M. (2002). Glyphosate-resistant goosegrass. Identification of a mutation in the target enzyme 5-enolpyruvylshikimate-3-phosphate synthase. *Plant Physiol.* 129(3), 1265-1275.

Barrett, S.H. (1983). Crop mimicry in weeds. *Econ. Bot.* 37(3), 255-282.

Baylis, A.D. (2000). Why glyphosate is a global herbicide: strengths, weaknesses and prospects. *Pest Manag. Sci.* 56(4), 299-308.

Beckie, H.J. (2011). Herbicide-resistant weed management: Focus on glyphosate. *Pest Manag. Sci.* 67(9), 1037-1048.

Bensch, C.N., Horak, M.J., and Peterson, D. (2003). Interference of redroot pigweed (*Amaranthus retroflexus*), Palmer amaranth (*A. palmeri)*, and common waterhemp (*A. rudis*) in soybean. *Weed Sci.* 51(1), 37-43.

Bradshaw, L.D., Padgette, S.R., Kimball, S.L., and Wells, B.H. (1997). Perspectives on glyphosate resistance. *Weed Technol.* 11(1), 189-198.

Burnside, O.C., Wilson, R.G., Weisberg, S., and Hubbard, K.G. (1996). Seed longevity of 41 weed species buried 17 years in eastern and western Nebraska. *Weed Sci.*, 74-86.

Busi, R., Neve, P., and Powles, S. (2013). Evolved polygenic herbicide resistance in *Lolium rigidum* by low-dose herbicide selection within standing genetic variation. *Evol. Appl.* 6(2), 231-242.

Calderbank, A., and Slade, P. (1976). Diquat and paraquat. *Herbicides* 2, 501-540.

Carvalho, F.P. (2006). Agriculture, pesticides, food security and food safety. *Environ. Sci. Policy* 9(7), 685-692.

Carvalho, F.P. (2017). Pesticides, environment, and food safety. *Food and Energy Security* 6(2), 48-60.

Cassidy, E.S., West, P.C., Gerber, J.S., and Foley, J.A. (2013). Redefining agricultural yields: from tonnes to people nourished per hectare. *Environ. Res. Lett.* 8(3), 034015.

Culpepper, A.S., Grey, T.L., Vencill, W.K., Kichler, J.M., Webster, T.M., Brown, S.M., et al. (2006). Glyphosate-resistant Palmer amaranth (*Amaranthus palmeri*) confirmed in Georgia. *Weed Sci.* 54(4), 620-626.

Delye, C. (2013). Unravelling the genetic bases of non-target-site-based resistance (NTSR) to herbicides: a major challenge for weed science in the forthcoming decade. *Pest Manag. Sci.* 69(2), 176-187.

Delye, C., Jasieniuk, M., and Le Corre, V. (2013). Deciphering the evolution of herbicide resistance in weeds. *Trends Genet.* 29(11), 649-658.

Duke, S.O. (2012). Why have no new herbicide modes of action appeared in recent years? *Pest Manag. Sci.* 68(4), 505-512.

Duke, S.O., and Powles, S.B. (2008). Glyphosate: a once-in-a-century herbicide. *Pest Management Science* 64(4), 319-325.

FAO (2014). *Arable land (% of land area)* [Online]. Food and Agriculture Organization. Available: https://data.worldbank.org/indicator/AG.LND.ARBL.ZS?end=2014&start=2014&view=map [Accessed Nov 16 2017].

Foley, J.A., Ramankutty, N., Brauman, K.A., Cassidy, E.S., Gerber, J.S., Johnston, M., et al. (2011). Solutions for a cultivated planet. *Nature* 478(7369)**,** 337-342.

Foyer, C., Descourvieres, P., and Kunert, K. (1994). Protection against oxygen radicals: an important defence mechanism studied in transgenic plants. *Plant, Cell Environ.* 17(5)**,** 507-523.

Franssen, A.S., Skinner, D.Z., Al-Khatib, K., Horak, M.J., and Kulakow, P.A. (2001). Interspecific hybridization and gene flow of ALS resistance in *Amaranthus* species. *Weed Sci.* 49(5)**,** 598-606.

Fried, G., Chauvel, B., Reynaud, P., and Sache, I. (2017). "Decreases in Crop Production by Non-native Weeds, Pests, and Pathogens," in *Impact of Biological Invasions on Ecosystem Services*. Springer), 83-101.

Gaines, T.A., Ward, S.M., Bukun, B., Preston, C., Leach, J.E., and Westra, P. (2012). Interspecific hybridization transfers a previously unknown glyphosate resistance mechanism in *Amaranthus* species. *Evol. Appl.* 5(1)**,** 29-38.

Gaines, T.A., Wright, A.A., Molin, W.T., Lorentz, L., Riggins, C.W., Tranel, P.J., et al. (2013). Identification of genetic elements associated with EPSPS gene amplification. *PLoS One* 8(6)**,** e65819. doi: 10.1371/journal.pone.0065819.

Gaines, T.A., Zhang, W., Wang, D., Bukun, B., Chisholm, S.T., Shaner, D.L., et al. (2010). Gene amplification confers glyphosate resistance in *Amaranthus palmeri*. *Proc. Nat. Acad. Sci. USA* 107(3)**,** 1029-1034.

Gardner, S.N., Gressel, J., and Mangel, M. (1998). A revolving dose strategy to delay the evolution of both quantitative vs major monogene resistances to pesticides and drugs. *Intl. J. Pest Manag.* 44(3)**,** 161-180.

Ge, X., d'Avignon, D.A., Ackerman, J.J., and Sammons, R.D. (2010). Rapid vacuolar sequestration: The horseweed glyphosate resistance mechanism. *Pest Manag. Sci.* 66(4)**,** 345-348.

Ge, X., d'Avignon, D.A., Ackerman, J.J., Collavo, A., Sattin, M., Ostrander, E.L., et al. (2012). Vacuolar glyphosate-sequestration correlates with glyphosate resistance in ryegrass (*Lolium* spp.) from Australia, South America, and Europe: a 31P NMR investigation. *J. Agric. Food Chem.* 60(5)**,** 1243-1250.

Gerland, P., Raftery, A.E., Ševčíková, H., Li, N., Gu, D., Spoorenberg, T., et al. (2014). World population stabilization unlikely this century. *Science* 346(6206)**,** 234-237.

GlobeNewswire. 2017. Global Herbicide Market 2016-2022: Market was $23.97 Billion in 2016 and is Estimated to Reach $34.10 Billion by 2022, https://globenewswire.com/news-release/2017/05/11/982371/0/en/Global-Herbicide-Market-2016-2022-Market-was-23-97-Billion-in-2016-and-is-Estimated-to-Reach-34-10-Billion-by-2022.html.

Hamill, A.S., Holt, J.S., and Mallory-Smith, C.A. (2004). Contributions of weed science to weed control and management. *Weed Technol.* 18(sp1)**,** 1563-1565.

Hausman, N.E., Singh, S., Tranel, P.J., Riechers, D.E., Kaundun, S.S., Polge, N.D., et al. (2011). Resistance to HPPD-inhibiting herbicides in a population of waterhemp (*Amaranthus tuberculatus*) from Illinois, United States. *Pest Manag. Sci.* 67(3)**,** 258-261.

Heap, I. (2014). "Herbicide resistant weeds," in *Integrated pest management*. Springer), 281-301.

Heap, I. (2018). *The International Survey of Herbicide Resistant Weeds. Online. Available:* www.weedscience.org [Online]. Available: www.weedscience.org [Accessed January 30, 2018].

Henchion, M., McCarthy, M., Resconi, V.C., and Troy, D. (2014). Meat consumption: Trends and quality matters. *Meat Sci.* 98(3)**,** 561-568.

Jasieniuk, M., Brûlé-Babel, A.L., and Morrison, I.N. (1996). The evolution and genetics of herbicide resistance in weeds. *Weed Sci.* 44(1)**,** 176-193. doi: 10.2307/4045802.

Jhala, A.J., Sandell, L.D., Rana, N., Kruger, G.R., and Knezevic, S.Z. (2014). Confirmation and control of triazine and 4-hydroxyphenylpyruvate dioxygenase-inhibiting herbicide-resistant Palmer amaranth (*Amaranthus palmeri*) in Nebraska. *Weed Technol.* 28(1)**,** 28-38.

Kartescz, J.T. (2014). *The Biota of North America Program (BONAP)* [Online]. Taxonomic Data Center. (http://www.bonap.net/tdc). Chapel Hill, N.C. Available: http://bonap.net/napa [Accessed 2017 July 28].

Kaundun, S.S., Hutchings, S.J., Dale, R.P., Howell, A., Morris, J.A., Kramer, V.C., et al. (2017). Mechanism of resistance to mesotrione in an *Amaranthus tuberculatus* population from Nebraska, USA. *PLoS One* 12(6)**,** 1-22. doi: 10.1371/journal.pone.0180095.

Kearney, J. (2010). Food consumption trends and drivers. *Philosophical Transactions of the Royal Society of London B: Biological Sciences* 365(1554)**,** 2793-2807.

Küpper, A., Borgato, E.A., Patterson, E.L., Netto, A.G., Nicolai, M., Carvalho, S.J.d., et al. (2017). Multiple resistance to glyphosate and acetolactate synthase inhibitors in Palmer amaranth (*Amaranthus palmeri*) identified in Brazil. *Weed Sci.* 65(3)**,** 317-326.

Lee, D.L., Knudsen, C.G., Michaely, W.J., Chin, H.L., Nguyen, N.H., Carter, C.G., et al. (1998). The structure–activity relationships of the triketone class of HPPD herbicides. *Pest Manag. Sci.* 54(4)**,** 377-384.

Leibtag, E. (2008). Corn prices near record high, but what about food costs? *Amber Waves* 6(1)**,** 10.

Lima, M.A., Gomez, L.D., Steele-King, C.G., Simister, R., Bernardinelli, O.D., Carvalho, M.A., et al. (2014). Evaluating the composition and processing potential of novel sources of Brazilian biomass for sustainable biorenewables production. *Biotechnology for Biofuels* 7(1)**,** 10.

Massinga, R.A., Currie, R.S., Horak, M.J., and Boyer Jr, J. (2001). Interference of Palmer amaranth in corn. *Weed Sci.* 49(2)**,** 202-208.

McMullan, P.M., and Green, J.M. (2011). Identification of a tall waterhemp (*Amaranthus tuberculatus*) biotype resistant to HPPD-inhibiting herbicides, atrazine, and thifensulfuron in Iowa. *Weed Technol.* 25(3)**,** 514-518.

Merriam-Webster (2004). *Merriam-Webster's collegiate dictionary.* Merriam-Webster.

Meyers, S.L., Jennings, K.M., Schultheis, J.R., and Monks, D.W. (2010). Interference of Palmer amaranth (*Amaranthus palmeri*) in sweetpotato. *Weed Sci.* 58(3)**,** 199-203.

Molin, W.T., Wright, A.A., Lawton-Rauh, A., and Saski, C.A. (2017). The unique genomic landscape surrounding the EPSPS gene in glyphosate resistant *Amaranthus palmeri*: A repetitive path to resistance. *BMC Genomics* 18(91)**,** doi: 10.1186/s12864-12016-13336-12864.

Mukherjee, S. (2017). *The gene: An intimate history.* Simon and Schuster.

Murphy, S.L., Xu, J., and Kochanek, K.D. (2013). Deaths: final data for 2010.

Nakka, S., Godar, A.S., Wani, P.S., Thompson, C.R., Peterson, D.E., Roelofs, J., et al. (2017). Physiological and molecular characterization of hydroxyphenylpyruvate dioxygenase (HPPD)-inhibitor resistance in Palmer amaranth (*Amaranthus palmeri* S. Wats.). *Front. Plant Sci.* 8**,** 555.

Neve, P., and Powles, S. (2005). Recurrent selection with reduced herbicide rates results in the rapid evolution of herbicide resistance in *Lolium rigidum*. *Theor. Appl. Genet.* 110(6)**,** 1154-1166. doi: 10.1007/s00122-005-1947-2.

Norris, S.R., Barrette, T.R., and DellaPenna, D. (1995). Genetic dissection of carotenoid synthesis in Arabidopsis defines plastoquinone as an essential component of phytoene desaturation. *The Plant Cell* 7(12)**,** 2139-2149.

Norsworthy, J.K., Griffith, G.M., Scott, R.C., Smith, K.L., and Oliver, L.R. (2008). Confirmation and control of glyphosate-resistant Palmer amaranth (*Amaranthus palmeri*) in Arkansas. *Weed Technol.* 22(1)**,** 108-113.

Norsworthy, J.K., Jha, P., Steckel, L.E., and Scott, R.C. (2010). Confirmation and control of glyphosate-resistant giant ragweed (*Ambrosia trifida*) in Tennessee. *Weed Technol.* 24(1)**,** 64-70.

Oerke, E.-C. (2006). Crop losses to pests. *J. Agri. Sci.* 144(01)**,** 31-43.

Oerke, E. (2002). Crop losses due to pests in major crops. *CAB International Crop Protection Compendium.*

Oliveira, M., Dayan, F., Gaines, T., Patterson, E., Jhala, A., and Knezevic, S. (2017). Reversing resistance to tembotrione in an *Amaranthus tuberculatus* (var. *rudis*) population from Nebraska, USA with cytochrome P450 inhibitors. *Pest Manag. Sci.***,** doi: 10.1002/ps.4697.

Owen, M.D. (2011). Weed resistance development and management in herbicide-tolerant crops: experiences from the USA. *Journal für Verbraucherschutz und Lebensmittelsicherheit* 6(1)**,** 85-89.

Perez-Jones, A., Martins, B.A., and Mallory-Smith, C.A. (2010). Hybridization in a commercial production field between imidazolinone-resistant winter wheat and jointed goatgrass (*Aegilops cylindrica*) results in pollen-mediated gene flow of Imi1. *Weed Sci.* 58(4)**,** 395-401.
Pimentel, D., Zuniga, R., and Morrison, D. (2005). Update on the environmental and economic costs associated with alien-invasive species in the United States. *Ecol. Econom.* 52(3)**,** 273-288.
Pollegioni, L., Schonbrunn, E., and Siehl, D. (2011). Molecular basis of glyphosate resistance–different approaches through protein engineering. *The FEBS Journal* 278(16)**,** 2753-2766.
Powles, S.B., Lorraine-Colwill, D.F., Dellow, J.J., and Preston, C. (1998). Evolved resistance to glyphosate in rigid ryegrass (*Lolium rigidum*) in Australia. *Weed Sci.***,** 604-607.
Powles, S.B., and Shaner, D.L. (2001). *Herbicide resistance and world grains.* Crc Press.
Pratley, J., Urwin, N., Stanton, R., Baines, P., Broster, J., Cullis, K., et al. (1999). Resistance to glyphosate in *Lolium rigidum.* I. Bioevaluation. *Weed Sci.***,** 405-411.
Preston, C., Tardif, F.J., Christopher, J.T., and Powles, S.B. (1996). Multiple resistance to dissimilar herbicide chemistries in a biotype of *Lolium rigidum* due to enhanced activity of several herbicide degrading enzymes. *Pest Biochem Physiol* 54(2)**,** 123-134.
Pretty, J., Sutherland, W.J., Ashby, J., Auburn, J., Baulcombe, D., Bell, M., et al. (2010). The top 100 questions of importance to the future of global agriculture. *International Journal of Agricultural Sustainability* 8(4)**,** 219-236.
Rayburn, A.L., McCloskey, R., Tatum, T.C., Bollero, G.A., Jeschke, M.R., and Tranel, P.J. (2005). Genome size analysis of weedy species. *Crop Sci.* 45(6)**,** 2557-2562.
Renton, M., Diggle, A., Manalil, S., and Powles, S. (2011). Does cutting herbicide rates threaten the sustainability of weed management in cropping systems? *J. Theor. Biol.* 283(1)**,** 14-27.
Rowland, M.W., Murray, D.S., and Verhalen, L.M. (1999). Full-season Palmer amaranth (*Amaranthus palmeri*) interference with cotton (*Gossypium hirsutum*). *Weed Sci.***,** 305-309.
Ruiz-Sola, M.Á., and Rodríguez-Concepción, M. (2012). Carotenoid biosynthesis in Arabidopsis: a colorful pathway. *The Arabidopsis Book* 10**,** 1-28.
Ryan, G. (1970). Resistance of common groundsel to simazine and atrazine. *Weed Sci.* 18(5)**,** 614-616.
Sammons, R.D., and Gaines, T.A. (2014). Glyphosate resistance: State of knowledge. *Pest Manag. Sci.* 70(9)**,** 1367-1377. doi: 10.1002/ps.3743.
Sauer, J. (1957). Recent migration and evolution of the dioecious amaranths. *Evol.* 11(1)**,** 11-31.
Schulte, W., and Köcher, H. (2009). Tembotrione and combination partner isoxadifen-ethyl–mode of herbicidal action. *Bayer CropSci. J.* 62(1)**,** 35-52.
Schultz, J.L., Chatham, L.A., Riggins, C.W., Tranel, P.J., and Bradley, K.W. (2015). Distribution of herbicide resistances and molecular mechanisms conferring resistance in Missouri waterhemp (*Amaranthus rudis* Sauer) populations. *Weed Sci.* 63(1)**,** 336-345.
Scott, K., and Putwain, P. (1981). Maternal inheritance of simazine resistance in a population of *Senecio vulgaris*. *Weed Res.* 21(3-4)**,** 137-140.
Scott, R., Steckel, L., Smith, K., Mueller, S., Oliver, L., and Norsworthy, J. (Year). "Glyphosate-resistant Palmer amaranth in Tennessee and Arkansas", in: *Proc. South. Weed. Sci. Soc.*), 226.
Sellers, B.A., Smeda, R.J., Johnson, W.G., Kendig, J.A., and Ellersieck, M.R. (2003). Comparative growth of six *Amaranthus* species in Missouri. *Weed Sci.* 51(3)**,** 329-333.
Shaner, D. (2014). Herbicide handbook. *Weed Science Society of America, Champaign, IL***,** 315.
Shaner, D.L. (2009). Role of translocation as a mechanism of resistance to glyphosate. *Weed Sci.* 57(1)**,** 118-123.
Shaner, D.L., Nadler-Hassar, T., Henry, W.B., and Koger, C.H. (2005). A rapid *in vivo* shikimate accumulation assay with excised leaf discs. *Weed Sci.* 53(6)**,** 769-774.
Smith, D.T., Baker, R.V., and Steele, G.L. (2000). Palmer amaranth (*Amaranthus palmeri*) impacts on yield, harvesting, and ginning in dryland cotton (*Gossypium hirsutum*). *Weed Technol.* 14(1)**,** 122-126.
Smith, P., and Gregory, P.J. (2013). Climate change and sustainable food production. *Proc. Nutr. Soc.* 72(1)**,** 21-28.

Soltani, N., Dille, J.A., Burke, I.C., Everman, W.J., VanGessel, M.J., Davis, V.M., et al. (2016). Potential corn yield losses from weeds in North America. *Weed Technol.* 30(4)**,** 979-984.
Soltani, N., Dille, J.A., Burke, I.C., Everman, W.J., VanGessel, M.J., Davis, V.M., et al. (2017). Perspectives on potential soybean yield losses from weeds in North America. *Weed Technol.* 31(1)**,** 148-154.
Sosnoskie, L.M., Webster, T.M., Kichler, J.M., MacRae, A.W., Grey, T.L., and Culpepper, A.S. (2012). Pollen-mediated dispersal of glyphosate-resistance in Palmer amaranth under field conditions. *Weed Sci.* 60(3)**,** 366-373.
Steckel, L.E., Main, C.L., Ellis, A.T., and Mueller, T.C. (2008). Palmer amaranth (*Amaranthus palmeri*) in Tennessee has low level glyphosate resistance. *Weed Technol.* 22(1)**,** 119-123.
Tomlinson, I. (2013). Doubling food production to feed the 9 billion: a critical perspective on a key discourse of food security in the UK. *Journal of Rural Studies* 29**,** 81-90.
USDA. 2017. Recent trends in GE adoption, https://www.ers.usda.gov/data-products/adoption-of-genetically-engineered-crops-in-the-us/recent-trends-in-ge-adoption.aspx.
Vencill, W.K., Nichols, R.L., Webster, T.M., Soteres, J.K., Mallory-Smith, C., Burgos, N.R., et al. (2012). Herbicide resistance: Toward an understanding of resistance development and the impact of herbicide-resistant crops.
Wang, D.-W., Lin, H.-Y., Cao, R.-J., Chen, T., Wu, F.-X., Hao, G.-F., et al. (2015). Synthesis and herbicidal activity of triketone–quinoline hybrids as novel 4-hydroxyphenylpyruvate dioxygenase inhibitors. *J. Agric. Food Chem.* 63(23)**,** 5587-5596.
Wang, J.-L., Klessig, D.F., and Berry, J.O. (1992). Regulation of C4 Gene Expression in Developing Amaranth Leaves. *The Plant Cell* 4(2)**,** 173-184.
Ward, S.M., Webster, T.M., and Steckel, L.E. (2013). Palmer amaranth (*Amaranthus palmeri*): A review. *Weed Technol.* 27(1)**,** 12-27.
Webster, T.M., and Nichols, R.L. (2012). Changes in the prevalence of weed species in the major agronomic crops of the Southern United States: 1994/1995 to 2008/2009. *Weed Sci.* 60(2)**,** 145-157.
Worldometers (2017). *World Population: Past, Present, and Future* [Online]. Available: http://www.worldometers.info/world-population/#pastfuture [Accessed Nov 16 2017].
WSSA. 2016. WSSA Survey Ranks Palmer Amaranth as the Most Troublesome Weed in the U.S., Galium as the Most Troublesome in Canada. *Weed Science Society of America* [Online].
Yu, Q., Jalaludin, A., Han, H., Chen, M., Sammons, R.D., and Powles, S.B. (2015). Evolution of a double amino acid substitution in the EPSP synthase in *Eleusine indica* conferring high level glyphosate resistance. *Plant Physiol.***,** DOI: https://doi.org/10.1104/pp.1115.00146.
Yuan, J.S., Tranel, P.J., and Stewart, C.N. (2007). Non-target-site herbicide resistance: A family business. *Trends Plant Sci.* 12(1)**,** 6-13.
Zimdahl, R.L. (2013). *Fundamentals of Weed Science.* Academic Press.

2. TEMBOTRIONE DETOXIFICATION IN HPPD-INHIBITOR RESISTANT PALMER AMARANTH (*AMARANTHUS PALMERI S. WATS*)[1]

INTRODUCTION

Due to its rapid growth rate, high fecundity, extended emergence period, and ability to tolerate adverse conditions (Chahal et al., 2015). In recent years Palmer amaranth (*Amaranthus palmeri* S. Wats.) has become one of the most difficult weeds to control in the United States in key crops including soybean, corn, and cotton (Webster and Nichols, 2012; Ward et al., 2013; Norsworthy et al., 2014). Furthermore, the cross-pollinating species has evolved resistance to multiple herbicides representing several modes of action, including microtubule-, photosystem II (PS II)-, acetolactate synthase (ALS)-, 5-enol-pyruvylshikimate-3-phosphate synthase (EPSPS)-, protoporphyrinogen oxidase (PPO) and 4-hydroxyphenylpyruvate dioxygenase (HPPD)-inhibitors with some populations resistant to herbicides spanning three different modes of action (Chahal et al., 2015; Nakka et al., 2017; Schwartz-Lazaro et al., 2017; Heap, 2018). The increasing frequency of glyphosate-resistant populations and the dwindling options of still effective modes of action increase the importance of HPPD-inhibitors in herbicide programs (Meyer et al., 2015).

The HPPD-inhibitor tembotrione (triketone chemistry), a post-emergence herbicide (Santel, 2009), inhibits the oxidative decarboxylation and rearrangement of 4-hydroxyphenylpyruvate (HPP) to homogentisate (HGA). This in turn inhibits the catabolism of tyrosine and results in a deficiency of plastoquinone and α-tocopherols (Lee et al., 1998). The end-products act as either co-factors in photosynthesis and carotenoid biosynthesis (Norris et al., 1995) or as antioxidants protecting membranes against photooxidative stress from reactive oxygen species (Foyer et al., 1994; Ruiz-Sola and Rodríguez-Concepción, 2012). When the production of plastoquinone and tocopherol is inhibited, radicals destroy

[1] Anita Küpper, Falco Peter, Peter Zöllner, Lothar Lorentz, Patrick J. Tranel, Roland Beffa, Todd A. Gaines

the UV-protecting chlorophyll shield and lead to bleaching followed by foliar necrosis and plant death (Santel, 2009; Schulte and Köcher, 2009; van Almsick, 2009; Ahrens et al., 2013).

The first triketone herbicide sulcotrione was commercialized in 1993, followed by mesotrione in 2001 and tembotrione in 2007 (Beaudegnies et al., 2009; Ahrens et al., 2013). In 2009 the first case of *A. palmeri* resistance to HPPD-inhibitors (mesotrione, topramezone, and tembotrione) was reported from a corn and sorghum field in Kansas. The reported biotype was also resistant to ALS and PS II inhibitors (Nakka et al., 2017). Additional cases of HPPD-inhibitor resistance in the same species were later reported from Nebraska in 2011 and 2014 (Jhala et al., 2014; Heap, 2018) with the latter biotype also resistant to ALS and PS II inhibitors (Jhala et al., 2014; Nakka et al., 2017). Resistance to HPPD inhibitors has been reported in common waterhemp (*A. tuberculatus* var. *rudis*) from Illinois (Hausman et al., 2011), Iowa (McMullan and Green, 2011), Nebraska (Nakka et al., 2017), and Missouri (Schultz et al., 2015). The population from Illinois is resistant to herbicides spanning five different modes of action (Evans, 2016).

The multiple resistant *A. palmeri* population from Kansas was 10 to 18-fold resistant to mesotrione (based on GR_{50} values) compared to a susceptible population from Mississippi and another one from Kansas (Nakka et al., 2017). Both target-site and non-target-site-based mechanisms of resistance were identified, including enhanced metabolism, and a 4 to 12-fold increase in *HPPD* transcript levels linked with an increase in HPPD protein in the resistant plants (Nakka et al., 2017). Enhanced metabolism but no change in *HPPD* expression was also shown in the HPPD-inhibitor resistant *A. tuberculatus* population from Illinois when compared to a susceptible line (Kaundun et al., 2017). Non-target site resistance (NTSR) via enhanced metabolism in weeds is associated with CYPs (Yun et al., 2005; Powles and Yu, 2010; Gaines et al., 2014; Han et al., 2014; Iwakami et al., 2014a; Yu and Powles, 2014; Busi et al., 2017a), glutathione S-transferases (GSTs) (Cummins et al., 2013; Busi et al., 2017b), glycosyl transferases (GTs) (Brazier et al., 2002), aryl acylamidases (Leah et al., 1994), and ABC transporters (Yuan et al., 2007; Yang et al., 2016; Duhoux et al., 2017).

The objective of this study was to characterize tembotrione resistance in resistant and susceptible *A. palmeri* populations from Nebraska, including tembotrione dose response, absorption, translocation, metabolism, *HPPD* gene copy number, and *HPPD* gene expression. Furthermore, environmental conditions and developmental stages of *A. palmeri* were investigated to identify optimal experimental parameters to measure differences in tembotrione metabolism between resistant and susceptible individuals for resistance diagnostic assays.

MATERIALS AND METHODS

Plant material

The resistant (NER) and susceptible (NES) *A. palmeri* populations investigated in this study were both collected from fields in Shickley, Nebraska in 2011, approximately 1.8 km apart from each other. NER was collected in a seed corn production field with a history of atrazine and HPPD-inhibitor use (Jhala et al., 2014). NER was not controlled by atrazine, or by the HPPD inhibitors mesotrione, tembotrione, and topramezone (Jhala et al., 2014). Two previous studies used HPPD-resistant *A. palmeri* collected from the same field but NER was collected at a different time (Jhala et al., 2014; Nakka et al., 2017). For all following experiments the seed was sown in plant tissue culture containers (PlantCon, MP Biomedicals, LLC, Santa Ana, CA) containing 0.7% agar type A (Sigma-Aldrich, St. Louis, MO), kept in the dark for two d at 4 °C, and then germinated in a growth chamber at 28 °C and 16/8h light/dark conditions at 400 µmol m^{-2} s^{-1} and 70% humidity. Once at the cotyledon stage, single seedlings were transplanted into 4 cm Fertil pots (Jiffy, Chelsea, MI) containing peat/loam 1:1 soil mixture and kept in the greenhouse at 30/25°C 17/7h light/dark conditions with a light intensity of 220 µE m^{-2} s^{-1} (Son-T AGRO, Philips, Amsterdam, Netherlands) and 60% humidity. Watering was performed twice daily.

Dose response

A greenhouse dose-response study was conducted to quantify the level of tembotrione resistance in NER compared to NES. The experimental setup contained five individuals per replicate in separate pots

with a total of four replicates per dose and population. Except for the non-treated control, the plants were treated at the four true-leaf stage with 12.5, 25, 50, 75, 100, 200, 300, and 400 g a.i. ha^{-1} tembotrione (Laudis, 419 g a.i. L^{-1}, Bayer, Leverkusen, Germany) together with 2200 g a.i. ha^{-1} of the wetting agent Mero (Bayer, Leverkusen, Germany) and 170 g a.i. ha^{-1} ammonium sulfate using a stationary research sprayer (Höchst AG, Höchst, Germany) calibrated to deliver a spray volume of 300 L ha^{-1}. Survival and herbicide injury were recorded 35 d after application. The dose-response experiment was not repeated.

Tembotrione metabolism, absorption and translocation

Metabolism of tembotrione was measured in NER and NES over time in eight individuals per population and treatment. The application was performed on the two youngest expanded leaves of individuals at the four-leaf stage with a total of ten 1 µL droplets (5 µL per leaf) of ^{14}C-tembotrione (Bayer, Leverkusen, Germany) in a 0.3% v/v Mero solution (Bayer, Leverkusen, Germany) with 3.3 kBq or 200,000 dpm μL^{-1}, corresponding to 0.762 µg μL^{-1} of tembotrione. The treated plants were kept in a growth chamber at 28°C under continuous light conditions with a light intensity of 400 µmol m^{-2} s^{-1} and 70% humidity. For the time course experiment the plants were harvested 1, 3, 6, 12, 24 and 48 h after treatment (HAT).

At harvest, the above ground tissue was washed in 80% acetone three times to remove any non-absorbed ^{14}C-tembotrione, and then disrupted in 600 µL methanol with 5 mm stainless steel beads at 30 Hz for 10 min. The homogenate was centrifuged at 6000xg for 10 min. The residue was re-extracted with 600 µL methanol followed by a final extraction with 600 µL 90% acetonitrile. All solvents used were HPLC-grade (Sigma-Aldrich, Steinheim, Germany, ≥ 99.9 % HPLC grade). The pooled supernatant was evaporated under continuous air flow at 55 °C and then re-suspended in 200 µL 90% acetonitrile using a shaker and ultrasonic bath and then filtered through a 0.45 µm low-binding hydrophilic PTFE mesh for 10 min at 2200xg in the centrifuge. The recovered radioactivity in the filtrate was 92% of total applied on average. A non-treated control sample, spiked with ^{14}C-tembotrione just prior to extraction, was also included. Separation and HPLC identification of the parent tembotrione herbicide and its metabolites

were performed on a reverse-phase HPLC (LC Net II/ADC with PU-980 pump unit, LC-980-02 gradient unit and CO-2060 Plus column thermostat, Jasco, Oklahoma City, OK). Chromatographic separation was achieved with a 150 x 2.0 or 3.0 mm I.D: Luna C18(2) column with a particle size of 3µm (Phenonemex, Aschaffenburg, Germany) at a flow rate of 0.5 mL min^{-1}. The mobile phases consisted of 0.05% phosphoric acid (A) and acetonitrile:0.2% formic acid (B) and were run at a 60 min linear gradient from 0 to 60% solvent B, followed by a 1 min linear gradient from 60 to 90% solvent B, plateauing for 4 min. The column was then flushed with 100% solvent A for 7 min. An in-line radio flow detector (Flowstar LB 513 with YG40-S6M detector cell, Berthold Technologies, Bad Wildbad, Germany) was used for radioactive peak determination. The parent herbicide ^{14}C-tembotrione and a non-radiolabeled tembotrione reference standard were both injected. The latter was detected via an inline UV-visible spectrophotometer (MD-910, Jasco, Oklahoma City, OK) to establish retention times. All experiments were conducted twice. Tembotrione absorption and translocation were measured as described in Supporting Information methods.

Tembotrione metabolite identification

In order to identify the tembotrione metabolites, four resistant and four susceptible plants, extracted 48 HAT, were analyzed using LC-MS. LC-MS analysis of all these samples was performed on a mass spectrometer (Q-TOF premier, Waters, Manchester, United Kingdom) connected to an HPLC (2795 HPLC system, Waters, Milford, USA) via a radioactivity detector (Berthold Technologies, Bad Wildbad, Germany) and an electrospray interface. The radioactivity detector was run at 2,250 V. The mass spectrophotometer was operated in positive and negative ion modes with capillary voltages of 1.5 and 2.3 kV, respectively. The ion source block and desolvation gas temperature were set at 80 and 450 °C, respectively, and the desolvation gas was set to a flow rate of 450 L/h. The cone voltage was set at 25 V in positive and negative ion mode and the cone gas flow rate was 25 L/h. Mass spectra were recorded within a range of 100 to 1000 u at a scan time of 0.2 sec and an inter scan time of 0.02 sec. Fifty µL of each sample was injected. The flow rate was 0.25 mL min^{-1} (2 mm I.D.) and 0. 50 mL min^{-1} (3 mm I.D.)

at a column temperature of 40 °C. Mixtures of water (A) and acetonitrile (B), each with 0.05 % (v/v) formic acid (Sigma-Aldrich, Steinheim, Germany, ≥ 98% p.a. grade), were used as mobile phases. All solvents used were HPLC-grade (Sigma-Aldrich, Steinheim, Germany, ≥ 99.9 % HPLC grade). The column and gradient protocol used were the same as described for the metabolism experiment. Instrument control and data evaluation were done with MassLynx® 4.1 (Waters, Manchester, United Kingdom). Compound identities were confirmed by high resolution mass spectrometry (determination of the elemental composition of molecular ions and fragment ions) in the MS and MS/MS mode (product ion scan).

Environmental conditions and developmental stages

Metabolism of tembotrione under different environmental conditions and developmental stages was measured in NER and NES in eight individuals per population and treatment. Application of ^{14}C-tembotrione was performed as mentioned in 2.4. The treated plants were kept in a growth chamber with a light intensity of 400 µmol m^{-2} s^{-1} and 70% humidity. The experiment on different environmental conditions used continuous light at 18 or 28°C (CL18/CL28) and 16/8h light/dark at 28°C (LD28) at the four-leaf stage (4L). For different developmental stages, plants were treated at the two- (2L), four- (4L), or eight leaf stage (10 cm tall, 8L) and kept at 16/8h light/dark and 28°C after treatment. The plants were harvested 16 HAT. HPLC analysis was performed as mentioned in 2.3.

Statistical analysis

The statistical program ‘R’ and the package ‘drc’ were used to calculate the three parameter sigmoidal log-logistic dose-response models, lethal dose to 50% (LD_{50}), lethal dose to 90% (L_{90}), and effected dose causing 50% visual injury (ED_{50}) values, as well as upper and lower limits (Ritz and Streibig, 2005; Knezevic et al., 2007). The resistance factor (RF) of the populations was calculated based on the quotient between the LD_{50}/ED_{50} values of NER and NES. Statistical tests for absorption, translocation, and metabolism data were done using two-way ANOVA in R followed by Tukey’s HSD

test for pairwise comparisons. The tembotrione and metabolite curves were fitted using SigmaPlot. Due to the non-monotonic curves of the non-linear logistic regression, the dose-response variable *e* was not compared between NER and NES. All eight NES individuals tested were used in analyses. Since NER is a segregating population containing resistant and susceptible individuals, out of the eight individuals examined per time point, only the three individuals that metabolized tembotrione the fastest were used for all analyses.

RESULTS

Dose response

A dose-response experiment was conducted with NER and NES populations from Nebraska to determine the level of resistance to tembotrione. Two d after treatment (DAT), NES expressed bleaching symptoms at the apical meristem and young leaves followed by bleaching and necrosis of all leaves six to nine d later. Often NER initially expressed a similar phenotype with bleaching of the youngest leaves at the area closest to the petiole while the area towards the leaf tip stayed either green or showed a patchy green pattern. Older leaves remained visually unaffected by the herbicide. Highly resistant plants were completely unaffected by the application. Over the course of the following 14 d, new green leaves grew from the meristems in the NER.

The LD_{50} values for NER and NES were 83.0 and 24.9 g a.i. ha^{-1} respectively, resulting in a resistance factor of 3.3 (Figure 2-1). Fifty percent injury (ED_{50}) was achieved at 73.4 and 25.0 g a.i. ha^{-1} for NER and NES, respectively (Appendix A, Figure 7-1). The NER population is still highly segregating, resulting in a population LD_{50} lower than the typical commercial tembotrione use rate (91 g a.i. ha^{-1}). However, NER would not be sufficiently controlled by the labeled rate of tembotrione in the field, as LD_{90} values were 329.0 and 38.9 g a.i. ha^{-1} for NER and NES, respectively. Both populations were controlled completely at 400 g a.i. ha^{-1} tembotrione (Figure 2-1).

Tembotrione metabolism, absorption and translocation

Due to results confirming increased mesotrione metabolism in *A. palmeri* populations from Nebraska and Kansas, it was hypothesized that tembotrione metabolism would be greater in NER than NES (Nakka et al., 2017). Even though phenotypic differences were not visible in NER and NES within the first 24 HAT, significant differences in ^{14}C-tembotrione metabolism were observed. Five major peaks were detected by HPLC forming an average of 89.9% (area) of the total radioactivity (64 - 99% at 1-3 HAT and > 75% for 6 HAT onwards). The standard ^{14}C-tembotrione resolved at a peak retention time of 50.8 min with reversed-phase HPLC. Its major metabolites resolved at retention times of 34.6 (M1), 35.7 (M2), 41.8 (M3), 43.9 (M4) and 53.0 (M5) min (Figure 2-2). M1 elutes as a single peak but occasionally exhibited a small shoulder on the tail end. The nature of this shoulder has not been elucidated and was integrated as part of the M1 peak area. Metabolites M3 and M4 occurred as double peaks with a smaller peak to the left side of the main peak but were counted as one peak area as well.

No qualitative differences were found in metabolite profiles between NER and NES. Significant differences in the rate of tembotrione metabolism between NER and NES were observed as early as 6 HAT ($P < 0.0001$) when 72% of parent ^{14}C-tembotrione was still detected in the NES while only 41% of the parent compound was detected in the NER. Significant differences were observed until 24 HAT ($P < 0.05$, Figure 2-3A). The half-life (T_{50}), the time for 50% of the parent compound to be degraded, was 7.3 and 17.1 h for NER and NES, respectively, confirming that NER individuals were able to metabolize tembotrione 2.3 times faster than NES. These findings are similar to T_{50} values found in a mesotrione-resistant *A. palmeri* population from Kansas which was able to metabolize mesotrione 2.5 times faster than a mesotrione-susceptible population from Mississippi (T_{50}: 5.9 and 14.6 h, respectively) (Nakka et al., 2017).

NER and NES production of M1, 2 and 5 (Figure 2-3B, C and F) were similar at each time point. However, NER formed M3 significantly faster 6 and 12 HAT ($P < 0.01$) than NES (Figure 2-3D). NES formed M4 significantly faster 48 HAT ($P < 0.01$) than NER (Figure 2-3E). The T_{50}, in this case the time it takes until 50% of the maximum production of the metabolite is reached, was 4.9 and 11.9 h for M3 and

5 and 7 h for M4 for NER and NES, respectively. The data indicate that NER accumulate more M3 and less M4 than NES within the first 48 HAT.

No significant differences for ^{14}C-tembotrione absorption or translocation were found but a trend towards reduced translocation in NER at 24 HAT compared to NES was observed (Appendix A, Figure 7-2 and Figure 7-3).

Tembotrione metabolite identification by LC-MS

The masses of all metabolites identified in this study are shown in Table 2-2. Metabolites M3 and M4, despite having two separate peaks on the HPLC, had the same mass, suggesting that they were isomers with the hydroxyl group possibly attached at different locations. When the peak areas of M3 and M4 were combined, NER were still faster in producing this metabolite at 6 and 12 HAT ($P < 0.05$) than NES (Figure 2-5). A reduced form of M7 was identified, which exhibits an additional double bond due to the loss of two hydrogen atoms (M8).

The data suggest that tembotrione could be metabolized in two different ways, either cleavage of the cyclohexane structure (M2) followed by oxidation and methylation of the cleaved site (M6), or by hydroxylation (M3/M4). After hydroxylation, a second hydroxy group (M9) or a mannose group (M7/M8) gets added to the hydroxylated molecule (M3/M4). The mannose group is then open for acetylation (M1) (Figure 2-4).

Environmental conditions and developmental stages

The following experiments were conducted to find the conditions under which the detectable differences in tembotrione metabolism between metabolic HPPD-resistant and -susceptible *A. palmeri* individuals were the largest, so optimal conditions could be utilized in diagnostic testing. When both populations of *A. palmeri* were treated at the four-leaf stage (4L) and kept at continuous light at 18 or 28°C (CL18/CL28) or under a 16/8 h light/dark at 28°C (LD28), the parent compound tembotrione found 16 HAT was significantly lower in NER compared to NES under all of the conditions, but with the most

significant difference at 4L CL28 ($P < 0.0001$). When comparing within a population, colder conditions significantly slowed down tembotrione metabolism ($P < 0.0001$). When comparing NER and NES at the two- (2L), four- (4L), and eight-leaf stage (8L) kept at LD28, significant differences were observed at the 4L stage only ($P < 0.05$, Figure 2-6).

HPPD gene copy number and expression

The methods for HPPD gene copy number and expression are in Supporting Information. Genomic *HPPD* copy numbers ranged from 1.0 to 1.1 for *HPPD:β-tubulin* and *HPPD:ALS* and from 1.3 to 1.6 for *HPPD:CPS* for both NER and NES individuals (Appendix A, Figure 7-4), confirming that NER did not show increased *HPPD* gene copy numbers when compared to NES. Relative gene expression of *HPPD* was not significantly different between NER compared to NES prior to tembotrione treatment (Appendix A, Figure 7-5A/B). When NER was treated with tembotrione, no differences or trends in *HPPD* transcription were observed 24 HAT compared to treated NES (Appendix A Figure 7-5C/D).

DISCUSSION

Under typical environmental conditions tembotrione can be found in its ionic form which is non-volatile, highly soluble, and stable in water (Dumas et al., 2016). The structure of the tembotrione molecule and other benzoylcyclohexanediones can be divided into a benzoyl and dione (cyclohexanedione) moiety, which have independent roles in the activity of the herbicide (Lee et al., 1998; Mitchell et al., 2001; Beaudegnies et al., 2009). The β-diketone moiety, which all triketones share, mimics the α-keto acid chain of HPP (Matringe et al., 2005). An *ortho*-chloro substituent on the phenyl ring (benzoyl moiety) is crucial for herbicidal activity. Higher herbicidal activity and binding affinity to the HPPD enzyme is strongly correlated to high electron deficiency of the phenyl ring caused by electron-withdrawing substituents at the 2- and 4-positions. The resulting acidification of the molecule (Lee et al., 1998; Beaudegnies et al., 2009) facilitates uptake to plant cells (Santel, 2009). Additions to the molecule

such as methyl groups produce better herbicidal activity but also decrease corn selectivity and increase soil residual time (Mitchell et al., 2001). If dione substituents are removed, and therefore the sites for hydroxylation are increased, this opens up sites for plant metabolism and increases the ability of maize to metabolize the compound (Mitchell et al., 2001; Beaudegnies et al., 2009). Tembotrione does not have any substitutions on the dione moiety, indicating that it may be more amenable to plant metabolism and, therefore, enhanced metabolism to occur as a resistance mechanism in weeds.

The main route of metabolism of the benzoylcyclohexanediones in plants is the monohydroxylation of the 4-position of the cyclohexanedione, or alternatively the 6-position in case the 4-position is blocked (Mitchell et al., 2001; Beaudegnies et al., 2009). Monohydroxylation of tembotrione has previously been observed in plants and mammals (AE 1444744) (Kelly et al., 2009) as well as during ozonation in water (Tawk et al., 2017). Kelly *et al.* (2009) identified both a 4-hydroxy and a 5-hydroxy metabolite, with the latter found in animals only (Kelly et al., 2009). We identified a hydroxy metabolite for both peaks M3 and M4, suggesting that two isomers of the molecule exist. Similar observations were made for a hydroxylated phototransformation product of the triketone herbicide sulcotrione which showed as three peaks on HPLC. Mass spectrometry showed that the product identified had gained an oxygen atom, suggesting that the three peaks represented three isomers of the hydroxylated form of sulcotrione (ter Halle et al., 2006).

Hydroxylation (M3) took place at a higher rate in NER compared to NES, as has been shown in mesotrione-resistant *A. tuberculatus* from Illinois and Nebraska (Ma et al., 2013; Kaundun et al., 2017). Tembotrione hydroxylation takes place faster than hydroxylation of mesotrione, which could be correlated to tembotrione being absorbed more than twice as fast as mesotrione (Kaundun et al., 2017). The process is presumed to be catalyzed by CYPs (Ma et al., 2013; Yu and Powles, 2014), the mechanism seen in triketone corn selectivity (Mitchell et al., 2001; Williams II and Pataky, 2008), where it provides tembotrione with a half-life of less than a day (Kelly et al., 2009). The CYP gene *Nsf1/Ben1* was identified as the single major resistance locus in corn (Kang, 1993; Nordby et al., 2008; Williams II and Pataky, 2008).

Results from this study suggest that an increase in CYP expression and activity are responsible for the rapid production of M3 in NER. Since the production of M3/M4 declined over time (Figure 2-3D/E), the compounds may be intermediate metabolites. Because the half-life of tembotrione is relatively short in NES, the relatively faster tembotrione metabolism in NER may be sufficient to confer survival. Kaundun *et al.* (2017) hypothesized that the resistance mechanisms for mesotrione and tembotrione were the same because both herbicides are prone to increased detoxification by 4-hydroxylation (Kaundun et al., 2017). In HPPD-inhibitor resistant *A. tuberculatus* from Nebraska susceptibility to mesotrione was restored by the cytochrome P450 monooxygenase inhibitor amitrole but not by malathion, while tembotrione resistance was reversed by malathion, amitrole and piperonyl butoxide. This suggests that different CYPs encoded by different genes which are differently susceptible to CYP inhibitors contribute to HPPD herbicide enhanced metabolism (Preston et al., 1996; Oliveira et al., 2017). Inheritance of mesotrione resistance is multi-genic in *A. tuberculatus* as well (Huffman et al., 2015). It is likely that different CYP genes capable of metabolizing HPPD herbicides may evolve in different combinations across populations and species (Powles and Yu, 2010).

As a downstream metabolite of M3/M4, the dihydroxy M9 has two hydroxy groups added most likely at the 4,6-position. The compound was previously identified (AE 1417268) as a major metabolite in plants (Kelly et al., 2009; Leake et al., 2009). Further detoxification in the form of conjugation was observed in NER by the addition of the hexose mannose in M7/M8, suggesting that *O*-glycosyl transferase (GT) plays a key role (Coutinho et al., 2003). None of the metabolites found were conjugated with glutathione making GSTs unlikely to play a role in detoxification of tembotrione in NER. Secondary conjugation was observed in NER in the form of acetylation in M1, most likely caused by an acetyltransferase. Figure 2-3B shows a time-dependent plateau of M1, suggesting that this compound might be an end-product in the tembotrione detoxification process.

A second major degradation pathway seems to exist featuring M2, a metabolite having undergone oxidative cleavage. M2 has been previously identified as a relatively persistent benzoic acid derivative (TCMBA (Calvayrac et al., 2013) or AE 0456148 (Kelly et al., 2009; Leake et al., 2009)) formed by the

splitting of 1,3-cyclohexanedione (CHD) from the benzoic ring. The compound is part of the tembotrione detoxification pathway in soil (Tarara et al., 2009), photolysis (Calvayrac et al., 2013), as well as plant metabolism (Leake et al., 2009). Similar benzoic acid derivatives are known from the degradation of sulcotrione (CMBA) (ter Halle et al., 2006; Chaabane et al., 2007; Chaabane et al., 2008) and mesotrione (MNBA) (Alferness and Wiebe, 2002). Previous studies identified further TCMBA breakdown products such as carboxy benzylic alcohol (AE 1392936) (Leake et al., 2009) and (methylated) phenol forms (Tarara et al., 2009), none of which were identified in this study. Instead, the addition of an acetyl group is suggested as a down-stream metabolite (M6) in the plant detoxification pathway. Aside from the metabolites mentioned above, the metabolite M5, a reduced form of the parent compound, was identified. Even though a major metabolite, its place and function in the detoxification pathway is unclear.

It was reported before that some triketone compounds can undergo an intramolecular cyclization to a dihydroxanthenone (Appendix A, Figure 7-6). Such formation of xanthone derivates occurs via the displacement of an *ortho*-substituent capable of being a leaving group or when the *meta*-substituent is electron-withdrawing because it opens the *ortho*-position towards nucleophilic attack (Lee et al., 1998; Calvayrac et al., 2013). It is likely that M5, M7, M8 and possibly other metabolites are able to undergo intramolecular cyclization and might be present in either one of the forms. In the literature, further tembotrione detoxification products such as xanthenedione type compound (TXD) (Tarara et al., 2009; Calvayrac et al., 2013), glutaric acid or 2-sulfofumaric acid (Tawk et al., 2017) were mentioned. None of these products were identified in this study.

M2 does not exhibit any herbicidal activity (Leake et al., 2009) while M9 is 5-fold less potent *in vitro* than tembotrione (Kelly et al., 2009). It is unclear if the remaining metabolites are still biologically active in the plant. M7/M8 and M1 have likely become too large to fit into the HPPD binding pocket but M3/M4 could still be toxic *in planta*.

No difference in tembotrione uptake was observed between NER and NES, as has been shown before in HPPD inhibitor-resistant *A. tuberculatus* and *A. palmeri* (Kaundun et al., 2017; Nakka et al., 2017). HPPD-inhibitors are translocated in both phloem and xylem (Leake et al., 2009). There may have

been a slightly reduced ^{14}C translocation in NER, similar to what was observed in HPPD-inhibitor resistant *A. tuberculatus* (Kaundun et al., 2017). The detected ^{14}C could be parent compound tembotrione or its various metabolites. Studies comparing ^{14}C mesotrione translocation between *Chenopodium album* and *Zea mays* (with maize being tolerant to HPPD inhibitors due to its capacity to metabolize the herbicide) showed that seven d after treatment 48% of the absorbed radioactive material had moved out of the applied leaf in *C. album* out of which 42% was still parent mesotrione whereas no parent mesotrione could be detected in the 14% of absorbed radioactive material which translocated outside the treated leaf in maize. This shows that rapid metabolism limits herbicide translocation (Wichert et al., 1999; Mitchell et al., 2001). It is possible that the slight difference observed in tembotrione translocation is due to the increased metabolism in NER. NER forms tembotrione metabolites more rapidly than NES and the metabolite(s) might be translocated less efficiently than the parent active compound. This is particularly true for glycosyl-conjugates stored in the vacuole (Gaillard et al., 1994).

Further experiments were carried out to determine the environmental factors and developmental stages under which the difference in metabolism was highest between NER and NES. Low temperatures significantly slowed metabolism in both NER and NES, as has been shown before in several weed species (Viger et al., 1991; Olson et al., 2000). In other studies, the efficacy of mesotrione (as well as absorption, translocation and metabolism) is influenced by temperature, with *A. palmeri* being more sensitive to the HPPD inhibitor mesotrione at low temperatures (Godar et al., 2015). At 10 cm tall, past the recommended spraying height according to the herbicide label, most NES were able to metabolize over 50% of tembotrione within 16 HAT. Therefore, for successful weed control it is crucial to time the herbicide application to small plants following the Herbicide Resistance Action Committee (HRAC) recommendations (HRAC, 2014), as NES can metabolize tembotrione rapidly enough to enable survival once they reach a certain developmental stage. The data suggest that tembotrione resistance diagnostics should be performed at the four-leaf stage (under continuous light conditions) to see the most prominent difference between resistant and susceptible populations.

Some evidence suggests an additional role for target-site resistance (TSR) in HPPD-inhibitor resistance via increased *HPPD* transcription in *A. palmeri* only (Nakka et al., 2017) but no target-site mutations (Ma et al., 2013; Kaundun et al., 2017; Nakka et al., 2017) or increased *HPPD* copy number in either species (Ma et al., 2013; Kaundun et al., 2017; Nakka et al., 2017). The differences in transcription still need to be confirmed by measuring active HPPD protein present in the chloroplast. Resistant *A. tuberculatus* populations showed no differences for *HPPD* transcription either before or after application with mesotrione (Ma et al., 2013; Kaundun et al., 2017). Between NER and NES, no change in *HPPD* gene copy number was found, but a trend for increased *HPPD* transcription was observed in NER compared to NES prior to tembotrione treatment. This trend was lost after treatment with tembotrione. Previous research has shown that *HPPD* expression in *A. palmeri* can be influenced by temperature when treated with mesotrione (Godar et al., 2015) as well as light intensity in *Arabidopsis thaliana* (Rossel et al., 2002). Further research on more populations from different origins is necessary to determine whether and to what extent increased *HPPD* transcription contributes to tembotrione resistance in *A. palmeri*.

CONCLUSION

This study identified that resistance to tembotrione in the *A. palmeri* population from Nebraska is due to enhanced herbicide metabolism as has previously been shown with HPPD inhibitor-resistant *A. tuberculatus* from Illinois (Ma et al., 2013) and Nebraska (Kaundun et al., 2017; Oliveira et al., 2017), as well as *A. palmeri* from Kansas (Nakka et al., 2017). The specific tembotrione metabolites formed were the same in both NER and NES. Nine degradation products were identified, some of which have not been identified before. Hydroxylated tembotrione was formed faster in NER than NES, suggesting that mainly CYPs are involved in the detoxification process. Further research is needed to identify the specific gene or genes involved in NTSR to HPPD-inhibitors in *A. palmeri*.

Enhanced herbicide metabolism is one of the main mechanisms of NTSR and its frequency has been increasing over the past decades (Beckie and Tardif, 2012). The ability of weeds to detoxify herbicide(s) represents a great threat for modern agriculture and sustainable weed control and strongly

impacts yields and quality (Powles and Yu, 2010). Even if herbicide detoxification is often limited to certain chemical classes, weed populations resistant to multiple herbicides from different chemical classes and modes of action are increasing (Délye et al., 2011; Yu and Powles, 2014). A further concern is that weed populations or individuals showing enhanced herbicide metabolism can be recurrently selected by the use of low herbicide doses (Yu et al., 2013). With *A. palmeri* populations being resistant to five different modes of action, it will become more challenging in the future to control with the currently available herbicides. Additionally, CYPs are suggested to be involved in metabolic cross resistance (Cocker et al., 2001; Letouzé and Gasquez, 2003) which might make it even more difficult to manage *A. palmeri* with NTSR because it limits the effectiveness of mixtures, rotations (Beckie and Tardif, 2012), and stacked herbicide-resistance traits in crop cultivars.

TABLES

Table 2-1: Confirmation of resistance to tembotrione of *A. palmeri* population NER compared to NES. Plant survival and injury expressed as a percentage were used in a three-parameter log-logistic equation to estimate *D* (upper limit), LD_{50}/ED_{50} (herbicide dose in g a.i. ha^{-1} results in 50% survival/injury), and *b* (slope). Ratio of LD_{50}/ED_{50} for NER to NES was expressed as resistance factor (R/S).

Experiment	Population	*D*	LD_{50}/ED_{50}	*b*	R/S	*P* value
Survival	NER	104.5 (3.1)	83.0 (5.9)	1.6	3.3	<0.0001
	NES	101.5 (3.4)	24.9 (0.9)	5.0		
Injury	NER	91.0 (3.1)	73.4 (4.4)	-2.2	2.9	<0.0001
	NES	100.0 (1.2)	25.0 (0.3)	-11.3		

Table 2-2: Molecular formulas and mass spectrum characteristics of tembotrione and its metabolites.

Name	Molecular formula	Detected molecular ions (m/z)
Tembotrione	$C_{17}H_{16}O_6ClF_3S$	439 $[M-H]^-$; 441 $[M+H]^+$; 458 $[M+NH_4]^+$
M1	$C_{25}H_{28}O_{13}ClF_3S$	659 $[M-H]^-$
M2	$C_{11}H_{10}O_5ClF_3S$	345 $[M-H]^-$
M3/M4	$C_{17}H_{16}O_7ClF_3S$	455 $[M-H]^-$; 457 $[M+H]^+$; 474 $[M+NH_4]^+$
M5	$C_{17}H_{14}O_6ClF_3S$	437 $[M-H]^-$; 439 $[M+H]^+$
M6	$C_{12}H_{10}O_5ClF_3S$	359 $[M-H]^-$
M7	$C_{23}H_{26}O_{12}ClF_3S$	617 $[M-H]^-$
M8	$C_{23}H_{24}O_{12}ClF_3S$	615 $[M-H]^-$
M9	$C_{17}H_{16}O_8ClF_3S$	471 $[M-H]^-$

FIGURES

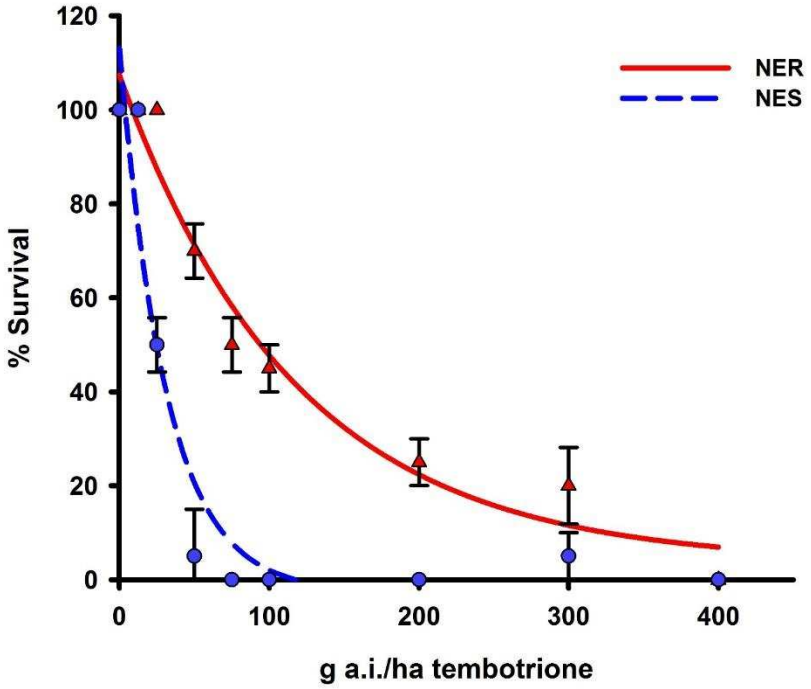

Figure 2-1: Non-linear regression analysis of survival for A. palmeri populations NER and NES 35 DAT with tembotrione. Percent survival obtained from averages of 20 replicates and fitted in a three-parameter log-logistic model with standard errors.

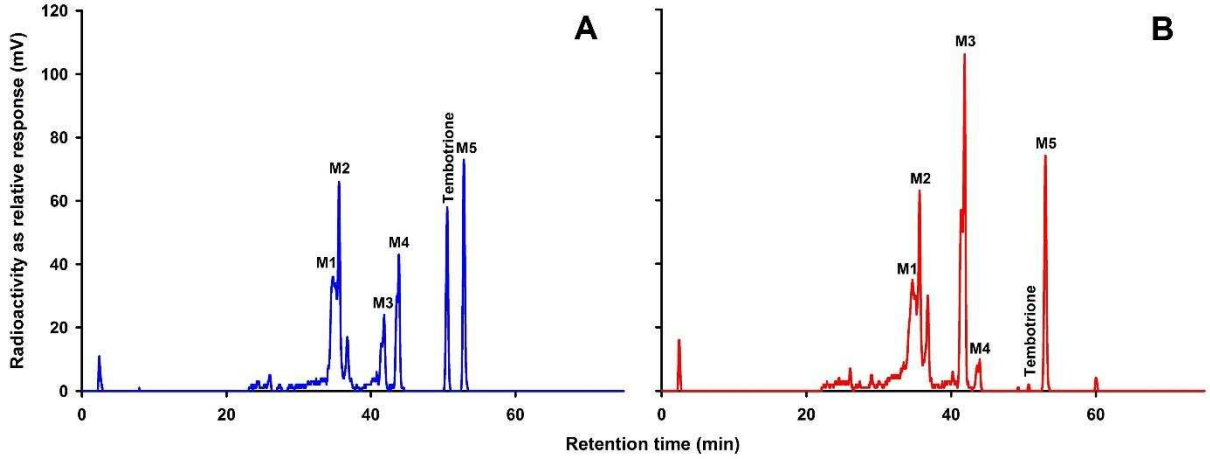

Figure 2-2: Representative reverse-phase HPLC chromatograms of NES (A) and NER (B) *A. palmeri* individuals 48 HAT with ^{14}C-tembotrione. The retention time at 50.8 min shows the tembotrione peak, the five major metabolites are labeled.

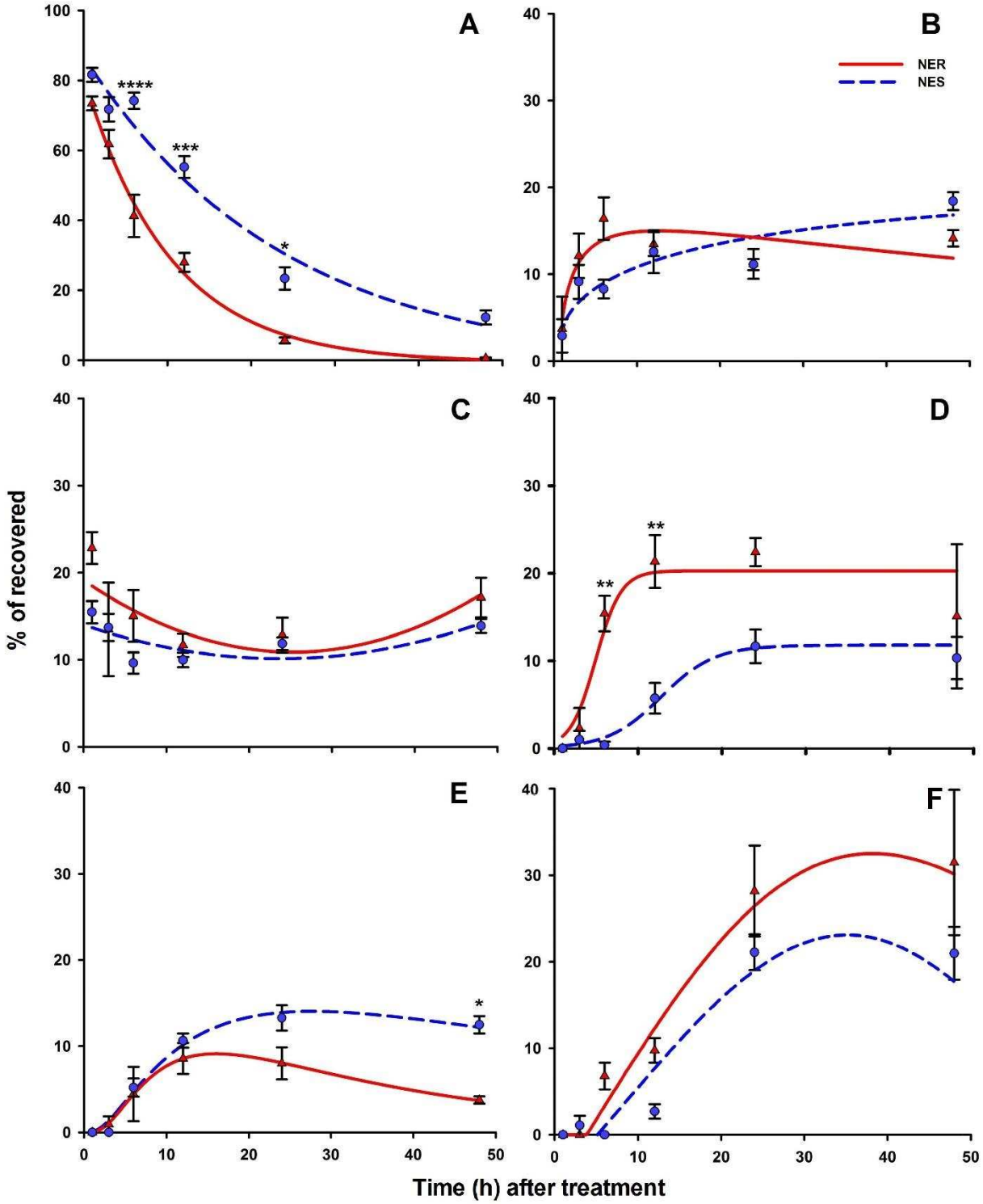

Figure 2-3: Tembotrione major metabolites in NER and NES *A. palmeri* over time fitted by non-linear regression analyses with standard error bars. A, parent tembotrione; B, Metabolite 1; C, Metabolite 2; D Metabolite 3; E, Metabolite 4; F, Metabolite 5. Asterisks indicate significant differences (* = $P < 0.05$, ** = $P < 0.1$, *** = $P < 0.001$, **** = $P < 0.0001$) between NER and NES at specific time points.

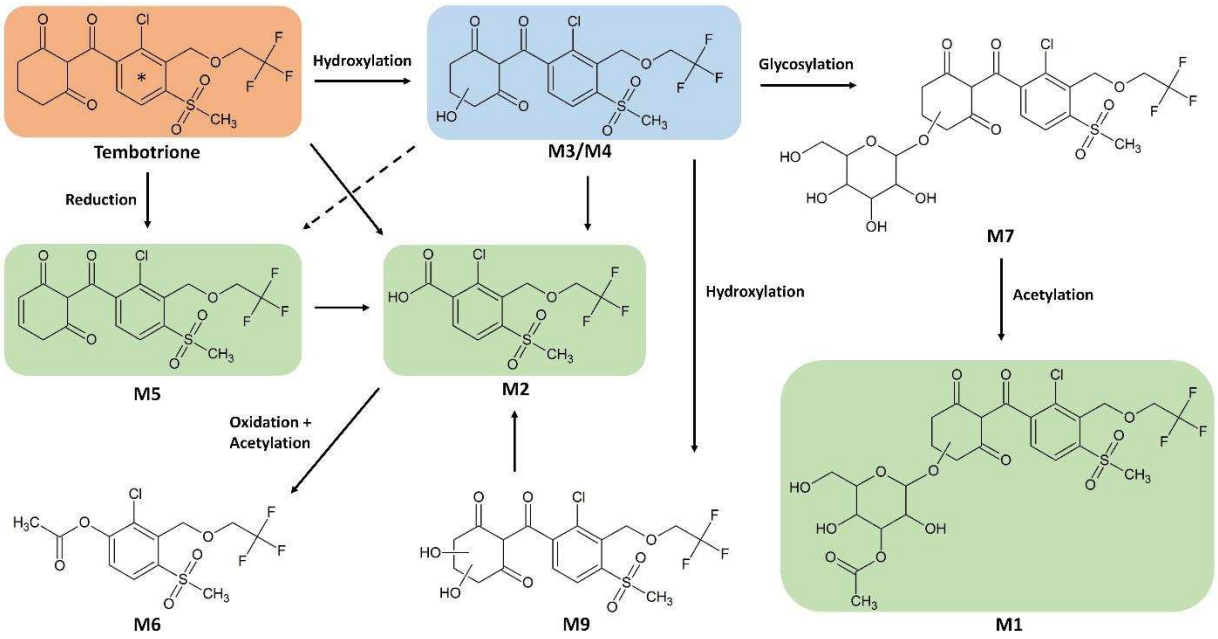

Figure 2-4: Chemical structures of tembotrione and detected metabolites from NER and NES arranged in their putative detoxification pathways. The asterisk in the tembotrione molecule (orange) marks the location of the ^{14}C-label. The major metabolites are shown in green with M3/M4, the metabolite that showed significant differences between NER and NES, shown in blue. The binding sites of the hexose and acetyl group in M7 and M1 are putative.

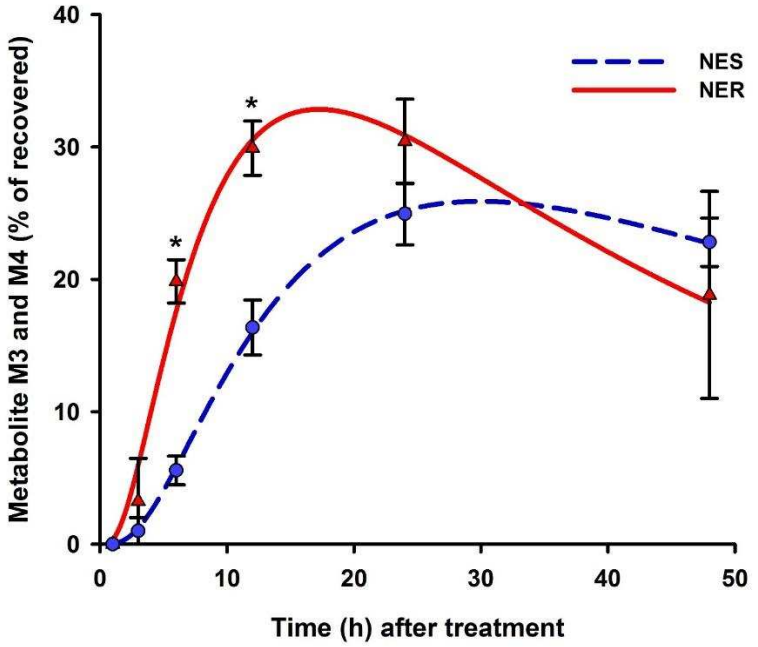

Figure 2-5: Formation of M3 and M4 combined in NER and NES over time fitted by non-linear regression analyses with standard error bars. Asterisks indicate significant differences ($P < 0.05$) between NER and NES at specific time points.

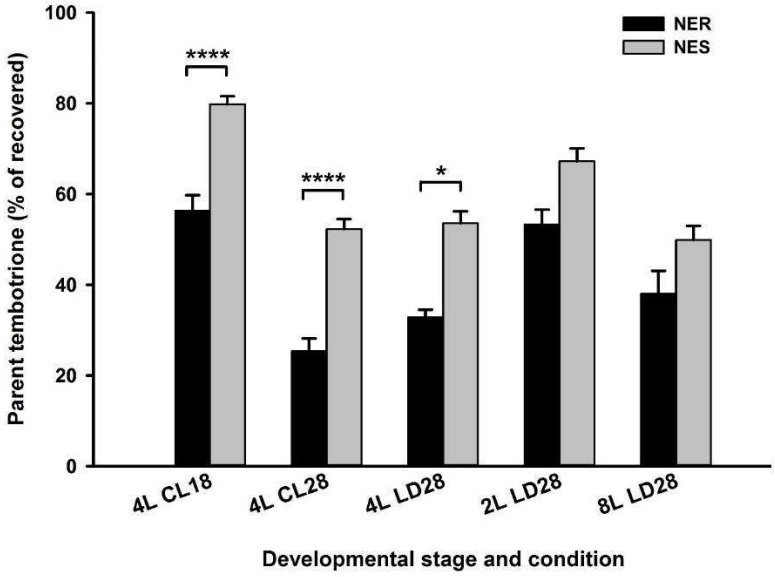

Figure 2-6: Tembotrione formation 16 HAT in NER and NES *A. palmeri* individuals treated at the two- (2L), four- (4L), or eight-leaf stage (8L) and kept under continuous light (CL) or 16/8h light/dark conditions (LD) at either 18 or 28°C (18/28). Error bars represent the standard error of individuals from two experiments. Asterisks indicate significant differences (* = $P < 0.05$, **** = $P < 0.0001$) between NER and NES.

REFERENCES

Ahrens, H., Lange, G., Müller, T., Rosinger, C., Willms, L., and van Almsick, A. (2013). 4-Hydroxyphenylpyruvate dioxygenase inhibitors in combination with safeners: Solutions for modern and sustainable agriculture. *Angew. Chem. Int. Ed.* 52(36)**,** 9388-9398.

Alferness, P., and Wiebe, L. (2002). Determination of mesotrione residues and metabolites in crops, soil, and water by liquid chromatography with fluorescence detection. *J. Agric. Food Chem.* 50(14)**,** 3926-3934.

Beaudegnies, R., Edmunds, A.J., Fraser, T.E., Hall, R.G., Hawkes, T.R., Mitchell, G., et al. (2009). Herbicidal 4-hydroxyphenylpyruvate dioxygenase inhibitors--a review of the triketone chemistry story from a Syngenta perspective. *Bioorg. Med. Chem.* 17(12)**,** 4134-4152. doi: 10.1016/j.bmc.2009.03.015.

Beckie, H.J., and Tardif, F.J. (2012). Herbicide cross resistance in weeds. *Crop Prot.* 35**,** 15-28.

Brazier, M., Cole, D.J., and Edwards, R. (2002). O-Glucosyltransferase activities toward phenolic natural products and xenobiotics in wheat and herbicide-resistant and herbicide-susceptible black-grass (*Alopecurus myosuroides*). *Phytochem* 59(2)**,** 149-156.

Busi, R., Gaines, T.A., and Powles, S. (2017a). Phorate can reverse P450 metabolism-based herbicide resistance in *Lolium rigidum*. *Pest Manag. Sci.* 73(2)**,** 410-417.

Busi, R., Porri, A., Gaines, T., and Powles, S. (2017b). Pyroxasulfone resistance in *Lolium rigidum* conferred by enhanced metabolic capacity. *bioRxiv***,** DOI: 10.1101/116269.

Calvayrac, C., Bontemps, N., Nouga-Bissoue, A., Romdhane, S., Coste, C.-M., and Cooper, J.-F. (2013). Photolysis of tembotrione and its main by-products under extreme artificial conditions:: Comparison with another β-triketone herbicide. *Sci. Total Environ.* 452**,** 227-232.

Chaabane, H., Vulliet, E., Calvayrac, C., Coste, C.M., and Cooper, J.F. (2008). Behaviour of sulcotrione and mesotrione in two soils. *Pest Manag. Sci.* 64(1)**,** 86-93.

Chaabane, H., Vulliet, E., Joux, F., Lantoine, F., Conan, P., Cooper, J.-F., et al. (2007). Photodegradation of sulcotrione in various aquatic environments and toxicity of its photoproducts for some marine micro-organisms. *Water Res* 41(8)**,** 1781-1789.

Chahal, P.S., Aulakh, J.S., Jugulam, M., and Jhala, A.J. (2015). *Herbicide-resistant Palmer amaranth (Amaranthus palmeri S. Wats.) in the United States—Mechanisms of resistance, impact, and management.* InTechOpen, Rijeka, Croatia.

Cocker, K.M., Northcroft, D.S., Coleman, J.O.D., and Moss, S.R. (2001). Resistance to ACCase-inhibiting herbicides and isoproturon in UK populations of *Lolium multiflorum*: mechanisms of resistance and implications for control. *Pest Manag. Sci.* 57(7)**,** 587-597.

Coutinho, P.M., Deleury, E., Davies, G.J., and Henrissat, B. (2003). An evolving hierarchical family classification for glycosyltransferases. *J. Mol. Biol.* 328(2)**,** 307-317.

Cummins, I., Wortley, D.J., Sabbadin, F., He, Z., Coxon, C.R., Straker, H.E., et al. (2013). Key role for a glutathione transferase in multiple-herbicide resistance in grass weeds. *Proc. Nat. Acad. Sci. USA* 110(15)**,** 5812-5817.

Délye, C., Gardin, J., Boucansaud, K., Chauvel, B., and Petit, C. (2011). Non-target-site-based resistance should be the centre of attention for herbicide resistance research: *Alopecurus myosuroides* as an illustration. *Weed Res.* 51(5)**,** 433-437.

Duhoux, A., Carrère, S., Duhoux, A., and Délye, C. (2017). Transcriptional markers enable identification of rye-grass (*Lolium sp.*) plants with non-target-site-based resistance to herbicides inhibiting acetolactate-synthase. *Plant Sci.* 257**,** 22-36.

Dumas, E., Giraudo, M., Goujon, E., Halma, M., Knhili, E., Stauffert, M., et al. (2016). Fate and ecotoxicological impact of new generation herbicides from the triketone family: An overview to assess the environmental risks. *J. Hazard. Mater.* 325**,** 136-156.

Evans, C.M. (2016). *Characterization of a novel five-way-resistant population of waterhemp (Amaranthus tuberculatus)*. University of Illinois at Urbana-Champaign.

Foyer, C., Descourvieres, P., and Kunert, K. (1994). Protection against oxygen radicals: an important defence mechanism studied in transgenic plants. *Plant, Cell Environ.* 17(5)**,** 507-523.

Gaillard, C., Dufaud, A., Tommasini, R., Kreuz, K., Amrhein, N., and Martinoia, E. (1994). A herbicide antidote (safener) induces the activity of both the herbicide detoxifying enzyme and of a vacuolar transporter for the detoxified herbicide. *FEBS Letters* 352(2)**,** 219-221.

Gaines, T.A., Lorentz, L., Figge, A., Herrmann, J., Maiwald, F., Ott, M.C., et al. (2014). RNA-Seq transcriptome analysis to identify genes involved in metabolism-based diclofop resistance in *Lolium rigidum*. *Plant J.* 78(5)**,** 865-876.

Godar, A.S., Varanasi, V.K., Nakka, S., Prasad, P.V., Thompson, C.R., and Mithila, J. (2015). Physiological and molecular mechanisms of differential sensitivity of Palmer amaranth (*Amaranthus palmeri*) to mesotrione at varying growth temperatures. *PLoS One* 10(5)**,** DOI: 10.1371/journal.pone.012673.

Han, H., Yu, Q., Vila-Aiub, M., and Powles, S. (2014). Genetic inheritance of cytochrome P450-mediated metabolic resistance to chlorsulfuron in a multiple herbicide resistant *Lolium rigidum* population. *Crop Prot.* 65**,** 57-63.

Hausman, N.E., Singh, S., Tranel, P.J., Riechers, D.E., Kaundun, S.S., Polge, N.D., et al. (2011). Resistance to HPPD-inhibiting herbicides in a population of waterhemp (*Amaranthus tuberculatus*) from Illinois, United States. *Pest Manag. Sci.* 67(3)**,** 258-261.

Heap, I. (2018). *The International Survey of Herbicide Resistant Weeds. Online. Available:* www.weedscience.org [Online]. Available: www.weedscience.org [Accessed January 30, 2018].

HRAC (2014). "HPPD-inhibitor Resistance Stewardship Fact Sheet - The Perspective of the HRAC HPPD-inhibitor Working Group. Online. Available: http://hracglobal.com/files/HPPD-inhibitor-Fact-Sheet.pdf". Herbicide Resistance Action Committee).

Huffman, J., Hausman, N.E., Hager, A.G., Riechers, D.E., and Tranel, P.J. (2015). Genetics and inheritance of nontarget-site resistances to atrazine and mesotrione in a waterhemp (*Amaranthus tuberculatus*) population from Illinois. *Weed Sci.* 63(4)**,** 799-809.

Iwakami, S., Endo, M., Saika, H., Okuno, J., Nakamura, N., Yokoyama, M., et al. (2014). Cytochrome P450 CYP81A12 and CYP81A21 are associated with resistance to two acetolactate synthase inhibitors in *Echinochloa phyllopogon*. *Plant Physiol.* 165(2)**,** 618-629.

Jhala, A.J., Sandell, L.D., Rana, N., Kruger, G.R., and Knezevic, S.Z. (2014). Confirmation and control of triazine and 4-hydroxyphenylpyruvate dioxygenase-inhibiting herbicide-resistant Palmer amaranth (*Amaranthus palmeri*) in Nebraska. *Weed Technol.* 28(1)**,** 28-38.

Kang, M. (1993). Inheritance of susceptibility to nicosulfuron herbicide in maize. *J. Hered.* 84(3)**,** 216-217.

Kaundun, S.S., Hutchings, S.J., Dale, R.P., Howell, A., Morris, J.A., Kramer, V.C., et al. (2017). Mechanism of resistance to mesotrione in an *Amaranthus tuberculatus* population from Nebraska, USA. *PLoS One* 12(6)**,** 1-22. doi: 10.1371/journal.pone.0180095.

Kelly, I., Leake, C., Diot, R., and Lemke, V. (2009). Dietary risk assessments for tembotrione using determinisic and probabilistic methods. *Bayer Crop Sci J.* 62**,** 79-93.

Knezevic, S.Z., Streibig, J.C., and Ritz, C. (2007). Utilizing R software package for dose-response studies: the concept and data analysis. *Weed Technol.* 21(3)**,** 840-848.

Leah, J.M., Caseley, J.C., Riches, C.R., and Valverde, B. (1994). Association between elevated activity of aryl acylamidase and propanil resistance in Jungle-rice, *Echinochloa colona*. *Pest Manag. Sci.* 42(4)**,** 281-289.

Leake, C., Diot, R., Glass, H., Newby, S., Semino, G., Tarara, G., et al. (2009). The human and environmental safety aspects of tembotrione. *Bayer Crop Sci J.* 62**,** 53-62.

Lee, D.L., Knudsen, C.G., Michaely, W.J., Chin, H.L., Nguyen, N.H., Carter, C.G., et al. (1998). The structure–activity relationships of the triketone class of HPPD herbicides. *Pest Manag. Sci.* 54(4)**,** 377-384.

Letouzé, A., and Gasquez, J. (2003). Enhanced activity of several herbicide-degrading enzymes: a suggested mechanism responsible for multiple resistance in blackgrass (*Alopecurus myosuroides* Huds.). *Agronomie* 23(7)**,** 601-608.

Ma, R., Kaundun, S.S., Tranel, P.J., Riggins, C.W., McGinness, D.L., Hager, A.G., et al. (2013). Distinct detoxification mechanisms confer resistance to mesotrione and atrazine in a population of waterhemp. *Plant Physiol.* 163(1)**,** 363-377.

Matringe, M., Sailland, A., Pelissier, B., Rolland, A., and Zink, O. (2005). p-Hydroxyphenylpyruvate dioxygenase inhibitor-resistant plants. *Pest Manag. Sci.* 61(3)**,** 269-276.

McMullan, P.M., and Green, J.M. (2011). Identification of a tall waterhemp (*Amaranthus tuberculatus*) biotype resistant to HPPD-inhibiting herbicides, atrazine, and thifensulfuron in Iowa. *Weed Technol.* 25(3)**,** 514-518.

Meyer, C.J., Norsworthy, J.K., Young, B.G., Steckel, L.E., Bradley, K.W., Johnson, W.G., et al. (2015). Herbicide program approaches for managing glyphosate-resistant Palmer amaranth (*Amaranthus palmeri*) and waterhemp (*Amaranthus tuberculatus* and *Amaranthus rudis*) in future soybean-trait technologies. *Weed Technol.* 29(4)**,** 716-729.

Mitchell, G., Bartlett, D.W., Fraser, T.E.M., Hawkes, T.R., Holt, D.C., Townson, J.K., et al. (2001). Mesotrione: A new selective herbicide for use in maize. *Pest Manag. Sci.* 57(2)**,** 120-128.

Nakka, S., Godar, A.S., Wani, P.S., Thompson, C.R., Peterson, D.E., Roelofs, J., et al. (2017). Physiological and molecular characterization of hydroxyphenylpyruvate dioxygenase (HPPD)-inhibitor resistance in Palmer amaranth (*Amaranthus palmeri* S. Wats.). *Front. Plant Sci.* 8**,** 555.

Nordby, J.N., Williams, M.M., Pataky, J.K., Riechers, D.E., and Lutz, J.D. (2008). A common genetic basis in sweet corn inbred Cr1 for cross sensitivity to multiple cytochrome P450-metabolized herbicides. *Weed Sci.* 56(3)**,** 376-382.

Norris, S.R., Barrette, T.R., and DellaPenna, D. (1995). Genetic dissection of carotenoid synthesis in Arabidopsis defines plastoquinone as an essential component of phytoene desaturation. *The Plant Cell* 7(12)**,** 2139-2149.

Norsworthy, J.K., Griffith, G., Griffin, T., Bagavathiannan, M., and Gbur, E.E. (2014). In-field movement of glyphosate-resistant Palmer amaranth (*Amaranthus palmeri*) and its impact on cotton lint yield: evidence supporting a zero-threshold strategy. *Weed Sci.* 62(2)**,** 237-249.

Oliveira, M., Dayan, F., Gaines, T., Patterson, E., Jhala, A., and Knezevic, S. (2017). Reversing resistance to tembotrione in an *Amaranthus tuberculatus* (var. *rudis*) population from Nebraska, USA with cytochrome P450 inhibitors. *Pest Manag. Sci.***,** doi: 10.1002/ps.4697.

Olson, B.L., Al-Khatib, K., Stahlman, P., and Isakson, P.J. (2000). Efficacy and metabolism of MON 37500 in *Triticum aestivum* and weedy grass species as affected by temperature and soil moisture. *Weed Sci.* 48(5)**,** 541-548.

Powles, S.B., and Yu, Q. (2010). Evolution in action: Plants resistant to herbicides. *Annu. Rev. Plant. Biol.* 61**,** 317-347. doi: 10.1146/annurev-arplant-042809-112119.

Preston, C., Tardif, F.J., Christopher, J.T., and Powles, S.B. (1996). Multiple resistance to dissimilar herbicide chemistries in a biotype of *Lolium rigidum* due to enhanced activity of several herbicide degrading enzymes. *Pest Biochem Physiol* 54(2)**,** 123-134.

Ritz, C., and Streibig, J.C. (2005). Bioassay analysis using R. *J. Stat. Softw.* 12(5)**,** 1-22.

Rossel, J.B., Wilson, I.W., and Pogson, B.J. (2002). Global changes in gene expression in response to high light in Arabidopsis. *Plant Physiol.* 130(3)**,** 1109-1120.

Ruiz-Sola, M.Á., and Rodríguez-Concepción, M. (2012). Carotenoid biosynthesis in Arabidopsis: a colorful pathway. *The Arabidopsis Book* 10**,** 1-28.

Santel, H. (2009). Laudis® OD–a new herbicide for selective post-emergence weed control in corn (*Zea mays L.*). *Bayer CropSci. J.* 62(2009)**,** 95-108.

Schulte, W., and Köcher, H. (2009). Tembotrione and combination partner isoxadifen-ethyl–mode of herbicidal action. *Bayer CropSci. J.* 62(1)**,** 35-52.

Schultz, J.L., Chatham, L.A., Riggins, C.W., Tranel, P.J., and Bradley, K.W. (2015). Distribution of herbicide resistances and molecular mechanisms conferring resistance in Missouri waterhemp (*Amaranthus rudis* Sauer) populations. *Weed Sci.* 63(1)**,** 336-345.

Schwartz-Lazaro, L.M., Norsworthy, J.K., Scott, R.C., and Barber, L.T. (2017). Resistance of two Arkansas *Palmer amaranth* populations to multiple herbicide sites of action. *Crop Prot.* 96**,** 158-163.

Tarara, G., Fliege, R., Desmarteau, D., Kley, C., and Peters, B. (2009). Environmental fate of tembotrione. *Bayer CropSci. J.* 62**,** 63-78.

Tawk, A., Deborde, M., Labanowski, J., Thibaudeau, S., and Gallard, H. (2017). Transformation of the B-triketone pesticides tembotrione and sulcotrione by reactions with ozone: Kinetic study, transformation products, toxicity and biodegradability. *Ozone: Sci. Eng.* 39(1)**,** 3-13.

ter Halle, A., Drncova, D., and Richard, C. (2006). Phototransformation of the herbicide sulcotrione on maize cuticular wax. *Environ. Sci. Technol.* 40(9)**,** 2989-2995.

van Almsick, A. (2009). New HPPD-inhibitors – A proven mode of action as a new hope to solve current weed problems. *Outlooks Pest Manag.* 20(1)**,** 27-30.

Viger, P.R., Eberlein, C.V., Fuerst, E.P., and Gronwald, J.W. (1991). Effects of CGA-154281 and temperature on metolachlor absorption and metabolism, glutathione content, and glutathione-S-transferase activity in corn (*Zea mays*). *Weed Sci.* 39(3)**,** 324-328.

Ward, S.M., Webster, T.M., and Steckel, L.E. (2013). Palmer amaranth (*Amaranthus palmeri*): a review. *Weed Technol.* 27(1)**,** 12-27.

Webster, T.M., and Nichols, R.L. (2012). Changes in the prevalence of weed species in the major agronomic crops of the Southern United States: 1994/1995 to 2008/2009. *Weed Sci.* 60(2)**,** 145-157.

Wichert, R., Townson, J., Bartlett, D., and Foxon, G. (Year). "Technical review of mesotrione, a new maize herbicide"), 105-112.

Williams II, M.M., and Pataky, J.K. (2008). Genetic basis of sensitivity in sweet corn to tembotrione. *Weed Sci.* 56(3)**,** 364-370.

Yang, Q., Deng, W., Li, X., Yu, Q., Bai, L., and Zheng, M. (2016). Target-site and non-target-site based resistance to the herbicide tribenuron-methyl in flixweed (*Descurainia sophia L.*). *BMC Genomics* 17(1)**,** 551.

Yu, Q., Han, H., Cawthray, G., Wang, S., and Powles, S. (2013). Enhanced rates of herbicide metabolism in low herbicide-dose selected resistant *Lolium rigidum*. *Plant Cell Environ.* 36(4)**,** 818-827.

Yu, Q., and Powles, S. (2014). Metabolism-based herbicide resistance and cross-resistance in crop weeds: a threat to herbicide sustainability and global crop production. *Plant Physiol.* 166(3)**,** 1106-1118.

Yuan, J.S., Tranel, P.J., and Stewart, C.N. (2007). Non-target-site herbicide resistance: A family business. *Trends Plant Sci.* 12(1)**,** 6-13.

Yun, M.-S., Yogo, Y., Miura, R., Yamasue, Y., and Fischer, A.J. (2005). Cytochrome P-450 monooxygenase activity in herbicide-resistant and-susceptible late watergrass (*Echinochloa phyllopogon*). *Pest Biochem. Physiol.* 83(2)**,** 107-114.

3. IDENTIFICATION OF GENES INVOLVED IN METABOLISM-BASED TEMBOTRIONE RESISTANCE IN PALMER AMARANTH (*AMARANTHUS PALMERI*) BY RNA-SEQ TRANSCRIPTOME ANALYSIS[2]

INTRODUCTION

Over the past decades hundreds of weed species have evolved resistance to numerous herbicide modes of action, reducing the number of herbicides available for successful chemical weed control in several agricultural cropping systems. Among the most troublesome weed species in the U.S. is Palmer amaranth (*Amaranthus palmeri*), having evolved resistance to five different modes of action including 4-hydroxyphenylpyruvate dioxygenase (HPPD)-inhibitors (Chahal et al., 2015; Nakka et al., 2017; Schwartz-Lazaro et al., 2017; Heap, 2018). The first case of HPPD-inhibitor resistance in this species was reported from Kansas in 2009 followed by Nebraska in 2011 (Jhala et al., 2014; Nakka et al., 2017). Resistance was also reported in common waterhemp (*A. tuberculatus* var. *rudis*) (Hausman et al., 2011; McMullan and Green, 2011; Schultz et al., 2015; Nakka et al., 2017).

HPPD-inhibitors interrupt the formation of homogentisic acid (HGA), the precursor for plastoquinone and vitamin E production, by mimicking the HPPD-substrate 4-hydroxyphenylpyruvate (HPP). Enzyme inhibition results in bleaching and plant death (Matringe et al., 2005). Crops have been engineered to be resistant to HPPD-inhibitors by over-expression of bacterial HPPD, by a HPPD point mutation, by bypassing HPPD in HGA synthesis, or by increasing the flux of HPP substrate (Matringe et al., 2005). Sweet corn and creeping bentgrass (*Agrostis stolonifera* L.) have shown tolerance to HPPD-inhibitors naturally by increasing their metabolism via the up-regulation of cytochrome P450 enzymes (CYPs) (Pallett et al., 1998; Bollman et al., 2008; Pataky et al., 2008; Elmore et al., 2015). This allows the plants to reduce the herbicide to a nonlethal dose reaching the target enzyme. HPPD-inhibitor

[2] Anita Küpper, Darci Giacomini, Patrick Tranel, Roland Beffa, Todd A. Gaines

resistance in *A. palmeri* and *A. tuberculatus* is due to enhanced metabolic resistance (EMR), likely conferred by CYPs, as well (Kaundun et al., 2017; Küpper et al., 2017b; Nakka et al., 2017; Oliveira et al., 2017).

CYPs have many biosynthetic pathway functions, but are also part of a pre-existing abiotic stress response pathway which allows plants to make biochemical modifications to herbicides to render them less toxic or less mobile, resulting in their compartmentalization (Schuler and Werck-Reichhart, 2003; Yuan et al., 2007). These modifications often start by transforming the herbicide into a more hydrophilic and less toxic metabolite, a process mainly carried out by CYPs. These transformation reactions can include oxidation, hydrolysis, reduction, dehydration, dimerization, deamination, dehydrogenation, dealkylation, epoxidation, and certain cleavage processes (Van Eerd et al., 2003). After this first phase, the metabolite can be conjugated and transported into the vacuole or cell walls where it is no longer toxic to the plant (Bartholomew et al., 2002; Van Eerd et al., 2003; Reade et al., 2004). Aside from CYPs, oxidases, peroxidases, esterases, hydrolases, glutathione-S-transferases (GST), glycosyltransferases (GT), aryl acylamidases, and ABC transporters have been implicated in plant detoxification processes (Leah et al., 1994; Brazier et al., 2002; Preston, 2004; Yuan et al., 2007; Cummins et al., 2013; Delye, 2013; Yang et al., 2016; Busi et al., 2017b; Duhoux et al., 2017).

CYP involvement in EMR is often limited to studies using CYP inhibitors such as malathion, 1-aminobenzo-triazole, tetcyclacis, piperonyl butoxide, or tridiphane, which induce susceptibility in resistant plants (Yuan et al., 2007). However, these experiments do not identify the specific CYPs involved. Determining CYPs that cause resistance is confounded by several factors. In comparison to animals, which are not forced to live a sessile lifestyle and have the option to evade exposure to xenobiotics, plants possess up to 500 highly diverse CYPs (Barrett, 2000). Their expression can be constitutive, inducible, or both (Barrett, 2000). It is possible for multiple CYPs to metabolize the same substrate (Schuler and Werck-Reichhart, 2003) but some single CYPs are also able to confer EMR to multiple chemically unrelated herbicide classes either fully or in combination with other genes. As an example, CYP2B6 has the ability to metabolize 13 different herbicides from several different modes of

action (Hirose et al., 2005). Thus, EMR to a herbicide depends on the combination of alleles present in the plant (Delye, 2013). EMR is most often a quantitative trait controlled by two or more additive genes, as has been shown with acetyl-CoA carboxylase (ACCase) and acetolactate synthase (ALS) inhibitors in monocots (Preston, 2003; Petit et al., 2010; Busi et al., 2011). Gradual selections with repeated applications of low herbicide doses favor multigenic resistance (Gardner et al., 1998; Neve and Powles, 2005; Renton et al., 2011; Busi et al., 2013; Yu et al., 2013). They allow resistance alleles to accumulate until a favorable combination enables the weed to survive (Busi et al., 2011; Delye, 2013). Furthermore, it has been suggested that multigenic resistance such as EMR is quicker to evolve than monogenic target-site resistance because minor resistance alleles occur in high frequency, especially in weed populations with high genetic diversity (Renton et al., 2011; Delye et al., 2013).

Currently, non-target site herbicide resistance is a major mechanism of resistance in weedy grasses (Beckie and Tardif, 2012; Delye, 2013; Gardin et al., 2015) and has the potential for cross-resistance. This not only threatens current modes of action, but also those that did not yet come to market (Letouzé and Gasquez, 2003). EMR has not been characterized well on the genetic level and its recent discovery in HPPD-resistant dicot weeds and in a species as problematic as *A. palmeri* make it urgent to identify the resistance genes involved. Previous research has shown that resistant *A. palmeri* is able to hydroxylate tembotrione faster than susceptible individuals which makes CYPs the most likely enzymes involved (Küpper et al., 2017b). Thus, the objective of this study was to identify candidate CYPs genes for tembotrione resistance in *A. palmeri* by comparing resistant and susceptible individuals from a Pseudo-F_2 generation using RNA-Seq transcriptome analysis.

MATERIALS AND METHODS

Plant material

The resistant (NER) and -susceptible (NES) *A. palmeri* populations investigated were collected from fields in Shickley, Nebraska in 2011 (Küpper et al., 2017b). NER is resistant to atrazine and the HPPD inhibitors tembotrione, mesotrione, and topramezone (Jhala et al., 2014). *A. palmeri* is a species

with high genetic variability. Therefore, plants with a similar genetic background were generated for the RNA-Seq experiment by controlled pairings of NER and NES parents to minimize genetic differences unrelated to EMR traits. For the crosses, the seed was sown on 0.7% agar medium (Sigma-Aldrich), placed in a refrigerator at 4 °C for seven d and then germinated on a germination bench at room temperature with 16/8h of day/night cycle. Germinated seedlings were transplanted into commercial potting soil (Professional Growing Mix, Sun Gro Horticulture) in 5x5 cm inserts and maintained in the greenhouse at 24±2 °C temperatures and 15/9 h day/night photoperiods supplemented with metal-halide lamps (400 µmol m^{-2} s^{-1}). Plants were watered daily. A pseudo-F_2 generation was generated by first spraying parental NER individuals at 7-10 cm height with a field rate of 91 a.i. ha^{-1} tembotrione (Laudis, Bayer CropScience) and 1% v/v methylated seed oil (MSO). Herbicide applications were made using an overhead track sprayer (DeVries Manufacturing) equipped with a flat-fan nozzle tip (TeeJet 8002EVS, Spraying System) calibrated to deliver 187 L ha^{-1} of spray solution at 172 kPa. Surviving NER were transplanted into 22.5 cm diameter pots and individually crossed with another NES individual using pollination bags. Five crosses with NER_{male} x NES_{female} and five crosses with NER_{female} x NES_{male} were performed and grown to seed. The resulting F_1 generations were grown out and sprayed again under the same conditions described above. Two F_1 individuals from each parental cross that survived the application were crossed with each other. The seed from the resulting Pseudo-F_2 generation was subsequently used for the RNA-Seq experiment (Figure 3-1).

Reference transcriptome

A *de novo* reference transcriptome was generated from three libraries containing samples from several NER parent individuals. The first library contained pooled samples from 20 NER seedlings, the second library contained pooled samples from two male and two female NER inflorescences, and the third library contained pooled samples from five stressed plants each exposed to field rates of tembotrione, 2,4-D (2,4-D amine, Alligare LLC), glyphosate (WeatherMax, Monsanto), lactofen (Cobra, Valent), and atrazine (Atrazine 90DF, Drexel), respectively. The libraries were generated using the same

kit mentioned above with an average cDNA fragment length of 600bp with a range of 80 – 900 bps. They were then run on one lane of an Illumina HiSeq 2500 platform yielding a total of 190 million 250nt paired-end reads with individual library yields ranging from 30.9 to 32.3 million reads.

Trimmomatic v.0.33 (Bolger et al., 2014) was used for adapter and quality trimming and *de novo* transcriptome assembly was performed using Trinity v.2.0.6 (Haas et al., 2013; Giacomini et al., 2016). Only the transcripts over 300nt containing the longest predicted open reading frames (ORF) predicted by TransDecoder v.2.0.1 were retained (Haas et al., 2013). The resulting 315-MB reference transcriptome contained 306,614 contigs with a N50 contig size of 730, mean length of 676 bp and GC content of 36%. The assignment of putative annotations to contigs was performed using BLASTx/p to identify matches with the UniProtKB/Swiss-Prot, Kegg, GO, and Eggnog databases. HMMER v.3.1 and signalP v.4.1 were used to identify and predict Pfam protein domains and signal peptides, respectively (Bendtsen et al., 2004; Finn et al., 2011).

RNA-Sequencing

For the RNA-Seq experiment, plants were grown from the Pseudo-F_2 generations generated from two parental NER_{male} x NES_{female} crosses (cross A and B, respectively) and one parental NER_{female} x NES_{male} cross (cross C). The seed was sown on 0.7% agar medium (Sigma-Aldrich), placed in a refrigerator at 4 °C for seven d and then germinated on a germination bench at room temperature with 16/8h of day/night cycle. About 150 seedlings from each Pseudo-F_2 cross were transplanted into 4x4 cm inserts each and maintained in a growth chamber at 25/22 °C day/night temperatures, 70% relative humidity, and 16h photoperiod with 700 µmol m^{-2} s^{-1} provided by incandescent and fluorescent bulbs. At 4-5 cm height and 4-5 leaf stage, the first fully expanded leaf from the apical meristem of each plant was cut and immediately frozen at -80 °C for timepoint 0. The plants were then sprayed at 77 g a.i. ha^{-1} (85% of the field rate) with 1% v/v MSO as described above to ensure resistant plants would be able to survive despite removing leaves for testing. Six hours after treatment (HAT) the second expanded leaf and twelve HAT the third expanded leaf were cut and immediately frozen at -80 °C, respectively. Visual damage and

survival data were recorded after treatment for 21 d to phenotype resistant and susceptible individuals. From each pseudo-F_2 cross only the six visually most resistant and the six visually most susceptible individuals were used for RNA-Sequencing (Table 3-1).

Total RNA was extracted from frozen ground tissue using the Direct-zol™ RNA MiniPrep Plus (Zymo Research) which includes DNAse treatment. Yield and purity were measured with a NanoDrop 2000 spectrophotometer (Thermo Scientific) and RNA integrity (RIN) was measured on an Agilent 2200 Bio TapeStation system (Agilent Technologies) using Agilent High Sensitivity RNA ScreenTape. RNA-Seq library preparation was performed with the TruSeq stranded mRNA library prep kit (Illumina) preparing for 150 nucleotide paired-end sequencing. The 108 libraries were run on an Illumina HiSeq 4000 platform on a total of 16 lanes (2 flow cells) with seven libraries per lane, yielding 5.2 billion paired-end reads. Individual library yields were 48.2 million on average and ranged from 35.0 to 71.5 million paired-end reads. On average over 93% of sequenced nucleotides met a quality score of 30 (Q30 Phred score).

Read pre-processing included the removal of library adapter sequences using TrimGalore v.0.4.5 (Krueger) and quality control checks using FastQC v.0.11.6 (Andrews, 2010). Read alignment of the 108 libraries to the *de novo* reference transcriptome was performed using Bowtie2 with the sensitive option for end-to-end alignment (Langmead and Salzberg, 2012). Most of the reads (>49%) aligned concordantly once, while >43% aligned concordantly more than one time and about 7% of reads aligned not concordantly. Raw read counts were extracted using SAMtools (Li et al., 2009).

Differential gene expression and SNP analysis

The package 'EdgeR' (Robinson et al., 2010) in the software R v.3.3 was used to estimate dispersion using the Cox-Reid profile-adjusted likelihood method and to normalize for effective library size in the dataset. Transcripts were removed from the analysis if they were not expressed in all of the samples of any one of the conditions or did not meet at least one count-per-million (CPM) criteria. Therefore, only transcripts were retained in the analysis that were found in all six replicates within a

condition. Differential transcript expression was estimated using the negative binomial generalized linear model (GLM). Differentially expressed transcripts were then filtered for a $\log_2$ fold-change ≥ 2 between compared groups and a false discovery rate (FDR) of $P \leq 0.01$. Expression differences were compared between resistant (R) and susceptible (S) plants of all crosses combined as well as separately for each time point. Furthermore, R and S plant samples from before treatment with tembotrione were compared with R and S sampled after treatment, respectively. Again, this was done for all crosses combined as well as for separate crosses. Contigs were selected based on the magnitude of expression differences, statistical difference, and annotations related to metabolic detoxification pathways, with particular emphasis on contigs annotated as CYPs. Redundant transcripts were merged using Clustal Omega multiple sequence alignment (Sievers et al., 2011). Identification of the transcript locations on the grain amaranth (*Amaranthus hypochondriacus*) genome (v.PGA2_1_2212017, id34733) was performed using the genomic mapping and alignment program GMAP with parameters for cross-species, coverage of ≥ 70%, and identity of ≥ 80% (Wu and Watanabe, 2005) and CoGe Comparative Genomics (CoGe, 2018). The bam files of differentially expressed contigs of samples taken 6 HAT were compared in the Integrative Genomics Viewer to determine possible SNPs co-segregating with resistance (Robinson et al., 2011).

RESULTS

Differences between all R and S plants

Differential expression ($\log_2$ fold-change (FC) ≥ 2, false discovery rate (FDR) ≤ 0.01) between all R and S individuals at 0 HAT was apparent with 61 contigs up-regulated in R of which over 45% were related to metabolism and over 29% were CYPs. After accounting for transcript redundancy, constitutive gene up-regulation in R at 0 HAT was apparent in several contigs that shared 76% identity with CYP72A219-like from common beet (*Beta vulgaris*, Accession: XM010696246.2). Another up-regulated contig shared 80% identity with CYP81E8-like (from *B. vulgaris*, Accession: XM010674481.2) and was also 76% identical with CYP81D11 from quinoa (*Chenopodium quinoa*, Accession: XM021868599.1). Even though the depicted CYP72A219 contigs did not show high sequence identity, it is possible that

they may represent the same gene, different segments of the same gene, or gene homologs (Table 3-2). In spinach (*Spinacia oleracea*), for example, three different transcript variants were found for CYP72A219-like. All up-regulated CYP72A219 contigs that could be mapped to the *A. hypochondriacus* genome mapped to scaffold 4 between 25.1-25.2 Mbp while CYP81E8 mapped to the same scaffold at 3.49 Mbp.

With a $\log_2$ FC of 4.3, CYP81E8 showed the highest and most significant up-regulation in R, followed by CYP72A219a with a $\log_2$ FC of 3.3 (Table 3-2). In addition, tembotrione triggers CYP72A219 up-regulation in both R and S with R showing a trend to up-regulate CYP72A219 quicker than S. Furthermore, CYP72A219 up-regulation seems to plateau 6 HAT for S while expression continues to rise until 12 HAT for R. Tembotrione treatment also triggers CYP81E8 expression in both R and S. However, the increase in S is minimal compared to R. For all plants CYP81E8 expression peaks at 6 HAT and decreases 12 HAT (Figure 3-2).

Aside from CYPs, several GTs, an oxidase and a GST enzyme were also up-regulated in R (for list of all differentially regulated transcripts 0 HAT see Appendix B, Table 8-1). They mapped to scaffolds 2, 3, and 7 of the *A. hypochondriacus* genome. GST U22 showed the highest up-regulation in R with $\log_2$ FC with 3.6 (Table 3-2). Treatment with tembotrione seemed to trigger continuous up-regulation of LPR2 and Sco-GT2 while the up-regulation of A3-GT1, A3-GT3, and UGT capped 6 HAT in both R and S. GST U22 was constitutively expressed in R only (Figure 3-3).

No significant gene expression differences were found between all R and S 6 HAT but 12 HAT R exhibited up-regulation of several ABC transporters (for a list of all differentially regulated transcripts 12 HAT see Appendix B, Table 8-2). None of the contigs mentioned above had any SNPs that correlated with tembotrione metabolic resistance.

Differences between R and S plants separated by cross

In previous experiments, 18.7, 36.9, and 17.2% of individuals from cross A, B, and C (91, 65, and 58 individuals tested, respectively) survived 91 g a.i. tembotrione with 1% v/v MSO, respectively. The strongest survivors could be found in cross A and B while R in Cross C took a longer time to recover

from tembotrione treatment. Thus, cross C was the least resistant of the three crosses. Not surprisingly, 0 HAT contigs CYP72A219 a and especially CYP81E8 were not as highly up-regulated in the R of cross C (R-C) as they were in R of crosses A (R-A) and cross B (R-B). However, R-C plants showed a trend towards higher up-regulation of the contigs CYP72A219 b-e than R-A and R-B plants (Figure 3-4).

Up-regulation after treatment varies between crosses, and individuals. Again, especially the up-regulation of CYP72A219 contigs at 6 HAT was very apparent in R-C plants. However, R-A and R-B plants continuously increase CYP72A219 contigs after treatment while R-C plants generally reach their expression peak 6 HAT and then slightly decrease at 12 HAT.CYP81E8 up-regulation in R-C plants even after treatment is hardly detectable compared to the other crosses (Figure 3-4).

Differential gene expression analysis suggested that aside from the CYPs already mentioned, only R-A plants showed significant constitutive up-regulation of a contig sharing 88% identity with CYP71A1-like from *C. quinoa* (Accession:021860844.1).

Effect of tembotrione on all R and S plants

Additionally to CYP71A219 and CYP81E8, which are up-regulated by treatment with tembotrione, the herbicide also triggered significant up-regulation of contigs that shared 79% identity with CYP71A1-like or 78% identity with CYP83B1-like from *B. vulgaris* (Accession: XM010675962.1 and XM010672697.2), 79% identity with CYP71A25-like from *C. quinoa* (Accession: XM021864488.1), 73% identity with CYP76C2-like from *C. quinoa* (Accession: XM021912709.1), 79% identity with CYP83B1-like from *S. oleracea* (Accession: XM021995517.1), 77% identity with CYP81F3-like from *B. vulgaris* (Accession: XM010697600.2), and 85% identity with CYP82D47-like from *C. quinoa* (Accession: XR002510196.1). Another contig shared 76% identity with CYP71A26-like in *B. vulgaris* or 75% identity with CYP71A3-like in *S. oleracea* (Accession: XM010697702.2 and XM022007837.1). Due to the ambiguity, the contig is therefore referred to as CYP71A. A similar observation was made for CYP78A which exhibited 81% shared identity with CYP78A3-like or CYP78A9-like from *C. quinoa* or

80% identity with CYP78A6-like from *S. oleracea* (Accession: XM021892787.1, XM021911584.1, or XM021991257.1).

Tembotrione treatment triggers the up-regulation of several CYPs in both R and S, some of them regardless of their susceptibility. However, S induced twice as many contigs as R (Table 3-3). This is especially evident with the up-regulation of CYP71A1, CYP71A, CYP76C2, and CYP83B1, which do not get significantly up-regulated in R. On the other hand, CYP78A was induced after treatment mainly in R only. All listed contigs are continually induced over the hours after treatment (Figure 3-5). Aside from CYPs, tembotrione also triggers the expression of GTs, oxidases, peroxidases, esterases, hydrolases, and an acetyltransferase in both R and S. S also up-regulate the expression of GSTs and ABC transporters.

DISCUSSION

Previous studies on the tembotrione metabolite profiles of NER and NES (see chapter 2) revealed that both biotypes produce the same metabolites. However, R hydroxylates tembotrione quicker than S which strongly suggests CYP involvement in the resistance mechanism. It also suggests that the CYPs that might be up-regulated in R would not differ from S in their composition but in the timing of their onset. After the addition of the hydroxy-group, it is likely that a GT adds a hexose group, potentially followed by an acetyltransferase adding an acetyl-group. This would allow for the transport of the metabolite to the vacuole or extracellular space by ABC transporters (Küpper et al., 2017b). Based on this knowledge, the hypothesis was tested that R individuals revealed differentially expressed contigs related to the first phase of metabolism.

CYP expression is induced by nuclear receptors which sense herbicide exposure (Waxman, 1999; Honkakoski and Negishi, 2000). Likely due to the diverse demands on the chemical defense system, this class of enzymes is subject to rapid, dynamic evolution of substrate specificity and expression regulation (Yuan et al., 2007) with diverse amino acid sequences sharing identities as low as 16% (Werck-Reichhart and Feyereisen, 2000). Most CYPs are anchored in the endoplasmatic reticulum. In order to function many require NADPH-dependent reductases for electron transfer (Schuler and Werck-Reichhart, 2003).

In plants a total of 59 CYP families exist which are sorted by a nomenclature depicting the family (share ≥ 40% of amino acid identity, represented by a number) and subfamilies (share ≥ 55% of amino acid identity, represented by a letter) (Schuler and Werck-Reichhart, 2003).

The first CYP identified to confer herbicide resistance was CYP76B1 in Jerusalem artichoke (*Helianthus tuberosus*) (Robineau et al., 1998) which was transferred to tobacco and *Arabidopsis thaliana* to confer resistance to phenylurea herbicides (Didierjean et al., 2002). Later, CYP1A1, CYP2B6, CYP51A1, and CYP71A10 were overexpressed to engineer herbicide-tolerant crop varieties (Grausem et al., 1995; Siminszky et al., 1999; Shiota et al., 2000; Yamada et al., 2002a; Yamada et al., 2002b; Hirose et al., 2005). Other CYPs like CYP71, CYP72A31, and CYP81A6 were also found to catalyze herbicide degradation in crops and model organisms (Werck-Reichhart et al., 2000; Pan et al., 2006; Xiang et al., 2006; Zhang et al., 2007; Saika et al., 2014). Herbicide safeners are used to selectively protect crops from herbicide damage because they induce the expression of genes involved in herbicide metabolism, among them several CYPs (Davies and Caseley, 1999; Persans et al., 2001). In weeds, resistance to ALS inhibitors was associated with CYP72A254, CYP81A12, and CYP81A21 in rice barnyardgrass (*Echinochloa phyllopogon*) (Iwakami et al., 2014a; Iwakami et al., 2014b), CYP71A, CYP71B, and CYP81D in blackgrass (*Alopecurus myosuroides*) (Gardin et al., 2015), and CYP72A and CYP81B1 in rye-grass (*Lolium sp.*) (Duhoux et al., 2015). EMR to ACCase inhibitors in annual ryegrass (*Lolium rigidum*) was traced to CYP72A as well (Gaines et al., 2014).

This study identified CYP72A219 and CYP81E8 (similar to CYP81D11) as candidates for metabolic resistance to tembotrione in *A. palmeri.* Interestingly, these genes fall into some of the same CYP families associated with metabolic resistance to ALS and ACCase inhibitors in grasses. This suggests that CYP72A and CYP81 act as key metabolic resistance gene families. Similar observations were made with metabolic resistance to insecticides where eight CYP families were identified, many of which belong to tight genomic clusters resulting from recent duplication or conversion events (David et al., 2013). For example, CYP6P9, which confers resistance to pyrethroids, was duplicated with extensive sequence variation (Wondji et al., 2009) and the simultaneous overexpression of the gene variants likely

increased the resistance level considerably (David et al., 2013). The variants found for CYP72A219 might be an indication for such a duplicated gene or homeologues derived from genome duplication.

CYPA219 has not been implicated in detoxification pathways before. The enzyme is thought to be closely related to CYP72A57 and CYP72A1 (Han et al., 2011) and is expressed in leaf tissue, but more so in roots in the medicinal plant *Nothapodytes nimmoniana* (Rather et al., 2018). CYP81E8, an isoflavone 2'-hydroxylase, is thought to be closely related to CYP81E1 and CYP81Q (Marques et al., 2013). The enzyme has previously been found in fungal infected leaves of barrelclover (*Medicago truncatula*) (Liu et al., 2003) and was also up-regulated in resistant citrus fruit after infection with the fungus *Penicillium digitatum* (Ballester et al., 2011). Furthermore, up-regulation of CYP81E8 was evident in glyphosate-susceptible soybean (*Glycine max*) 24 HAT with the herbicide (Zhu et al., 2008) as well as following the treatment with the photosystem II-inhibitor atrazine (log_2 FC 1.5, 2 HAT) or bentazon (log_2 FC 4.2, 4 HAT) (Zhu et al., 2009). This suggests that the enzyme is part of a pathogen- and herbicide-induced response that attempts to chemically reduce toxic effects in the plant.

Gene expression differences for CYP72A219 and CYP81E8 between R and S were detectable before treatment with tembotrione, but not after, thus resistance is probably constitutive. This expression pattern allows R to implement detoxification before the herbicide damage becomes irreversible. Point mutations, insertions or deletions consistent with resistance could not be found in the contigs, but they may appear in an upstream gene-specific regulator such as a promoter or an enhancer motif, instead of the locus itself. As an example, a partial transposable element upstream of CYP6M10 was implicated in the induced expression of the gene which confers resistance to insecticides (Wilding et al., 2012). Alternatively, an increase in gene copy number could cause the overexpression of the candidate CYP genes (Gaines et al., 2010). Differences in the presence of transcription factors may also be the reason for the observed differential gene expression, e.g. the increased expression of several genes associated with resistance to ALS inhibitors in *E. phyllopogon* was suggested to be simultaneously regulated by a trans-element (Iwakami et al., 2014a). Epigenetic regulation may also play a role if the candidate genes were methylated in S individuals only.

Treatment with tembotrione further induced the expression of candidate genes in both R and S. CYP activation can be caused by a wide range of stimuli, among them pathogen attacks and pollutants, but also light, nutrient stress, and wounding (Schuler and Werck-Reichhart, 2003). For the RNA-Seq experiment the same individuals were sampled at different time points it cannot be excluded that the increase in CYP expression is at least partially caused by wounding. It is possible that the higher up-regulation of CYP81E8 in R plants of crosses A and B allowed them to recover quicker than R from cross C, which did not show significant up-regulation of CYP81E8 at either of the timepoints. Therefore, the up-regulation of CYP72A might be enough to confer resistance on its own even though resistance is less prominent than if CYP81E8 was involved as well. The increased constitutive expression and induction of GTs after treatment in R may also play a role in the resistance mechanism because a trend towards faster creation of glycolysylated metabolites was apparent in R (Figure 2-3). This would also explain the increased expression of ABC transporters in R 12 HAT. At this point in time, metabolites in R would have undergone phase I and II metabolism enough to be available for phase III enzymes.

Aside from candidate genes for resistance, tembotrione also triggered the up-regulation of various other CYPs in R and S individuals which is consistent with transcriptome studies in *Arabidopsis thaliana* that found 10% of all CYPs to be upregulated after herbicide exposure (Glombitza et al., 2004). The higher number of up-regulated CYPs in S might reflect stronger herbicide stress. Previous research in *A. myosuroides* described an initial shock phase after treatment with an ALS inhibitor with stress-signaling pathways being triggered (6-12 HAT) followed by an acclimation phase in which resources were diverted to defense processes (24-73HAT) (Gardin et al., 2015).

This study identified two CYP genes associated with metabolic herbicide resistance in the dicot weed *A. palmeri*. Future research is going to focus on sequencing of the two candidate genes CYP72A219 and CYP81E8 to verify their assembly and annotation. Quantitative polymerase chain reaction (qPCR) will be performed to investigate copy number variations for the candidate genes. In a series of steps for functional validation, reverse transcription (RT)-qPCR will be used to validate the results of the RNA-Seq experiment. Furthermore, the candidate genes will be tested in samples from other populations with

increased metabolic resistance to HPPD inhibitors (e.g. *A. palmeri* from Kansas and *A. tuberculatus* from Nebraska). The candidate sequences will also be cloned into yeast to test if they are sufficient to confer resistance to tembotrione or other HPPD inhibitors and to investigate herbicide-specificity and cross-resistance to herbicides from different chemical classes. Gaining knowledge about the connection between specific CYPs and herbicides they confer resistance to is crucial to predict compound liabilities, improve the design of herbicides, and allow for better diagnostics and management of metabolic resistance in the field.

TABLES

Table 3-1: Setup of the RNA-Seq experiment with Pseudo-F_2 *A. palmeri* originating from three separate crosses of parental tembotrione-resistant (R) and -susceptible (S) individuals. Six individuals that were highly resistant and highly susceptible were chosen from each cross and sampled at three different timepoints including before, 6 and 12 h after treatment with tembotrione (HAT).

		0 HAT	6 HAT	12 HAT
Cross A	R	6	6	6
R_{male} x S_{female}	S	6	6	6
Cross B	R	6	6	6
R_{male} x S_{female}	S	6	6	6
Cross C	R	6	6	6
R_{female} x S_{male}	S	6	6	6

Table 3-2: Identification and *A. hypochondriacus* genome location of putative differentially expressed contigs at timepoint 0 between all tembotrione-resistant and -susceptible Pseudo-F_2 *A. palmeri* using RNA-Seq. Fold change in CPM (counts-per-million). False discovery rate (FDR), fold change (FC), cytochrome P450 monooxygenase (CYP), 7-deoxyloganetic acid glucosyltransferase (UGT), Anthocyanidin 3-O-glyosyltranserse (A3-GT), scopoletin glucosyltransferase (Sco-GT), multicopper oxidase (LPR2), glutathione-S-transferase (GST).

Annotation	Log_2FC	FDR	Scaffold
CYP 72A219 a	3.3	0.0004	4
CYP 72A219 b	2.5	0.003	4
CYP 72A219 c	2.7	0.002	4
CYP 72A219 d	2.4	0.005	4
CYP 72A219 e	2.4	0.007	4
CYP 81E8	4.3	0.0008	4
A3-GT1	2.5	0.007	2
A3-GT3	2.2	0.005	unknown
A3-GT6	2.2	0.003	3
GST U22	3.6	0.004	unknown
LPR2	2.5	0.006	2
Sco-GT1	2.1	0.0007	2
Sco-GT2	2.1	0.0003	unknown

Table 3-3: Putative differentially expressed cytochrome P450 monooxygenase (CYP) contigs comparing tembotrione-resistant and -susceptible Pseudo-F_2 *A. palmeri* after treatment with tembotrione, respectively. Hours after treatment (HAT), false discovery rate (FDR), fold change (FC).

Annotation	6 HAT				12 HAT			
	Tembotrione-resistant		Tembotrione-susceptible		Tembotrione-resistant		Tembotrione-susceptible	
	Log_2FC	FDR	Log_2FC	FDR	Log_2FC	FDR	Log_2FC	FDR
CYP71A1							4.0	< 0.0001
CYP71A3	3.4	0.004	3.4	0.0003	3.8	< 0.0001	3.8	< 0.0001
CYP71A							2.6	0.002
CYP76C2							2.5	< 0.0001
CYP78A	2.3	0.01			4.5	< 0.0001	4.7	< 0.0001
CYP83B1							3.8	< 0.0001
CYP81F3					2.3	< 0.0001	2.3	< 0.0001
CYP82D47					2.2	0.001	2.9	< 0.001

FIGURES

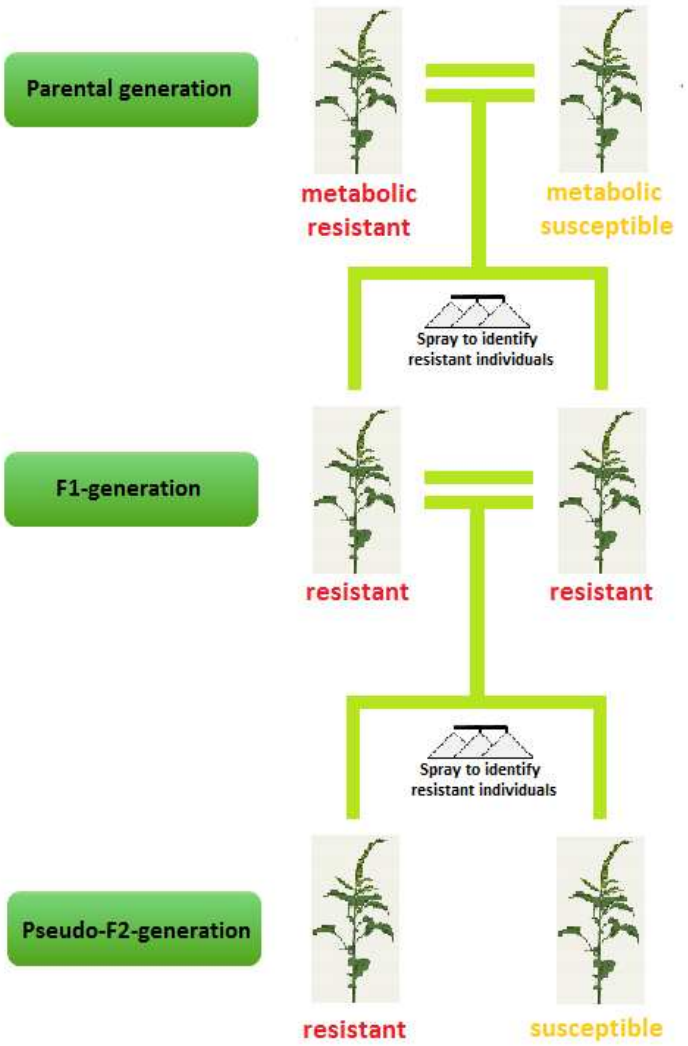

Figure 3-1: Generation of the pseudo-F_2 crosses in preparation for the RNA-Sequencing experiment with F_2 *A. palmeri*. Three separate crosses with tembotrione-resistant and -susceptible parents were performed followed by crossing of tembotrione-surviving F_1 individuals. The resulting pseudo-F_2 generation was used for RNA-Sequencing.

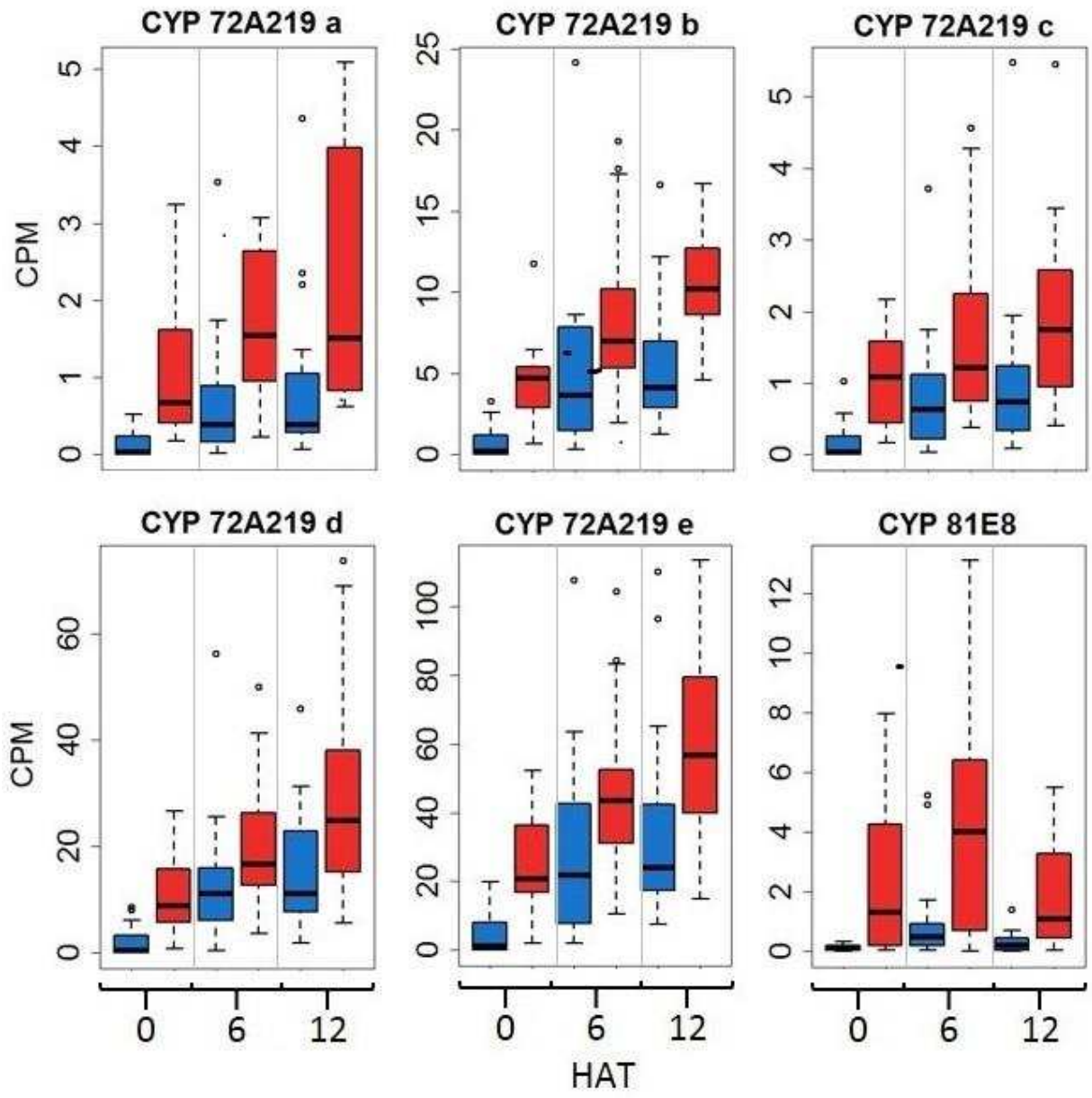

Figure 3-2: Cytochrome P450 monooxygenase (CYP) contigs that are candidate genes for metabolic resistance to tembotrione. Their expression differences in tembotrione-susceptible (blue) and -resistant (red) Pseudo-F_2 *A. palmeri* at 0, 6, and 12 h after treatment (HAT) with tembotrione. Counts-per-million reads (CPM).

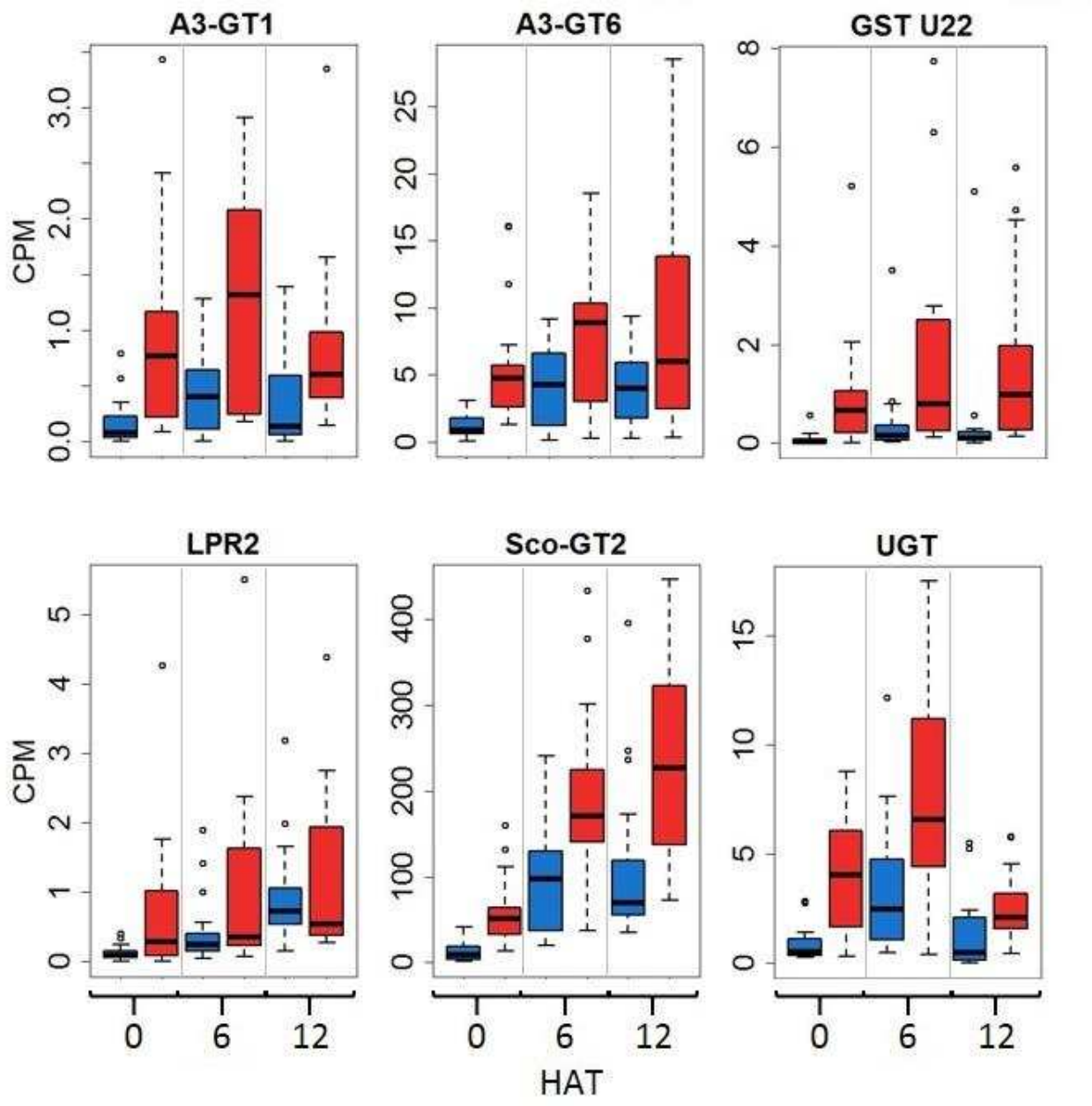

Figure 3-3: Gene expression differences of selected putative non-cytochrome P450 monooxygenase contigs that co-segregate with metabolic resistance to tembotrione in tembotrione-susceptible (blue) and -resistant (red) Pseudo-F_2 *A. palmeri* at 0, 6, and 12 h after treatment (HAT) with tembotrione. Counts-per-million reads (CPM). 7-deoxyloganetic acid glucosyltransferase (UGT), Anthocyanidin 3-O-glyosyltranserse (A3-GT), scopoletin glucosyltransferase (Sco-GT), multicopper oxidase (LPR2), glutathione-S-transferase (GST).

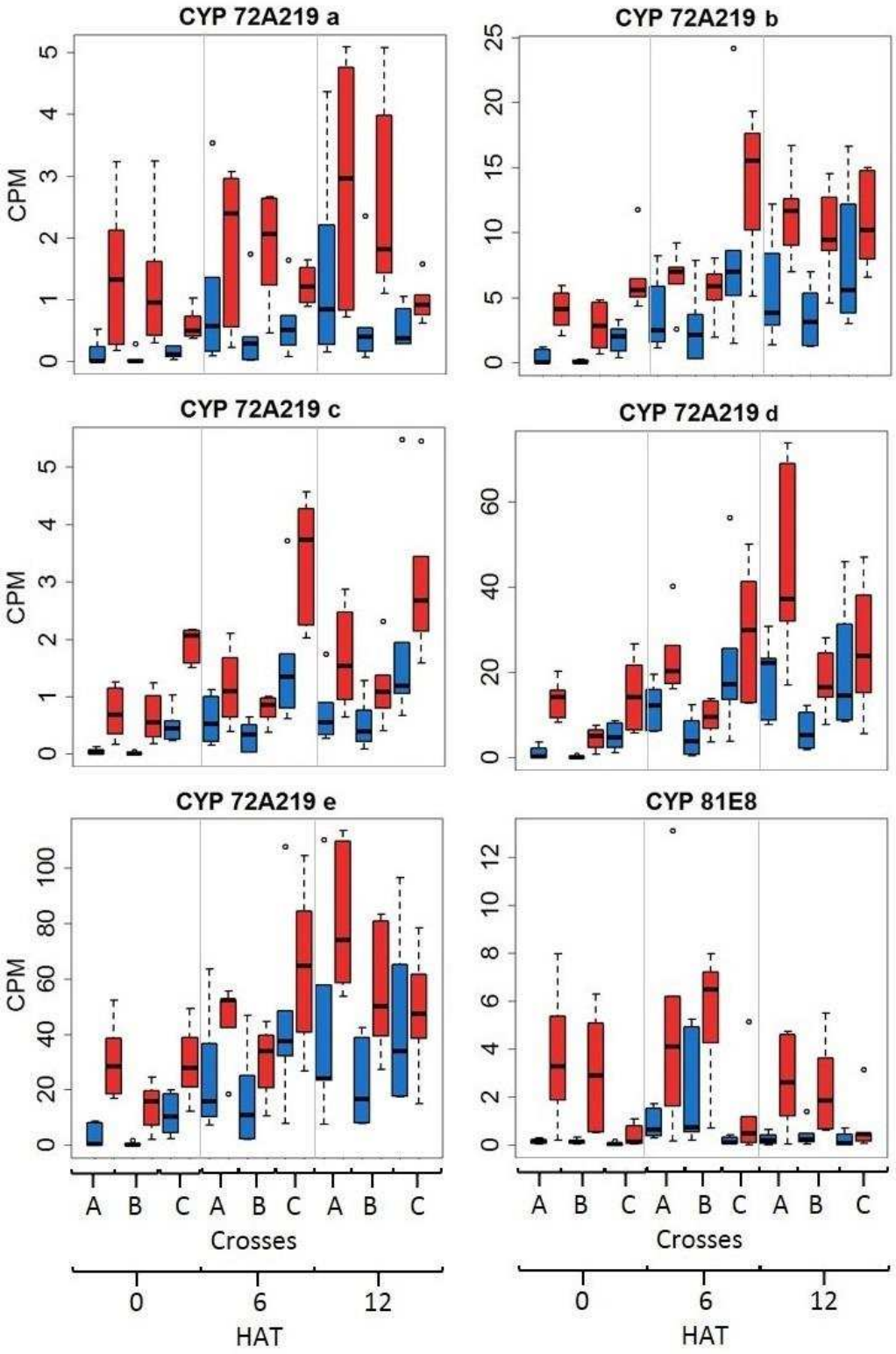

Figure 3-4: Cytochrome P450 monooxygenase (CYP) contigs that are candidate genes for metabolic resistance to tembotrione. Their expression differences in tembotrione-susceptible (blue) and -resistant (red) Pseudo-F_2 *A. palmeri* at 0, 6, and 12 h after treatment (HAT) with tembotrione, separated by cross. Counts-per-million reads (CPM).

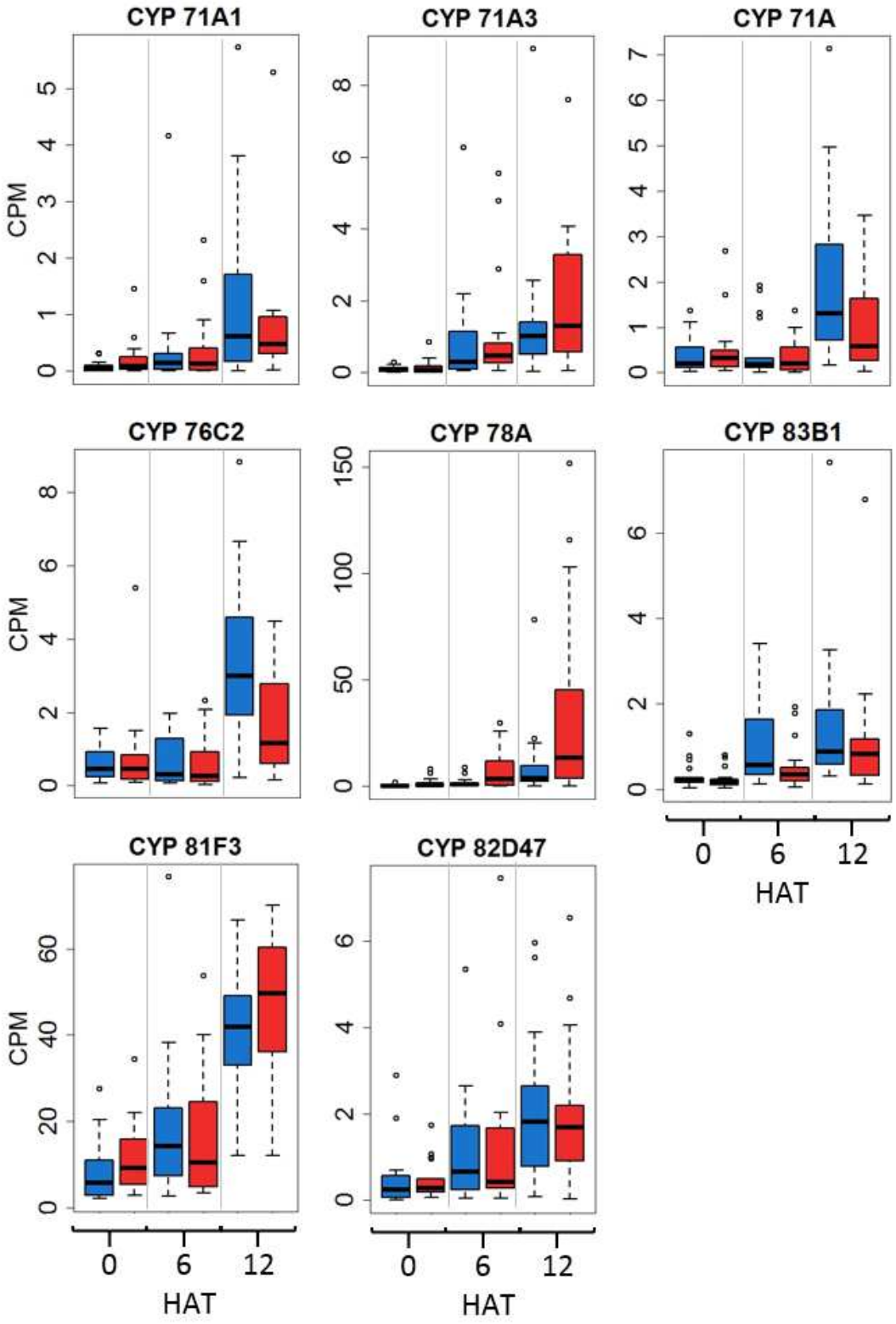

Figure 3-5: Gene expression differences of putative cytochrome P450 monooxygenase (CYP) contigs comparing tembotrione-susceptible (blue) and -resistant (red) Pseudo-F_2 *A. palmeri* after treatment with tembotrione, respectively. Hours after treatment (HAT), counts-per-million reads (CPM).

REFERENCES

Andrews, S. (2010). *FastQC: a quality control tool for high throughput sequence data. Reference Source* [Online]. http://www.bioinformatics.babraham.ac.uk/projects/fastqc.

Ballester, A.-R., Lafuente, M.T., Forment, J., Gadea, J., De Vos, R.C., Bovy, A.G., et al. (2011). Transcriptomic profiling of citrus fruit peel tissues reveals fundamental effects of phenylpropanoids and ethylene on induced resistance. *Mol. Plant Pathol.* 12(9)**,** 879-897.

Barrett, M. (2000). The role of cytochrome P450 enzymes in herbicide metabolism. *Herbicides and Their Mechanisms of Action. Boca Raton, FL: CRC***,** 25-37.

Bartholomew, D.M., Van Dyk, D.E., Lau, S.-M.C., O'Keefe, D.P., Rea, P.A., and Viitanen, P.V. (2002). Alternate energy-dependent pathways for the vacuolar uptake of glucose and glutathione conjugates. *Plant Physiol.* 130(3)**,** 1562-1572.

Beckie, H.J., and Tardif, F.J. (2012). Herbicide cross resistance in weeds. *Crop Prot.* 35**,** 15-28.

Bendtsen, J.D., Nielsen, H., von Heijne, G., and Brunak, S. (2004). Improved prediction of signal peptides: SignalP 3.0. *J. Mol. Biol.* 340(4)**,** 783-795.

Bolger, A.M., Lohse, M., and Usadel, B. (2014). Trimmomatic: a flexible trimmer for Illumina sequence data. *Bioinformatics* 30(15)**,** 2114-2120.

Bollman, J.D., Boerboom, C.M., Becker, R.L., and Fritz, V.A. (2008). Efficacy and tolerance to HPPD-inhibiting herbicides in sweet corn. *Weed Technol.* 22(4)**,** 666-674.

Brazier, M., Cole, D.J., and Edwards, R. (2002). O-Glucosyltransferase activities toward phenolic natural products and xenobiotics in wheat and herbicide-resistant and herbicide-susceptible black-grass (*Alopecurus myosuroides*). *Phytochem.* 59(2)**,** 149-156.

Busi, R., Neve, P., and Powles, S. (2013). Evolved polygenic herbicide resistance in *Lolium rigidum* by low-dose herbicide selection within standing genetic variation. *Evol. Appl.* 6(2)**,** 231-242.

Busi, R., Porri, A., Gaines, T., and Powles, S. (2017). Pyroxasulfone resistance in *Lolium rigidum* conferred by enhanced metabolic capacity. *bioRxiv***,** DOI: 10.1101/116269.

Busi, R., Vila-Aiub, M., and Powles, S. (2011). Genetic control of a cytochrome P450 metabolism-based herbicide resistance mechanism in Lolium rigidum. *Heredity* 106(5)**,** 817.

Chahal, P.S., Aulakh, J.S., Jugulam, M., and Jhala, A.J. (2015). *Herbicide-resistant Palmer amaranth (Amaranthus palmeri S. Wats.) in the United States—Mechanisms of resistance, impact, and management.* InTechOpen, Rijeka, Croatia.

CoGe (2018). *Comparatice Genomics* [Online]. https://genomevolution.org/coge/. [Accessed].

Cummins, I., Wortley, D.J., Sabbadin, F., He, Z., Coxon, C.R., Straker, H.E., et al. (2013). Key role for a glutathione transferase in multiple-herbicide resistance in grass weeds. *Proc. Nat. Acad. Sci. USA* 110(15)**,** 5812-5817.

David, J.-P., Ismail, H.M., Chandor-Proust, A., and Paine, M.J.I. (2013). Role of cytochrome P450s in insecticide resistance: impact on the control of mosquito-borne diseases and use of insecticides on Earth. *Phil. Trans. R. Soc. B* 368(1612)**,** 20120429.

Davies, J., and Caseley, J.C. (1999). Herbicide safeners: A review. *Pest Manag. Sci.* 55(11)**,** 1043-1058.

Delye, C. (2013). Unravelling the genetic bases of non-target-site-based resistance (NTSR) to herbicides: a major challenge for weed science in the forthcoming decade. *Pest Manag. Sci.* 69(2)**,** 176-187.

Delye, C., Jasieniuk, M., and Le Corre, V. (2013). Deciphering the evolution of herbicide resistance in weeds. *Trends Genet.* 29(11)**,** 649-658.

Didierjean, L., Gondet, L., Perkins, R., Lau, S.-M.C., Schaller, H., O'Keefe, D.P., et al. (2002). Engineering herbicide metabolism in tobacco and Arabidopsis with CYP76B1, a cytochrome P450 enzyme from Jerusalem artichoke. *Plant Physiol.* 130(1)**,** 179-189.

Duhoux, A., Carrère, S., Duhoux, A., and Délye, C. (2017). Transcriptional markers enable identification of rye-grass (*Lolium sp.*) plants with non-target-site-based resistance to herbicides inhibiting acetolactate-synthase. *Plant Sci.* 257**,** 22-36.

Duhoux, A., Carrère, S., Gouzy, J., Bonin, L., and Délye, C. (2015). RNA-Seq analysis of rye-grass transcriptomic response to an herbicide inhibiting acetolactate-synthase identifies transcripts linked to non-target-site-based resistance. *Plant Mol. Biol.* 87(4-5)**,** 473-487.

Elmore, M.T., Brosnan, J.T., Armel, G.R., Kopsell, D.A., Best, M.D., Mueller, T.C., et al. (2015). Cytochrome P450 inhibitors reduce creeping bentgrass (*Agrostis stolonifera*) tolerance to topramezone. *PloS One* 10(7)**,** e0130947.

Finn, R.D., Clements, J., and Eddy, S.R. (2011). HMMER web server: Interactive sequence similarity searching. *Nucl. Acid Res.* 39(suppl_2)**,** W29-W37.

Gaines, T.A., Lorentz, L., Figge, A., Herrmann, J., Maiwald, F., Ott, M.C., et al. (2014). RNA-Seq transcriptome analysis to identify genes involved in metabolism-based diclofop resistance in *Lolium rigidum*. *Plant J.* 78(5)**,** 865-876.

Gaines, T.A., Zhang, W., Wang, D., Bukun, B., Chisholm, S.T., Shaner, D.L., et al. (2010). Gene amplification confers glyphosate resistance in *Amaranthus palmeri*. *Proc. Nat. Acad. Sci. USA* 107(3)**,** 1029-1034.

Gardin, J.A.C., Gouzy, J., Carrère, S., and Délye, C. (2015). ALOMYbase, a resource to investigate non-target-site-based resistance to herbicides inhibiting acetolactate-synthase (ALS) in the major grass weed *Alopecurus myosuroides* (black-grass). *BMC Genomics* 16(1)**,** 590.

Gardner, S.N., Gressel, J., and Mangel, M. (1998). A revolving dose strategy to delay the evolution of both quantitative vs major monogene resistances to pesticides and drugs. *Intl. J. Pest Manag.* 44(3)**,** 161-180.

Giacomini, D.A., Kuepper, A., Gaines, T.A., Beffa, R., and Tranel, P.J. (2016). A comparative analysis of the Palmer amaranth and waterhemp transcritpomes. *Proceedings of the North Central Weed Science Society, Des Moines, IA* 71: 63.

Glombitza, S., Dubuis, P.-H., Thulke, O., Welzl, G., Bovet, L., Götz, M., et al. (2004). Crosstalk and differential response to abiotic and biotic stressors reflected at the transcriptional level of effector genes from secondary metabolism. *Plant Mol. Biol.* 54(6)**,** 817-835.

Grausem, B., Chaubet, N., Gigot, C., Loper, J.C., and Benveniste, P. (1995). Functional expression of Saccharomyces cerevisiae CYP51A1 encoding lanosterol-14-demethylase in tobacco results in bypass of endogenous sterol biosynthetic pathway and resistance to an obtusifoliol-14-demethylase herbicide inhibitor. *Plant J.* 7(5)**,** 761-770.

Haas, B.J., Papanicolaou, A., Yassour, M., Grabherr, M., Blood, P.D., Bowden, J., et al. (2013). *De novo* transcript sequence reconstruction from RNA-seq using the Trinity platform for reference generation and analysis. *Nat. Protoc.* 8(8)**,** 1494.

Han, J.-Y., Kim, H.-J., Kwon, Y.-S., and Choi, Y.-E. (2011). The Cyt P450 enzyme CYP716A47 catalyzes the formation of protopanaxadiol from dammarenediol-II during ginsenoside biosynthesis in *Panax ginseng*. *Plant Cell Physiol.* 52(12)**,** 2062-2073.

Hausman, N.E., Singh, S., Tranel, P.J., Riechers, D.E., Kaundun, S.S., Polge, N.D., et al. (2011). Resistance to HPPD-inhibiting herbicides in a population of waterhemp (*Amaranthus tuberculatus*) from Illinois, United States. *Pest Manag. Sci.* 67(3)**,** 258-261.

Heap, I. (2018). *The International Survey of Herbicide Resistant Weeds. Online. Available:* www.weedscience.org [Online]. Available: www.weedscience.org [Accessed January 30, 2018].

Hirose, S., Kawahigashi, H., Ozawa, K., Shiota, N., Inui, H., Ohkawa, H., et al. (2005). Transgenic rice containing human CYP2B6 detoxifies various classes of herbicides. *J. Agric. Food Chem.* 53(9)**,** 3461-3467.

Honkakoski, P., and Negishi, M. (2000). Regulation of cytochrome P450 genes by nuclear receptors. *Biochem. J.* 347. doi: 10.1042/bj3470321.

Iwakami, S., Endo, M., Saika, H., Okuno, J., Nakamura, N., Yokoyama, M., et al. (2014a). Cytochrome P450 CYP81A12 and CYP81A21 are associated with resistance to two acetolactate synthase inhibitors in *Echinochloa phyllopogon*. *Plant Physiol.* 165(2)**,** 618-629.

Iwakami, S., Uchino, A., Kataoka, Y., Shibaike, H., Watanabe, H., and Inamura, T. (2014b). Cytochrome P450 genes induced by bispyribac-sodium treatment in a multiple-herbicide-resistant biotype of *Echinochloa phyllopogon*. *Pest Manag. Sci.* 70(4)**,** 549-558.

Jhala, A.J., Sandell, L.D., Rana, N., Kruger, G.R., and Knezevic, S.Z. (2014). Confirmation and control of triazine and 4-hydroxyphenylpyruvate dioxygenase-inhibiting herbicide-resistant Palmer amaranth (*Amaranthus palmeri*) in Nebraska. *Weed Technol.* 28(1)**,** 28-38.

Kaundun, S.S., Hutchings, S.J., Dale, R.P., Howell, A., Morris, J.A., Kramer, V.C., et al. (2017). Mechanism of resistance to mesotrione in an *Amaranthus tuberculatus* population from Nebraska, USA. *PLoS One* 12(6)**,** 1-22. doi: 10.1371/journal.pone.0180095.

Krueger, F. *Trim Galore!* [Online]. http://www.bioinformatics.babraham.ac.uk/projects/trim_galore/. [Accessed].

Küpper, A., Peter, F., Zöllner, P., Lorentz, L., Tranel, P.J., Beffa, R., et al. (2017). Tembotrione detoxification in 4-hydroxyphenylpyruvate dioxygenase (HPPD) inhibitor-resistant Palmer amaranth (*Amaranthus palmeri* S. Wats.). *Pest Manag. Sci.*

Langmead, B., and Salzberg, S.L. (2012). Fast gapped-read alignment with Bowtie 2. *Nature Methods* 9(4)**,** 357.

Leah, J.M., Caseley, J.C., Riches, C.R., and Valverde, B. (1994). Association between elevated activity of aryl acylamidase and propanil resistance in Jungle-rice, *Echinochloa colona*. *Pest Manag. Sci.* 42(4)**,** 281-289.

Letouzé, A., and Gasquez, J. (2003). Enhanced activity of several herbicide-degrading enzymes: a suggested mechanism responsible for multiple resistance in blackgrass (*Alopecurus myosuroides* Huds.). *Agronomie* 23(7)**,** 601-608.

Li, H., Handsaker, B., Wysoker, A., Fennell, T., Ruan, J., Homer, N., et al. (2009). The sequence alignment/map format and SAMtools. *Bioinformatics* 25(16)**,** 2078-2079.

Liu, C.J., Huhman, D., Sumner, L.W., and Dixon, R.A. (2003). Regiospecific hydroxylation of isoflavones by cytochrome p450 81E enzymes from *Medicago truncatula*. *Plant J.* 36(4)**,** 471-484.

Marques, J.V., Kim, K.-W., Lee, C., Costa, M.A., May, G.D., Crow, J.A., et al. (2013). Next generation sequencing in predicting gene function in podophyllotoxin biosynthesis. *J. Biol. Chem.* 288(1)**,** 466-479.

Matringe, M., Sailland, A., Pelissier, B., Rolland, A., and Zink, O. (2005). p-Hydroxyphenylpyruvate dioxygenase inhibitor-resistant plants. *Pest Manag. Sci.* 61(3)**,** 269-276.

McMullan, P.M., and Green, J.M. (2011). Identification of a tall waterhemp (*Amaranthus tuberculatus*) biotype resistant to HPPD-inhibiting herbicides, atrazine, and thifensulfuron in Iowa. *Weed Technol.* 25(3)**,** 514-518.

Nakka, S., Godar, A.S., Wani, P.S., Thompson, C.R., Peterson, D.E., Roelofs, J., et al. (2017). Physiological and molecular characterization of hydroxyphenylpyruvate dioxygenase (HPPD)-inhibitor resistance in Palmer amaranth (*Amaranthus palmeri* S. Wats.). *Front. Plant Sci.* 8**,** 555.

Neve, P., and Powles, S. (2005). Recurrent selection with reduced herbicide rates results in the rapid evolution of herbicide resistance in *Lolium rigidum*. *Theor. Appl. Genet.* 110(6)**,** 1154-1166. doi: 10.1007/s00122-005-1947-2.

Oliveira, M., Dayan, F., Gaines, T., Patterson, E., Jhala, A., and Knezevic, S. (2017). Reversing resistance to tembotrione in an *Amaranthus tuberculatus* (var. *rudis*) population from Nebraska, USA with cytochrome P450 inhibitors. *Pest Manag. Sci.***,** doi: 10.1002/ps.4697.

Pallett, K., Little, J., Sheekey, M., and Veerasekaran, P. (1998). The mode of action of isoxaflutole: I. Physiological effects, metabolism, and selectivity. *Pest. Biochem. Physiol.* 62(2)**,** 113-124.

Pan, G., Zhang, X., Liu, K., Zhang, J., Wu, X., Zhu, J., et al. (2006). Map-based cloning of a novel rice cytochrome P450 gene CYP81A6 that confers resistance to two different classes of herbicides. *Plant Mol. Biol.* 61(6)**,** 933-943.

Pataky, J.K., Meyer, M.D., Bollman, J.D., Boerboom, C.M., and Williams, M.M. (2008). Genetic basis for varied levels of injury to sweet corn hybrids from three cytochrome P450-metabolized herbicides. *J. Am. Soc. Hortic. Sci.* 133(3)**,** 438-447.

Persans, M.W., Wang, J., and Schuler, M.A. (2001). Characterization of maize cytochrome P450 monooxygenases induced in response to safeners and bacterial pathogens. *Plant Physiol.* 125(2)**,** 1126-1138.

Petit, C., Duhieu, B., Boucansaud, K., and Délye, C. (2010). Complex genetic control of non-target-site-based resistance to herbicides inhibiting acetyl-coenzyme A carboxylase and acetolactate-synthase in *Alopecurus myosuroides* Huds. *Plant Sci.* 178(6)**,** 501-509.

Preston, C. (2003). Inheritance and linkage of metabolism-based herbicide cross-resistance in rigid ryegrass (*Lolium rigidum*). *Weed Sci.* 51(1)**,** 4-12.

Preston, C. (2004). Herbicide resistance in weeds endowed by enhanced detoxification: Complications for management. *Weed Sci.* 52(3)**,** 448-453.

Rather, G.A., Sharma, A., Pandith, S.A., Kaul, V., Nandi, U., Misra, P., et al. (2018). *De novo* transcriptome analyses reveals putative pathway genes involved in biosynthesis and regulation of camptothecin in *Nothapodytes nimmoniana* (Graham) Mabb. *Plant Mol. Biol.* 96(1-2)**,** 197-215.

Reade, J.P., Milner, L.J., and Cobb, A.H. (2004). A role for glutathione S-transferases in resistance to herbicides in grasses. *Weed Sci.* 52(3)**,** 468-474.

Renton, M., Diggle, A., Manalil, S., and Powles, S. (2011). Does cutting herbicide rates threaten the sustainability of weed management in cropping systems? *J. Theor. Biol.* 283(1)**,** 14-27.

Robineau, T., Batard, Y., Nedelkina, S., Cabello-Hurtado, F., LeRet, M., Sorokine, O., et al. (1998). The chemically inducible plant cytochrome P450 CYP76B1 actively metabolizes phenylureas and other xenobiotics. *Plant Physiol.* 118(3)**,** 1049-1056.

Robinson, J.T., Thorvaldsdóttir, H., Winckler, W., Guttman, M., Lander, E.S., Getz, G., et al. (2011). Integrative genomics viewer. *Nat. Biotechnol.* 29(1)**,** 24.

Robinson, M.D., McCarthy, D.J., and Smyth, G.K. (2010). edgeR: a Bioconductor package for differential expression analysis of digital gene expression data. *Bioinformatics* 26(1)**,** 139-140.

Saika, H., Horita, J., Taguchi-Shiobara, F., Nonaka, S., Nishizawa-Yokoi, A., Iwakami, S., et al. (2014). A novel rice cytochrome P450 gene, CYP72A31, confers tolerance to acetolactate synthase-inhibiting herbicides in rice and Arabidopsis. *Plant Physiol.* 166(3)**,** 1232-1240.

Schuler, M.A., and Werck-Reichhart, D. (2003). Functional genomics of P450s. *Annu. Rev. Plant Biol.* 54**,** 629-667. doi: 10.1146/annurev.arplant.54.031902.134840.

Schultz, J.L., Chatham, L.A., Riggins, C.W., Tranel, P.J., and Bradley, K.W. (2015). Distribution of herbicide resistances and molecular mechanisms conferring resistance in Missouri waterhemp (*Amaranthus rudis* Sauer) populations. *Weed Sci.* 63(1)**,** 336-345.

Schwartz-Lazaro, L.M., Norsworthy, J.K., Scott, R.C., and Barber, L.T. (2017). Resistance of two Arkansas *Palmer amaranth* populations to multiple herbicide sites of action. *Crop Prot.* 96**,** 158-163.

Shiota, N., Kodama, S., Inui, H., and Ohkawa, H. (2000). Expression of human cytochromes P450 1A1 and P450 1A2 as fused enzymes with yeast NADPH-cytochrome P450 oxidoreductase in transgenic tobacco plants. *Biosci. Biotechnol. Biochem.* 64(10)**,** 2025-2033.

Sievers, F., Wilm, A., Dineen, D., Gibson, T.J., Karplus, K., Li, W., et al. (2011). Fast, scalable generation of high-quality protein multiple sequence alignments using Clustal Omega. *Mol. Syst. Biol.* 7(1)**,** 539.

Siminszky, B., Corbin, F.T., Ward, E.R., Fleischmann, T.J., and Dewey, R.E. (1999). Expression of a soybean cytochrome P450 monooxygenase cDNA in yeast and tobacco enhances the metabolism of phenylurea herbicides. *Proc. Nat. Acad. Sci. USA* 96(4)**,** 1750-1755.

Van Eerd, L.L., Hoagland, R.E., Zablotowicz, R.M., and Hall, J.C. (2003). Pesticide metabolism in plants and microorganisms. *Weed Sci.* 51(4)**,** 472-495.

Waxman, D.J. (1999). P450 gene induction by structurally diverse xenochemicals: Central role of nuclear receptors CAR, PXR, and PPAR. *Arch. Biochem. Biophys.* 369(1)**,** 11-23.

Werck-Reichhart, D., and Feyereisen, R. (2000). Cytochromes P450: A success story. *Genome Biol.* 1(6)**,** 3003. 3001-3003.3009.

Werck-Reichhart, D., Hehn, A., and Didierjean, L. (2000). Cytochromes P450 for engineering herbicide tolerance. *Trends Plant Sci.* 5(3)**,** 116-123.

Wilding, C.S., Smith, I., Lynd, A., Yawson, A.E., Weetman, D., Paine, M.J., et al. (2012). A cis-regulatory sequence driving metabolic insecticide resistance in mosquitoes: functional characterisation and signatures of selection. *Insect Biochem. Mol. Biol.* 42(9)**,** 699-707.

Wondji, C.S., Irving, H., Morgan, J., Lobo, N.F., Collins, F.H., Hunt, R.H., et al. (2009). Two duplicated P450 genes are associated with pyrethroid resistance in *Anopheles funestus*, a major malaria vector. *Genome Res.* 19(3)**,** 452-459.

Wu, T.D., and Watanabe, C.K. (2005). GMAP: a genomic mapping and alignment program for mRNA and EST sequences. *Bioinformatics* 21(9)**,** 1859-1875.

Xiang, W., Wang, X., and Ren, T. (2006). Expression of a wheat cytochrome P450 monooxygenase cDNA in yeast catalyzes the metabolism of sulfonylurea herbicides. *Pest. Biochem. Physiol.* 85(1)**,** 1-6.

Yamada, T., Ishige, T., Shiota, N., Inui, H., Ohkawa, H., and Ohkawa, Y. (2002a). Enhancement of metabolizing herbicides in young tubers of transgenic potato plants with the rat CYP1A1 gene. *Theor. Appl. Genet.* 105(4)**,** 515-520.

Yamada, T., Ohashi, Y., Ohshima, M., Inui, H., Shiota, N., Ohkawa, H., et al. (2002b). Inducible cross-tolerance to herbicides in transgenic potato plants with the rat CYP1A1 gene. *Theor. Appl. Genet.* 104(2-3)**,** 308-314.

Yang, Q., Deng, W., Li, X., Yu, Q., Bai, L., and Zheng, M. (2016). Target-site and non-target-site based resistance to the herbicide tribenuron-methyl in flixweed (*Descurainia sophia L.*). *BMC Genomics* 17(1)**,** 551.

Yu, Q., Han, H., Cawthray, G., Wang, S., and Powles, S. (2013). Enhanced rates of herbicide metabolism in low herbicide-dose selected resistant *Lolium rigidum*. *Plant Cell Environ.* 36(4)**,** 818-827.

Yuan, J.S., Tranel, P.J., and Stewart, C.N. (2007). Non-target-site herbicide resistance: A family business. *Trends Plant Sci.* 12(1)**,** 6-13.

Zhang, L., Lu, Q., Chen, H., Pan, G., Xiao, S., Dai, Y., et al. (2007). Identification of a cytochrome P450 hydroxylase, CYP81A6, as the candidate for the bentazon and sulfonylurea herbicide resistance gene, Bel, in rice. *Molecular breeding* 19(1)**,** 59-68.

Zhu, J., Patzoldt, W.L., Radwan, O., Tranel, P.J., and Clough, S.J. (2009). Effects of photosystem-II-interfering herbicides atrazine and bentazon on the soybean transcriptome. *The Plant Genome* 2(2)**,** 191-205.

Zhu, J., Patzoldt, W.L., Shealy, R.T., Vodkin, L.O., Clough, S.J., and Tranel, P.J. (2008). Transcriptome response to glyphosate in sensitive and resistant soybean. *J. Agric. Food Chem.* 56(15)**,** 6355-6363.

4. MULTIPLE RESISTANCE TO GLYPHSATE AND ALS INHIBITORS IN PALMER AMARANTH (*AMARANTHUS PALMERI*) IDENTIFIED IN BRAZIL[3]

INTRODUCTION

Palmer amaranth (*Amaranthus palmeri* S. Watson) is native to the United States and is originally from semiarid regions (Sauer, 1957). The weed is rarely found in South American countries: however, recent surveys conducted in Argentina have found that Palmer amaranth is established and problematic in southern Córdoba and San Luis states in soybean, peanuts, sorghum, and corn (Morichetti et al., 2013). It was reported in Brazil for the first time in 2015 where it was found growing in cotton fields in Mato Grosso State (Andrade Júnior et al., 2015; Carvalho et al., 2015).

Before Palmer amaranth's recent introduction, Brazilian weed scientists reported ten *Amaranthus* species (Kissman and Groth, 1999), including low amaranth (*A. deflexus*), smooth pigweed (*A. hybridus*), spiny amaranth (*A. spinosus*), redroot pigweed (*A. retroflexus*), and slender amaranth (*A. viridis*) (Carvalho et al., 2008). Palmer amaranth can be distinguished from other species by the absence of pubescence on the stem, with a petiole longer than the leaf blade and the presence of slightly spiny structures on the female flowers (Sauer, 1957). Palmer amaranth is dioecious (Sauer, 1957) and no other dioecious *Amaranthus* species are known to occur in Brazil. This flowering structure ensures cross-pollination (Franssen et al., 2001) and high genetic variability, factors that contribute to its adaptive and evolutionary success (Ward et al., 2013).

Palmer amaranth is an annual dicotyledonous species with C4 photosynthesis and is able to survive extreme conditions of low humidity and high temperatures. It is a problematic species because it is highly competitive with agricultural crops (Ward et al., 2013). Palmer amaranth has become one of the most important weeds in cotton and soybean fields in the United States, especially since many

[3] Anita Küpper, Ednaldo A. Borgato, Eric L. Patterson, Acácio Gonçalves Netto, Marcelo Nicolai, Saul J. P. de Carvalho, Scott J. Nissen, Todd A. Gaines, Pedro J. Christoffoleti

populations have multiple herbicide resistance (Sosnoskie et al., 2011; Nandula et al., 2012). A major problem in managing Palmer amaranth is the rapid selection and the potential for rapid dispersion of herbicide resistance.

Palmer amaranth introduced in Brazil is resistant to glyphosate, requiring doses higher than 4,500 g ae ha^{-1} to reduce plant growth by 80%, a threshold where control with glyphosate is no longer considered economically viable (Carvalho et al., 2015). Dose-response studies also confirmed that these populations were cross-resistant to the ALS inhibitors chlorimuron, imazethapyr and cloransulan, confirming a case of multiple resistance (Gonçalves Netto et al., 2016).

Given the importance of accurate species identification and determining herbicide response to inform appropriate management decisions, the objectives of this research were to 1) confirm the identification of the new *Amaranthus* species discovered in Brazil; 2) confirm and characterize the multiple resistance to glyphosate and ALS inhibitor herbicides; and 3) identify the mechanisms conferring ALS and glyphosate resistance in the Brazilian population.

MATERIALS AND METHODS

Plant Material

The glyphosate-resistant (BR-R) Palmer amaranth population was collected from a field site in Ipiranga do Norte, Mato Grosso, Brazil. The glyphosate-susceptible (GA-S) Palmer amaranth population was originally collected in 2004 from the University of Georgia Ponder Farm Research Station (Culpepper et al., 2006). A known waterhemp (*A. tuberculatus*) population from Nebraska was used for species identification (Bernards et al., 2012).

Species-Diagnostic Marker

Waterhemp is another dioecious species in the *Amaranthus* genus but not known to be present in Brazil. Additionally, a single nucleotide polymorphism in the acetolactate synthase (ALS) gene has been utilized to genetically identify waterhemp and Palmer amaranth (Tranel et al., 2002). To determine if the

dioecious Amaranthus individuals collected in Brazil were Palmer amaranth or waterhemp, a genotyping protocol was developed using the ALS polymorphism. Approximately 50 mg of young leaf tissue from three untreated GA-S individuals, six untreated BR-R individuals, and three known waterhemp individuals were used for DNA extraction using a modified CTAB extraction protocol (Doyle, 1991). Samples were placed in tubes, a metal bead was added and then the tubes were frozen in liquid nitrogen. The samples were ground using a Qiagen TissueLyser II (Qiagen Inc., Valencia, CA 91355) for 1 min at 30 oscillations per second. The ground tissue was incubated with 500 µL of 2× CTAB buffer with 4 µL of 2-mercaptoethanol at 50 C for 15 min. The suspension was then incubated for 15 min with 500 µL of 24:1 chloroform:isoamyl alcohol with gentle agitation and then centrifuged for 15 min at 15,000×g. The aqueous phase was removed and re-separated using another 500 µL of 24:1 chloroform:isoamyl alcohol and centrifuged for 5 min at 15,000×g. The aqueous phase was once again removed and then precipitated with 50 µL sodium acetate (3M, pH 5.2) and 1650 µL of 100% ethanol. After 15-min at room temperature, samples were centrifuged for 15,000×g for 15 min. All liquid was removed and the pellets were rinsed with 70% ethanol and allowed to dry. Dry pellets were re-suspended in water. DNA concentration and quality were determined using a micro-spectrophotometer (NanoDrop 2000 Spectrophotometer, Thermo Fisher Scientific, Wilmington, DE 19810).

Amaranthus KASP Genotyping. To determine whether individuals in the BR-R population were Palmer amaranth or waterhemp, a KASP assay was developed to genotype a species-diagnostic single nucleotide polymorphism (SNP) located at base-pair 678 in the acetolacetate synthase (*ALS*) coding sequence (Tranel et al., 2002). The assay was performed using six control individuals, (three GA-S Palmer amaranth individuals, three Nebraska waterhemp individuals) and six untreated individuals from the BR-R population. SNP678 is a cytosine (C) in waterhemp individuals and a thymine (T) in Palmer amaranth individuals. Two species-diagnostic forward primers for SNP_{678} were developed that were identical except the final 3' nucleotide which pairs with SNP_{678}. Additionally, each forward primer contained nucleotides at its 5' end specific for either a HEX or FAM labeled oligo contained in the LGC Genomics Master Mix (waterhemp forward primer: 5'-

GAAGGTGACCAAGTTCATGCTAAAAAGAAAGCTTCCTTAACAATTCTAGGG-3’; Palmer amaranth forward primer: 5’-GAAGGTCGGAGTCAACGGATTAAAAAGAAAGCTTCCTTAACAATTCTAGGA-3’). For PCR a universal reverse primer (5'-GTTGAGGTAACTCGATCCATTACTAAGC-3') was developed that was complementary in both *Amaranthus* species.

Forward and reverse primers were mixed according to manufacturer recommendations and included 18 µL waterhemp forward primer (FAM label) at 12 µM, 18 µL Palmer amaranth forward primer (HEX label) at 12 µM, and 45 µL of universal reverse primer at 30 µM. Primer mix was brought up to 150 µL with 10 mM Tris-HCl, pH 8.3. A master-mix was then generated from 11.8 µL of primer mix and 432 µL of LGC Genomics Master Mix. Final reactions were mixed in a 96 well, optically clear plate by combining 4 µL of *Amaranthus* DNA at 5 ng/µL with 4 µL of LGC Genomics Master Mix plus primers. PCR was performed on a Biorad CFX Connect with the following cycling protocol: 94 C for 15 min; followed by 10 cycles of 94 C° for 20 sec, 61 decreasing to 55 C° for 60 sec (0.6 C° touchdown per cycle); followed by 26 cycles of 94 C° for 20 sec, and 55 C° for 60 sec. An end point fluorescence read was taken by cooling the plate to 30 C° for 30 sec, and reading the plate in both the HEX and FAM fluorescent channels. HEX and FAM fluorescence were corrected by removing the background fluorescence observed in a no-template control. Fluorescence was plotted in a 2D scatterplot so that the test BR-R population individuals could be compared to known waterhemp and Palmer amaranth samples. Waterhemp samples (primers labeled with FAM) were expected to have high fluorescence intensity for FAM but not HEX, while Palmer amaranth samples (primers labeled with HEX) were expected to have high fluorescence intensity for HEX but not FAM. Clustering of the test BR-R individuals with either high FAM or high HEX fluorescence intensity would indicate their identity as waterhemp or Palmer amaranth, respectively. Each KASP genotyped sample was independently confirmed using the *Eco*RV PCR-RFLP developed by Tranel et al. (2002) (data not shown).

Greenhouse Glyphosate Dose-Response

A dose-response experiment was carried out in the greenhouse of the Weed Research Laboratory at Colorado State University in Fort Collins, CO to quantify the level of glyphosate resistance. Seeds from the BR-R and GA-S Palmer amaranth populations were planted on 1% agar medium and placed in a refrigerator at 4 C for 7 d. They were then transferred to a germination bench at room temperature with 12/12 h of day/night to stimulate rapid and simultaneous germination. Germinated seedlings were then transplanted into commercial potting soil (Professional Growing Mix, Sun Gro Horticulture, Vancouver, Canada) in 5 by 5 cm inserts. They were treated with glyphosate at 8-10 cm height and kept in a greenhouse where they were maintained at 24 ± 2 C temperatures and 15/9 h day/night photoperiods supplemented with metal halide lamps (400 µmol m^{-2} s^{-1}) and watered twice daily. The experiment was arranged in a randomized complete block design with three replicates. Each replicate contained six individuals for each population and dose, and four individuals for each population and dose when the experiment was repeated. A glyphosate dose response was conducted using 0, 0.05, 0.08, 0.2, 0.4, 0.8, 1.6, 4.8 kg ae glyphosate ha^{-1} with commercially formulated glyphosate (potassium salt, Roundup Weather Max, Monsanto Co., St. Louis, MO). When the experiment was repeated an additional dose of 8 kg glyphosate ha^{-1} was included. Applications were made using an overhead track sprayer (DeVries Manufacturing, Hollandale, MN) equipped with a flat-fan nozzle tip (TeeJet 8002EVS, Spraying System Co. Wheaton, IL) calibrated to deliver 187 L ha^{-1} of spray solution at 172 kPa. Survival was recorded after 21 d, defined as any plant showing new growth. Dose response analysis was conducted using the drc package in R (Knezevic et al., 2007; R, 2015). Survival data (proportion) were analyzed using the three-parameter log-logistic model in the drc package:

$$y = \frac{D}{\left[1+\left(\frac{x}{LD_{50}}\right)^{b}\right]} \quad [1]$$

Where y = survival; x = glyphosate dose (g ae ha^{-1}); D = upper limit; b = slope; and LD_{50} = dose causing 50% reduction in survival.

Shikimate Assay

Twenty individuals each from the BR-R and the GA-S populations were grown in the greenhouse and tested for glyphosate resistance using an *in vivo* leaf-disc assay. Three technical replicates (5 mm leaf discs) from each individual per population were sampled, following the procedure described by Shaner et al. (2005). The excised leaf discs were placed into 96-well microtiter plates containing 10 mM ammonium phosphate buffer and molecular grade glyphosate at the doses of 100, 500 and 1000 µM. Shikimate levels were read at 380 nm on a fluorescence plate reader (BioTek™ Synergy™ 2 multi-mode microplate reader, Winooski, VT). A shikimate standard curve was used to quantify shikimate accumulation (ng shikimate μL^{-1}) in the samples. Data were analyzed using a t-test to compare shikimate accumulation between BR-R and GA-S.

EPSPS Gene Copy Number

Genomic DNA was used to determine 5-enolpyruvylshikimate-3-phosphate synthase (*EPSPS*) copy number using real-time quantitative PCR (qPCR). Twenty individuals each from the GA-S and BR-R populations were grown in small pots, and young leaf tissue was collected from each individual for genomic DNA. The samples were immediately frozen in liquid nitrogen and stored at -80 C. Genomic DNA was extracted using the Qiagen DNEasy Plant Mini Kit (Qiagen, Valencia, CA) and quantified using a NanoDrop spectrophotometer (Thermo Scientific, Wilmington, DE). DNA concentrations were adjusted to 5 ng μL^{-1} and primer sets and qPCR conditions were used as previously described (primers ALSF2 and ALSR2, EPSF1 and EPSR8) (Gaines et al., 2010). Threshold cycles (C_t) for *EPSPS* and *ALS* were recorded by a CFX Connect™ Real-Time PCR Detection System thermal cycler (Bio-Rad Laboratories, Hercules, CA). Relative *EPSPS* gene copy number was calculated as $2^{-\Delta Ct}$, with ΔCt = [(Ct, *ALS*) – (Ct, *EPSPS*)] (Gaines et al., 2010). Triplicate technical replications were used to calculate the mean and standard error of the increase in *EPSPS* gene copy number relative to *ALS*.

Single Dose ALS Testing

Single-dose experiments were conducted to assess resistance to the ALS inhibitors chlorsulfuron, sulfometuron-methyl (both sulfonylureas) and imazethapyr (imidazolinone). These experiments were conducted in the greenhouse at Colorado State University in Fort Collins, CO under the same conditions as described in the glyphosate dose-response experiment. Individuals from BR-R and GA-S were treated at 8-10 cm height. The experiments with sulfonylureas used 28 individuals per population and treatment combination, and the experiments with imazethapyr used 36 individuals for each population. Chlorsulfuron (Glean, DuPont) and sulfometuron-methyl (Oust, Bayer CropScience) were applied at 88 g ai ha^{-1} and 315 g ai ha^{-1}, respectively. Imazethapyr (Pursuit, BASF) was applied at 61 g ai ha^{-1} with 1.25% v/v crop oil concentrate (COC). Height (cm), dry weight (g), and survival data were collected 21 d after treatment. The data were analyzed using ANOVA and LSD with P=0.05 was used for multiple comparison adjustment.

ALS Gene Sequence

Approximately 50 mg of young leaf tissue was samples from each of three untreated GA-S individuals, six untreated BR-R individuals, nine BR-R individuals that survived 315 g ai ha^{-1} sulfometuron-methyl, and nine BR-R individuals that survived 88 g ai ha^{-1} chlorsulfuron. DNA was extracted as described for the species-diagnostic marker. The full-length *ALS* gene was amplified by PCR using the forward primer: 5'- ATGGCGTCCACTTCAACAAACC -3' and reverse primer 5'-CTAATAAGCCCTTCTTCCATCACCC -3'. Thirty µL reactions were mixed following the standard protocol provided with Thermo Scientific Phusion polymerase and 20 ng of template genomic DNA. Reactions were cycled 32 times with the following three step protocol: 98 C° for 10 sec, 62 C° for 20 sec, and 72 C° for 90 sec. PCR products were run on a 1% agarose gel to verify single band amplification. The expected bands at 2010 bp were excised from the gel and purified following the standard protocol provided by the QIAquick gel extraction kit from Qiagen. Purified PCR products were sequenced using both the amplification primers listed above as well as the following four sequencing primers: Seq_FP1 5'-

AGTTTGTATTGCCACTTCTGGTCC-3', Seq_FP2 5'-GAAATCCTCGCCAATGGCTGAC-3', Seq_RP1 5'- GTCAGCCATTGGCGAGGATTTC-3', Seq_RP2 5'-TGGACCAGAAGTGGCAATACAAAC-3'. Sanger sequencing reads were analyzed using A Plasmid Editor (aPe) and heterozygous base-pairs were identified in the sequence trace files by manual inspection. Translated amino acid sequences obtained from BR-R and GA-S were compared to a known susceptible Palmer amaranth ALS amino acid sequence (Molin et al., 2016), GenBank protein accession AMS38337.1.

RESULTS AND DISCUSSION

Species-Diagnostic Marker

The genotyping assay used to amplify a SNP within the *ALS* gene that distinguishes Palmer amaranth from waterhemp clearly grouped the BR-R individuals with Palmer amaranth GA-S individuals (Figure 4-1) due to the high HEX fluorescence intensity produced from the Palmer amaranth HEX-labeled forward primer. Known waterhemp individuals were clearly distinguished by the waterhemp allele at this SNP position, as shown by high FAM fluorescence intensity produced from the FAM-labeled forward primer specific for waterhemp. Therefore, the dioecious *Amaranthus* population collected from Mato Grosso State, Brazil is Palmer amaranth and not waterhemp. The *Eco*RV PCR-RFLP developed by Tranel et al. (2002) also produced the same species identification as our KASP assay (data not shown).

Greenhouse Dose-Response Curves

The data from two repeated greenhouse dose-response experiments were combined for analysis. The BR-R population was glyphosate resistant (Table 4-1, Figure 4-2), with an LD_{50} of 3,982 g ae ha^{-1}. The LD_{50} for GA-S was 169 g ae ha^{-1}, resulting in a resistance factor (R/S) of 24 (Table 4-1, Figure 4-2). This resistance factor confirms the resistance of the Brazilian Palmer amaranth population to glyphosate, and

demonstrates that the BR-R population has an LD_{50} higher than two times the typical commercial glyphosate rate (ranging from 800 to 1,000 g ae ha^{-1}).

Shikimate Assay

Shikimate is an important intermediate in the biosynthesis of the aromatic amino acids phenylalanine, tyrosine, and tryptophan. EPSPS inhibition by glyphosate results in shikimate accumulation (Steinrücken and Amrhein, 1980; Herrmann and Weaver, 1999; Shaner et al., 2005). There was a clear difference in shikimate accumulation between the two populations tested at all three glyphosate doses (Figure 4-3), with GA-S accumulating significantly more shikimate than BR-R. Increasing glyphosate doses, up to 1000 µM, did not cause shikimate accumulation in BR-R, a clear metabolic marker for glyphosate resistance. The lack of shikimate accumulation in the BR-R corroborates results obtained from the dose-response curves (Table 4-1, Figure 4-2), both confirming glyphosate resistance in the BR-R population. These results also confirm the findings of Carvalho et al. (2015) reporting glyphosate resistance of this Palmer amaranth population from the state of Mato Grosso, Brazil.

EPSPS Gene Copy Number

The qPCR technique was used to quantify *EPSPS* gene copy number relative to *ALS*. Between 1.1 and 1.5 relative *EPSPS* gene copies were measured in the GA-S population and between 50 and 179 relative *EPSPS* gene copies were measured in the BR-R population. Increased *EPSPS* gene copy number was highly correlated with reduced shikimate accumulation in BR-R individuals, while wild-type, single copy *EPSPS* was highly correlated with high shikimate accumulation in GA-S individuals (Figure 4-4). Individuals in the BR-R population have *EPSPS* gene duplication that results in EPSPS overexpression as a mechanism of glyphosate resistance, first reported in Palmer amaranth (Gaines et al., 2010).

A previously reported glyphosate-resistant Palmer amaranth population from Georgia, USA had a reported LD_{50} of 1,600 g e.a. ha^{-1} and between 40 and 100 relative *EPSPS* gene copies (Gaines et al., 2011). The BR-R population had an LD_{50} of 3,982 g ae ha^{-1} (Table 4-1) and *EPSPS* gene duplication

between 50 and 179 copies, suggesting that glyphosate resistance in BR-R is due to increased *EPSPS* gene copies. Increased *EPSPS* gene copy number as a glyphosate resistance mechanism has also been reported in Italian ryegrass (*Lolium perenne* var. *multiflorum*) (Salas et al., 2012), waterhemp (Lorentz et al., 2014; Chatham et al., 2015), spiny amaranth (*A. spinosus*) (Nandula et al., 2014), ripgut brome (*Bromus diandrus*) (Malone et al., 2016), kochia (*Kochia scoparia*) (Wiersma et al., 2015), and goosegrass (*Eleusine indica*) (Chen et al., 2015).

Single-Dose ALS Testing

A high percentage of BR-R individuals survived following treatment with chlorsulfuron, sulfometuron, and imazethapyr (Table 4-2). The GA-S population was completely controlled by all three ALS herbicides. Plant height and dry weight also indicated that BR-R individuals were resistant to all three ALS herbicides, while GA-S individuals were susceptible (Table 4-2). The high survival rate of BR-R after ALS herbicide treatment is consistent with previous observations of high-level ALS herbicide resistance in Palmer amaranth (Burgos et al., 2001; Whaley et al., 2007; Wise et al., 2009; Guo et al., 2015).

ALS Gene Sequencing

Sequencing the *ALS* gene from both populations resulted in the identification of two independent mutations in the BR-R *ALS* gene sequence, resulting in a change from tryptophan to leucine at position 574 ($W_{574}L$) and serine to asparagine at position 653 ($S_{653}N$) (Table 4-4, Figure 4-5). The $W_{574}L$ mutation confers resistance to both imidazolinones and sulfonylureas, while the $S_{653}N$ mutation confers resistance only to imidazolinones (Sprague et al., 1997; Burgos et al., 2001; Franssen et al., 2001; Tranel and Wright, 2002; McCourt et al., 2006; Patzoldt and Tranel, 2007; Powles and Yu, 2010). Nearly all BR-R individuals were either heterozygous or homozygous for $W_{574}L$, while 10 of 24 sequenced individuals were heterozygous for $S_{653}N$; none were homozygous for $S_{653}N$. No individuals carried both $W_{574}L$ and $S_{653}N$ mutations within the same allele. ALS resistance is inherited as a dominant trait (Tranel and

Wright, 2002; Powles and Yu, 2010), which explains the high survival rate of heterozygous *ALS* mutants in BR-R. No other *ALS* mutations were detected, but four BR-R individuals that survived either chlorsulfuron or sulfometuron were homozygous for the susceptible allele at W_{574}, and all four were heterozygous for $S_{653}N$ (Table 4-4). Since the S653N is not known to confer resistance to sulfonylurea herbicides, these four individuals may have a different, non-target-site resistance mechanism. A different and undetected *ALS* target-site mutation is considered unlikely as the entire *ALS* gene was sequenced. All sequenced GA-S individuals were homozygous susceptible for both W_{574} and S_{653} (Table 4-4, Figure 4-5).

In wild radish (*Raphanus raphanistrum*), the $S_{653}N$ mutation confers resistance to the imidazolinones, while homozygous $W_{574}L$ confers resistance to sulfonylureas, imidazolinones and triazolpirimidines, three chemical families of ALS inhibitors (Yu et al., 2012). The presence of $W_{574}L$ gives high levels of resistance to these three chemical groups in waterhemp, while $S_{653}N$ is usually linked to imidazolinone resistance (Patzoldt and Tranel, 2007) as observed here.

Molin et al. (2016) reported both the $W_{574}L$ and the $S_{653}N$ mutation in Palmer amaranth, and showed the transfer of the $W_{574}L$ mutation from Palmer amaranth to hybrids between Palmer amaranth and spiny amaranth. Resistance to ALS inhibitors was reported in mucronate amaranth (*A. quitensis*) and Palmer amaranth from Argentina, with the $S_{653}N$ mutation observed only in mucronate amaranth but not in Palmer amaranth (Berger et al., 2016). The study concluded that the Palmer amaranth population in Argentina likely has a different ALS resistance mechanism than target-site mutation. While not definitive, the absence of $S_{653}N$ in Palmer amaranth from Argentina and the presence of both $W_{574}L$ and $S_{653}N$ in Palmer amaranth from Brazil suggests that independent introductions of Palmer amaranth may have occurred in the two countries.

This is the first study confirming through molecular methods the introduction of Palmer amaranth in Brazil and the molecular mechanisms of multiple resistance within this population to glyphosate and ALS inhibitors. The resistance mechanisms are, respectively, increased *EPSPS* gene copy number and target-site mutations in *ALS* ($W_{574}L$ and $S_{653}N$). Both mechanisms confer high resistance levels to these herbicides. Other known glyphosate resistance mechanisms such as vacuole sequestration (Ge et al.,

2010; Ge et al., 2012) and reduced translocation (Wakelin et al., 2004; Vila-Aiub et al., 2012) were not investigated. Increased *ALS* gene expression was also not investigated as a potential resistance mechanism. While these mechanisms have not yet been reported in Palmer amaranth, they cannot be ruled out based on the results of this study. Integrated management practices should be adopted in places where Palmer amaranth is found in Brazil, such as tank mixing herbicides with different modes of action, using pre-emergence herbicides, crop rotation, and integrating cover crops (Price et al., 2012; DeVore et al., 2013) for more effective Palmer amaranth control. Future research should focus on population genetics to determine the geographic route by which Palmer amaranth was introduced in Brazil and how to prevent possible new introductions of this and other species.

TABLES

Table 4-1: Confirmation of glyphosate resistance in Palmer amaranth from Brazil (BR-R) compared to a known glyphosate-susceptible population from Georgia (GA-S) in two repeated greenhouse dose-response experiments. Plant survival expressed as a proportion was used in a three-parameter log-logistic equation (Equation 1).

Population	D[a]	LD_{50}[b]	b[c]	R/S[d]	P value
BR-R	1.0	3,982 (310)	3.1	23.5 (3.3)	<0.0001
GA-S	0.96	169 (19)	1.8		

a: upper limit, b: herbicide dose in g ae ha-1 that causes 50% reduction in survival, standard error in parentheses, c: slope, d: ratio of LD50 for BR-R to LD50 for GA-S expressed as R/S resistance factor, standard error in parentheses

Table 4-2: A glyphosate-resistant Palmer amaranth population from Brazil (BR-R) is resistant to sulfonylurea and imidazolinone ALS herbicides. Plants were treated at 8-10 cm height. Survival, height, and dry weight data collected 21 DAT for single-dose treatments of chlorsulfuron (88 g ha^{-1}), sulfometuron (315 g ha^{-1}), and imazethapyr (61 g ha^{-1}) on BR-R and GA-S (glyphosate- and ALS-susceptible Palmer amaranth from Georgia). Standard deviation shown in parentheses; n, number of individuals tested per dose; letters within a column indicate significant difference at P=0.05.

Line	n	Herbicide	Alive (%)		Height (cm)		Dry weight (g)	
BR-R	28	Untreated	100 (0)	A	22.8 (8.2)	AB	2.3 (0.5)	A
BR-R	28	Chlorsulfuron	96 (20)	A	16.4 (6.0)	C	1.8 (0.8)	BC
BR-R	28	Sulfometuron	88 (33)	A	18.7 (8.4)	BC	1.5 (0.7)	C
GA-S	28	Untreated	100 (0)	A	27.5 (6.4)	A	2.1 (0.7)	AB
GA-S	28	Chlorsulfuron	0 (0)	B	8.1 (5.2)	D	0.9 (0.5)	D
GA-S	28	Sulfometuron	0 (0)	B	8.0 (4.3)	D	0.8 (0.5)	D
BR-R	36	Untreated	100 (0)	A	17.8 (3.3)	B	1.3 (0.5)	B
BR-R	36	Imazethapyr	100 (0)	A	19.3 (3.0)	AB	1.8 (0.3)	A
GA-S	36	Untreated	100 (0)	A	20.5 (4.8)	A	1.5 (0.5)	B
GA-S	36	Imazethapyr	0 (0)	B	7.4 (3.3)	C	0.8 (0.4)	C

Table 4-3: Alignment of *ALS* amino acid sequences from a known ALS-inhibitor-susceptible *A. palmeri* (GenBank AMS38337.1) and three glyphosate-resistant individuals from Georgia, Tennessee, and Arizona.

AMS38337.1-S	NNQHLGMVVQ**W**EDRFYKANRA	HQEHVLPMIP**S**GAAFKDTITE
GA-R 1-3	NNQHLGMVVQ**W**EDRFYKANRA	HQEHVLPMIP**S**GAAFKDTITE
TN-R 1	NNQHLGMVVQ**(W/L)**EDRFYKANRA	HQEHVLPMIP**S**GAAFKDTITE
TN-R 2-3	NNQHLGMVVQ**W**EDRFYKANRA	HQEHVLPMIP**S**GAAFKDTITE
AZ-R 1	NNQHLGMVVQ**W**EDRFYKANRA	HQEHVLPMIP**(S/N)**GAAFKDTITE
AZ-R 2	NNQHLGMVVQ**(W/L)**EDRFYKANRA	HQEHVLPMIP**S**GAAFKDTITE
AZ-R 3	NNQHLGMVVQ**W**EDRFYKANRA	HQEHVLPMIP**S**GAAFKDTITE

Table 4-4: Two target-site *ALS* mutations are present in ALS-resistant Palmer amaranth from Brazil (BR-R). All BR-R individuals that survived a single-dose treatment with chlorsulfuron or sulfometuron had at least one ALS-resistance conferring allele at position W574 (resistant allele L) or S653 (resistant allele N) of ALS. All individuals from GA-S were homozygous for the susceptible allele at W574 and S653. Homozygous resistant allele (HOMO R, dark cells); heterozygous (HET, gray cells); homozygous susceptible allele (HOMO S, light cells).

			Mutation and Genotype	
			W574L	S653N
Population	Treatment	Individual	TGG → TTG	AGC → AAC
BR-R	Chlorsulfuron	1	HET	HOMO S
		2	HET	HOMO S
		3	HOMO S	HET
		4	HOMO R	HOMO S
		5	HET	HOMO S
		6	HOMO S	HET
		7	HET	HET
		8	HOMO S	HET
		9	HET	HOMO S
	Sulfometuron	1	HOMO S	HET
		2	HET	HOMO S
		3	HET	HOMO S
		4	HOMO R	HOMO S
		5	HET	HOMO S
		6	HET	HET
		7	HET	HET
		8	HOMO R	HOMO S
		9	HET	HET
	Untreated	1	HET	HOMO S
		2	HET	HET
		3	HOMO R	HOMO S
		4	HET	HOMO S
		5	HET	HET
		6	HOMO R	HOMO S
GA-S	Untreated	1	HOMO S	HOMO S
		2	HOMO S	HOMO S
		3	HOMO S	HOMO S

FIGURES

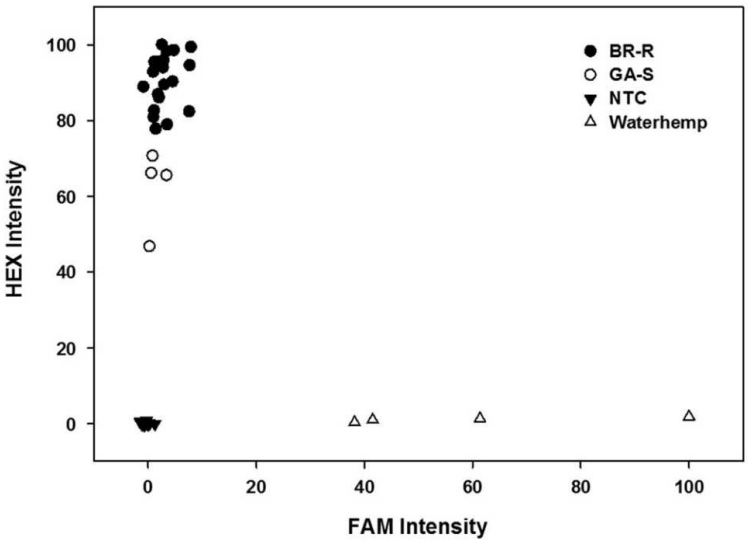

Figure 4-1: Genotyping assay using KASP where Palmer amaranth forward primers in the KASP assay were labeled with HEX, and waterhemp forward primers were labeled with FAM. Clustering of the Brazilian population (BR-R) together with known Palmer amaranth (GA-S) for high HEX fluorescence intensity confirms that BR-R is Palmer amaranth. Known waterhemp samples showed expected high FAM fluorescence intensity, and no template control (NTC) had no fluorescence for HEX or FAM.

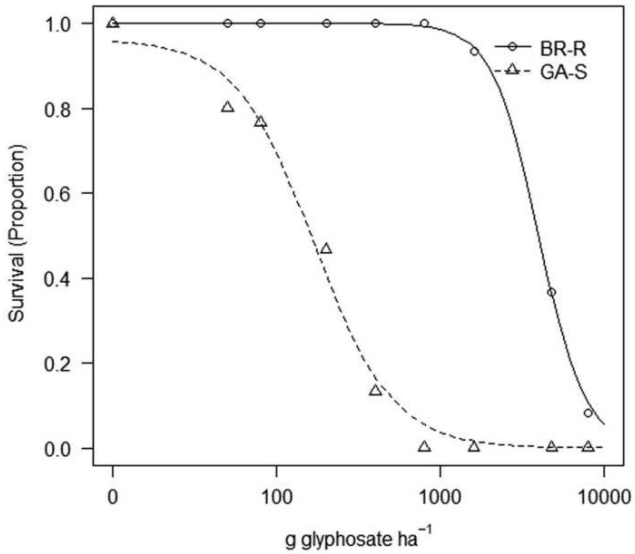

Figure 4-2: Greenhouse glyphosate dose-response curves for plant survival of a glyphosate-resistant Palmer amaranth population from Brazil (BR-R) and glyphosate-susceptible Palmer amaranth from Georgia (GA-S) expressed as the proportion of survivors (Equation 1).

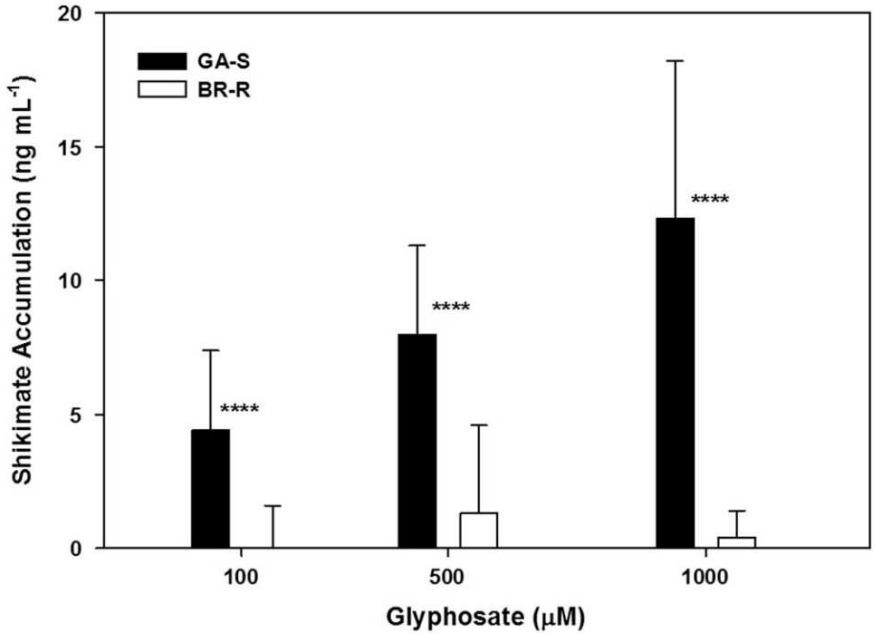

Figure 4-3: Shikimate accumulation in glyphosate-resistant Palmer amaranth from Brazil (BR-R) and glyphosate-susceptible Palmer amaranth from Georgia (GA-S) at three glyphosate doses. Mean from 20 biological replications with standard deviation; **** indicates p-value < 0.0001 between GA-S and BR-R at each dose.

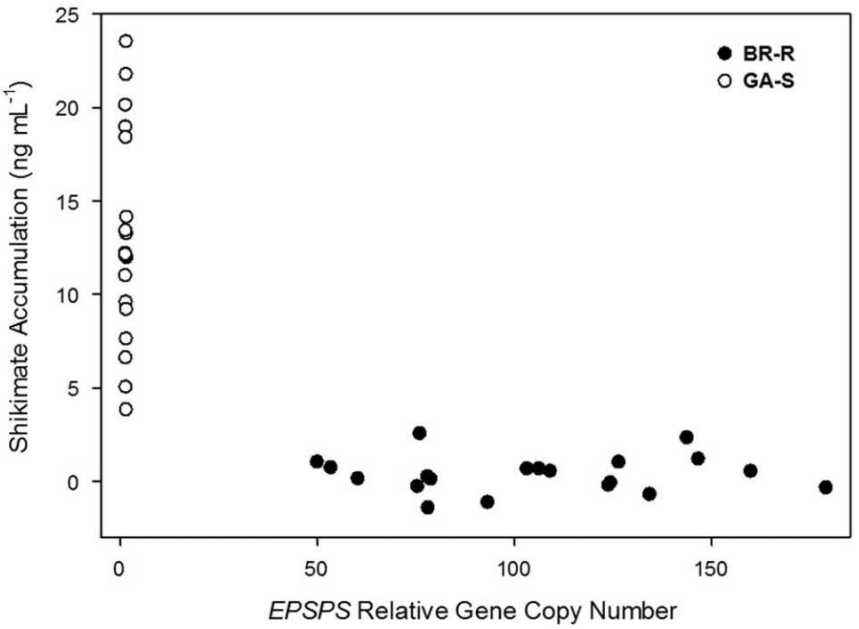

Figure 4-4: *EPSPS* relative genomic copy number and shikimate accumulation after treatment of leaf discs with 1000 µM glyphosate in glyphosate-resistant Palmer amaranth from Brazil (BR-R) and glyphosate-susceptible Palmer amaranth from Georgia (GA-S).

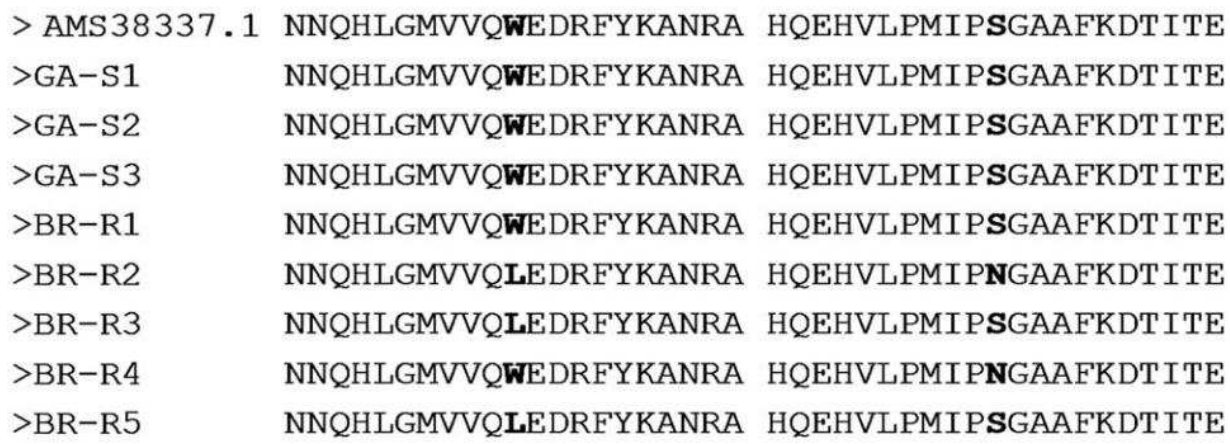

Figure 4-5: Alignment of ALS amino acid sequences from known ALS-susceptible Palmer amaranth (GenBank AMS38337.1), glyphosate- and ALS-susceptible Palmer amaranth from Georgia (GA-S), and glyphosate- and ALS-resistant Palmer amaranth from Brazil (BR-R) individuals showing W574L and S653N mutations in BR-R individuals.

REFERENCES

Andrade Júnior, E., Cavaenaghi, A., Guimarães, S., and Carvalho, S. (2015). Primeiro relato de *Amaranthus palmeri* no Brasil em áreas agrícolas no estado de Mato Grosso (First report of *Amaranthus palmeri* in Brazil in agricultural areas in the state of Mato Grosso, Portuguese). *Circular Técnica IMA-MT* 19**,** 1-8.

Berger, S., Madeira, P.T., Ferrell, J., Gettys, L., Morichetti, S., Cantero, J.J., et al. (2016). Palmer amaranth (*Amaranthus palmeri*) identification and documentation of ALS-resistance in Argentina. *Weed Sci.* 64(2)**,** 312-320.

Bernards, M.L., Crespo, R.J., Kruger, G.R., Gaussoin, R., and Tranel, P.J. (2012). A waterhemp (*Amaranthus tuberculatus*) population resistant to 2,4-D. *Weed Sci.* 60(3)**,** 379-384.

Burgos, N.R., Kuk, Y.I., and Talbert, R.E. (2001). Amaranthus palmeri resistance and differential tolerance of *Amaranthus palmeri* and *Amaranthus hybridus* to ALS-inhibitor herbicides. *Pest Manag. Sci.* 57(5)**,** 449-457.

Carvalho, S., Goncalves Netto, A., Nicolai, M., Cavenaghi, A., Lopez-Ovejero, R., and Christoffoleti, P. (2015). Detection of glyphosate-resistant Palmer Amaranth (*Amaranthus palmeri*) in agricultural areas of Mato Grosso, Brazil. *Planta Daninha* 33(3)**,** 579-586.

Carvalho, S.J.P., López-Ovejero, R.F., and Christoffoleti, P.J. (2008). Crescimento e desenvolvimento de cinco espécies de plantas daninhas do gênero Amaranthus (Growth and development of five weed species of the genus Amaranthus, Portuguese). *Bragantia* 67(2)**,** 317-326.

Chatham, L.A., Wu, C., Riggins, C.W., Hager, A.G., Young, B.G., Roskamp, G.K., et al. (2015). EPSPS gene amplification is present in the majority of glyphosate-resistant Illinois waterhemp (*Amaranthus tuberculatus*) populations. *Weed Technol.* 29(1)**,** 48-55.

Chen, J., Huang, H., Zhang, C., Wei, S., Huang, Z., Chen, J., et al. (2015). Mutations and amplification of EPSPS gene confer resistance to glyphosate in goosegrass (*Eleusine indica*). *Planta* 242(4)**,** 859-868.

Culpepper, A.S., Grey, T.L., Vencill, W.K., Kichler, J.M., Webster, T.M., Brown, S.M., et al. (2006). Glyphosate-resistant Palmer amaranth (*Amaranthus palmeri*) confirmed in Georgia. *Weed Sci.* 54(4)**,** 620-626.

DeVore, J.D., Norsworthy, J.K., and Brye, K.R. (2013). Influence of deep tillage, a rye cover crop, and various soybean production systems on *Palmer amaranth* emergence in soybean. *Weed Technol.* 27(2)**,** 263-270.

Doyle, J. (1991). *DNA protocols for plants–CTAB total DNA isolation.* Springer: Berlin.

Franssen, A.S., Skinner, D.Z., Al-Khatib, K., Horak, M.J., and Kulakow, P.A. (2001). Interspecific hybridization and gene flow of ALS resistance in *Amaranthus* species. *Weed Sci.* 49(5)**,** 598-606.

Gaines, T.A., Shaner, D.L., Ward, S.M., Leach, J.E., Preston, C., and Westra, P. (2011). Mechanism of resistance of evolved glyphosate-resistant Palmer amaranth (*Amaranthus palmeri*). *J. Agric. Food Chem.* 59(11)**,** 5886-5889.

Gaines, T.A., Zhang, W., Wang, D., Bukun, B., Chisholm, S.T., Shaner, D.L., et al. (2010). Gene amplification confers glyphosate resistance in *Amaranthus palmeri*. *Proc. Nat. Acad. Sci. USA* 107(3)**,** 1029-1034.

Ge, X., d'Avignon, D.A., Ackerman, J.J., and Sammons, R.D. (2010). Rapid vacuolar sequestration: The horseweed glyphosate resistance mechanism. *Pest Manag. Sci.* 66(4)**,** 345-348.

Ge, X., d'Avignon, D.A., Ackerman, J.J., Collavo, A., Sattin, M., Ostrander, E.L., et al. (2012). Vacuolar glyphosate-sequestration correlates with glyphosate resistance in ryegrass (*Lolium* spp.) from Australia, South America, and Europe: a 31P NMR investigation. *J. Agric. Food Chem.* 60(5)**,** 1243-1250.

Gonçalves Netto, A., Nicolai, M., Carvalho, S.J.P., Borgato, E.A., and Christoffoleti, P.J. (2016). Multiple resistance of *Amaranthus palmeri* to ALS and EPSPS inhibiting herbicides in the State of Mato Grosso, Brazil. *Planta Daninha* 34(3)**,** 581-587.

Guo, J., Riggins, C.W., Hausman, N.E., Hager, A.G., Riechers, D.E., Davis, A.S., et al. (2015). Nontarget-site resistance to ALS inhibitors in waterhemp (*Amaranthus tuberculatus*). *Weed Sci.* 63(2)**,** 399-407.

Herrmann, K.M., and Weaver, L.M. (1999). The shikimate pathway. *Ann. Rev. Plant Biol.* 50(1)**,** 473-503.

Kissman, K., and Groth, D. (1999). Plantas infestantes e nocivas (Weeds and harmful plants, Portuguese). *Editora BASF* 2**,** 978.

Knezevic, S.Z., Streibig, J.C., and Ritz, C. (2007). Utilizing R software package for dose-response studies: the concept and data analysis. *Weed Technol.* 21(3)**,** 840-848.

Lorentz, L., Gaines, T.A., Nissen, S.J., Westra, P., Strek, H.J., Dehne, H.W., et al. (2014). Characterization of glyphosate resistance in *Amaranthus tuberculatus* populations. *J. Agric. Food Chem.* 62(32)**,** 8134-8142.

Malone, J.M., Morran, S., Shirley, N., Boutsalis, P., and Preston, C. (2016). EPSPS gene amplification in glyphosate-resistant *Bromus diandrus*. *Pest Manag. Sci.* 72(1)**,** 81-88.

McCourt, J.A., Pang, S.S., King-Scott, J., Guddat, L.W., and Duggleby, R.G. (2006). Herbicide-binding sites revealed in the structure of plant acetohydroxyacid synthase. *Proc. Nat. Acad. Sci. USA* 103(3)**,** 569-573.

Molin, W.T., Nandula, V.K., Wright, A.A., and Bond, J.A. (2016). Transfer and expression of ALS inhibitor resistance from Palmer Amaranth (*Amaranthus palmeri*) to an *A. spinosus* × *A. palmeri* hybrid. *Weed Sci.* 64(2)**,** 240-247.

Morichetti, S., Cantero, J.J., Núñez, C., Barboza, G.E., Amuchastegui, A., and Ferrell, J. (2013). On the presence of *Amaranthus palmeri* (Amaranthaceae) in Argentina. *Boletín de la Sociedad Argentina de Botánica* 48(2)**,** 347-353.

Nandula, V.K., Reddy, K.N., Koger, C.H., Poston, D.H., Rimando, A.M., Duke, S.O., et al. (2012). Multiple resistance to glyphosate and pyrithiobac in Palmer amaranth (*Amaranthus palmeri*) from Mississippi and response to flumiclorac. *Weed Sci.* 60(2)**,** 179-188.

Nandula, V.K., Wright, A.A., Bond, J.A., Ray, J.D., Eubank, T.W., and Molin, W.T. (2014). EPSPS amplification in glyphosate-resistant spiny amaranth (*Amaranthus spinosus*): a case of gene transfer via interspecific hybridization from glyphosate-resistant Palmer amaranth (*Amaranthus palmeri*). *Pest Manag. Sci.* 70(12)**,** 1902-1909.

Patzoldt, W.L., and Tranel, P.J. (2007). Multiple ALS mutations confer herbicide resistance in waterhemp (*Amaranthus tuberculatus*). *Weed Sci.* 55(5)**,** 421-428.

Powles, S.B., and Yu, Q. (2010). Evolution in action: Plants resistant to herbicides. *Annu. Rev. Plant. Biol.* 61**,** 317-347.

Price, A.J., Balkcom, K.S., Duzy, L.M., and Kelton, J.A. (2012). Herbicide and cover crop residue integration for *Amaranthus* control in conservation agriculture cotton and implications for resistance management. *Weed Technol.* 26(3)**,** 490-498.

R (2015). "R Core Team (2015). R: A language and environment for statistical computing. R Foundation for Statistical Computing, Vienna, Austria. URL http://www.R-project/org/.".).

Salas, R.A., Dayan, F.E., Pan, Z., Watson, S.B., Dickson, J.W., Scott, R.C., et al. (2012). EPSPS gene amplification in glyphosate-resistant Italian ryegrass (*Lolium perenne* ssp. *multiflorum*) from Arkansas. *Pest Manag. Sci.* 68(9)**,** 1223-1230.

Sauer, J. (1957). Recent migration and evolution of the dioecious amaranths. *Evol.* 11(1)**,** 11-31.

Shaner, D.L., Nadler-Hassar, T., Henry, W.B., and Koger, C.H. (2005). A rapid *in vivo* shikimate accumulation assay with excised leaf discs. *Weed Sci.* 53(6)**,** 769-774.

Sosnoskie, L.M., Kichler, J.M., Wallace, R.D., and Culpepper, A.S. (2011). Multiple resistance in Palmer amaranth to glyphosate and pyrithiobac confirmed in Georgia. *Weed Sci.* 59(3)**,** 321-325.

Sprague, C.L., Stoller, E.W., Wax, L.M., and Horak, M.J. (1997). Palmer amaranth (*Amaranthus palmeri*) and common waterhemp (*Amaranthus rudis*) resistance to selected ALS-inhibiting herbicides. *Weed Sci.* 45(2)**,** 192-197.

Steinrücken, H., and Amrhein, N. (1980). The herbicide glyphosate is a potent inhibitor of 5-enolpyruvylshikimic acid-3-phosphate synthase. *Biochem. Biophys. Res. Commun.* 94(4)**,** 1207-1212.

Tranel, P., Wassom, J., Jeschke, M., and Rayburn, A. (2002). Transmission of herbicide resistance from a monoecious to a dioecious weedy *Amaranthus* species. *Theor. Appl. Genet.* 105(5)**,** 674-679.

Tranel, P.J., and Wright, T.R. (2002). Resistance of weeds to ALS-inhibiting herbicides: what have we learned? *Weed Sci.* 50(6)**,** 700-712.

Vila-Aiub, M.M., Balbi, M.C., Distéfano, A.J., Fernández, L., Hopp, E., Yu, Q., et al. (2012). Glyphosate resistance in perennial *Sorghum halepense* (Johnsongrass), endowed by reduced glyphosate translocation and leaf uptake. *Pest Manag. Sci.* 68(3)**,** 430-436.

Wakelin, A., Lorraine-Colwill, D., and Preston, C. (2004). Glyphosate resistance in four different populations of *Lolium rigidum* is associated with reduced translocation of glyphosate to meristematic zones. *Weed Res.* 44(6)**,** 453-459.

Ward, S.M., Webster, T.M., and Steckel, L.E. (2013). Palmer amaranth (*Amaranthus palmeri*): A review. *Weed Technol.* 27(1)**,** 12-27.

Whaley, C.M., Wilson, H.P., and Westwood, J.H. (2007). A new mutation in plant ALS confers resistance to five classes of ALS-inhibiting herbicides. *Weed Sci.* 55(2)**,** 83-90.

Wiersma, A.T., Gaines, T.A., Preston, C., Hamilton, J.P., Giacomini, D., Buell, C.R., et al. (2015). Gene amplification of 5-enol-pyruvylshikimate-3-phosphate synthase in glyphosate-resistant *Kochia scoparia*. *Planta* 241(2)**,** 463-474.

Wise, A.M., Grey, T.L., Prostko, E.P., Vencill, W.K., and Webster, T.M. (2009). Establishing the geographical distribution and level of acetolactate synthase resistance of Palmer amaranth (*Amaranthus palmeri*) accessions in Georgia. *Weed Technol.* 23(2)**,** 214-220.

Yu, Q., Han, H., Li, M., Purba, E., Walsh, M., and Powles, S. (2012). Resistance evaluation for herbicide resistance–endowing acetolactate synthase (ALS) gene mutations using *Raphanus raphanistrum* populations homozygous for specific ALS mutations. *Weed Res.* 52(2)**,** 178-186.

5. POPULATION GENETIC STRUCTURE IN GLYPHOSATE-RESISTANT AND -SUSCEPTIBLE PALMER AMARANTH (*AMARANTHUS PALMERI*) POPULATIONS USING GENOTYPING-BY-SEQUENCING (GBS)[4]

INTRODUCTION

Since the introduction of transgenic soybean, corn, and cotton in the mid-1990s, herbicide-resistant varieties of these crops have largely replaced conventional varieties in the United States (Coupe and Capel, 2016). In 1996, glyphosate-resistant (GR) (Roundup Ready) crops were commercialized and as a result global glyphosate usage rose by about 15-fold (Benbrook, 2016), dominating the current herbicide market (Duke, 2017). The widespread reliance on glyphosate to the exclusion of all other weed control methods has resulted in high selection pressure and the evolution of GR weeds, including Palmer amaranth (*Amaranthus palmeri* S. Wats.) (Culpepper et al., 2006), which is now a major threat to many U.S. food production systems (Beckie, 2011).

A. palmeri is a dioecious, annual species with prolific seed production, pollen-mediated gene flow due to obligate outcrossing, and high genetic variability (Franssen et al., 2001; Sellers et al., 2003; Ward et al., 2013). As a member of the *Amaranthaeceae* family, *A. palmeri* is native to the southwestern United States and northwestern Mexico, having first been documented in Sonora, California, Arizona, New Mexico, and Texas in the late 19th century. During the early 20th century, the species started to spread east and northeast, probably because of human mediated seed dispersal (Sauer, 1957; Ward et al., 2013). In recent years, *A. palmeri* has expanded its distribution as far north as Ontario, Canada and as far east as Massachusetts, USA (Karteszc, 2014). The species made its first occurrence on the annual listing of most troublesome weeds in South Carolina in 1989 (Webster and Coble, 1997). By 2009 the weed was ranked

[4] Anita Küpper, Harish K. Manmathan, Darci Giacomini, Eric L. Patterson, William B. McCloskey, Todd A. Gaines

the most troublesome weed in cotton in the Southern U.S. (Webster and Nichols, 2012; Ward et al., 2013).

Resistance to glyphosate in *A. palmeri* was first reported from a GR cotton field in Georgia in 2004. Shortly after, another case was reported from North Carolina in 2005 (Culpepper et al., 2006; Culpepper et al., 2008). As of 2017, GR *A. palmeri* was found in 27 U.S. states, Argentina, and Brazil (Scott et al., 2007; Norsworthy et al., 2008; Steckel et al., 2008; Berger et al., 2016; Küpper et al., 2017a; Heap, 2018). The primary mechanism of glyphosate resistance in *A. palmeri* has been identified as the amplification of the gene encoding the target enzyme 5-enolpyruvylshikimate-3-phosphate synthase (EPSPS) which produces increased *EPSPS* transcription and protein activity (Gaines et al., 2010). The same glyphosate resistance mechanism has independently evolved in six other species (Salas et al., 2012; Jugulam et al., 2014; Lorentz et al., 2014; Chatham et al., 2015; Chen et al., 2015; Wiersma et al., 2015; Malone et al., 2016; Ngo et al., 2017). *EPSPS* gene amplification has also transferred via pollen-mediated inter-specific hybridization from *A. palmeri* to *A. spinosus* (Nandula et al., 2014).

Evolutionary models have identified that herbicide resistance dynamics are largely influenced by gene flow, seed immigration, and fitness cost (Maxwell et al., 1990). Further factors include mutation rate, the mode of inheritance, dominance of the resistance trait, seed bank turnover rate, herbicide chemistry and persistence, as well as herbicide usage patterns (Georghiou and Taylor, 1986; Jasieniuk et al., 1996a; Neve, 2008). For instance, glyphosate used prior to crop emergence is predicted to have a low risk of resistance evolution while post-emergence use increases the risk, and reliance on glyphosate exclusively increases the risk even further (Neve, 2008). A simulation model for *A. palmeri* predicted that five applications of glyphosate each year with no other herbicides would result in resistance evolving in 74% of the simulated populations (Neve et al., 2011).

A. palmeri management is complicated by the fact that *A. palmeri* evolved resistance to five different modes of action (Chahal et al., 2015; Nakka et al., 2017; Schwartz-Lazaro et al., 2017; Heap, 2018), the lack of discovery of new modes of action for the past three decades, and the high cost of bringing new herbicides to the market (Duke, 2012). The overuse of and sole reliance on glyphosate and

the resulting evolution of resistant weeds exhausted the lifespan of a once-in-a-century herbicide (Duke and Powles, 2008b) and threatens current crop production practices by diminishing available weed management options further. Therefore, knowledge about the origin and geographical pathways of glyphosate resistance in *A. palmeri*, one of the most problematic GR weeds in the USA, is crucial to avoid repeating the same mistakes made with glyphosate with other modes of action that are still successful at controlling weeds in the field.

This study focuses on a GR population identified in a no-till cotton-wheat double crop system near Phoenix, Arizona (AZ), USA. Glyphosate was used as the sole weed management technique for the cotton portion of the production cycle for more than 10 yr before glyphosate resistance was first suspected in 2012, eight years after the first report in the species. The objective was to determine whether GR *A. palmeri* immigrated to the AZ locality from an outside location via seed or pollen-mediated gene flow, or if resistance evolved at or nearby the location in AZ independently via parallel evolution. To answer this question, single nucleotide polymorphisms (SNPs) generated by genotyping-by-sequencing (GBS) to identify numerous sequence differences at presumably random parts of the genome (Brumfield et al., 2003), were used. The GR population from AZ and seven other populations from different locations in the USA were investigated for their degree of genetic relatedness to identify patterns of phylogeography and variation on an intraspecific level.

MATERIALS AND METHODS

Plant material and DNA isolation

Twelve *A. palmeri* individuals (six males and six females) from each of eight different locations in the USA were used for the analyses (Table 5-1), except for AZ-S2 for which only eleven individuals were used to leave a blank on the plate. Locations AZ-S1, AZ-S2, KS-S, GA-S and NE-S were verified as glyphosate susceptible (GS) and locations AZ-R (Molin et al., 2017b), GA-R (Culpepper et al., 2006), and TN-R (Steckel et al., 2008) were verified as resistant. The populations were collected between 2004 and 2012, except for AZ-S2 which was maintained by the USDA-ARS Germplasm Resource Information

Network (accession number: Ames 5370) since its collection in 1981 and serves as an outgroup to prevent ascertainment bias (Wakeley et al., 2001; Akey et al., 2003). AZ-S1 was collected about 240 km southeast of Buckeye, AZ (AZ-R) where no agronomic crop production has occurred since the 1960s to provide a recently collected Arizona-native GS population that is fairly sympatric with AZ-R.

For DNA extraction, young leaf tissue was collected, immediately frozen in liquid nitrogen, and stored at -80 °C. For glyphosate-resistant (GR) samples only individuals that survived 800 g a.e. ha^{-1} glyphosate (Roundup Weathermax, Monsanto) were used. DNA extraction was performed following a modified cetyltrimethylammonium bromide (CTAB) extraction protocol (Doyle, 1991; Küpper et al., 2017a) and quantified on a NanoDrop spectrophotometer (Thermo Scientific) followed by normalization. Gel electrophoresis and enzyme digestion with *Hind*III (Thermo Scientific) were performed on all or 10% of the samples, respectively, to confirm DNA quality and normalization.

Herbicide resistance characterization

To confirm glyphosate resistance and susceptibility for the individuals used for GBS, an *in vivo* shikimate accumulation assay with excised leaf tissue (Shaner et al., 2005) was conducted. Additionally, *EPSPS* gene copy number was determined for all samples. Four-mm leaf discs from each individual were exposed to glyphosate at 0, 100, 500 and 1000 µM glyphosate for 16 h. Shikimate accumulation was measured on a spectrophotometer (Synergy 2 Multi-Mode Reader, BioTek). A shikimate standard curve was used to calculate the ng shikimate μL^{-1} accumulation above the background level. Each biological sample was run in three technical replicates for each dose.

For *EPSPS* gene copy number determination, DNA concentrations were adjusted to 5 ng μL^{-1} and primer sets (ALSF2 and ALSR2, EPSF1 and EPSR8) and qPCR conditions were used as previously described (Gaines et al., 2010). Quantitative PCR was performed using SYBR green master-mix (BioRad) on a CFX Connect™ Real-Time PCR Detection System (BioRad). *EPSPS* gene copy number relative to *ALS* was determined using the $2\Delta C_T$ method where $\Delta C_T = C_{T(ALS)} - C_{T(EPSPS)}$. Each biological sample was run in three technical replicates.

Greenhouse dose-response studies were conducted to confirm pyrithiobac-sodium [acetolactate synthase (ALS inhibitor)] resistance in AZ-R with AZ-S1 as a susceptible control. The experiments took place at the University of Arizona Campus Agricultural Center in Tucson, Arizona. Seeds were planted in artificial soil mix in 10 cm pots and after emergence seedlings were thinned, fertilized, and irrigated as needed. ALS-inhibitor treatments included 0, 0.0001, 0.0005, 0.001, 0.002, 0.005, 0.01, 0.02, 0.05, 0.1, 0.2, 0.5, and 1 kg a.i. ha^{-1} pyrithiobac-sodium (Staple LX, DuPont) with 0.25% v/v non-ionic surfactant (Activator 90, Loveland Products). Plants were sprayed at the six-leaf stage using a CO_2 pressurized backpack sprayer equipped with a three nozzle (TeeJet XR8001VS) boom delivering a carrier volume of 112 L ha^{-1} at 172 kPa at 4 km h^{-1}. The experimental design was random with five replications per dose. Above-ground biomass was harvested 27 DAT, dried at 60°C and dry weight was measured.

The *ALS* gene was sequenced from three individuals each of the AZ-R, GA-R, and TN-R populations using the same DNA used for the *EPSPS* copy number test and SNP calling. *ALS* gene sequencing was conducted as previously described (Küpper et al., 2017a).

Genotyping and SNP filtering

After DNA extraction, GBS and bi-allelic SNP calling was conducted by the Biotechnology Resource Center at Cornell University, Ithaca, New York (Elshire et al., 2011). A total of 95 samples (eleven samples for AZ-S2 and twelve samples for the remaining populations) were digested with *Ape*KI, individually barcoded, run on an Illumina HiSeq2500 single-end 100 bp sequencing lane, and later trimmed to 64 bp for analysis. The GBS UNEAK pipeline in TASSEL v. 3.0.173 (Bradbury et al., 2007; Lu et al., 2013; Glaubitz et al., 2014) was used for *de novo* clustering of the sequences. The resulting SNP calls were then filtered for depth and missing values at any given locus with VCFtools v. 0.1.11 (Danecek et al., 2011) after which 4,566 filtered SNPs remained. Through further pruning, 70.4% of the filtered SNPs were excluded due to percentage of missing data points (>5%), minor allele frequency (MAF) values lower than 0.05, or more than 80% loci with more than one allele, leaving 1,351 SNPs which were

informative (Appendix C, Figure 9-2). Except where indicated, all analyses were performed on the panel of 1,351 SNPs.

EPSPS gene copies in GR *A. palmeri* individuals are randomLy dispersed throughout the whole genome (Gaines et al., 2010). They can be found embedded in a complex array of repetitive elements and putative helitron sequences referred to as the '*EPSPS* cassette' (Molin et al., 2017a). Because SNPs are called genome-wide, an overrepresentation of called SNPs within these sequences could potentially lead to clustering of GR individuals regardless of their actual genetic relatedness. To avoid such bias, the sequences flanking the 1,351 SNPs were aligned to the *A. palmeri* 1,044 bp *EPSPS* sequence (Gaines et al., 2010) and the 297,445 bp *A. palmeri EPSPS* cassette (Molin et al., 2017a). The 1,351 SNP sequences were also aligned to the chloroplast genome of spinach (*Spinacia oleracea*) and the mitochondrial genome of sugar beet (*Beta vulgaris*) to identify SNPs specific to the cytoplasmic regions.

Analysis of genetic structure

The putative population genetic structure was explored using the model-based Bayesian analysis implemented in STRUCTURE v2.3.4 (Pritchard et al., 2000). The number of sub-populations K in the dataset was determined by the averaged likelihood at each K [ln Pr(X | K) or Ln(K_n)] and the variance between replicates was determined by running a continuous series of K = 1-15 to determine the optimal number of populations present within the 95 individuals. The analysis was carried out using a burn-in of 30,000 iterations and a run length of 100,000 Markov Chain Monte Carlo (MCMC) replications in ten independent runs. Prior knowledge about the number of populations was not included. The optimum number of clusters was predicted following the *ad hoc* statistic ΔK (Evanno et al., 2005) using Structure Harvester v0.6.94 (Earl, 2012). For the final K analysis a burn-in of 30,000 with a run length of 500,000 MCMC replications and 20 independent runs were used. To be conservative, the analyses were run assuming admixture and correlated allele frequencies (Porras-Hurtado et al., 2013). The Greedy algorithm by CLUMPP v1.1.2 (Jakobsson and Rosenberg, 2007) was used to obtain the individual and cluster

membership coefficient matrices over the 20 runs which were then plotted using *distruct* 1.1 (Rosenberg, 2004).

The following information and tests were calculated in R v3.4.1. The number of alleles (N_a) and allelic richness (A_R) per population were calculated using the package 'PopGenReport'. Observed (H_O) and expected heterozygosity (H_E) were calculated with 'adegenet' (Jombart and Ahmed, 2011; Adamack and Gruber, 2014). The inbreeding coefficient (F_{IS}) was calculated following the formula 1 - (H_O/H_E). Principal component analysis (PCA) was conducted using 'SNPRelate' and 'gdsfmt' (Zheng et al., 2012). Calculations for Nei's distance (D_{ST}) (Nei, 1972) and pairwise fixation index (F_{ST}) among populations were performed with 1,000 bootstrap replications using 'StAMPP' (Pembleton et al., 2013). The analysis of molecular variance (AMOVA) (10,000 permutations) and the Mantel test (10,000 permutations) for isolation by distance analysis were performed using 'poppr' (Kamvar et al., 2014) and 'adegenet' (Dray and Dufour, 2007), respectively. The phylogenetic analysis was based on the UPGMA clustering method using the Hasegawa-Kishono-Yano (HKY) genetic distance model in the software Geneious v10.0.6.

RESULTS

Herbicide resistance characterization

GS *A. palmeri* populations showed higher shikimate accumulation (11.8 – 146.3 ng μL^{-1} at 500 µM glyphosate) than GR populations (0 – 3.8 ng μL^{-1}) (Figure 5-1A) while GR populations showed higher genomic *EPSPS* copy number (individuals measured from 25 – 250-fold) than GS populations (individuals measured from 1 – 2-fold) (mean *EPSPS* copy number shown in Figure 5-1B). Thus, the mechanism of glyphosate resistance was determined to be *EPSPS* gene duplication in all the sampled GR populations (Gaines et al., 2010). The average copy numbers for the GR populations were within a similar range (Figure 5-1B). The 500 µM glyphosate concentration was a clear discriminating dose between GR and GS individuals.

Resistance to the acetolactate synthase (ALS)-inhibitors, commonly used in cotton, was suspected in AZ-R as well, thus a dose-response with pyrithiobac-sodium and sequencing of the *ALS* gene was

conducted. The ED_{50} values for dry weight (pyrithiobac-sodium dose causing 50% reduction in dry weight) were 6.9 and 1.3 g a.i. ha^{-1} for AZ-R and AZ-S1, respectively ($P = 0.027$) (Appendix C, Figure 9-1).

Sequencing the *ALS* gene in three GR individuals each from AZ-R, GA-R and TN-R, showed that one TN and one AZ plant were heterozygous for a mutation from TGG → TTG resulting in an amino acid change from tryptophan to leucine at position 574 ($W_{574}L$). A different AZ plant was heterozygous for a AGC → AAC mutation resulting in a change from serine to asparagine at position 653 ($S_{653}N$). No individual carried both mutations within the same allele. The remaining individuals tested showed no mutations at these positions (Table 4-3). Both mutations have been reported before in *A. palmeri* from MS and Brazil (Molin et al., 2016; Küpper et al., 2017a) while only $S_{653}N$ was reported from GA (Berger et al., 2016). The mutation at $W_{574}L$ confers resistance to triazolpirimidines, sulfonylureas, imidazolinones, and pyrimidinylthioenzoates (including pyrithiobac-sodium), whereas the $S_{653}N$ mutation confers resistance to imidazolinones and the pyrimidinylthiobenzoates only (McNaughton et al., 2005; Whaley et al., 2006; Patzoldt and Tranel, 2007; Laplante et al., 2009; Yu et al., 2012). Both mutations are known to be inherited as a dominant trait (Tranel and Wright, 2002; Powles and Yu, 2010). It is suspected that a non-target site mechanism conferring resistance to ALS inhibitors exists (Küpper et al., 2017a) and such a mechanism may also be present in AZ-R ALS-resistant individuals that lack target-site ALS mutations.

Influence of glyphosate resistance mechanism on GBS analysis

The *EPSPS* gene has five potential cutting sites for the enzyme *Ape*KI used in this GBS study, while the entire *EPSPS* cassette has 289 potential cutting sites. No SNPs were called within the *EPSPS* gene and only one SNP was called from within the *EPSPS* cassette which was removed from further analysis. Thus, the mechanism of glyphosate resistance (repetitive *EPSPS* gene copies) is not expected to influence the analysis of genetic relatedness in this case.

Within Population Genetic Diversity

The 1,351 loci used for this study had an average percentage of missing data of 1.07% and an average minor allele frequency (MAF) of 0.159. A high degree of polymorphism (MAF ≥ 0.30) was found in 14.41% of the dataset. The proportion of MAF <0.1 was 45.37%. One AZ-S2 individual was removed from all future analysis because it was an extreme outlier. The observed number of alleles within a population ranged from 2,017 (AZ-S2) to 2,395 (KS-S), with an average of 2,217. Levels of heterogeneity were compared among populations to examine genetic variability within populations. Allelic richness (A_R) ranged from 1.445 (AZ-S2) to 1.654 (KS-S) with an average of 1.560. The observed (H_O) and expected heterozygosity (H_E) values ranged from 0.161 (AZ-S1) to 0.219 (TN-R) and from 0.163 (AZ-S2) to 0.211 (KS-S/GA-R), respectively, with an average of 0.193. Low values for H_O indicate small effective population sizes or population bottlenecks. The H_O values in most populations were less than the H_E values (Appendix C, Figure 9-3), with the exception of GA-S, TN-R and AZ-S2. The inbreeding coefficient (F_{IS}) for these three populations was negative. AZ-R was the population with the highest F_{IS} value (0.121) (Appendix C, Table 9-1).

Consensus tree

The consensus tree separated GA-S, TN-R, NE-S, and AZ-S2 with over 86% certainty with GAS, TN-R, and AZ-S2 being the most divergent populations. AZ-S1, AZ-R, and KS-S clustered together. Except for KS-S and AZ-R, all individuals clustered within their sampling location (Figure 5-2), The long branch lengths for the individuals indicate high within-individual genetic variability.

Principal component analysis

To confirm this clustering, a similar pattern of differentiation among populations was constructed using PCA which is used to bring out strong patterns in the dataset based on their variance. The first two principal component (PC) axes cumulatively accounted for 16.69% of the total variation. PCA showed that all individuals clustered according to their collection site. Three distinct outgroups (GA-S, TN-R, and

AZ-S2) emerged while the remaining individuals from the other five populations clustered into one group. The first dimension (PC 1) accounted for 8.91% of the variation and roughly separated GR from GS individuals (Figure 5-3A). After removing GA-S, TN-R, and AZ-S2, AZ-R did not separate from the cluster with KS-S and AZ-S1, while GA-R and NE-S clustered distinctively according to PC 2, supporting the UPGMA consensus tree. PC 1 in the second PCA on the subset of populations accounted for 6.87% of the variation in the dataset and again roughly separated GR from GS individuals. Individuals from the same population occupied different areas of the cluster, which indicates a population substructure (Figure 5-3B).

Bayesian analysis

Model-based clustering was used to assign individuals to sub-populations based on allele frequency differences. Initially, the putative number of populations (*K*) in the dataset required to explain the total sum of genetic variation observed was determined. Evanno's test (Evanno et al., 2005) on the whole dataset of 1,351 SNPs indicated that the *K* distribution was bimodal and that the most informative numbers of subpopulations were four and six with $K = 6$ being most probable (Appendix C, Figure 9-4). At $K = 4$, consistent with the previous findings, sub-population structure analysis revealed that individuals from GA-S, TN-R, and AZ-S2 appeared distinct from the other populations. The same analysis also showed that individuals from AZ-R and GA-R shared a proportion of their alleles with TN-R while AZ-S1 shared a small proportion with AZ-S2. At $K = 6$, AZ-R, KS-S, and AZ-S1 showed the highest membership coefficient for a shared cluster (beige) while the remaining populations contained unique alleles. This is supported by a high number of shared alleles among these three populations at $K = 8$ where KS-S displayed a high degree of admixture with AZ-R and AZ-S1. Although less than with KS-S and AZ-S1, AZ-R still shared alleles with GA-R while AZ-S1 and GA-R shared none (Figure 5-4). Investigating the dataset without the three outgroups GA-S, TN-R, and AZ-S2 at $K = 5$ supports that AZ-R shares alleles with KS-S, AZ-S1 and GA-R and very few with NE-S (Appendix C, Figure 9-5).

Pairwise comparison of genetic distances

As expected, very high genetic distances (D_{ST}) (Nei, 1972) and F_{ST} values were found for the three outgroups (TN-R, AZ-S2 and GA-S) while the genetic distance was lower among AZ-R, AZ-S1, and KS-S. Thus, AZ-R was most closely related to AZ-S1 (F_{ST} = 0.052, D_{ST} = 0.026) and KS-S (F_{ST} = 0.049, D_{ST} = 0.028) and most distantly related to the three outgroups GA-S (F_{ST} = 0.201, D_{ST} = 0.079), TN-R (F_{ST} = 0.176, D_{ST} = 0.067), and AZ-S2 (F_{ST} = 0.179, D_{ST} = 0.067). This was further visualized by a heatmap in Appendix C, Figure 9-6. The bootstrap analysis of F_{ST} values indicated that all populations were significantly different from each other, except for AZ-R and KS-S, where only 5% of the genetic differences between populations were attributable to their geographic origin (Table 5-3).

Analysis of molecular variance and isolation by distance

An analysis of molecular variance (AMOVA) revealed that 17.78% ($P < 0.001$) of the total genetic variation was among populations, 4.87% was among individuals within a population ($P < 0.01$) and the remaining 77.35% ($P < 0.001$) of the genetic variation was within individuals (Appendix C, Figure 9-7). Population differentiation exists at all levels but the variation within individuals was the largest. The high genetic variation within individuals suggests a lack of population structure, even though F_{ST} values up to 0.324 (Table 5-3) indicate that genetic differentiation between populations was high.

The geographical distance between any two populations ranged from about 60 to 1,930 km. The Mantel test revealed that no pattern of isolation by distance was evident between genetic and geographic distance (R^2 = 0.006, P = 0.259). The observed correlation of 0.076 further suggests that the two distances are not associated (Appendix C, Figure 9-8).

Genetic relatedness based on SNPs within the chloroplast and mitochondrial genome

Forty-two SNPs specific to the chloroplast genome and 54 SNPs specific to the mitochondrial genome were identified. PCA with chloroplast SNPs identified GA-S and TN-R as distinct groups (Figure 5-5A). Structure analysis with the identified sub-populations of K=4 and K=5 (Appendix C, Figure 9-9A)

supported this observation. AZ-S2, however, shared considerably more alleles with NE-S, AZ-S1, KS-S, and GA-R than previously observed when including the loci from the nuclear and mitochondrial genomes (Figure 5-6A). At *K*=8 AZ-R was closest related to AZ-S1 (F_{ST} = 0.058, D_{ST} = 0.279) (Appendix C, Table 9-1).

Consistent with the analysis with all 1,351 SNPs, mitochondrial SNPs identified GA-S, TN-R, NE-S, and also AZ-S2 as distinct groups (Figure 5-5A), while the remaining populations AZ-R, AZ-S1, GA-R and KS-S clustered together (Figure 5-6B) leaving *K*=5 identifiable clusters among the eight populations (Appendix C, Figure 9-9B). At *K* = 8, AZ-R was closest related to KS-S (F_{ST} = 0.053, D_{ST} = 0.23) (Appendix C, Table 9-2).

DISCUSSION

Previous population genetics studies investigating the phylogeographic structure of pesticide resistant organisms reveal either a single origin (Raymond and Callaghan, 1991; Linda and Alan, 1997; Daborn et al., 2002) or, more frequently, redundant independent, parallel evolution events shaped by variations in selection pressure (Cavan et al., 1998; Anstead et al., 2005; Menchari et al., 2006; Chen et al., 2007; Pinto et al., 2007; Délye et al., 2010). As an example, glyphosate resistance in horseweed (*Conyza canadensis*) from California had multiple independent origins within the Central Valley and evolved many years before its first detection. From there it spread, possibly due to increased selection by the herbicide (Okada et al., 2013). The resistance mechanism(s) for the *C. canadensis* populations used in this study were unknown but most likely involved reduced translocation (Wang et al., 2014) and vacuolar sequestration (Ge et al., 2010). Similarly, investigations into the frequency of target site mutations in the *EPSPS* gene of GR Italian ryegrass (*Lolium perenne* L. ssp. *multiflorum*) populations (Karn and Jasieniuk, 2017) as well as simple sequence repeats (SSR) genotyping of GR common morning glory (*Ipomea purpurea*) (Kuester et al., 2015), and GR Johnsongrass (*Sorghum halepense* L. Pers) (Fernández et al., 2013) found multiple evolutionary origins for glyphosate resistance.

Two previous studies have examined population genetics in *A. palmeri* with glyphosate resistance due to *EPSPS* gene amplification. An investigation using four genomic loci as markers of GR *A. palmeri* from several sampling sites within North Carolina suggested that adaptation to glyphosate application took place in parallel. The authors based this conclusion on the fact that four out of five identified population clusters were statistically associated with increased glyphosate resistance (Beard et al., 2014). In contrast, sequencing of selected regions of the 287 kb *EPSPS* cassette in GR populations from geographically distant locations within the U.S showed strong homology between sequences and the authors concluded that the conserved nature of the cassette indicated that glyphosate resistance via amplification evolved once from a point source and then rapidly spread across the USA (Molin et al., 2017b).

Information on the factors that influence the evolutionary origin, demographic history, and geographical pathways of glyphosate resistance in *A. palmeri* is crucial for the formulation of successful strategies to delay and manage herbicide resistance. The aim of this study was to investigate population structure and genetic differentiation among eight geographically distant *A. palmeri* populations to assess if glyphosate resistance evolved in the southeastern USA and migrated to the southwestern USA, or if it evolved independently in AZ as a result of local management practices. Glyphosate resistance and susceptibility were determined by *EPSPS* copy number and shikimate assay test in all sampled individuals confirming that the resistance mechanism was *EPSPS* gene amplification. *EPSPS* genomic copy number was similar among the resistant populations; thus, spread of glyphosate resistance from a single origin is possible. GBS was used to identify numerous genome-wide sequence differences used as putative neutral markers due to its fast and simple application, cost-effectiveness and high resolution (Brumfield et al., 2003; Morin et al., 2004; Deschamps et al., 2012; Narum et al., 2013). The technique is widely applicable for studying non-model organisms, such as weeds, because the consensus of read clusters around the sequence site becomes the reference sequence and therefore a complete reference genome sequence is not required (Baxter et al., 2011; Elshire et al., 2011; Reitzel et al., 2013). For this study, 1,351 SNPs were used that remained after filtering.

Genetic diversity for each of the *A. palmeri* populations was estimated by the number of alleles, allelic richness, observed and expected heterozygosity, as well as inbreeding coefficient. The varying levels of heterozygosity found can most likely be attributed to differing collection dates and subsequent seed increase events which may have caused inbreeding depression. In particular AZ-S2, collected in 1981, is expected to have undergone severe inbreeding, as is indicated by the negative F_{IS} value. Similar observations were made for GA-S and TN-R.

UPGMA phylogenetic tree analysis, PCA, Bayesian model-based clustering, and pairwise comparisons of genetic distances were used to determine the genetic relationship among the eight different *A. palmeri* populations and yielded congruent results. GA-S, TN-R, and AZ-S2 were genetically distinct while the remaining populations AZ-R, KS-S, AZ-S1, GA-R, and NE-S clustered together more closely. AZ-R was most closely related to KS-S, followed by AZ-S1, with GA-R being the next most similar population to AZ-R.

Cytoplasmic genomes are maternally inherited and do not undergo recombination. Thus, they permit a more conserved examination of intraspecific phylogeography in plants. They further have the potential to allow for higher differentiation (Petit et al., 2005). Chloroplast and mitochondrial SNPs were evaluated separately because they might support different phylogenies (Washburn et al., 2015; Zhu et al., 2016), since mitochondrial genomes have lower nucleotide sequence variation than chloroplast genomes (Wolfe et al., 1987). Analyses with SNPs in cytoplasmic genomes supported GA-S and TN-R to be genetically distinct. Chloroplast SNPs, however, placed AZ-S2 closer to the remaining populations than NE-S, consistent with the geographical distribution. AZ-R was closest to AZ-S1 based on chloroplast SNPs while mitochondrial SNPs placed the population closest to KS-S. Sequencing of the *ALS* gene revealed that two out of three AZ-R individuals carried a $W_{574}L$ and $S_{653}N$ mutation each, showing high diversity of the *ALS* sequence within the population. Since only the $W_{574}L$ mutation was found in one out of three individuals from TN-R, while GA-R and GA-S individuals had none (Küpper et al., 2017a), mutations in the *ALS* gene do not support clustering of AZ-R and GA-R.

According to the observed population genetic structure, two scenarios are possible for AZ-R: Either glyphosate resistance evolved independently in AZ or GR *A. palmeri* from GA migrated west via KS to AZ, against the species expansion direction (Appendix C, Figure 9-10). The small amount of shared sequences with GA-R and the moderate amount of shared sequences with KS-S individuals support such an introduction route, as does the chronological order of reports of glyphosate resistance (Georgia: 2004, Kansas: 2011, Arizona: 2012). AZ-R individuals shared alleles with AZ-S1 which could be attributed to crossing events with the native, GS population since resistance is likely to have been reported some time after the introduction event (Cavan et al., 1998). The high degree of unique sequence in AZ-R suggests that the exact origin of the population could not be identified. It can, however, be predicted that AZ-R individuals were not introduced from around the sampling location in TN.

Interestingly, TN-R and GA-R did not share any alleles and seemed unrelated in all analyses. Such strong population differentiation and monophyly can stem from a past divergence event and subsequent adaptation to environmental conditions through intraspecies convergent evolution (Ralph and Coop, 2015) and isolation due to limited dispersal and low connectivity (Reitzel et al., 2013). Further, agricultural practices might have strongly modified weed communities and disturbed genetic equilibrium (Menchari et al., 2007). TN and GA/NC coastal regions are geographically separated by the Appalachian mountain range and have dissimilar cropping systems with one primarily focusing on soybean and corn production and the other on cotton. As resistance to glyphosate was reported within a time frame of two years in these states, it is very possible that the populations represent independent glyphosate resistance origins. GA-R and GA-S, however, were genetically distinct from each other in all analyses even though collected from about 115 km apart and without any major geographical obstacles in the way. If glyphosate resistance evolved at the GA-R location, a more panmictic structure would have been expected (Chauvel and Gasquez, 1994). Such differences could be attributed to locally differing conditions, a high degree of natural spatial genetic diversity within the species, or the possibility that glyphosate resistance did not originate in GA. It is also possible that continuous selection with glyphosate created a genetic bottleneck and subsequent inbreeding of resistant individuals.

A. palmeri is a species with high genetic variability which makes it a challenge to draw a definite conclusion about an introduction event without very specific sampling. This study has shown that genetic relatedness does not decrease with distance. Hence, if GS individuals collected from within a 50 km radius can have the high level of genetic differentiation observed in this study (e.g., AZ-S1 and AZ-S2), it may be difficult to identify a parallel adaptation event. The nativity of *A. palmeri* to the southwestern USA and adaptation to local and heterogenous environments (Clements et al., 2004) as well as the species' obligate outcrossing nature are drivers for heterozygosity. Genetic diversity, in turn, increases the likelihood of resistance to evolve, as does high selection pressure due to frequent usage of glyphosate which has been the case in all areas of GR *A. palmeri* collection sites. Future research should incorporate a more extensive collection of GR *A. palmeri* populations, always coupled with at least one geographically close GS population. Furthermore, all seed should be collected by the exact same sampling technique to increase the precision and accuracy with which questions of genetic relatedness and geographic migration patterns can be answered.

CONCLUSION

A major management question for growers is how much of the resistance issue results from previous selection intensity from management practices in their own fields, and how much results from gene flow from neighboring fields. Although this study was not able to definitively determine whether AZ-R evolved independently or if glyphosate resistance migrated to AZ, the recent geographical expansion of *A. palmeri* to the upper USA Midwest (Kartescz, 2014), Argentina (Berger et al., 2016), and Brazil (Küpper et al., 2017a) shows that migration via seed movement is an important factor for *A. palmeri*. Long-distance seed dispersal is possible through irrigation and rainfall events (Norsworthy et al., 2014), buying and selling of used harvest equipment, custom harvesting crews moving around the country (Schwartz et al., 2016), contaminated crop seed and feed, as well as transportation through migrating wildlife such as ducks and geese (Farmer et al., 2017).Aside from harvest equipment hygiene requirements, it is difficult to prevent such seed dispersal. Early detection and rapid response approaches already used in invasive

species management (Westbrooks, 2004) and disease outbreaks (Fasina et al., 2014) could be useful to adopt for herbicide resistance management. Delaying resistance evolution and prolonging the utility of remaining effective modes of actions for which resistance is not yet widespread, such as synthetic auxins, glutamine synthetase-, and phytoene desaturase (PDS)-inhibitors, is critical for future *A. palmeri* management.

TABLES

Table 5-1: *A. palmeri* populations, their origin and time of collection.

Abbreviation	Origin	Collection year
AZ-R	Buckeye, Arizona	2012
AZ-S1	Sahuarita, Arizona	2012
AZ-S2	Tucson, Arizona	1981
GA-R	Macon, Georgia	2006
GA-S	Worth County, Georgia	2004
KS-S	Ottawa, Kansas	2005
NE-S	Shickley, Nebraska	2011
TN-R	Jackson, Tennessee	2007

Table 5-2: Population information and genetic variability estimates based on 1,351 SNP loci in eight populations of *A. palmeri*. N, number of individuals per population; N_a, observed number of alleles; A_R, allelic richness; observed (H_O) and expected (H_E) heterozygosity; F_{IS}, inbreeding coefficient.

Population	n	N_a	A_R	H_O	H_E	F_{IS}
AZ-R	12	2,381	1.650	0.182	0.207	0.121
AZ-S1	12	2,299	1.581	0.161	0.181	0.110
GA-R	12	2,307	1.617	0.193	0.211	0.085
GA-S	12	2,031	1.474	0.191	0.183	-0.044
NE-S	12	2,245	1.579	0.184	0.199	0.075
KS-S	12	2,395	1.654	0.194	0.211	0.081
TN-R	12	2,059	1.477	0.219	0.183	-0.197
AZ-S2	10	2,017	1.445	0.180	0.163	-0.104

Table 5-3: Pairwise estimates of F_{ST} and Nei's standard genetic distance (D_{ST}) between eight *A. palmeri* populations. Pairwise estimates of F_{ST} and D_{ST} are shown above and below the diagonal, respectively. †Non-significant value ($P > 0.05$)

	AZ-R	AZ-S1	GA-R	GA-S	NE-S	KS-S	TN-R	AZ-S2
AZ-R		0.052	0.080	0.201	0.106	0.049†	0.176	0.179
AZ-S1	0.026		0.126	0.202	0.108	0.051	0.215	0.170
GA-R	0.038	0.050		0.225	0.154	0.100	0.209	0.228
GA-S	0.079	0.072	0.090		0.233	0.196	0.316	0.308
NE-S	0.046	0.042	0.064	0.090		0.085	0.257	0.228
KS-S	0.028	0.026	0.046	0.077	0.039		0.191	0.171
TN-R	0.067	0.077	0.082	0.125	0.101	0.074		0.324
AZ-S2	0.067	0.058	0.088	0.115	0.084	0.064	0.122	

FIGURES

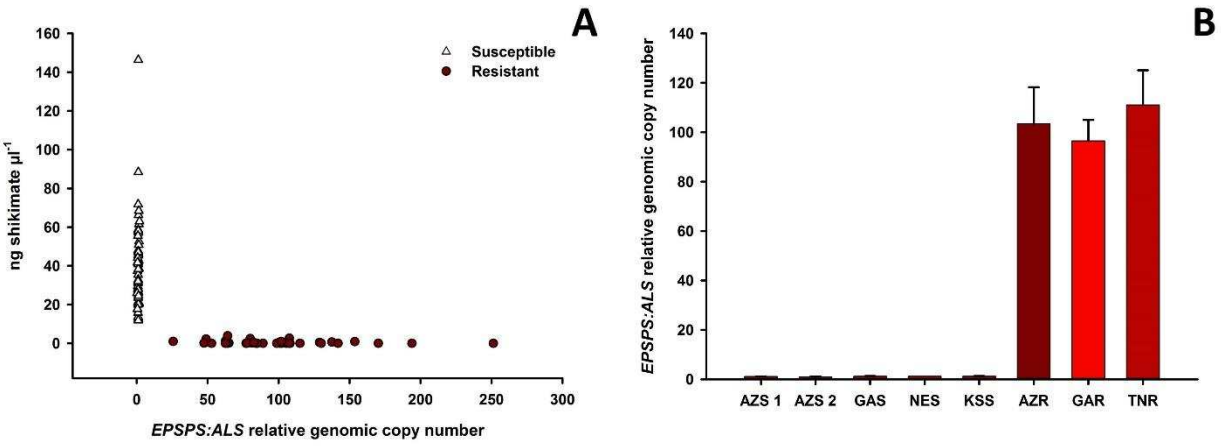

Figure 5-1: Correlation of shikimate accumulation and EPSPS genomic copy number in all individuals of each of the glyphosate-resistant and -susceptible *A. palmeri* populations. Shikimate accumulation was measured after incubation in 500 µM glyphosate in an in vivo leaf disc assay Increase in genomic copy number of EPSPS is relative to ALS as measured using qPCR on genomic DNA (A). EPSPS genomic copy number by population (B).

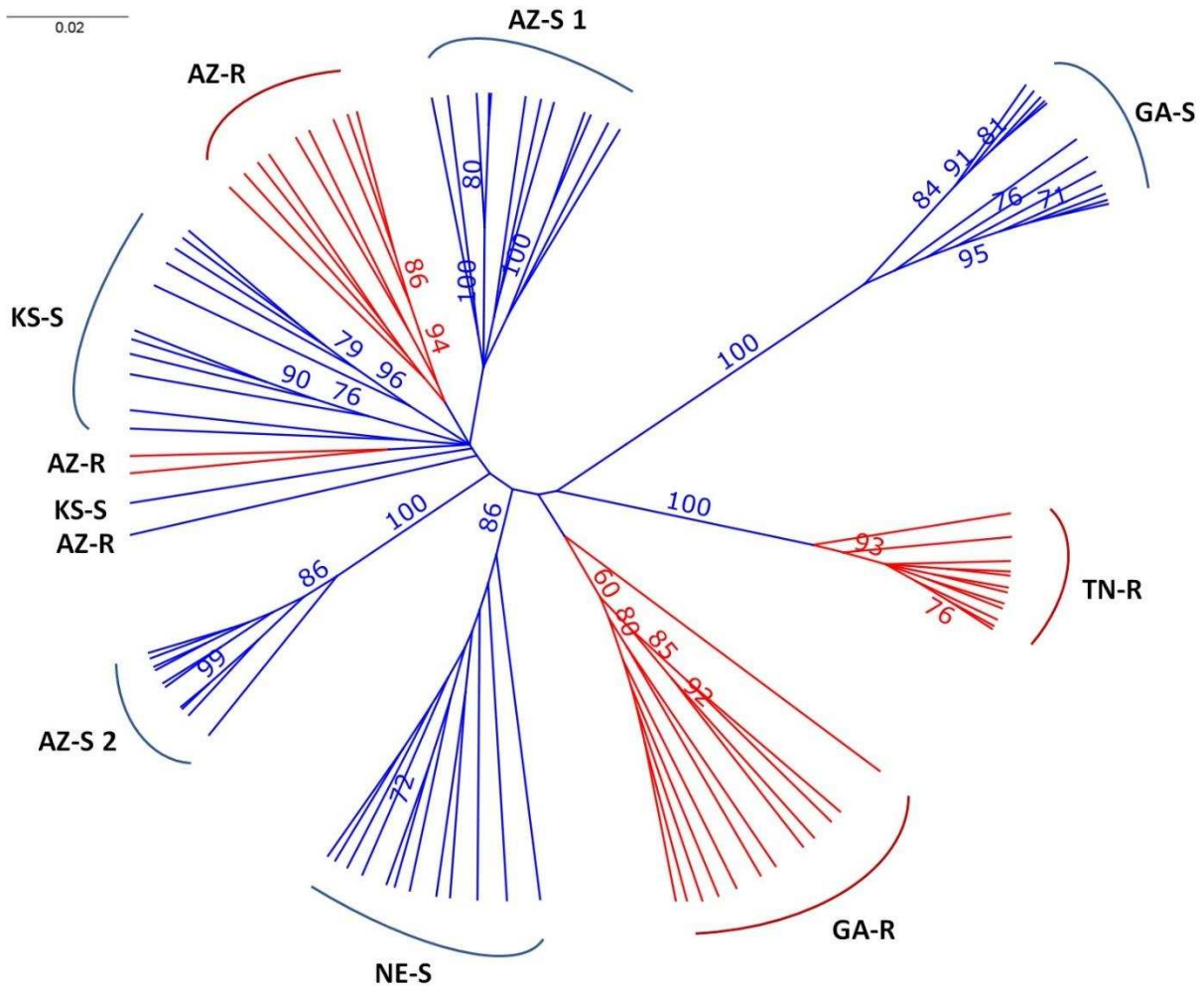

Figure 5-2: Unrooted UPGMA consensus tree after 1,000 bootstrap replications depicting the relationships of *A. palmeri* individuals from eight populations. Bootstrap values >70% at nodes are indicated.

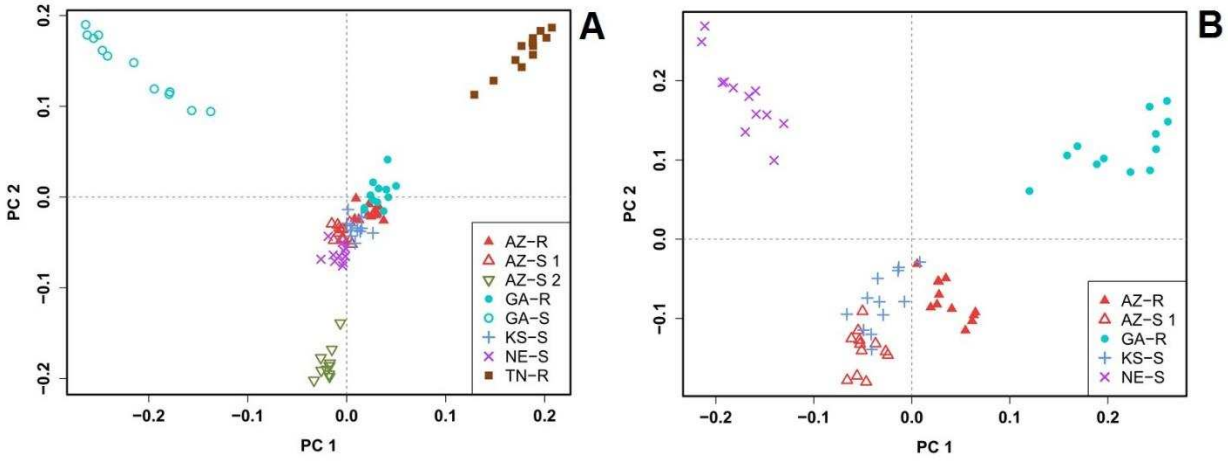

Figure 5-3: Clustering of *A. palmeri* populations based on principal component analysis (PCA) using the filtered and pruned whole dataset of 1,351 SNPs. Analysis was done on all eight populations (A) and on a subset of populations removing the three outlier groups AZ-S2, GA-S, and TN-R (B). Each point represents an individual colored according to the collection site. Glyphosate-resistant individuals are marked by filled symbols and susceptible individuals are marked by empty symbols. Individuals from the same U.S. state have the same symbols.

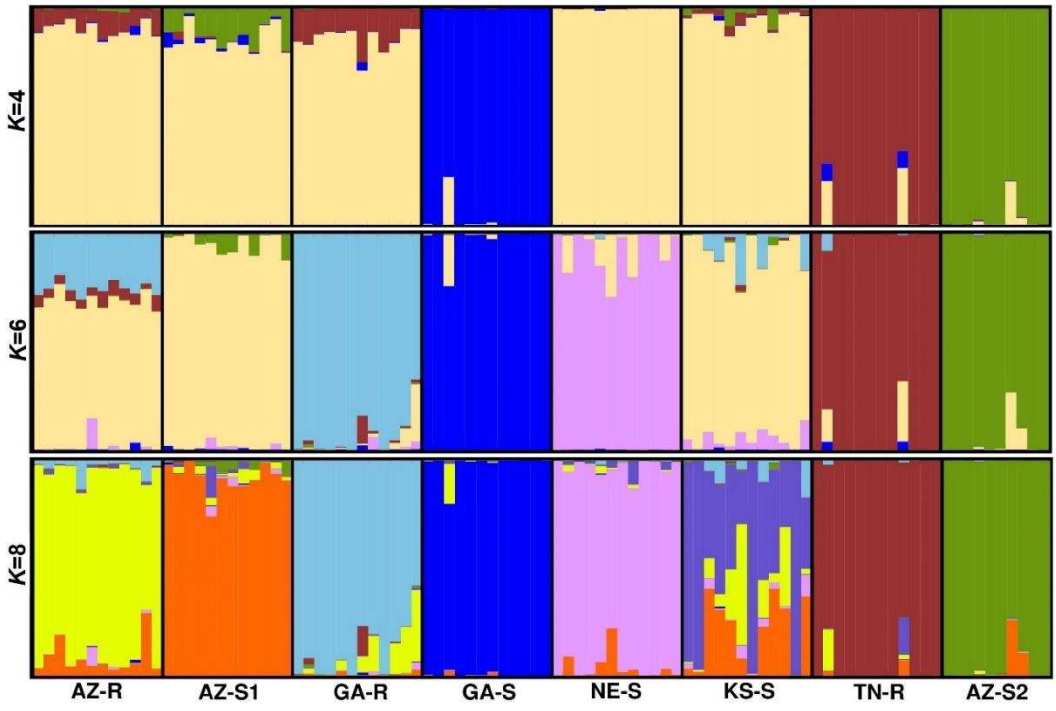

Figure 5-4: Population structure analysis with $K = 4$, $K = 6$, and $K = 8$ based on 1,351 SNPs of eight *A. palmeri* populations. Each individual is represented by a vertical bar that is divided by K colored segments representing the likelihood of a membership to each cluster.

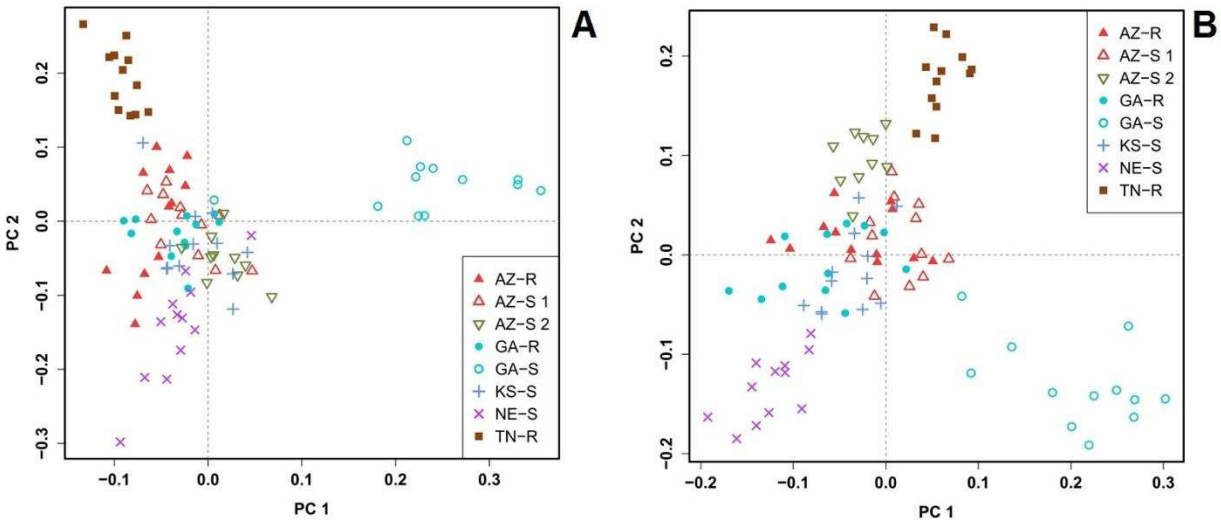

Figure 5-5: Clustering of *A. palmeri* populations based on principal component analysis (PCA) for SNPs found in all eight populations in the chloroplast genome (A) and the mitochondrial genome (B) using the filtered and pruned whole dataset. Each point represents an individual colored according to the collection site. Glyphosate-resistant individuals are marked by filled symbols and susceptible individuals are marked by empty symbols. Individuals from the same U.S. state have the same symbols.

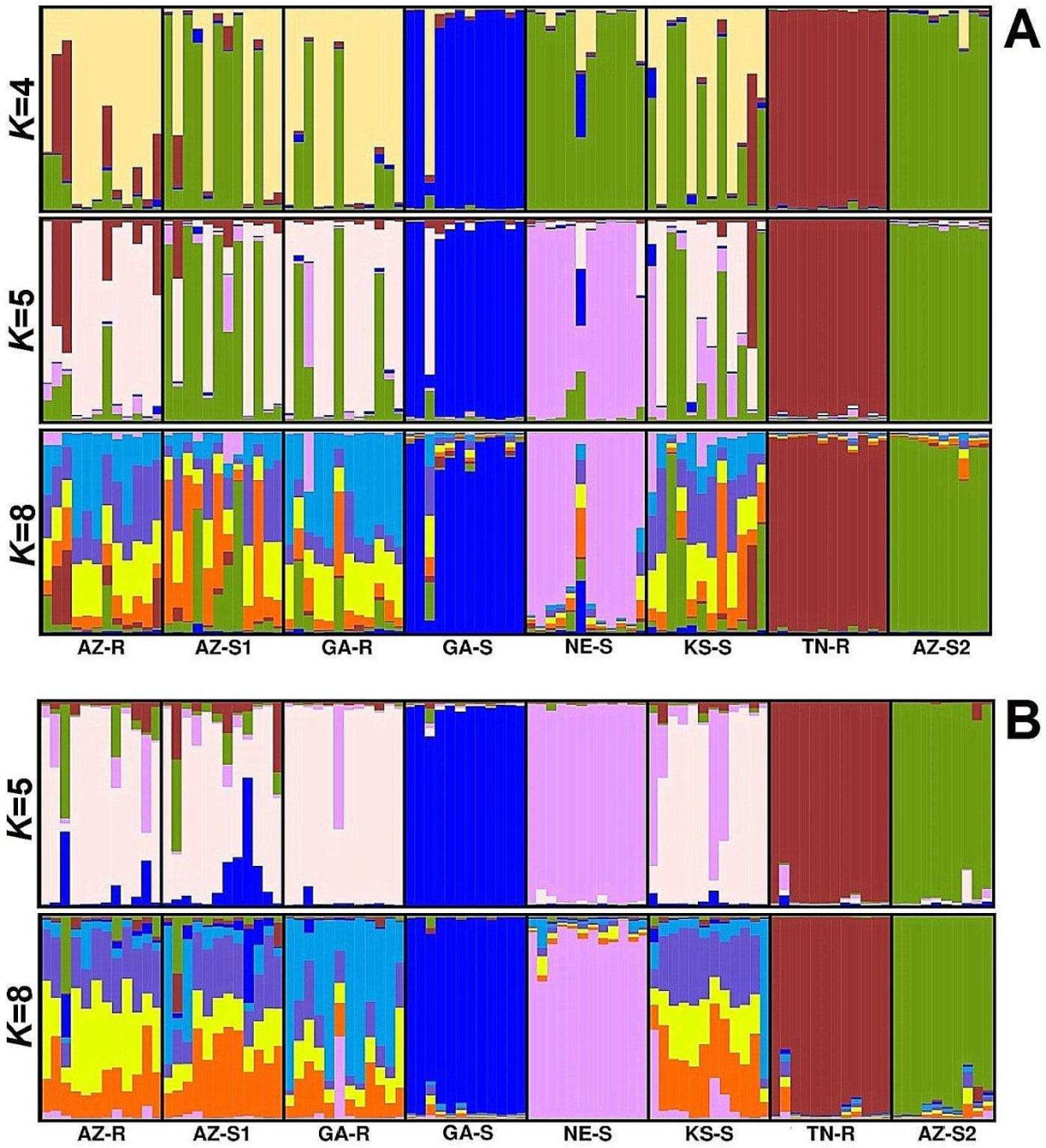

Figure 5-6: Population structure analysis with $K = 4$, $K = 5$, and $K = 8$ based on SNPs from the chloroplast genome for eight *A. palmeri* populations (A) and $K = 5$, and $K = 8$ based on SNPs from the mitochondrial genome for eight *A. palmeri* populations (B). Each individual is represented by a vertical bar that is divided by K colored segments representing the likelihood of a membership to each cluster.

REFERENCES

Adamack, A.T., and Gruber, B. (2014). PopGenReport: Simplifying basic population genetic analyses in R. *Methods Ecol. Evol.* 5(4)**,** 384-387.

Akey, J.M., Zhang, K., Xiong, M., and Jin, L. (2003). The effect of single nucleotide polymorphism identification strategies on estimates of linkage disequilibrium. *Mol. Biol. Evol.* 20(2)**,** 232-242.

Anstead, J.A., Williamson, M.S., and Denholm, I. (2005). Evidence for multiple origins of identical insecticide resistance mutations in the aphid *Myzus persicae*. *Insect Biochem. Mol. Biol.* 35(3)**,** 249-256.

Baxter, S.W., Davey, J.W., Johnston, J.S., Shelton, A.M., Heckel, D.G., Jiggins, C.D., et al. (2011). Linkage mapping and comparative genomics using next-generation RAD sequencing of a non-model organism. *PLoS One* 6(4)**,** doi: 10.1371/journal.pone.0019315.

Beard, K.E., Lay, K.S., Burton, J.D., Burgos, N., and Lawton-Rauh, A.L. (2014). Can very rapid adaptation arise without ancestral variation? Insight from the molecular evolution of herbicide resistance in genus *Amaranthus*. [dissertation]. [Clemson (SC)]: Clemson University.

Beckie, H.J. (2011). Herbicide-resistant weed management: Focus on glyphosate. *Pest Manag. Sci.* 67(9)**,** 1037-1048.

Benbrook, C.M. (2016). Trends in glyphosate herbicide use in the United States and globally. *Env. Sci. Eur.* 28(1)**,** 3.

Berger, S., Madeira, P.T., Ferrell, J., Gettys, L., Morichetti, S., Cantero, J.J., et al. (2016). Palmer amaranth (*Amaranthus palmeri*) identification and documentation of ALS-resistance in Argentina. *Weed Sci.* 64(2)**,** 312-320.

Bradbury, P.J., Zhang, Z., Kroon, D.E., Casstevens, T.M., Ramdoss, Y., and Buckler, E.S. (2007). TASSEL: software for association mapping of complex traits in diverse samples. *Bioinformatics* 23(19)**,** 2633-2635.

Brumfield, R.T., Beerli, P., Nickerson, D.A., and Edwards, S.V. (2003). The utility of single nucleotide polymorphisms in inferences of population history. *Trends Ecol. Evol.* 18(5)**,** 249-256. doi: 10.1016/s0169-5347(03)00018-1.

Cavan, G., Biss, P., and Moss, S. (1998). Localized origins of herbicide resistance in *Alopecurus myosuroides*. *Weed Res.* 38**,** 239-245.

Chahal, P.S., Aulakh, J.S., Jugulam, M., and Jhala, A.J. (2015). *Herbicide-resistant Palmer amaranth (Amaranthus palmeri S. Wats.) in the United States—Mechanisms of resistance, impact, and management*. InTechOpen, Rijeka, Croatia.

Chatham, L.A., Wu, C., Riggins, C.W., Hager, A.G., Young, B.G., Roskamp, G.K., et al. (2015). EPSPS gene amplification is present in the majority of glyphosate-resistant Illinois waterhemp (*Amaranthus tuberculatus*) populations. *Weed Technol.* 29(1)**,** 48-55.

Chauvel, B., and Gasquez, J. (1994). Relationships between genetic polymorphism and herbicide resistance within *Alopecurus myosuroides* Huds. *Heredity* 72(4)**,** 336-344.

Chen, J., Huang, H., Zhang, C., Wei, S., Huang, Z., Chen, J., et al. (2015). Mutations and amplification of EPSPS gene confer resistance to glyphosate in goosegrass (*Eleusine indica*). *Planta* 242(4)**,** 859-868.

Chen, W.-J., Delmotte, F., Cervera, S.R., Douence, L., Greif, C., and Corio-Costet, M.-F. (2007). At least two origins of fungicide resistance in grapevine downy mildew populations. *Appl. Environ. Microbiol.* 73(16)**,** 5162-5172.

Clements, D.R., DiTommaso, A., Jordan, N., Booth, B.D., Cardina, J., Doohan, D., et al. (2004). Adaptability of plants invading North American cropland. *Agric. Ecosyst. Environ.* 104(3)**,** 379-398.

Coupe, R.H., and Capel, P.D. (2016). Trends in pesticide use on soybean, corn and cotton since the introduction of major genetically modified crops in the United States. *Pest Manag. Sci.* 72(5)**,** 1013-1022.

Culpepper, A., Whitaker, J., MacRae, A., and York, A. (2008). Distribution of glyphosate-resistant Palmer amaranth (*Amaranthus palmeri*) in Georgia and North Carolina during 2005 and 2006. *J. Cotton Sci.* 12(3)**,** 306-310.

Culpepper, A.S., Grey, T.L., Vencill, W.K., Kichler, J.M., Webster, T.M., Brown, S.M., et al. (2006). Glyphosate-resistant Palmer amaranth (*Amaranthus palmeri*) confirmed in Georgia. *Weed Sci.* 54(4)**,** 620-626.

Daborn, P., Yen, J., Bogwitz, M., Le Goff, G., Feil, E., Jeffers, S., et al. (2002). A single P450 allele associated with insecticide resistance in *Drosophila*. *Science* 297(5590)**,** 2253-2256.

Danecek, P., Auton, A., Abecasis, G., Albers, C.A., Banks, E., DePristo, M.A., et al. (2011). The variant call format and VCFtools. *Bioinformatics* 27(15)**,** 2156-2158.

Délye, C., Michel, S., Bérard, A., Chauvel, B., Brunel, D., Guillemin, J.P., et al. (2010). Geographical variation in resistance to acetyl-coenzyme A carboxylase-inhibiting herbicides across the range of the arable weed *Alopecurus myosuroides* (black-grass). *New Phytol.* 186(4)**,** 1005-1017.

Deschamps, S., Llaca, V., and May, G.D. (2012). Genotyping-by-sequencing in plants. *Biology* 1(3)**,** 460-483.

Doyle, J. (1991). *DNA protocols for plants–CTAB total DNA isolation.* Springer: Berlin.

Dray, S., and Dufour, A.-B. (2007). The ade4 package: Implementing the duality diagram for ecologists. *J. Stat. Softw.* 22(4)**,** 1-20.

Duke, S.O. (2012). Why have no new herbicide modes of action appeared in recent years? *Pest Manag. Sci.* 68(4)**,** 505-512.

Duke, S.O. (2017). The history and current status of glyphosate. *Pest Manag. Sci.*

Duke, S.O., and Powles, S.B. (2008). Glyphosate: A once-in-a-century herbicide. *Pest Manag. Sci.* 64(4)**,** 319-325.

Earl, D.A. (2012). STRUCTURE HARVESTER: a website and program for visualizing STRUCTURE output and implementing the Evanno method. *Conserv. Genet. Resour.* 4(2)**,** 359-361.

Elshire, R.J., Glaubitz, J.C., Sun, Q., Poland, J.A., Kawamoto, K., Buckler, E.S., et al. (2011). A robust, simple genotyping-by-sequencing (GBS) approach for high diversity species. *PLoS One* 6(5)**,** e19379. doi: 10.1371/journal.pone.0019379.

Evanno, G., Regnaut, S., and Goudet, J. (2005). Detecting the number of clusters of individuals using the software STRUCTURE: a simulation study. *Mol. Ecol.* 14(8)**,** 2611-2620. doi: 10.1111/j.1365-294X.2005.02553.x.

Farmer, J.A., Webb, E.B., Pierce, R.A., and Bradley, K.W. (2017). Evaluating the potential for weed seed dispersal based on waterfowl consumption and seed viability. *Pest Manag. Sci.*

Fasina, F.O., Shittu, A., Lazarus, D., Tomori, O., Simonsen, L., Viboud, C., et al. (2014). Transmission dynamics and control of Ebola virus disease outbreak in Nigeria, July to September 2014. *Euro Surveill.* 19(40)**,** pii: 20920.

Fernández, L., Haro, L.A., Distefano, A.J., Carolina Martínez, M., Lía, V., Papa, J.C., et al. (2013). Population genetics structure of glyphosate-resistant Johnsongrass (*Sorghum halepense* L. Pers) does not support a single origin of the resistance. *Ecol. Evol.* 3(10)**,** 3388-3400.

Franssen, A.S., Skinner, D.Z., Al-Khatib, K., Horak, M.J., and Kulakow, P.A. (2001). Interspecific hybridization and gene flow of ALS resistance in *Amaranthus* species. *Weed Sci.* 49(5)**,** 598-606.

Gaines, T.A., Zhang, W., Wang, D., Bukun, B., Chisholm, S.T., Shaner, D.L., et al. (2010). Gene amplification confers glyphosate resistance in *Amaranthus palmeri*. *Proc. Nat. Acad. Sci. USA* 107(3)**,** 1029-1034.

Ge, X., d'Avignon, D.A., Ackerman, J.J., and Sammons, R.D. (2010). Rapid vacuolar sequestration: The horseweed glyphosate resistance mechanism. *Pest Manag. Sci.* 66(4)**,** 345-348.

Georghiou, G.P., and Taylor, C.E. (1986). *Factors influencing the evolution of resistance.* Washington, D.C.: National Academy Press.

Glaubitz, J.C., Casstevens, T.M., Lu, F., Harriman, J., Elshire, R.J., Sun, Q., et al. (2014). TASSEL-GBS: a high capacity genotyping by sequencing analysis pipeline. *PLoS One* 9(2)**,** doi: 10.1371/journal.pone.0090346. doi: 10.1371/journal.pone.0090346.

Heap, I. (2018). *The International Survey of Herbicide Resistant Weeds. Online. Available:* www.weedscience.org [Online]. Available: www.weedscience.org [Accessed January 30, 2018].

Jakobsson, M., and Rosenberg, N.A. (2007). CLUMPP: a cluster matching and permutation program for dealing with label switching and multimodality in analysis of population structure. *Bioinformatics* 23(14)**,** 1801-1806.

Jasieniuk, M., Brûlé-Babel, A.L., and Morrison, I.N. (1996). The evolution and genetics of herbicide resistance in weeds. *Weed Sci.***,** 176-193.

Jombart, T., and Ahmed, I. (2011). adegenet 1.3-1: New tools for the analysis of genome-wide SNP data. *Bioinformatics* 27(21)**,** 3070-3071.

Jugulam, M., Niehues, K., Godar, A.S., Koo, D.-H., Danilova, T., Friebe, B., et al. (2014). Tandem amplification of a chromosomal segment harboring 5-enolpyruvylshikimate-3-phosphate synthase locus confers glyphosate resistance in *Kochia scoparia. Plant Physiol.* 166(3)**,** 1200-1207.

Kamvar, Z.N., Tabima, J.F., and Grünwald, N.J. (2014). Poppr: an R package for genetic analysis of populations with clonal, partially clonal, and/or sexual reproduction. *PeerJ* 2**,** doi: 10.7717/peerj.7281.

Karn, E., and Jasieniuk, M. (2017). Nucleotide diversity at site 106 of EPSPS in *Lolium perenne* L. ssp. *multiflorum* from California indicates multiple evolutionary origins of herbicide resistance. *Front. Plant Sci.* 8**,** doi: 10.3389/fpls.2017.00777.

Kartescz, J.T. (2014). *The Biota of North America Program (BONAP)* [Online]. Taxonomic Data Center. (http://www.bonap.net/tdc). Chapel Hill, N.C. Available: http://bonap.net/napa [Accessed 2017 July 28].

Kuester, A., Chang, S.M., and Baucom, R.S. (2015). The geographic mosaic of herbicide resistance evolution in the common morning glory, Ipomoea purpurea: Evidence for resistance hotspots and low genetic differentiation across the landscape. *Evol. Appl.* 8(8)**,** 821-833.

Küpper, A., Borgato, E.A., Patterson, E.L., Netto, A.G., Nicolai, M., Carvalho, S.J.d., et al. (2017). Multiple resistance to glyphosate and acetolactate synthase inhibitors in Palmer amaranth (*Amaranthus palmeri*) identified in Brazil. *Weed Sci.* 65(3)**,** 317-326.

Laplante, J., Rajcan, I., and Tardif, F.J. (2009). Multiple allelic forms of acetohydroxyacid synthase are responsible for herbicide resistance in *Setaria viridis*. *Theor. Appl. Genet.* 119(4)**,** 577-585.

Linda, M., and Alan, L. (1997). Structure and organization of amplicons containing the E4 esterase genes responsible for insecticide resistance in the aphid *Myzus persicae* (Sulzer). *Biochem. J.* 322(3)**,** 867-871.

Lorentz, L., Gaines, T.A., Nissen, S.J., Westra, P., Strek, H.J., Dehne, H.W., et al. (2014). Characterization of glyphosate resistance in *Amaranthus tuberculatus* populations. *J. Agric. Food Chem.* 62(32)**,** 8134-8142.

Lu, F., Lipka, A.E., Glaubitz, J., Elshire, R., Cherney, J.H., Casler, M.D., et al. (2013). Switchgrass genomic diversity, ploidy, and evolution: Novel insights from a network-based SNP discovery protocol. *PLoS Genetics* 9(1)**,** doi: 10.1371/journal.pgen.1003215.

Malone, J.M., Morran, S., Shirley, N., Boutsalis, P., and Preston, C. (2016). EPSPS gene amplification in glyphosate-resistant *Bromus diandrus*. *Pest Manag. Sci.* 72(1)**,** 81-88.

Maxwell, B.D., Roush, M.L., and Radosevich, S.R. (1990). Predicting the evolution and dynamics of herbicide resistance in weed populations. *Weed Technol.***,** 2-13.

McNaughton, K.E., Letarte, J., Lee, E.A., and Tardif, F.J. (2005). Mutations in ALS confer herbicide resistance in redroot pigweed (*Amaranthus retroflexus*) and Powell amaranth (*Amaranthus powellii*). *Weed Sci.* 53(1)**,** 17-22.

Menchari, Y., Camilleri, C., Michel, S., Brunel, D., Dessaint, F., Le Corre, V., et al. (2006). Weed response to herbicides: regional-scale distribution of herbicide resistance alleles in the grass weed *Alopecurus myosuroides*. *New Phytol.* 171(4)**,** 861-874.

Menchari, Y., Délye, C., and Le Corre, V. (2007). Genetic variation and population structure in black-grass (*Alopecurus myosuroides* Huds.), a successful, herbicide-resistant, annual grass weed of winter cereal fields. *Mol. Ecol.* 16(15)**,** 3161-3172.

Molin, W.T., Nandula, V.K., Wright, A.A., and Bond, J.A. (2016). Transfer and expression of ALS inhibitor resistance from Palmer Amaranth (*Amaranthus palmeri*) to an *A. spinosus* × *A. palmeri* hybrid. *Weed Sci.* 64(2)**,** 240-247.

Molin, W.T., Wright, A.A., Lawton-Rauh, A., and Saski, C.A. (2017a). The unique genomic landscape surrounding the EPSPS gene in glyphosate resistant *Amaranthus palmeri*: A repetitive path to resistance. *BMC Genomics* 18(91)**,** doi: 10.1186/s12864-12016-13336-12864.

Molin, W.T., Wright, A.A., VanGessel, M.J., McCloskey, W.B., Jugulam, M., and Hoagland, R.E. (2017b). Survey of the genomic landscape surrounding the EPSPS gene in glyphosate resistant *Amaranthus palmeri* from geographically distant populations in the United States. *Pest Manag. Sci.*

Morin, P.A., Luikart, G., Wayne, R.K., and the, S.N.P.w.g. (2004). SNPs in ecology, evolution and conservation. *Trends Ecol. Evol.* 19(4)**,** 208-216. doi: 10.1016/j.tree.2004.01.009.

Nakka, S., Godar, A.S., Wani, P.S., Thompson, C.R., Peterson, D.E., Roelofs, J., et al. (2017). Physiological and molecular characterization of hydroxyphenylpyruvate dioxygenase (HPPD)-inhibitor resistance in Palmer amaranth (*Amaranthus palmeri* S. Wats.). *Front. Plant Sci.* 8**,** 555.

Nandula, V.K., Wright, A.A., Bond, J.A., Ray, J.D., Eubank, T.W., and Molin, W.T. (2014). EPSPS amplification in glyphosate-resistant spiny amaranth (*Amaranthus spinosus*): a case of gene transfer via interspecific hybridization from glyphosate-resistant Palmer amaranth (*Amaranthus palmeri*). *Pest Manag. Sci.* 70(12)**,** 1902-1909.

Narum, S.R., Buerkle, C.A., Davey, J.W., Miller, M.R., and Hohenlohe, P.A. (2013). Genotyping-by-sequencing in ecological and conservation genomics. *Mol. Ecol.* 22(11)**,** 2841-2847. doi: 10.1111/mec.12350.

Nei, M. (1972). Genetic distance between populations. *Amer. Nat.* 106(949)**,** 283-292.

Neve, P. (2008). Simulation modelling to understand the evolution and management of glyphosate resistance in weeds. *Pest Manag. Sci.* 64(4)**,** 392-401.

Neve, P., Norsworthy, J.K., Smith, K.L., and Zelaya, I.A. (2011). Modelling evolution and management of glyphosate resistance in *Amaranthus palmeri*. *Weed Res.* 51(2)**,** 99-112.

Ngo, T.D., Malone, J.M., Boutsalis, P., Gill, G., and Preston, C. (2017). EPSPS gene amplification conferring resistance to glyphosate in windmill grass (*Chloris truncata*) in Australia. *Pest Manag. Sci.*

Norsworthy, J.K., Griffith, G., Griffin, T., Bagavathiannan, M., and Gbur, E.E. (2014). In-field movement of glyphosate-resistant Palmer amaranth (*Amaranthus palmeri*) and its impact on cotton lint yield: evidence supporting a zero-threshold strategy. *Weed Sci.* 62(2)**,** 237-249.

Norsworthy, J.K., Griffith, G.M., Scott, R.C., Smith, K.L., and Oliver, L.R. (2008). Confirmation and control of glyphosate-resistant Palmer amaranth (*Amaranthus palmeri*) in Arkansas. *Weed Technol.* 22(1)**,** 108-113.

Okada, M., Hanson, B.D., Hembree, K.J., Peng, Y., Shrestha, A., Stewart, C.N., et al. (2013). Evolution and spread of glyphosate resistance in *Conyza canadensis* in California. *Evol. Appl.* 6(5)**,** 761-777. doi: 10.1111/eva.12061.

Patzoldt, W.L., and Tranel, P.J. (2007). Multiple ALS mutations confer herbicide resistance in waterhemp (*Amaranthus tuberculatus*). *Weed Sci.* 55(5)**,** 421-428.

Pembleton, L.W., Cogan, N.O., and Forster, J.W. (2013). StAMPP: An R package for calculation of genetic differentiation and structure of mixed-ploidy level populations. *Mol. Ecol. Resour.* 13(5)**,** 946-952.

Petit, R.J., Duminil, J., Fineschi, S., Hampe, A., Salvini, D., and Vendramin, G.G. (2005). Comparative organization of chloroplast, mitochondrial and nuclear diversity in plant populations. *Mol. Ecol.* 14(3)**,** 689-701.

Pinto, J., Lynd, A., Vicente, J.L., Santolamazza, F., Randle, N.P., Gentile, G., et al. (2007). Multiple origins of knockdown resistance mutations in the Afrotropical mosquito vector *Anopheles gambiae*. *PLoS One* 2(11)**,** e1243.

Porras-Hurtado, L., Ruiz, Y., Santos, C., Phillips, C., Carracedo, Á., and Lareu, M.V. (2013). An overview of STRUCTURE: Applications, parameter settings, and supporting software. *Front Genet.* 4**,** doi: 10.3389/fgene.2013.00098.

Powles, S.B., and Yu, Q. (2010). Evolution in action: Plants resistant to herbicides. *Annu. Rev. Plant. Biol.* 61**,** 317-347.

Pritchard, J.K., Stephens, M., and Donnelly, P. (2000). Inference of population structure using multilocus genotype data. *Genetics* 155(2)**,** 945-959.

Ralph, P.L., and Coop, G. (2015). Convergent evolution during local adaptation to patchy landscapes. *PLoS Genetics* 11(11)**,** doi: 10.1371/journal.pgen.1005630.

Raymond, M., and Callaghan, A. (1991). Worldwide migration of amplified insecticide resistance genes in mosquitoes. *Nature* 350(6314)**,** 151.

Reitzel, A.M., Herrera, S., Layden, M.J., Martindale, M.Q., and Shank, T.M. (2013). Going where traditional markers have not gone before: Utility of and promise for RAD sequencing in marine invertebrate phylogeography and population genomics. *Mol. Ecol.* 22(11)**,** 2953-2970. doi: 10.1111/mec.12228.

Rosenberg, N.A. (2004). DISTRUCT: A program for the graphical display of population structure. *Mol. Ecol. Resour.* 4(1)**,** 137-138.

Salas, R.A., Dayan, F.E., Pan, Z., Watson, S.B., Dickson, J.W., Scott, R.C., et al. (2012). EPSPS gene amplification in glyphosate-resistant Italian ryegrass (*Lolium perenne* ssp. *multiflorum*) from Arkansas. *Pest Manag. Sci.* 68(9)**,** 1223-1230.

Sauer, J. (1957). Recent migration and evolution of the dioecious amaranths. *Evol.* 11(1)**,** 11-31.

Schwartz-Lazaro, L.M., Norsworthy, J.K., Scott, R.C., and Barber, L.T. (2017). Resistance of two Arkansas *Palmer amaranth* populations to multiple herbicide sites of action. *Crop Prot.* 96**,** 158-163.

Schwartz, L.M., Norsworthy, J.K., Young, B.G., Bradley, K.W., Kruger, G.R., Davis, V.M., et al. (2016). Tall waterhemp (*Amaranthus tuberculatus*) and palmer amaranth (*Amaranthus palmeri*) seed production and retention at soybean maturity. *Weed Technol.* 30(1)**,** 284-290.

Scott, R., Steckel, L., Smith, K., Mueller, S., Oliver, L., and Norsworthy, J. (Year). "Glyphosate-resistant Palmer amaranth in Tennessee and Arkansas", in: *Proc. South. Weed. Sci. Soc.*), 226.

Sellers, B.A., Smeda, R.J., Johnson, W.G., Kendig, J.A., and Ellersieck, M.R. (2003). Comparative growth of six *Amaranthus* species in Missouri. *Weed Sci.* 51(3)**,** 329-333.

Shaner, D.L., Nadler-Hassar, T., Henry, W.B., and Koger, C.H. (2005). A rapid *in vivo* shikimate accumulation assay with excised leaf discs. *Weed Sci.* 53(6)**,** 769-774.

Steckel, L.E., Main, C.L., Ellis, A.T., and Mueller, T.C. (2008). Palmer amaranth (*Amaranthus palmeri*) in Tennessee has low level glyphosate resistance. *Weed Technol.* 22(1)**,** 119-123.

Tranel, P.J., and Wright, T.R. (2002). Resistance of weeds to ALS-inhibiting herbicides: what have we learned? *Weed Sci.* 50(6)**,** 700-712.

Wakeley, J., Nielsen, R., Liu-Cordero, S.N., and Ardlie, K. (2001). The discovery of single-nucleotide polymorphisms—and inferences about human demographic history. *Am. J. Hum. Genet.* 69(6)**,** 1332-1347.

Wang, W., Xia, H., Yang, X., Xu, T., Si, H.J., Cai, X.X., et al. (2014). A novel 5-enolpyruvoylshikimate-3-phosphate (EPSP) synthase transgene for glyphosate resistance stimulates growth and fecundity in weedy rice (*Oryza sativa*) without herbicide. *New Phytol.* 202(2)**,** 679-688.

Ward, S.M., Webster, T.M., and Steckel, L.E. (2013). Palmer amaranth (*Amaranthus palmeri*): A review. *Weed Technol.* 27(1)**,** 12-27.

Washburn, J.D., Schnable, J.C., Davidse, G., and Pires, J.C. (2015). Phylogeny and photosynthesis of the grass tribe *Paniceae*. *Am. J. Bot.* 102(9)**,** 1493-1505.

Webster, T.M., and Coble, H.D. (1997). Changes in the weed species composition of the southern United States: 1974 to 1995. *Weed Technol.*, 308-317.

Webster, T.M., and Nichols, R.L. (2012). Changes in the prevalence of weed species in the major agronomic crops of the Southern United States: 1994/1995 to 2008/2009. *Weed Sci.* 60(2), 145-157.

Westbrooks, R.G. (2004). New approaches for early detection and rapid response to invasive plants in the United States. *Weed Technol.* 18(sp1), 1468-1471.

Whaley, C.M., Wilson, H.P., and Westwood, J.H. (2006). ALS resistance in several smooth pigweed (*Amaranthus hybridus*) biotypes. *Weed Sci.* 54(5), 828-832.

Wiersma, A.T., Gaines, T.A., Preston, C., Hamilton, J.P., Giacomini, D., Buell, C.R., et al. (2015). Gene amplification of 5-enol-pyruvylshikimate-3-phosphate synthase in glyphosate-resistant *Kochia scoparia*. *Planta* 241(2), 463-474.

Wolfe, K.H., Li, W.-H., and Sharp, P.M. (1987). Rates of nucleotide substitution vary greatly among plant mitochondrial, chloroplast, and nuclear DNAs. *Proc. Nat. Acad. Sci. USA* 84(24), 9054-9058.

Yu, Q., Han, H., Li, M., Purba, E., Walsh, M., and Powles, S. (2012). Resistance evaluation for herbicide resistance–endowing acetolactate synthase (ALS) gene mutations using *Raphanus raphanistrum* populations homozygous for specific ALS mutations. *Weed Res.* 52(2), 178-186.

Zheng, X., Levine, D., Shen, J., Gogarten, S.M., Laurie, C., and Weir, B.S. (2012). A high-performance computing toolset for relatedness and principal component analysis of SNP data. *Bioinformatics* 28(24), 3326-3328.

Zhu, Q., Gao, P., Liu, S., Amanullah, S., and Luan, F. (2016). Comparative analysis of single nucleotide polymorphisms in the nuclear, chloroplast, and mitochondrial genomes in identification of phylogenetic association among seven melon (*Cucumis melo L.*) cultivars. *Breed. Sci.* 66(5), 711-719.

6. OUTLOOK

The research described in this dissertation confirmed that enhanced metabolism is the sole tembotrione resistance mechanism in *A. palmeri* from Nebraska, identified new tembotrione metabolites in plants and furthered the knowledge about metabolic resistance in dicot weeds by identifying differences in metabolism and gene expression. Many of these findings open up new questions that remain to be answered by the generation of weed scientists. For example, how can metabolic resistance be predicted? Are there structural characteristics that make a compound more liable for degradation in plants? Can these structures be predicted and avoided? How exactly is the up-regulation of metabolic resistance genes regulated and how did it evolve? Does it come with a fitness penalty for resistant plants? So far weed scientists have given the recommendation to farmers to rotate between different herbicide modes of action to combat the evolution of resistant plants. But if certain metabolic genes are able to confer resistance to herbicides from different modes of action, do we have to switch to grouping herbicides according to resistance genes now and rather recommend to rotate between these different groups? The research on population structure gave novel insights into the distribution, dispersal and evolutionary patterns of glyphosate-resistant and -susceptible *A. palmeri* but new questions about the dispersal corridors and ways of transportation remain.

Answering these questions is important to maintain the effectiveness of currently commercialized herbicides and to bring successful new herbicides to the market. The rapid developments in the areas of genomics, transcriptomics and molecular genetic techniques have helped to gain more genomic information about weedy species and enabled faster and cheaper identification of candidate genes. Future research will have to focus on cloning and validating the many candidate genes that are identified. Continuing to gain knowledge about resistance mechanisms, their evolution and their dispersal is crucial to develop optimized and new strategies to manage herbicide resistance in the field.

7. APPENDIX A

METHODS

^{14}C-tembotrione absorption and translocation

To assess tembotrione uptake, nine plants from NER and NES each were used for this experiment. The youngest fully expanded leaf of 8-10 cm tall plants was treated with a total of 7000 Bq of ^{14}C-tembotrione (Bayer) with a specific activity of 4.33 MBq mg^{-1}, applied in six 0.5 µL droplets. The treated plants were then incubated in a growth chamber at 25/18 °C and 16/8 h day/night period for 24 h. Subsequently, they were cut above soil level and the treated leaf was washed in 5 mL 33% methanol and 0.01 % Triton X100 solution. 500 µL of the solution was then measured on a liquid scintillation counter (Packard TriCarb 2000CA, GMI Inc, Ramsey, MN) to determine the amount of tembotrione that was not absorbed. The plants were then pressed and dried at 60°C. Three plants from each population were exposed to a phosphor-imaging film (BAS-MS-2040, Fuji, Tokyo, Japan) for 48 h before reading them on a phosphor imager (BAS-reader 1000, Fuji, Tokyo, Japan) to visualize differences in ^{14}C-radioactivity translocation. To quantify the extent of the translocation, the remaining six plants per population were separated into treated leaf, meristem, and stem as well as second, third, fourth, and fifth leaf. The radioactivity absorbed into the different plant parts was quantified by combustion using a biological oxidizer (OX-300, R.J. Harvey Instrument Corp., Hillsdale, NJ). The released CO_2 was collected in 10 mL scintillation solution (Oxysolve C400, Zinsser Analytics, Frankfurt, Germany) after a 2 min oxidation period (1.5 min oxygen, 0.5 min nitrogen) at 900 °C. The radioactivity was measured on a liquid scintillation counter. The radioactive leaf uptake was calculated as % of total radioactivity applied, and the radioactive translocation was calculated as % of total radioactivity absorbed.

HPPD gene copy number and expression

Young leaf tissue of three individuals each from NER and NES was collected and immediately frozen in liquid nitrogen and stored at -80°C. DNA was extracted using a modified cetyltrimethylammonium bromide (CTAB) extraction method(Doyle, 1991; Küpper et al., 2017a) and quantified on a NanoDrop spectrophotometer (Thermo Scientific, Waltham, MA). Q-PCR (CFX Connect™ Real-Time PCR Detection System thermal cycler, BioRad, Hercules, CA) was used to determine *HPPD* gene copy number. The qPCR reaction mix consisted of 12.5 µL of SYBR Green (BioRad, Hercules, CA), 1 µL each of forward and reverse primers (5 µM), and 20 ng of DNA to make the total reaction volume of 25 µL. Primer sets used were *HPPD* forward and reverse (F 5'-CTGTCGAAGTAGAAGACGCAG-3' and R 5'-TACATACCGAAGCACAACATCC-3') as well as *β-tubulin* (F 5'-ATGTGGGATGCCAAGAACATGATGTG-3' and R 5'-TCCACTCCACAAAGTAGGAAGAGTTCT-3'); carbamoyl phosphate synthetase (*CPS*) (F 5'-ATTGATGCTGCCGAGGATAG-3' and R 5'-GATGCCTCCCTTAGGTTGTTC-3') and acetolactate synthase (*ALS*) (F 5′-GCTGCTGAAGGCTACGCT-3′ and R 5′- GCGGGACTGAGTCAAGAAGTG-3′) for normalization.(Gaines et al., 2010; Godar et al., 2015) Q-PCR conditions were 50°C for 2 min, 95°C for 10 min, and 40 cycles of 95°C for 30 s and 60°C for 1 min.(Ma et al., 2013) For relative expression quantification a modification of the 2-ΔΔCt method (Schmittgen and Livak, 2008) was used with *HPPD:reference gene* relative expression quantification calculated as $\Delta C_T = C_{T(\text{reference gene})} - C_{T(\text{HPPD}).}$ Each biological sample was run in three technical replicates.

PCR experiments on cDNA were performed to determine *HPPD* expression. Young leaf tissue from at least three individuals at the 7-9 cm stage from the NER and NES populations, respectively, was collected before and 24 HAT with 91 g a.i. ha^{-1} tembotrione (Laudis, Bayer CropScience, Leverkusen, Germany) and 1% MSO. Additionally, leaf tissue from an HPPD inhibitor-resistant (KSR) and susceptible (KSS) *A. palmeri* population from Kansas (Nakka et al., 2017) was used. Due to the resistant populations segregating for resistance, only resistant plants that survived the field rate application 21 DAT were used. Applications were made inside a stationary cabinet spray chamber (DeVries

Manufacturing, Hollandale, MN) equipped with a flat-fan nozzle tip (TeeJet 8002EVS, Spraying System Co., Glendale Heights, IL) calibrated to deliver 187 L ha^{-1} of spray solution at 172 kPa. The samples were immediately frozen in liquid nitrogen and stored at -80 °C. RNA was extracted using Quick-RNA™ MiniPrep Plus (Zymo Research, Irvine, CA) which includes DNAse treatment and was then quantified on a NanoDrop spectrophotometer (Thermo Scientific, Waltham, MA). For cDNA synthesis, 1 µg of total RNA using iScript™ Reverse Transcription Supermix for RT-qPCR (Bio-Rad, Hercules, CA) was used. The qPCR reaction mix consisted of 12.5 µL of SYBR Green (BioRad, Hercules, CA), 1 µL each of forward and reverse primers (5 µM), and 1 µL of cDNA to make the total reaction volume of 25 µL. The primer sets and qPCR conditions used were the same as described for the *HPPD* gene copy number experiment. *HPPD:reference gene* expression was determined following a modification of the 2-ΔΔCt method (Schmittgen and Livak, 2008) with ΔC_T being $C_{T(\text{reference gene})} - C_{T(\text{HPPD}).}$ - Each biological sample was run in three technical replicates.

RESULTS

^{14}C-tembotrione absorption and translocation

To determine if resistance could be due to decreased absorption or translocation, ^{14}C-tembotrione was used to measure absorption and translocation in NER and NES. The recovery rate of the applied ^{14}C-tembotrione in the experiment was 92% on average. Tembotrione remaining on the leaf surface was measured 24 HAT in nine individuals of NER and NES each. Both populations exhibited high and not significantly different radioactivity absorption (89%) showing similar parent compound uptake between NER and NES (Supporting Information Fig. 2A). However, there was a trend towards more ^{14}C-radioactivity ($P = 0.066$) remaining in the treated leaf of NER than in NES at 24 HAT, which is also reflected by a trend towards less ^{14}C-radioactivity found in other parts of the plant ($P = 0.067$, Supporting Information Fig. 2B). Phosphor-imaging of the treated plants shows that within 24 HAT the labeled compounds move through the stem and to every leaf in the plant. However, in the majority of NER translocation to the older leaves was visually reduced compared to the NES (Supporting Information Fig.

3). This can be the consequence of an inhibition of transport of the parent compound, tembotrione, or the weaker transport of metabolites of tembotrione. Therefore, *in planta* metabolism was studied in more detail.

HPPD gene copy number and expression

Q-PCR was used to measure relative genomic copy numbers of the *HPPD* gene relative to the reference genes *ALS*, *CPS*, and *β-tubulin* in NER and NES individuals. Genomic *HPPD* copy numbers ranged from 1.0 to 1.1 for *HPPD:β-tubulin* and *HPPD:ALS* and from 1.3 to 1.6 for *HPPD:CPS* for both NER and NES individuals (Appendix A, Figure 7-2), confirming that NER did not show increased *HPPD* gene copy numbers when compared to NES. The mRNA gene expression pattern of *HPPD* was tested in individuals from NER, NES, KSR, and KSS before and 24 HAT with the recommended field rate of tembotrione (91 g a.i. ha^{-1}). In the untreated plants a trend towards increased *HPPD* transcription was observed in NER and KSR. However, none of the differences were significant (Appendix A, Figure 7-5A/B). In contrast to Nakka *et al.* (2017), the untreated plants in this study were not treated with adjuvants, which could explain the differences in expression level. Increasing *HPPD* transcription trends were lost 24 HAT (Appendix A, Figure 7-5C/D). *HPPD* relative expression between plants within the population was quite variable, as has been found before (Kaundun et al., 2017). Hence, it is important to use a sufficiently large number of biological replicates.

FIGURES

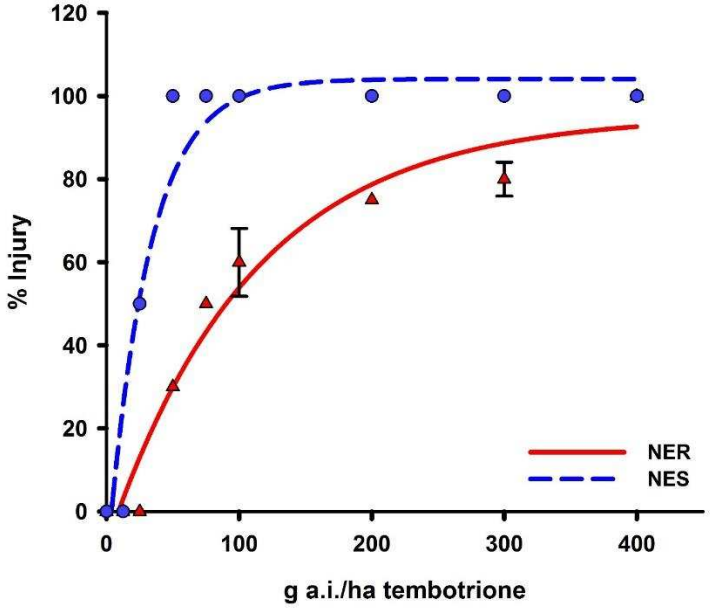

Figure 7-1: Non-linear regression analysis of injury for *A. palmeri* populations NER and NES 35 DAT with tembotrione. Symbols are averages of 20 replicates fitted in a three-parameter log-logistic model with standard errors.

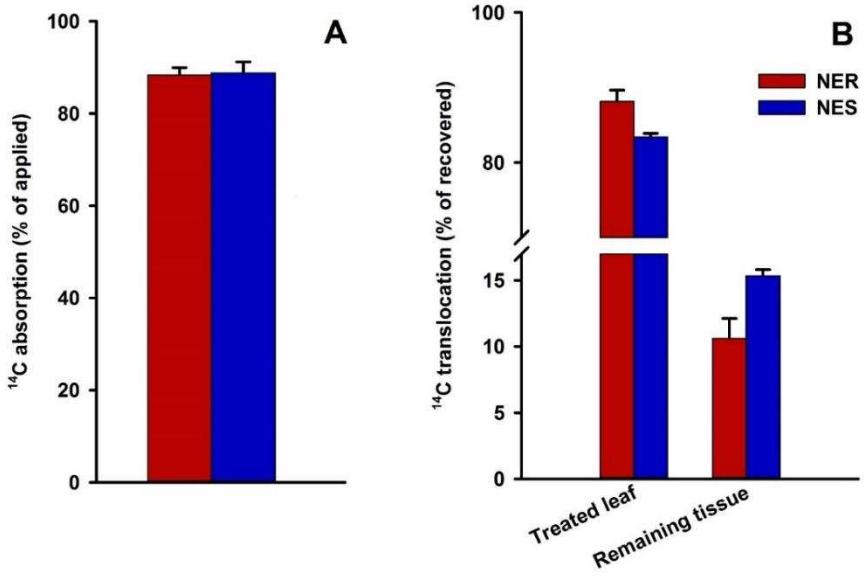

Figure 7-2: Tembotrione absorption and translocation in *A. palmeri*. ^{14}C-tembotrione absorption as % of applied radioactivity to NER and NES, 24 HAT (A). ^{14}C-tembotrione translocation to different parts of the plant as % applied radioactivity to NER and NES, 24 HAT (B). Error bars show standard errors.

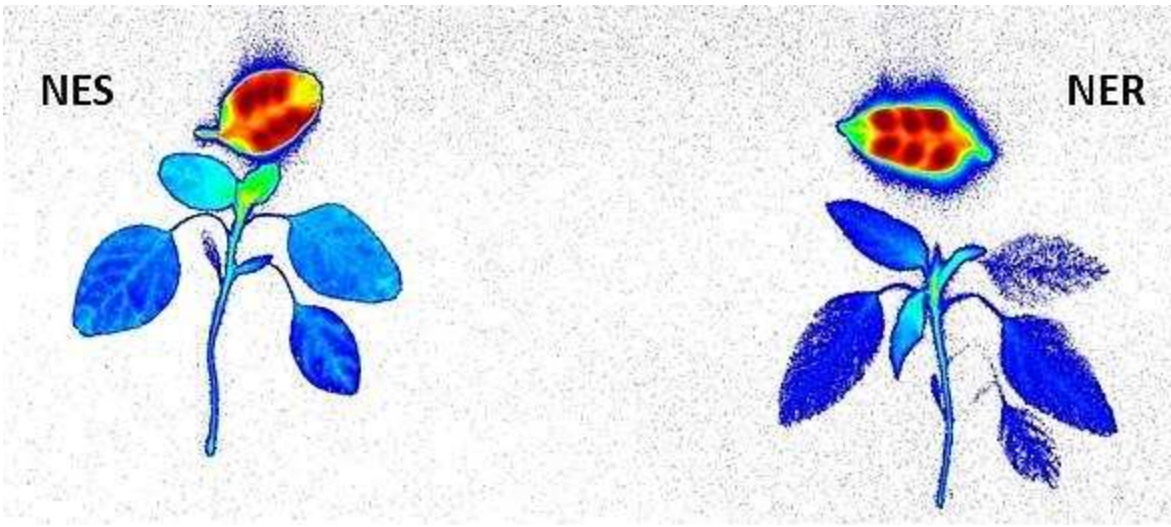

Figure 7-3: Phosphor-imager images of ^{14}C-radioactivity distribution within a NES and NER plant. Red shows high radioactivity, blue shows low radioactivity.

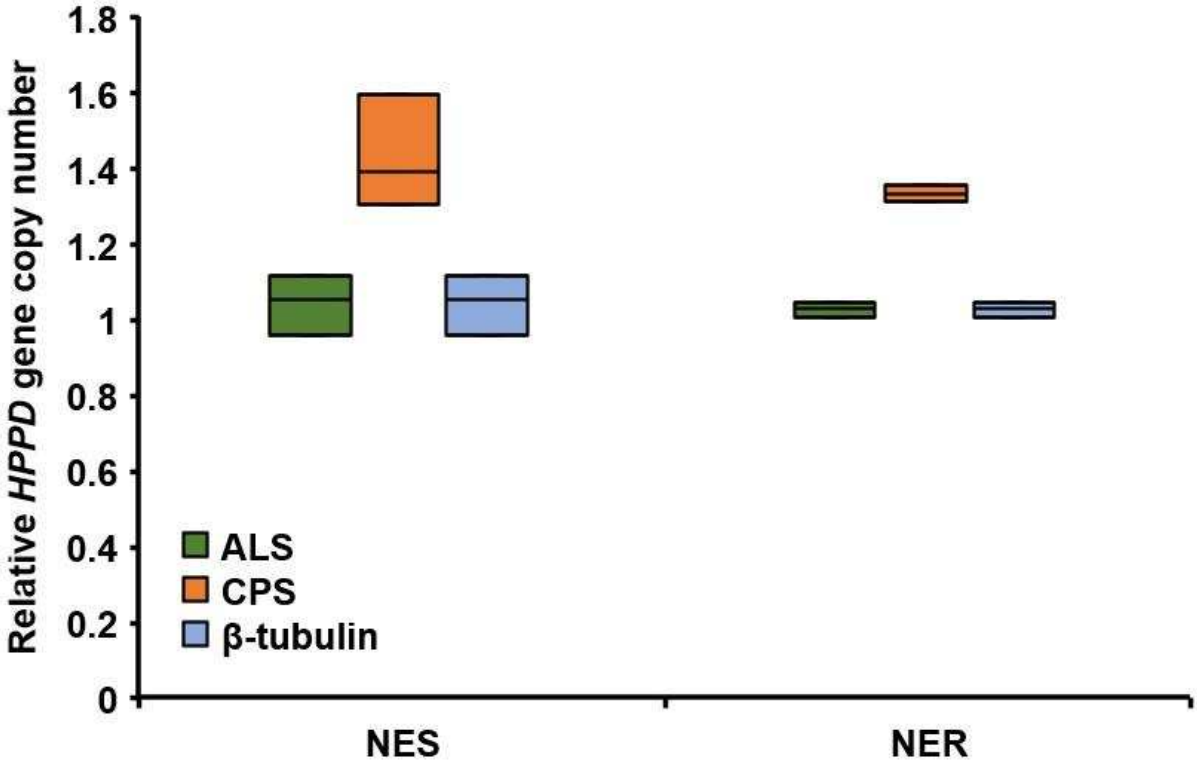

Figure 7-4: HPPD genomic copy number of NES and NER A. palmeri individuals relative to the reference genes ALS, CPS and β-tubulin.

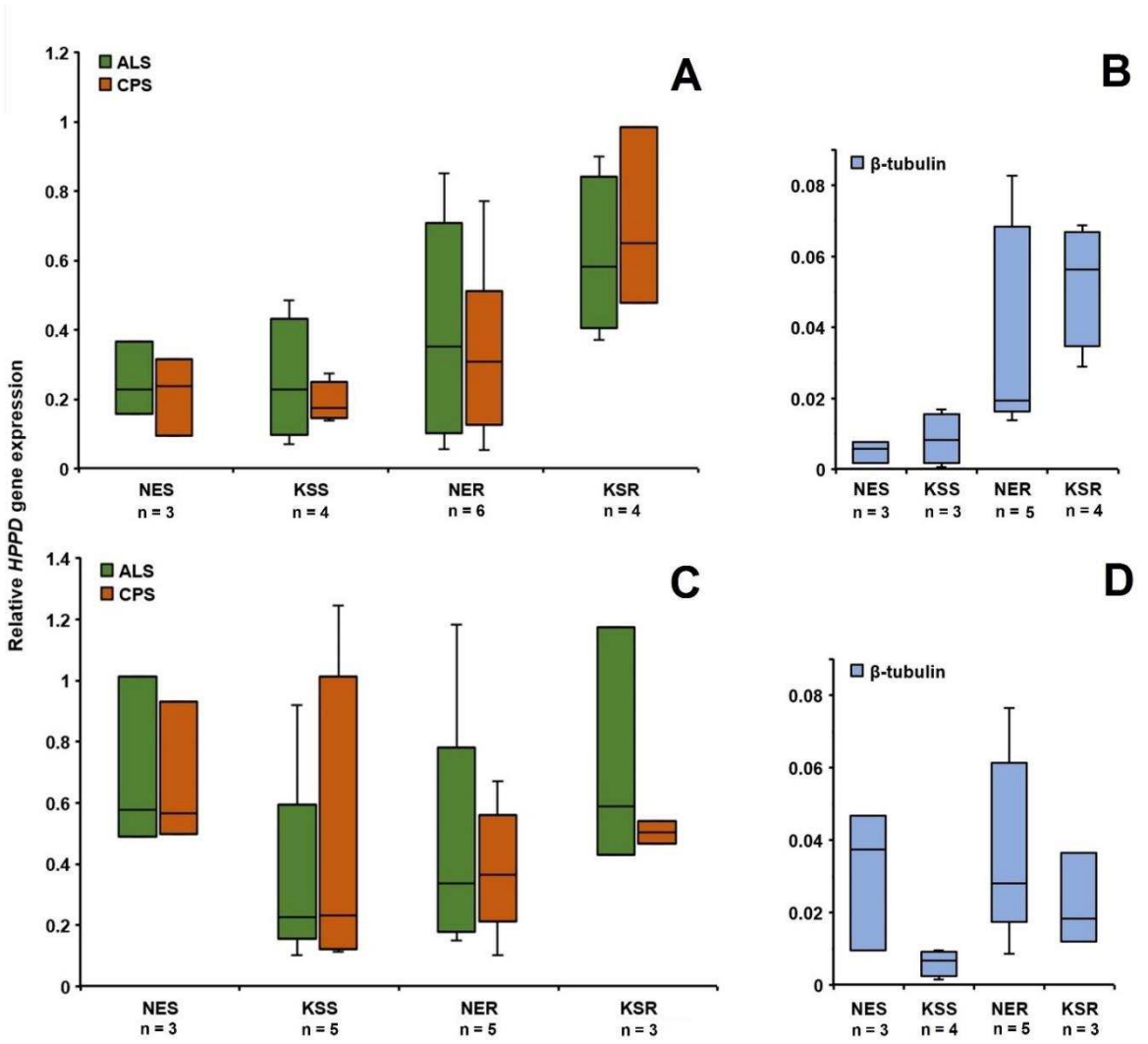

Figure 7-5: HPPD gene expression in A. palmeri individuals from NES, KSS, NER, and KSR without herbicide treatment and normalized to the reference genes ALS, CPS (A), and β-tubulin (B) as well as 24 HAT with tembotrione and normalized to the reference genes ALS, CPS (C), and β-tubulin (D). The number of individuals used per population (n) is indicated.

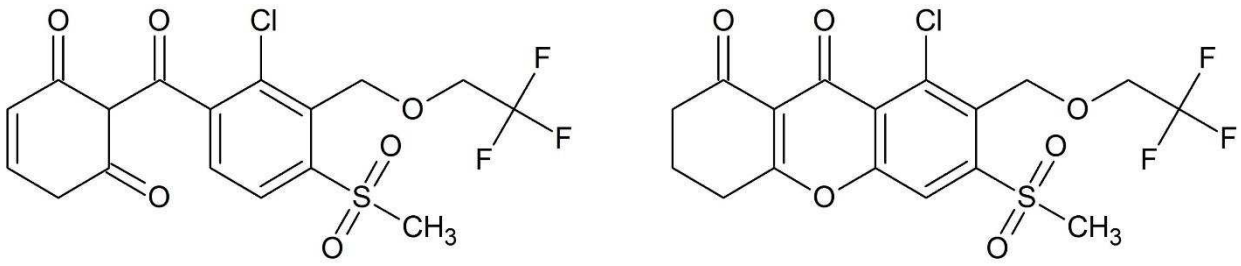

Figure 7-6: Example of intramolecular cyclization for the metabolite M5.

8. APPENDIX B

TABLES

Table 8-1: Identification of differentially expressed transcripts (log_2 FC ≥|2|, FDR ≤0.01) between tembotrione-resistant (NER) and -susceptible (NES) *A. palmeri* 0 h after treatment (HAT) using RNA-Seq, fold change (FC) in counts per million (CPM).

Transcript ID	Putative annotation	Length (nt)	Mean CPM S	Mean CPM R	log_2 FC	FDR
TR139772|c1_g53_i1	Cytochrome P450 81E8	307	0.120	2.361	4.28	<0.001
TR103704|c9_g15_i2	Cytochrome P450 CYP72A219	746	0.107	1.080	3.31	<0.001
TR101518|c10_g55_i2	Cytochrome P450 CYP72A219	1154	0.116	1.114	3.23	<0.001
TR145786|c6_g538_i1	Scopoletin glucosyltransferase	868	13.205	58.408	2.14	<0.001
TR106590|c58_g2_i1	unknown	659	0.164	4.325	4.70	<0.001
TR141711|c12_g19_i1	Homoserine kinase	425	0.100	2.567	4.65	<0.001
TR106346|c6_g1_i1	Homoserine kinase	406	0.300	3.282	3.44	<0.001
TR101518|c10_g58_i1	unknown	337	0.049	0.421	3.06	<0.001
TR107224|c27_g10_i1	unknown	720	0.590	3.789	2.67	<0.001
TR105503|c2_g21_i1	unknown	2832	12.259	2.421	-2.36	<0.001
TR139772|c1_g91_i1	Cytochrome P450 81E8	447	0.232	4.967	4.40	0.001
TR105338|c17_g169_i1	Cytochrome P450 CYP72A219	442	0.315	2.287	2.84	0.001
TR103704|c9_g20_i1	Cytochrome P450 CYP72A219	855	0.081	0.521	2.65	0.001
TR104899|c0_g12_i1	Scopoletin glucosyltransferase	838	16.132	70.616	2.12	0.001
TR19936|c1_g1_i1	2,3-bisphosphoglycerate-independent phosphoglycerate mutase	333	0.050	1.831	5.14	0.001
TR101852|c9_g265_i1	MLP-like protein 43	683	8.526	56.705	2.73	0.001
TR139918|c4_g41_i1	Thaumatin-like protein 1	453	6.410	0.172	-5.23	0.001
TR139918|c4_g15_i1	Thaumatin-like protein	539	5.613	0.084	-6.08	0.001
TR45397|c0_g1_i2	Zeamatin	981	3.285	0.009	-8.31	0.001
TR45397|c0_g1_i1	Zeamatin	1032	4.298	0.008	-8.82	0.001
TR105338|c17_g52_i1	Cytochrome P450 CYP72A219	319	1.236	8.671	2.80	0.002
TR95333|c7_g68_i1	Cytochrome P450 CYP72A219	471	0.886	5.856	2.71	0.002
TR105338|c17_g121_i1	Cytochrome P450 CYP72A219	325	1.666	10.584	2.66	0.002
TR104706|c3_g2_i1	Protein OS-9 homolog	356	0.105	2.093	4.30	0.002
TR107224|c27_g4_i1	unknown	531	0.274	2.900	3.39	0.002
TR143018|c1_g19_i1	Gibberellin-regulated protein 8	1568	10.375	1.240	-3.07	0.002
TR91790|c1_g4_i3	Glutamate receptor ionotropic, kainanate 5	1770	1.838	0.215	-3.11	0.002
TR143018|c1_g5_i1	Peamaclein	524	8.084	0.817	-3.31	0.002
TR111734|c0_g1_i1	Biotin synthase	517	0.932	0.015	-5.80	0.002
TR44811|c0_g1_i2	Pathogenesis-related protein 1C	746	2.939	0.021	-7.04	0.002
TR104899|c0_g30_i1	Scopoletin glucosyltransferase	561	5.822	34.151	2.54	0.003
TR103704|c7_g1_i1	Cytochrome P450 CYP72A219	951	0.774	4.452	2.51	0.003
TR103827|c0_g54_i2	Anthocyanidin 3-O-glucosyltransferase 6	557	1.207	5.593	2.21	0.003
TR95333|c7_g68_i2	unknown	665	0.144	3.135	4.44	0.003
TR101518|c10_g10_i1	unknown	521	0.112	1.093	3.26	0.003
TR103366|c3_g1_i1	Dynein heavy chain, cytoplasmic	631	0.167	0.952	2.50	0.003
TR45369|c0_g5_i1	Protein TolB 1	401	2.839	14.468	2.34	0.003
TR95971|c3_g1_i1	Non-specific lipid-transfer protein	526	21.083	1.735	-3.62	0.003
TR95971|c3_g2_i1	Non-specific lipid-transfer protein	930	63.224	5.165	-3.63	0.003
TR95971|c3_g1_i3	Non-specific lipid-transfer protein	378	21.460	1.705	-3.67	0.003
TR96971|c2_g46_i1	Late embryogenesis abundant protein 76	867	8.455	0.352	-4.60	0.003
TR138835|c4_g13_i1	unknown	303	0.339	0.003	-6.39	0.003
TR25925|c1_g2_i1	Serine/threonine-protein kinase TAO1	436	4.579	0.043	-6.69	0.003
TR141923|c7_g155_i1	Glutathione S-transferase U22	409	0.072	0.915	3.64	0.004
TR103704|c9_g22_i1	Cytochrome P450 CYP72A219	501	0.143	0.938	2.69	0.004
TR105338|c17_g25_i1	Cytochrome P450 CYP72A219	320	0.290	1.643	2.48	0.004
TR101852|c9_g326_i1	MLP-like protein 43	436	1.317	9.230	2.81	0.004
TR83615|c0_g19_i1	Protein transparent testa 12	686	1.172	6.067	2.36	0.004

TR105773|c15_g56_i1	Peptidyl-prolyl cis-trans isomerase FKBP15-1	419	1.158	0.240	-2.27	0.004
TR106658|c1_g2_i3	Probable WRKY transcription factor 50	1397	1.415	0.181	-2.97	0.004
TR93324|c1_g1_i1	Probable WRKY transcription factor 50	913	1.095	0.130	-3.08	0.004
TR146600|c1_g1_i1	Cytochrome P450 CYP72A219	369	0.180	1.090	2.58	0.005
TR133585|c0_g1_i1	Cytochrome P450 CYP72A219	619	2.068	10.988	2.40	0.005
TR145210|c1_g4_i3	Putative UDP-glucose flavonoid 3-O-glucosyltransferase 3	1015	0.882	4.056	2.19	0.005
TR33045|c6_g9_i1	Interleukin-22 receptor subunit alpha-1	1068	0.054	0.929	4.07	0.005
TR139772|c1_g38_i1	Isoflavone 2-hydroxylase	308	0.568	6.615	3.54	0.005
TR46076|c1_g3_i1	snRna-activating protein complex subunit 4	330	1.097	6.359	2.53	0.005
TR93324|c1_g6_i1	Probable WRKY transcription factor 50	804	1.904	0.286	-2.74	0.005
TR139918|c4_g33_i1	Pathogenesis-related protein	720	1.405	0.065	-4.44	0.005
TR147520|c3_g8_i1	Copia protein	1040	0.388	0.000	-8.21	0.005
TR111921|c0_g1_i1	Multicopper oxidase LPR2	472	0.132	0.753	2.49	0.006
TR144046|c1_g9_i1	Dna-directed Rna polymerase subunit beta	1001	0.035	0.634	4.14	0.006
TR100466|c2_g51_i1	Odorant receptor 94a	647	0.262	2.447	3.22	0.006
TR140600|c2_g229_i1	unknown	406	5.401	29.767	2.46	0.006
TR96893|c2_g1_i1	unknown	579	2.399	0.602	-2.01	0.006
TR89056|c0_g1_i1	Translocator protein homolog	971	1.697	0.383	-2.17	0.006
TR135378|c0_g9_i1	unknown	579	2.229	0.376	-2.58	0.006
TR86829|c0_g8_i1	Probable calcium-binding protein CML45	1494	1.492	0.116	-3.70	0.006
TR147036|c0_g6_i3	Cysteine-rich secretory protein 1	2103	0.788	0.025	-4.89	0.006
TR134773|c0_g30_i1	Anthocyanidin 3-O-glucosyltransferase 1	1278	0.174	0.964	2.45	0.007
TR105338|c13_g2_i1	Cytochrome P450 CYP72A219	692	4.760	24.682	2.36	0.007
TR96838|c0_g2_i1	unknown	306	0.004	0.448	6.49	0.007
TR95971|c3_g1_i2	Non-specific lipid-transfer protein	459	21.047	1.730	-3.62	0.007
TR44811|c0_g1_i1	Pathogenesis-related protein 1A	1174	2.039	0.059	-5.08	0.007
TR134826|c0_g3_i1	7-deoxyloganetic acid glucosyltransferase	542	0.223	1.199	2.41	0.008
TR102618|c0_g72_i2	Probable carboxylesterase 15	646	3.009	0.343	-3.15	0.008
TR40608|c1_g1_i4	unknown	2477	0.005	0.355	5.72	0.008
TR140709|c10_g324_i1	unknown	311	0.039	1.897	5.54	0.008
TR148918|c0_g2_i1	unknown	735	0.033	1.492	5.40	0.008
TR22853|c0_g1_i1	Riparin-1.5 acid	423	0.025	0.565	4.42	0.008
TR89576|c0_g1_i1	Protein transparent testa 12	606	0.788	4.024	2.34	0.008
TR97117|c0_g3_i1	Transcriptional regulator MraZ	698	0.099	0.491	2.28	0.008
TR106658|c1_g2_i2	Probable WRKY transcription factor 50	1493	1.177	0.191	-2.63	0.008
TR105360|c1_g7_i1	Lysine histidine transporter-like 8	1751	1.252	0.084	-3.90	0.008
TR105338|c17_g227_i1	Cytochrome P450 CYP72A219	305	0.985	5.516	2.48	0.009
TR101518|c10_g31_i1	Cytochrome P450 CYP72A219	588	0.270	1.499	2.45	0.009
TR133585|c0_g2_i1	Cytochrome P450 CYP72A219	1687	37.670	185.084	2.29	0.009
TR103827|c0_g9_i1	Anthocyanidin 3-O-glucosyltransferase 6	500	0.985	4.649	2.24	0.009
TR11697|c0_g1_i1	Probable carboxylesterase 15	524	2.766	0.350	-3.00	0.009
TR136244|c1_g5_i1	Uncharacterized protein F40H6.2	556	0.030	0.777	4.64	0.009
TR81691|c0_g1_i1	Ethylene-responsive transcription factor ERF098	617	0.111	0.733	2.71	0.009
TR142963|c1_g3_i1	4-hydroxyphenylpyruvate dioxygenase	848	0.769	3.553	2.20	0.009
TR140724|c5_g8_i2	Ethylene-responsive transcription factor ERF114	1584	0.606	0.079	-2.94	0.009
TR147511|c0_g9_i1	Receptor-like protein 12	837	5.829	0.283	-4.38	0.009
TR134919|c3_g3_i1	Zeamatin	438	1.125	0.022	-5.63	0.009
TR134933|c2_g3_i1	unknown	581	0.017	1.256	6.14	0.010
TR101852|c9_g238_i1	MLP-like protein 43	317	2.404	17.147	2.83	0.010
TR146622|c1_g22_i1	Alpha-glucosidase YihQ	1805	2.449	0.314	-2.96	0.010
TR146622|c1_g18_i5	Alpha-glucosidase YihQ	1473	1.827	0.208	-3.13	0.010
TR139918|c4_g9_i1	Thaumatin-like protein	458	1.162	0.071	-4.03	0.010
TR68255|c0_g6_i1	Pathogenesis-related protein PR-4A	419	4.005	0.173	-4.55	0.010

Table 8-2: Identification of differentially expressed transcripts (log_2 FC ≥|2|, FDR ≤0.01) between tembotrione-resistant (NER) and -susceptible (NES) *A. palmeri* 12 h after treatment (HAT) using RNA-Seq, fold change (FC) in counts per million (CPM).

Transcript ID	Putative annotation	Length (nt)	Mean CPM S	Mean CPM R	log2 FC	FDR
TR104519|c0_g1_i1	ABC transporter C family member 3	1425	2.019438	38.28181	4.10	<0.001
TR104519|c0_g3_i3	ABC transporter C family member 6	868	0.503379	10.43923	4.24	<0.001
TR104519|c0_g3_i1	ABC transporter C family member 3	1397	2.23986	49.22892	4.36	<0.001
TR138835|c4_g13_i1	unknown	303	0.425992	0.000656	-7.13	0.002
TR111734|c0_g1_i1	Biotin synthase	517	3.508165	0.02883	-6.23	0.001
TR95971|c2_g16_i1	Non-specific lipid-transfer protein	384	1.811397	0.033615	-6.06	0.006
TR95971|c2_g47_i1	Non-specific lipid-transfer protein	315	4.83148	0.11358	-5.77	0.001
TR95971|c2_g16_i2	Non-specific lipid-transfer protein	518	11.05545	0.372687	-5.27	0.006
TR95971|c2_g7_i1	Non-specific lipid-transfer protein	478	0.898729	0.02943	-5.24	0.005
TR95971|c2_g25_i1	Non-specific lipid-transfer protein	517	5.841105	0.23156	-5.03	0.004
TR158179|c0_g1_i1	Miraculin	885	11.16661	0.78397	-4.21	0.005
TR98249|c4_g22_i1	unknown	690	0.081066	0.004446	-4.04	0.008
TR137253|c0_g1_i2	Maturase K	1002	0.684304	0.048278	-3.82	0.000
TR146234|c1_g15_i1	Chaperone protein DnaJ	443	0.181085	0.017024	-3.45	0.003
TR145711|c1_g9_i1	Probable serine/threonine-protein kinase pats1	732	0.113083	0.011302	-3.37	0.008
TR103701|c8_g35_i2	Natterin-4	2090	24.09593	1.874598	-3.25	0.008
TR96073|c5_g18_i1	unknown	689	1.324207	0.178444	-3.20	0.005
TR42614|c0_g4_i1	Endogenous alpha-amylase/subtilisin inhibitor	804	17.04275	2.296033	-3.19	0.008
TR146234|c1_g3_i3	Probable terpene synthase 13	1358	0.538498	0.097945	-2.61	0.005
TR98701|c0_g16_i1	ADP-ribosylation factor GTPase-activating protein AGD12	761	0.510003	0.10586	-2.59	0.007
TR147385|c3_g15_i1	Linoleate 13S-lipoxygenase 2-1, chloroplastic	416	41.38774	8.296235	-2.45	0.001
TR102020|c2_g69_i1	Flavonol synthase/flavanone 3-hydroxylase	714	0.98794	0.185919	-2.36	0.007
TR144480|c0_g26_i1	unknown	657	0.604088	0.13807	-2.36	0.001
TR89050|c0_g4_i1	Endogenous alpha-amylase/subtilisin inhibitor	974	32.34506	6.717122	-2.33	0.008
TR99108|c3_g49_i1	Linolenate hydroperoxide lyase, chloroplastic	414	7.003397	1.633861	-2.08	0.003
TR35766|c0_g3_i1	Oligopeptide transporter 3	478	0.929379	3.694346	2.03	0.001
TR146644|c4_g91_i2	Probable plastid-lipid-associated protein 14, chloroplastic	818	4.947787	23.19134	2.08	0.002
TR103177|c5_g5_i1	unknown	307	0.436163	2.063939	2.10	0.005
TR75678|c0_g2_i1	Transcription factor bHLH47	380	0.191238	0.841515	2.11	0.007
TR146644|c4_g91_i1	Probable plastid-lipid-associated protein 14, chloroplastic	1020	6.256362	29.70738	2.13	0.001
TR60722|c0_g2_i1	Oligopeptide transporter 3	361	0.609293	2.710888	2.15	0.000
TR39253|c0_g2_i1	unknown	869	0.213202	1.057233	2.16	0.002
TR145597|c3_g46_i1	Oligopeptide transporter 3	483	8.12346	35.83426	2.16	0.000
TR103177|c5_g7_i1	unknown	352	0.521314	2.644067	2.20	0.005
TR146644|c4_g82_i1	Probable plastid-lipid-associated protein 14, chloroplastic	628	0.574806	2.990553	2.23	0.001
TR146644|c4_g8_i1	unknown	365	0.191479	1.023653	2.26	0.001
TR146644|c4_g43_i1	unknown	334	0.180244	0.944221	2.29	0.000
TR146644|c4_g84_i1	Probable plastid-lipid-associated protein 14, chloroplastic	781	4.438114	23.82234	2.30	0.001
TR103506|c2_g14_i1	Hippocampus abundant transcript-like protein 2	634	2.681888	13.40648	2.31	0.000
TR146644|c4_g15_i1	Probable plastid-lipid-associated protein 14, chloroplastic	713	3.972846	21.34175	2.33	0.001
TR146644|c4_g82_i2	Probable plastid-lipid-associated protein 14, chloroplastic	650	0.433104	2.423324	2.37	0.001
TR100466|c2_g59_i1	Odorant receptor 94a	657	0.257389	1.469713	2.40	0.008
TR103506|c2_g42_i1	Hippocampus abundant transcript-like protein 1	1743	25.86775	136.2032	2.41	0.000
TR9391|c0_g1_i1	unknown	437	0.169263	0.84052	2.46	0.007
TR68408|c0_g1_i1	Probable plastid-lipid-associated protein 14, chloroplastic	449	1.252602	8.131071	2.60	0.003
TR132110|c0_g1_i1	unknown	314	0.10675	0.620568	2.61	0.000
TR105434|c1_g76_i1	Cadmium/zinc-transporting ATPase HMA2	1980	17.20365	134.9203	2.97	0.008
TR44913|c0_g1_i1	Probable plastid-lipid-associated protein 14, chloroplastic	668	0.093773	0.862583	2.97	0.005
TR58548|c0_g1_i1	Probable plastid-lipid-associated protein 14, chloroplastic	417	0.159826	1.367668	3.03	0.005
TR42311|c0_g1_i1	unknown	460	0.086955	0.798062	3.08	0.000
TR105434|c1_g72_i1	Cadmium/zinc-transporting ATPase HMA2	1417	17.34825	153.0099	3.10	0.004
TR34953|c0_g4_i1	4-diphosphocytidyl-2-C-methyl-D-erythritol kinase	365	0.211842	2.117644	3.12	0.006

TR105434|c1_g3_i1	Cadmium/zinc-transporting ATPase HMA2	477	0.648138	6.016718	3.15	0.004
TR102196|c3_g62_i1	unknown	858	19.33973	162.9345	3.19	0.004
TR48510|c0_g1_i1	unknown	504	0.040031	0.415009	3.19	0.005
TR138017|c2_g4_i1	tRNA-2-methylthio-N(6)-dimethylallyladenosine synthase	414	1.728337	13.14628	3.26	0.008
TR34050|c0_g2_i1	Probable plastid-lipid-associated protein 14, chloroplastic	520	0.136088	1.439028	3.27	0.000
TR135414|c0_g2_i1	ORC1-type DNA replication protein	921	0.183785	1.585002	3.31	0.001
TR138017|c2_g7_i1	tRNA-2-methylthio-N(6)-dimethylallyladenosine synthase	432	0.622977	5.592293	3.45	0.001
TR145964|c1_g3_i3	ABC transporter C family member 5	1540	0.367693	5.246593	3.49	0.007
TR88111|c0_g7_i1	Octanoyltransferase	598	3.638411	43.12319	3.69	0.001
TR141660|c0_g23_i1	unknown	555	2.988986	43.53749	3.73	0.004
TR141660|c0_g9_i1	unknown	868	12.96066	160.9667	3.77	0.002
TR104519|c0_g6_i1	unknown	346	0.077228	1.38391	3.83	0.008
TR14276|c0_g2_i1	unknown	347	0.061444	0.802265	3.85	0.000
TR145964|c1_g3_i2	ABC transporter C family member 5	2665	2.443039	40.60342	3.90	0.000
TR14276|c0_g1_i1	unknown	392	0.036855	0.492796	3.98	0.002
TR145964|c1_g1_i2	unknown	441	0.10609	2.086313	4.03	0.003
TR41396|c0_g2_i1	unknown	1052	0.319158	4.959102	4.08	0.001
TR34790|c1_g1_i1	unknown	340	0.049669	0.868263	4.09	0.005
TR19936|c1_g1_i1	2,3-bisphosphoglycerate-independent phosphoglycerate mutase	333	0.121933	2.25996	4.09	0.004
TR41396|c0_g2_i2	unknown	1116	0.302999	5.59807	4.20	0.001
TR26144|c0_g3_i1	unknown	480	0.116361	1.866071	4.33	0.002
TR68635|c0_g3_i1	D(1B) dopamine receptor	362	0.051493	1.25551	4.40	0.001
TR67717|c0_g3_i1	unknown	335	0.10081	1.998588	4.46	0.001
TR97093|c0_g5_i1	unknown	528	0.386913	8.191069	4.73	0.004
TR136244|c1_g5_i1	Uncharacterized protein F40H6.2	556	0.026825	0.726526	4.93	0.007
TR95800|c4_g1_i1	unknown	442	0.204526	6.145185	5.02	0.000
TR97093|c0_g3_i1	unknown	583	0.32136	12.05658	5.31	0.000
TR103347|c8_g2_i1	NACHT, LRR and PYD domains-containing protein 9A	501	0.005114	0.320145	5.54	0.010
TR73879|c0_g2_i1	unknown	366	0.046618	2.000102	5.69	0.003
TR172023|c0_g1_i1	unknown	393	0.036527	2.155153	5.98	0.000
TR96878|c1_g5_i1	unknown	1184	0.007647	0.62862	5.99	0.009
TR91014|c0_g2_i1	unknown	724	0.010302	0.67347	6.07	0.009
TR134933|c2_g2_i1	unknown	567	0.059515	4.093334	6.13	0.000
TR134933|c2_g3_i1	unknown	581	0.022341	1.35484	6.50	0.009

9. APPENDIX C

TABLES

Table 9-1: Pairwise estimates of F_{ST} and Nei's standard genetic distance (D_{ST}) among eight *A. palmeri* populations using SNPs from the chloroplast genome. Pairwise estimates of F_{ST} and D_{ST} are shown above and below the diagonal, respectively.

	AZ-R	AZ-S1	GA-R	GA-S	NE-S	KS-S	TN-R	AZ-S2
AZ-R		0.058	0.068	0.223	0.178	0.215	0.169	0.205
AZ-S1	0.028		0.096	0.236	0.167	0.050	0.252	0.158
GA-R	0.035	0.039		0.222	0.181	0.068	0.248	0.190
GA-S	0.098	0.088	0.096		0.276	0.187	0.344	0.236
NE-S	0.070	0.056	0.071	0.073		0.112	0.358	0.212
KS-S	0.035	0.026	0.036	0.081	0.046		0.215	0.152
TN-R	0.057	0.075	0.088	0.132	0.126	0.072		0.152
AZ-S2	0.080	0.052	0.073	0.132	0.072	0.060	0.129	

Table 9-2: Pairwise estimates of F_{ST} and Nei's standard genetic distance (D_{ST}) among eight *A. palmeri* populations using SNPs from the mitochondrial genome. Pairwise estimates of F_{ST} and D_{ST} are shown above and below the diagonal, respectively.

	AZ-R	AZ-S1	GA-R	GA-S	NE-S	KS-S	TN-R	AZ-S2
AZ-R		0.057	0.091	0.198	0.152	0.053	0.213	0.202
AZ-S1	0.057		0.121	0.143	0.169	0.047	0.214	0.191
GA-R	0.033	0.041		0.216	0.154	0.061	0.307	0.306
GA-S	0.070	0.051	0.076		0.230	0.171	0.338	0.338
NE-S	0.056	0.062	0.055	0.094		0.096	0.342	0.288
KS-S	0.023	0.022	0.024	0.062	0.039		0.255	0.228
TN-R	0.055	0.054	0.085	0.108	0.116	0.079		0.404
AZ-S2	0.056	0.052	0.092	0.115	0.097	0.066	0.102	

FIGURES

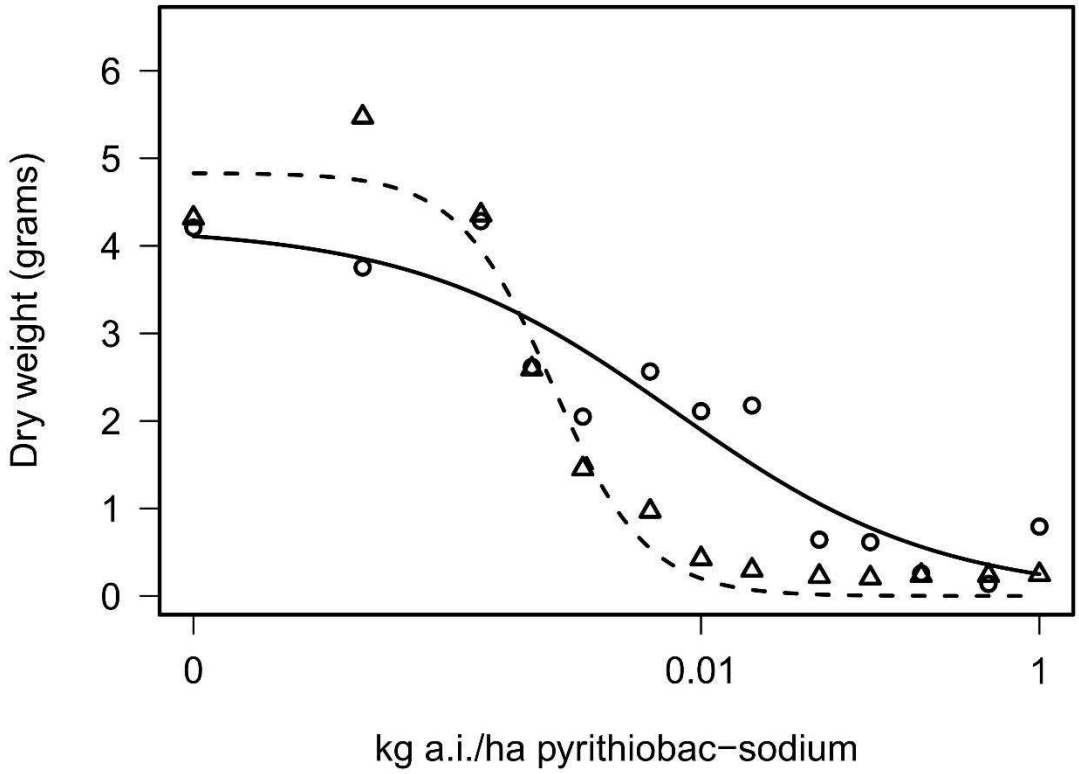

Figure 9-1: Non-linear regression analysis of dry weight for *A. palmeri* populations AZ-R (solid line) and AZ-S1 (dashed line) 27 DAT with pyrithiobac-sodium. Symbols are averages of 5 replicates fitted in a three-parameter log-logistic model.

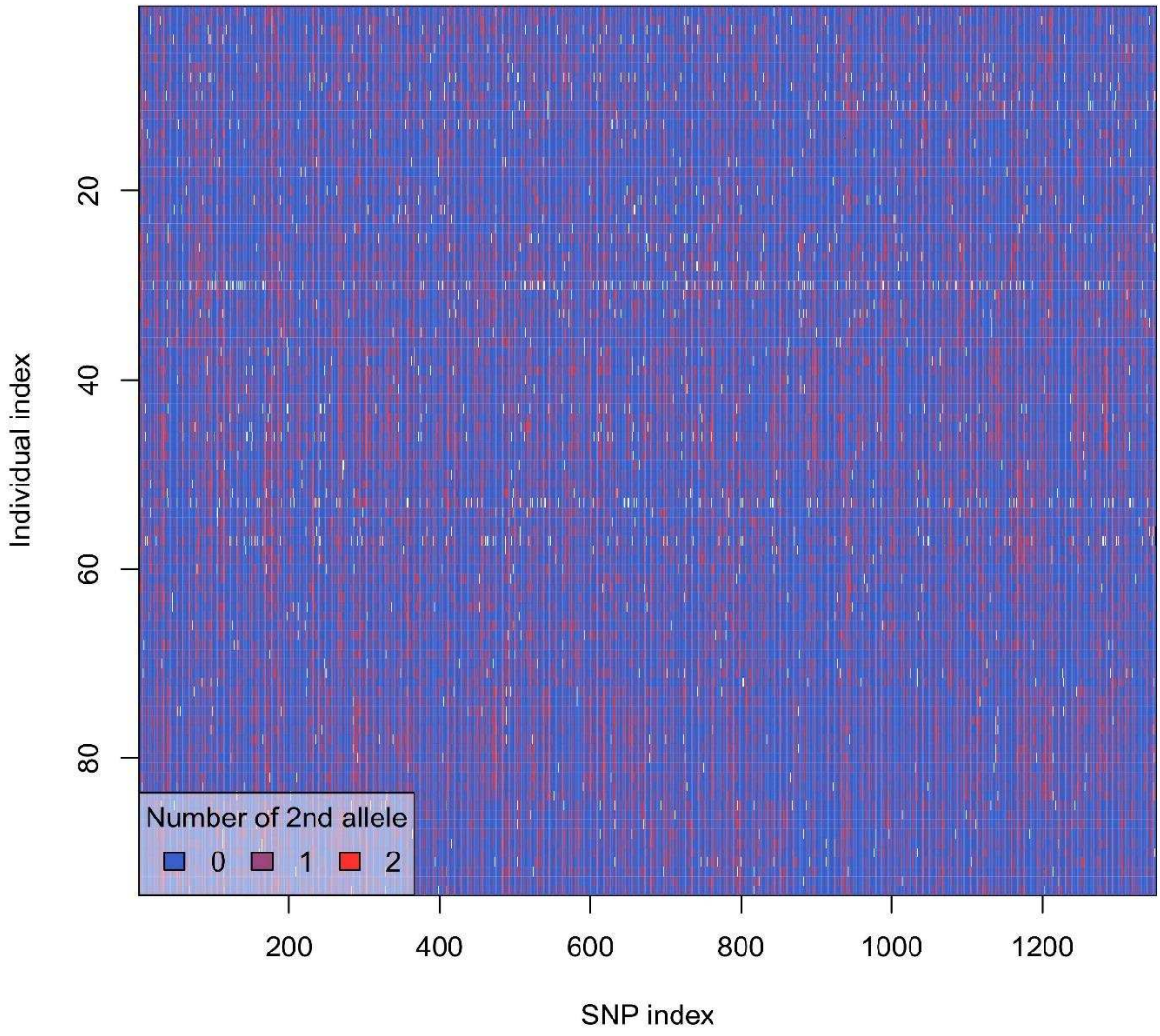

Figure 9-2: Allele structure of individuals versus loci. Blue/0 = homozygous for the most common allele (major allele), violet/1 = heterozygous, red/2 = homozygous for the least common allele (minor allele), white = missing data.

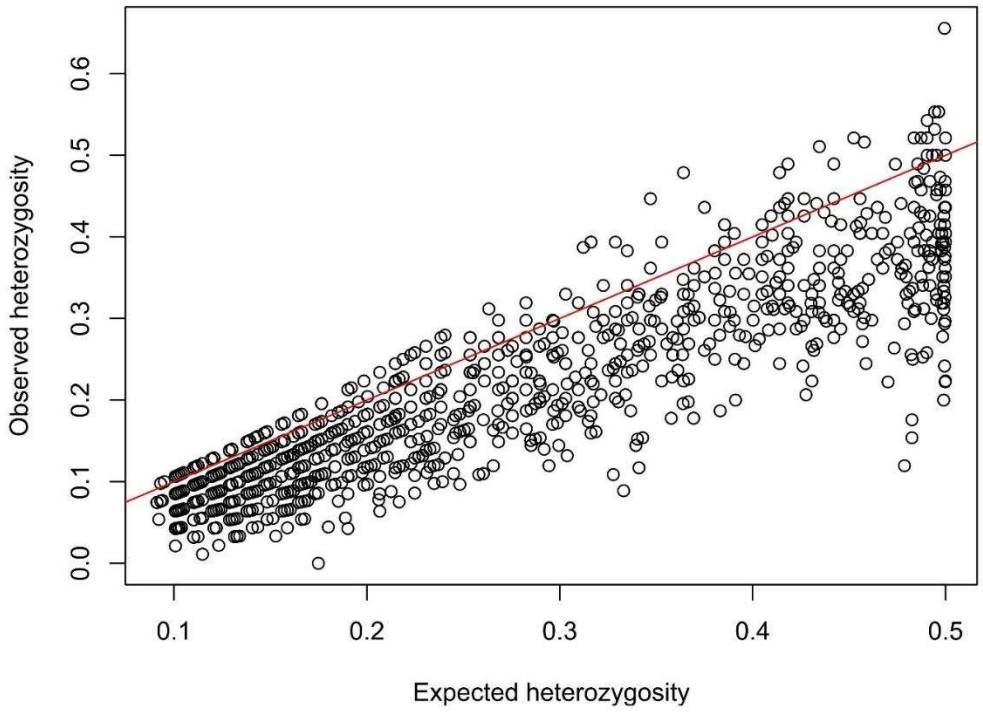

Figure 9-3: Observed heterozygosity as a function of expected heterozygosity per locus for the whole dataset of 1,351 SNPs.

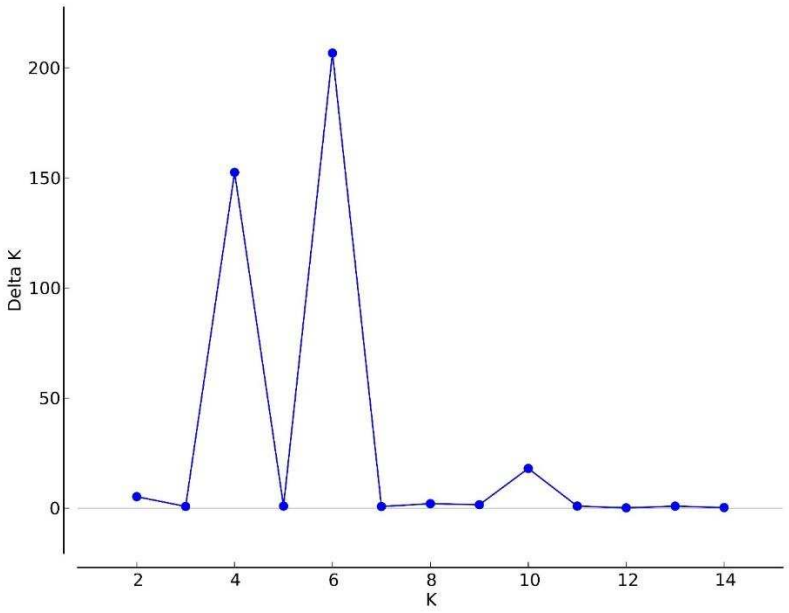

Figure 9-4: *Ad hoc* ΔK test (Evanno et al., 2005) with the whole dataset of 1,351 SNPs. The analysis suggests $K = 4$ and $K = 6$ to be the most likely amount of sub-populations.

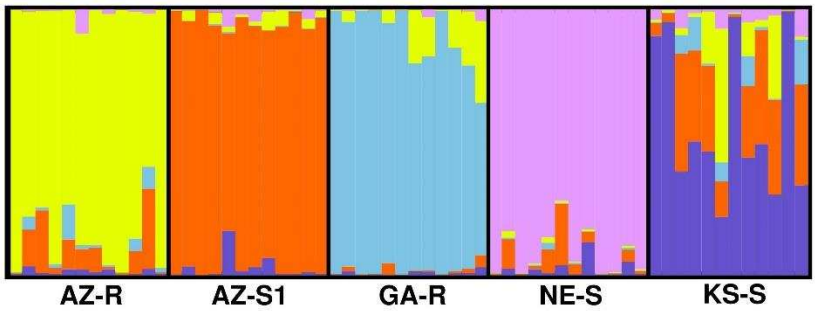

Figure 9-5: Population structure analysis with $K = 5$ for the 1,351 SNPs of the five *A. palmeri* populations which clustered together in Fig. 4A, excluding GA-S, TN-R, and AZ-S2. Each individual is represented by a vertical bar that is divided by K colored segments representing the likelihood of a membership to each cluster.

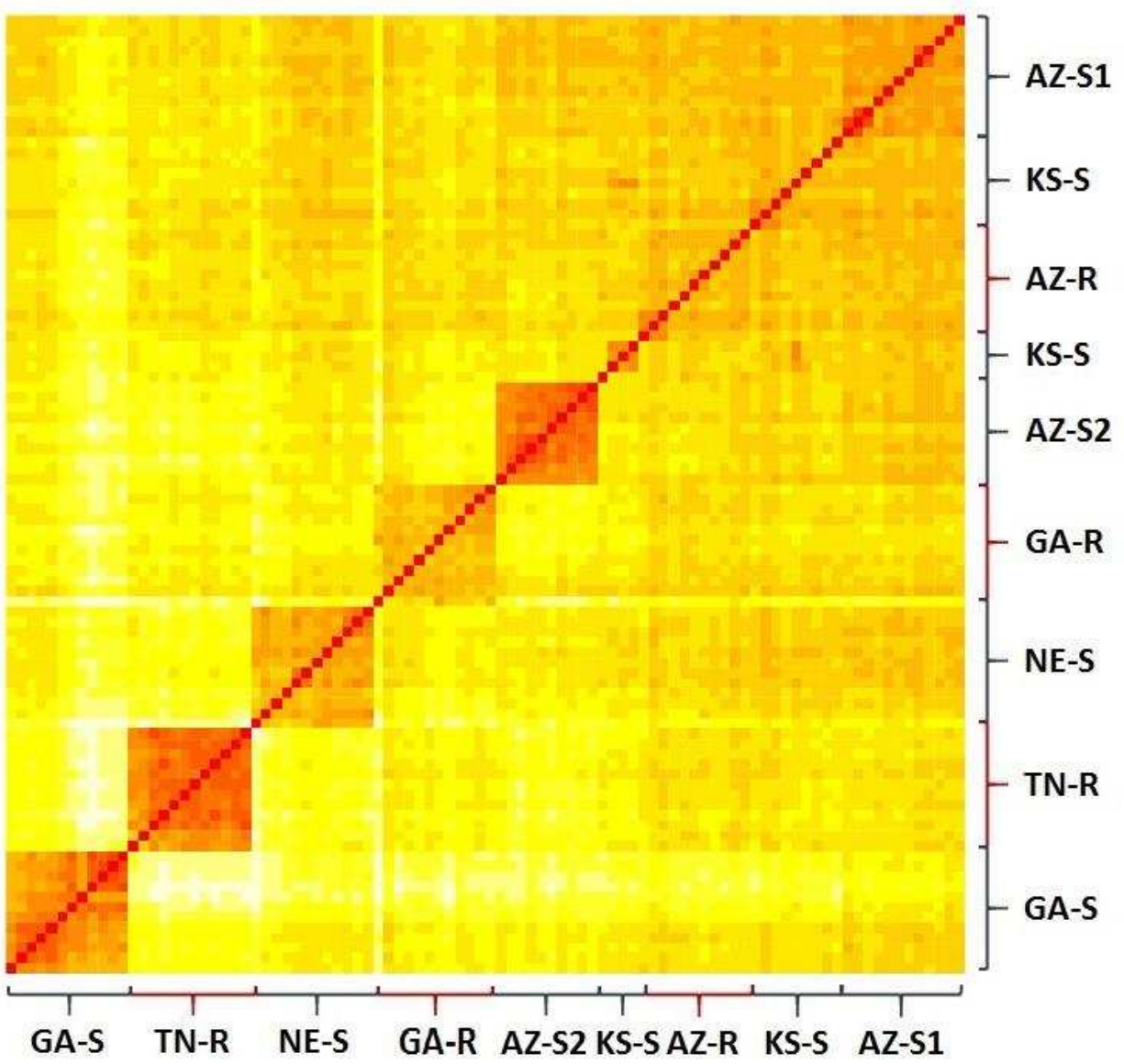

Figure 9-6: Visualization of Nei's distance (1972) as a heatmap. Each pixel refers to one individual being compared to another individual. Red marks a low degree of genetic distance while white and light yellow mark a high degree of genetic distance between these individuals. The diagonal line shows an individual being compared to itself while red squares indicate members of the same population. The missing square structures for KS-S, AZ-S1, and AZ-R are an indication for their high genetic variability.

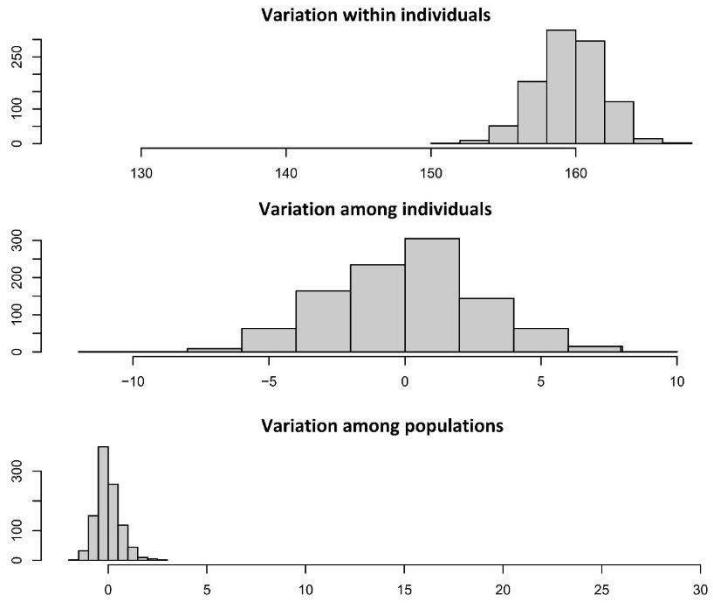

Figure 9-7: Three histograms that represent the distribution of randomized strata for variation within individuals, variation among individuals and variation among populations. Variation within individuals is very high while variation among individuals and among populations is low.

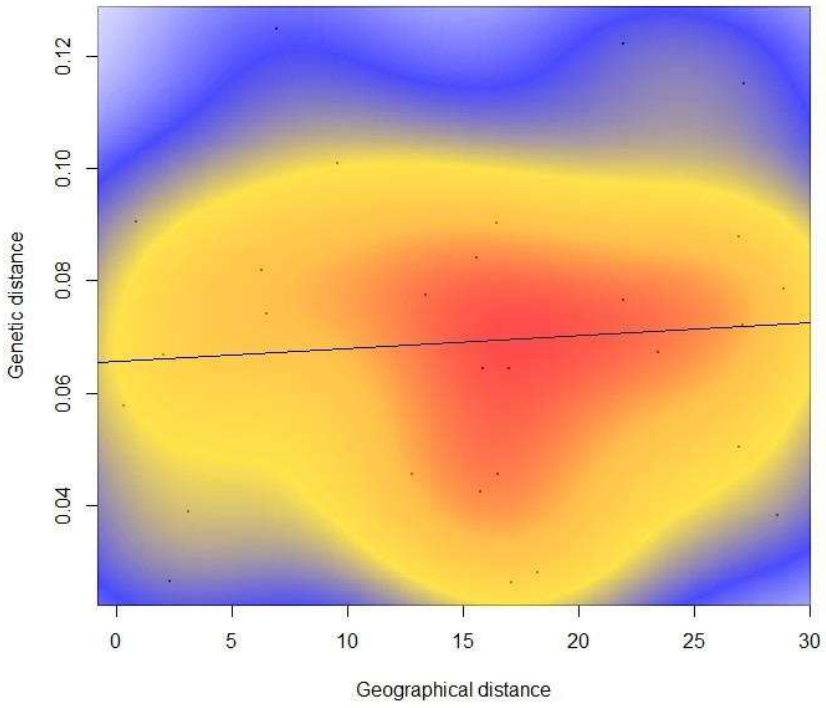

Figure 9-8: Correlation of genetic and geographical distance of eight *A. palmeri* populations from several U.S. states. The denser areas in the plot indicate sub-groups. With an R^2 of 0.006, no correlation between genetic and geographical distance was found.

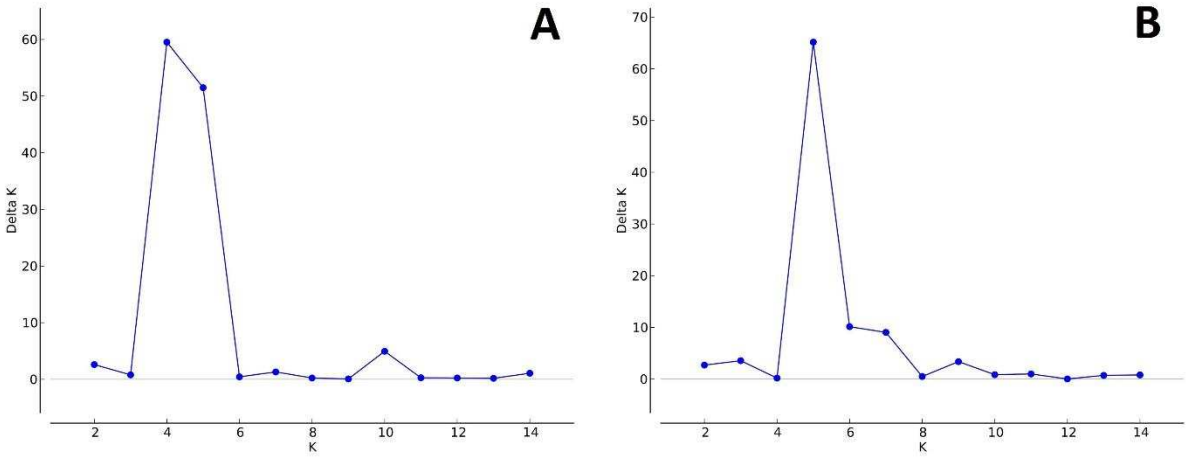

Figure 9-9: *Ad hoc* ΔK test with SNPs from the chloroplast genome (A) and the mitochondrial genome (B). The analysis suggests $K = 4$ and $K = 5$ as well as $K = 5$ to be the most likely amount of sub-populations, respectively.

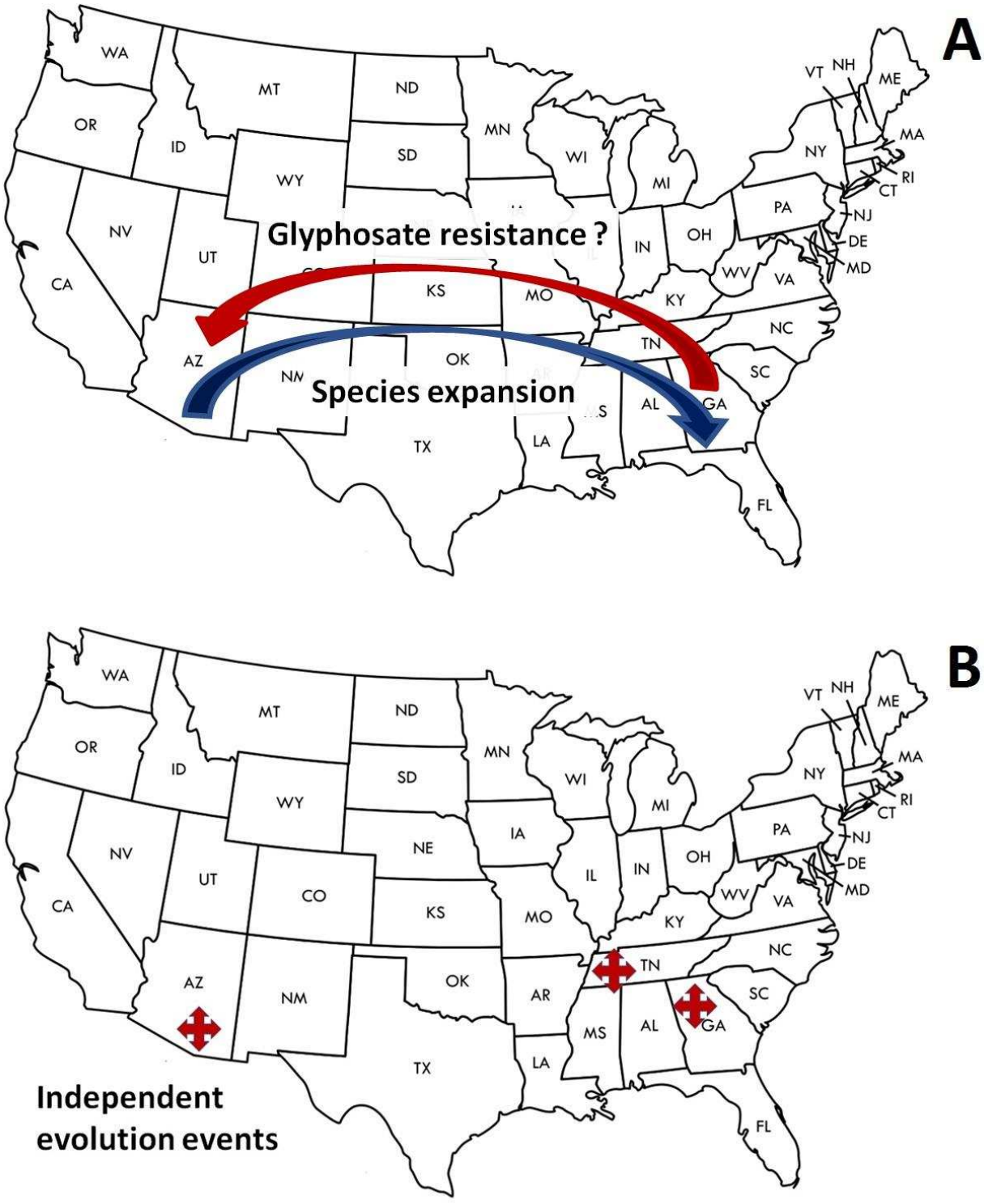

Figure 9-10: Two possible scenarios of glyphosate resistance origin in *A. palmeri* with either glyphosate resistance spread from Georgia over Kansas to Arizona in the counter-direction of species expansion to the southeast (A) or independent evolution events in Arizona, Georgia and Tennessee (B).